BIOCHEMICAL AND GENETIC CHARACTERIZATION OF IspC, AN IMMUNOGENIC SURFACE PROTEIN WITH PEPTIDOGLYCAN HYDROLASE ACTIVITY ESSENTIAL FOR VIRULENCE OF *LISTERIA MONOCYTOGENES*

A thesis submitted to the School of Graduate and Post-doctoral Studies, University of Ottawa, in partial fulfillment of the requirements for the degree of

Doctor of Philosophy of Science

Department of Biochemistry, Microbiology and Immunology

Faculty of Medicine

By

Lin Ru Wang

Your file Votre référence
ISBN: 978-0-494-46526-4
Our file Notre référence
ISBN: 978-0-494-46526-4

FACULTÉ DES ÉTUDES SUPÉRIEURES ET POSTOCTORALES

uOttawa

L'Université canadienne
Canada's university

FACULTY OF GRADUATE AND POSDOCTORAL STUDIES

Linru Wang
AUTEUR DE LA THÈSE / AUTHOR OF THESIS

Ph.D. (Microbiology and Immunology)
GRADE / DEGREE

Department of Biochemistry, Microbiology and Immunology
FACULTÉ, ÉCOLE, DÉPARTEMENT / FACULTY, SCHOOL, DEPARTMENT

Biochemical and Genetic Characterization of IspC, an Immunogenic Surface Protein with Peptidoglycan Hydrolase Activity Essential for Virulence of *Listeria Monocytogenes*

TITRE DE LA THÈSE / TITLE OF THESIS

Min Lin
DIRECTEUR (DIRECTRICE) DE LA THÈSE / THESIS SUPERVISOR

CO-DIRECTEUR (CO-DIRECTRICE) DE LA THÈSE / THESIS CO-SUPERVISOR

EXAMINATEURS (EXAMINATRICES) DE LA THÈSE / THESIS EXAMINERS

Brian Coombes

Jeffrey Farber

Susan Nadia-Davis

Susan Logan

Gary W. Slater
Le Doyen de la Faculté des études supérieures et postdoctorales / Dean of the Faculty of Graduate and Postdoctoral Studies

ABSTRACT

Listeria monocytogenes is a Gram-positive intracellular bacterial pathogen responsible for a severe foodborne disease referred to as listeriosis in humans. A novel 86-kDa protein of unknown function, designated IspC, was previously identified by differential immunoscreening of a *L. monocytogenes* genomic expression library using two kinds of antisera, one (RαL) from rabbits infected with live bacteria and the other (RαK) from animals immunized with heat-killed bacteria. IspC reacted only with RαL but not with RαK, suggesting that it is induced only or significantly upregulated *in vivo* during *L. monocytogenes* infection and thus may be important in pathogenicity. IspC is a putative peptidoglycan hydrolase that is likely surface localized, as predicted from its deduced amino acid sequence. The biochemical properties and biological function (s) of IspC and its role in pathogenesis remain to be elucidated.

The IspC protein was expressed in *Escherichia coli* and purified to electrophoretic homogeneity by chromatographic methods. This resulted in sufficient amount of purified recombinant IspC (rIspC) required for production of rabbit polyclonal antibodies to IspC (RαIspC) and for biochemical and structural studies. N-terminal sequencing and mass spectrometry analysis showed that IspC contained a 23-residue N-terminal peptide being processed in *E. coli*. Circular dichroism and Raman spectroscopy analysis of purified rIspC revealed that the dominant secondary structure for the protein is β-sheet, consistent with the prediction by the PSIPRED method. Renaturing SDS-PAGE analysis demonstrated that IspC was capable of hydrolyzing bacterial cell wall substrates from several bacterial sources

including *L. monocytogenes* itself, indicating IspC is an autolysin. The native IspC was detected in all growth phases at a relatively stable, low level during a 22-h *in vitro* culture, although its gene was transiently transcribed only in the early exponential growth phase. This and the previous findings suggest that IspC is upregulated *in vivo* during infection. The protein was unevenly distributed in clusters on the cell surface, as shown by immunofluorescence and immunogold electron microscopy. Analysis of various truncated forms of IspC has defined two separate functional domains: the N-terminal catalytic domain (aa 24 to 197) responsible for the hydrolytic activity and the C-terminal domain (aa 198 to 774) made up of seven GW (glycine-tryptophan dipeptide) modules responsible for anchoring the protein to the cell wall. The IspC autolysin exhibited peptidoglycan hydrolase activity over a broad pH range between 3 and 9 with an alkaline pH optimum of 7.5 to 9. Interestingly, the separated N-terminal catalytic domain showed hydrolytic activity at acidic pHs with a pH optimum between 4 and 6 and negligible activity at alkaline pHs. This suggests that the cell wall binding domain (CWBD) may be of importance in modulating the activity of the N-terminal enzyme domain.

To determine if this enzyme has any biological functions and/or plays a role in virulence, an *ispC* in-frame deletion mutant was created from the wild type *L. monocytogenes*. This Δ*ispC* mutant exhibited complete abrogation of expression of IspC and had no defect in the *in vitro* growth, colony and microscopic morphologies, or biochemical characteristics. Comparison of bacteriolytic profiles of the surface protein extracts of the wild type and the mutant strains indicated that IspC was a minor autolysin *in vitro*. Lack of

IspC led to attenuating the virulence of *L. monocytogenes* in mice, evidenced by a significant reduction of bacterial counts in liver and brain and no mortality compared with the wild type. Further, the data from the assays using various eukaryotic cells for adhesion, invasion, actin tail formation, plaque formation, and intracellular growth indicated that IspC expression was required for cell-type dependent adhesion and invasion, early-stage actin tail formation and late-stage intracellular survival and growth. The findings that (i) the mutant was impaired for adhesion to certain eukaryotic cells, (ii) both purified IspC and its C-terminal CWBD were capable of binding sheep choroid plexus (SCP) epithelial cells and Vero cells, and (iii) both purified IspC and its C-terminal CWBD were capable of binding to GAG heparin (extensively used as a representative glycosaminoglycan) *in vitro* supported the role of IspC as an adhesin in virulence. The Δ*ispC* mutant exhibited a marked defect in adhesion and invasion for SCP cells but not human brain microvascular endothelial cells (HBMEC), suggesting that IspC is necessary for crossing the blood-cerebrospinal fluid barrier. Proteomic and immunological analysis showed a reduced surface expression of some known or putative virulence factors (e.g., ActA, InlC2, and a flagellin homologue FlaA) due to the IspC deficiency. Together, these results demonstrate that IspC, expressed as a minor autolysin *in vitro*, is not important for cell division or separation but essential for full virulence of *L. monocytogenes in vivo*.

In conclusion, IspC plays a dual role in *L. monocytogenes* virulence, i.e., promoting the bacterium-host cell interaction through the adhesive properties of its C-terminal CWBD (direct role as an adhesin) and regulating the surface display of other virulence factors

(indirect role) presumably by the autolytic activity of its N-terminal catalytic domain. The study has shed new light on our understanding of molecular mechanisms by which a minor surface peptidoglycan hydrolase contributes to bacterial pathogenesis.

DEDICATION

This thesis is dedicated to my dearest father Rongjiang Wang and mother Shulan Tian for giving me a wonderful life, happy childhood and so nice white lies, to my husband Qiang Yue for your constant encouragements, to my sisters and brother Linhong Wang, Linmei Wang, and Linjun Wang for your deepest love, and also to my most dearest friends, Yong Liu, Zhijie Zhang, Lina Wu (The Clinical Laboratory of the 2nd affiliated Hospital of China Medical University), Ying Zhou, Guijie Wang, Hong Qi, Hui Kang (The Clinical Laboratory of the 1st affiliated Hospital of China Medical University), my loved classmates including Yue An, Guanghua Niu, Xu Shun, Yuling Liu, Tong Liu, Wenna Chen (Dalian Medical University).

ACKNOWLEDGEMENTS

First of all, I would love to thank from the bottom of my heart my supervisor, Dr. Min Lin from Canadian Food Inspection Agency, Canada. He taught me a lot of nice laboratory skills and his rich research experience, which made my Ph.D project progress very efficiently. He is open-minded and insightful, which greatly stimulated my creativity. The much energy and time he has devoted to science is much impressive and his strict attitude toward research sets a good example for me. Moreover, I respect him also for his appreciable personalities-generosity and kindness, who always stands out and provides help to so many people within and outside our lab. I am honored to be one of his students!

I am also extremely grateful to my advisory committee: Dr. Craig Lee, Dr. Douglas J. Franks, and Dr. Alain Stintzi (University of Ottawa, Canada), for your time, insight, suggestions and acknowledgements on my progress which greatly encourage me to keep on improving myself.

I would like to acknowledge our collaborators Dr. Terry D. Cyr and Lisa Walrond (Centre for Biologics Research, Health Canada, Ottawa, Ontario, Canada) for determination of the molecular weight of IspC by mass spectrometry, Dr. Zhanna Potetinova (Institute for Biological Science, NRC, Ottawa, Ontario, Canada) for Circular dichroism (CD) experiment, and Dr. Li-Lin Tay (National Research Council, Ottawa, Ontario, Canada) for Raman analysis of rIspC.

I wish to express my gratitude to B. Phipps-Todd for technical support and excellent training me on how to use transmission electron microscopes, to M. Wiedmann and E. D. Fortes (Department of Food Science, Cornell University, NY, USA) for providing useful advice on plaque assay, to the Small Animal Colony (Canadian Food Inspection Agency, Ottawa Laboratory, Fallowfield) for mouse infection experiments, to Prof. T. Chakraborty (Institute of Medical Microbiology, Justus-Liebig University, Germany) for providing the plasmid vector pAUL-A, to Prof. J. Wehland (Technical University of Braunschweig, Braunschweig, Germany) for providing rabbit anti-InlA and -InlB antibodies, and to M. Kuhn (Biocenter (Microbiology), University of Würzburg, Würzburg, Germany) for providing rabbit anti-ActA antibody. We also thank T. Abujamel, H. McRae, H. Dan, M-E. Auclair and K. Coulombe for your editorial comments and suggestions.

I owe to H. Dan for technical assistance, advices, and accompanying me when I worked late and on weekends.

Special thanks to two wonderful girls, Brook and Tiffany, for your friendship and teaching me English.

TABLE OF CONTENTS

LIST OF MAJOR ABBREVIATIONS

A
aa Amino Acid
APS Ammonium Persulfate

B
BBB Blood-Brain Barrier
BCSFB Blood-Cerebrospinal Fluid Blood
BHI Brain Heart Infusion
BPW Buffered Peptone Water
BSA Bovine Serum Albumin

C
CB Coomassie Blue
CD Circular Dichroism
CDC Cholesterol-Dependent Cytolysin
CEC Cation Exchange Chromatography
Co-IP Co-Immunoprecipitation
CNS Central Nervous System
CSF Cerebrospinal Fluid
CWBD Cell Wall Binding Domain

D
d.d H_2O Distilled/Deionized Water
DEPC Diethylpyrocarbonate
dH_2O Deionized Water
DMEM Dulbecco's Modified Eagle Medium

E
ε Extinction Coefficient
EAD Enzymatic Activity Domain
EC or ***E. coli*** *Escherichia coli*
EDTA Ethylenediaminetetraacetic Acid
EGF Human Recombinant Epidermal Growth Factor
Em Erythromycin
Ena Drosophila Enabled
ESI Electrospray Ionization

F
FA Formic Acid

FBS Fetal Bovine Serum
FITC Fluorescein Isothiocyanate

G
gC1q-R Receptor of the Globular Part of the Complement Component C1q
GAGs Glycosaminoglycans
GFPuv Green Fluorescent Protein Variant
GW Glycine-Tryptophan Dipeptide

H
HBMEC Human Brain Microvascular Endothelial Cell
HGF/SF Hepatocyte Growth Receptor/Scatter Factor
HPLC High Pressure Liquid Chromatography
HSPG Heparan Sulphate Proteoglycans
Hsp60 Heat Shock Protein 60

I
IgG Immunoglobulin G
IPTG Isopropyl-1-Thio-β-D-Galactopyranoside
I.V. Intravenous

L
LA Lipoic Acid
LB Luria-Bertani
LBMOPS Luria-Bertani (LB) Broth Containing MOPS
LIPI-1 *Listeria* Pathogenicity Island 1
LM *Listeria monocytogenes*
LRR Leucine-Rich Repeat
LTA Lipoteichoic Acid

M
MB Methylene Blue
MEM Minimal Essential Medium
ML *Micrococcus lysodeikticus*
MOI Multiplicity of Infection
MOPS Morpholinepropanesulfonic Acid
MS Mass Spectrometry

N
NAG or **GlcNAc** N-Acetyl Glucosamine
NAM or **MurNAc** N-Acetyl Muramic Acid

NEAA Non-Essential Amino Acids
Ni-NTA Ni-Nitrilotriacetic Acid

O
OD Optical Density
ORF Open Reading Frame

P
PBS Phosphate Buffered Saline
PBS-CC PBS Containing Proteinase Inhibitor Cocktail and Chloramphenicol
PCR Polymerase Chain Reaction
PDH Pyruvate Dehydrogenase
PFO Perfringolysin O
PG Peptidoglycan
pI Isoelectric Point
PI-PLC Phosphatidylinositol-Specific PLC
PI 3-Kinase Phosphoinositide 3-Kinase
PLC Phospholipase C
PLY Pneumolysin
PMSF Phenylmethylsulfonylfluoride

R
RαIspC Rabbit Antiserum Raised Against Purified Recombinant IspC Protein
RαK Rabbit Antiserum from Rabbit Immunized with Heat-Killed *L. monocytogenes* Serotype 4b
RαL Rabbit Antiserum from Rabbit Infected with Live *L. monocytogenes* Serotype 4b
rIspC Recombinant IspC Protein
RT-PCR Reverse Transcription-PCR

S
SCP Sheep Choroid Plexus
SDS-PAGE Sodium Dodecyl Sulfate Polyacrylamide Gel Electrophoresis
SP Signal Peptide

T
TAE Tris-Acetate-EDTA
TCA Trichloroacetic Acid
TEM Transmission Electron Microscopy
TSBA Tryptic Soy Sheep Blood Agar

V

VASP Vasodilator-Stimulated Phosphoprotein

W
WB Western Blot
WASP Wiskott-Aldrich Syndrome Protein
WT Wild Type

X
X-gal 5-Bromo-4-Chloro-3-Indolyl-β-D-Galactopyranoside

LIST OF FIGURES AND TABLES

CHAPTER I

Literature Review

1.1 *Listeria monocytogenes* and the Disease

The genus *Listeria*, closely related phylogenetically to *Bacillus, Clostridium, Enterococcus, Streptococcus*, and *Staphylococcus*, consists of a group of Gram-positive, facultative anaerobic, motile, rod-shaped bacteria of 0.4 by 1 to 1.5 μm that do not form spores and have no capsule or fimbriae (Vazquez-Boland et al., 2001). Among the six known *Listeria* spp., i.e., *L. monocytogenes, L. ivanovii, L. seeligeri, L. innocua, L. welshimeri*, and *L. grayi*, only *L. monocytogenes* and *L. ivanovii* are pathogenic (Vazquez-Boland et al., 2001). *L. monocytogenes* can cause a disease referred to as listeriosis in both humans and animals whereas *L. ivanovii* is principally associated with animal disease and causes only extremely rare cases of infection in humans (Snapir et al., 2006; Vazquez-Boland et al., 2001).

Epidemiological investigation of major outbreaks and sporadic cases have demonstrated that human listeriosis is most frequently acquired by consumption of food products contaminated with *L. monocytogenes* (Davies et al., 1984; Fleming et al., 1985; Gottlieb et al., 2006; Kvenberg, 1988; MacDonald et al., 2005; Makino et al., 2005; Mead et al., 2006). After ingestion of contaminated foods, the offending bacteria cross the intestinal barrier and then rapidly translocate to the primary target organs such as mesenteric lymph nodes, spleen, and liver (Marco et al., 1992a; Vazquez-Boland et al., 2001). Most of the organisms are captured and killed by resident macrophages in the liver and spleen (Armstrong and Sword, 1966; Conlan and North, 1991; Conlan and North, 1992; Cousens and Wing, 2000; Ebe et al., 1999; Lepay et al., 1985; Mackaness, 1962; Mandel and Cheers, 1980). Three major factors, the host immune response, the amount of bacteria ingested, and the virulence of a strain determine the subsequent development of listerial infection (Vazquez-Boland et al., 2001). If infection is not efficiently controlled at this stage, surviving bacteria not only replicate in

macrophages themselves but also infect and grow extensively in adjoining hepatocytes in the liver and eventually cause systemic infection in secondary target organs, in particular, the brain and/or the placenta and fetuses via hematogenous dissemination (Berche et al., 1988; Conlan and North, 1992; Hof et al., 1997; Mackaness, 1962; Mandel and Cheers, 1980; Vazquez-Boland et al., 2001). Listeriosis is characterized by a number of clinical symptoms including meningitis, meningoencephalitis, septicaemia, abortion, stillbirth, and gastroenteritis (Vazquez-Boland et al., 2001). The pregnant women, the elderly, neonates, and the immunocompromised individuals are more susceptible to listerial infection (Lyytikainen et al., 2000). Despite the low incidence of listeriosis (about 2-8 cases annually per million population in Europe and the United States), the disease has a high mortality rate (20% to 30%) (Farber and Peterkin, 1991; Rocourt et al., 2000; Vazquez-Boland et al., 2001), rendering *L. monocytogenes* the leading cause of death amongst food-borne bacterial pathogens.

L. monocytogenes is widespread in nature and can be isolated from a variety of environmental sources such as water, soil, decomposing plants, faeces of humans and animals, and a diversity of raw or "ready-to-eat" foods (Vazquez-Boland et al., 2001). It can grow in a wide range of pH (4.3–9.6) and temperature (-1.5–50 °C), and tolerate severe conditions such as high salt concentrations (10% NaCl) and freezing and drying (Donnelly, 2001), thus rendering *L. monocytogenes* a difficult organism to be eliminated from the food chain. Of 13 serotypes of *Listeria* recognized to date, only three serotypes 4b, 1/2a, and 1/2b, are responsible for almost all human infections (Donnelly, 2001; Hearty et al., 2006; Lorber, 1997; Vines and Swaminathan, 1998). *L. monocytogenes* serotype 1/2a strains are the predominant ones recovered from foods or food processing plants, whereas serotype 4b strains account for almost all major outbreaks of listeriosis and a large portion of sporadic

cases (Buchrieser, 2007; Nelson et al., 2004; Rocourt and Bille, 1997). These observations suggest that there are differences in pathogenic potential among different strains in causing human infections and in their ability to survive and grow in diverse environmental niches.

Recently, the genome sequences have been determined and annotated (Glaser et al., 2001; Hain et al., 2006; Nelson et al., 2004) for four pathogenic *L. monocytogenes* strains, two serotype 1/2a strains EGD-e (GenBank/EMBL accession number AL591824) and F6854 (DDBJ/GenBank/EMBL accession number AADQ00000000) and two serotype 4b strains H7858 (DDBJ/GenBank/EMBL accession number AADR00000000) and F2365 (DDBJ/GenBank/EMBL accession number AE017262), and two strains of nonpathogenic *Listeria species L. innocua* serotype 6a Clip11262 (GenBank/EMBL accession number AL592022) and *L. welshimeri* serotype 6b SLCC5334 (EMBL accession number AM263198). The complete genome sequences of four *L. monocytogenes* strains (EGD-e, F6854, H7858, F2365) are 2,893,921 to 2,953,211 bp in size with an average G+C content of 38% and 2847 to 3024 known and predicted protein-coding genes (Buchrieser, 2007). The *L. innocua* CLIP11626 genome has a similar size of 3,011,209 bp with a G+C content of 37.4% and 2973 known and predicted protein-coding genes (Buchrieser, 2007). *L. welshimeri* has the smallest *Listeria* genome sequenced to date of 2,814,130 bp with a slightly lower G+C content of 36.4% and 2780 known and predicted protein-coding genes (Hain et al., 2006). Phylogenetic analyses show that *L. monocytogenes* has a closer relationship to *L. innocua* than to *L. welshimeri* (Hain et al., 2006; Schmid et al., 2005). Among the ~2800 known and predicted protein-coding genes in the *Listeria* genomes sequenced, ~40% of them could not be assigned putative functions and those that have been assigned putative functions require biochemical conformation (Nelson et al., 2004). Comparative genomic analyses of *L. monocytogenes*, *L. innocua*, and *L. welshimeri* (Buchrieser, 2007; Glaser et al., 2001; Hain et

al., 2006; Nelson et al., 2004) reveals a strong overall conservation of synteny, the core gene set for the three listerial species, and a set of serotype- and strain-specific genes. Further in-depth studies in the postgenomic era are necessary to unveil the functions of these predicated protein-coding genes and their products, which will help increase our understanding of the biology, ecology and virulence of *L. monocytogenes* and evolution of the *Listeria* genus.

1.2 Intracellular Life Cycle

L. monocytogenes has a multi-step complex intracellular life cycle involving entry, escape from phagosome, intracytosolic multiplication, actin-based intracellular movement, and direct cell-to-cell spread (Tilney and Portnoy, 1989). Figure 1-1 illustrates the infection life cycle for *L. monocytogenes* and the virulence factors involved. *L. monocytogenes* is capable of entry into both professional phagocytes like macrophages via phagocytosis and nonprofessional phagocytic cells such as epithelial cells, endothelial cells, hepatocytes, and fibroblasts through induced phagocytosis (Dramsi et al., 1995; Drevets et al., 1995; Gaillard et al., 1987; Kuhn, 1998; Mackaness, 1962; Racz et al., 1970; Racz et al., 1973). These observations suggest that multiple invasins of *L. monocytogenes* are involved in mediating bacterial invasion into different types of eukaryotic cells. Two well studied internalins, InlA and InlB, mediate entry into host cells by their interactions with specific cell receptors (Braun et al., 2000; Dramsi et al., 1995; Gaillard et al., 1991; Mengaud et al., 1996). Other surface-exposed proteins such as ActA, p60, Ami, and LAP were also reported to be involved in adhesion (Alvarez-Dominguez et al., 1997; Jaradat et al., 2003; Milohanic et al., 2001; Pandiripally et al., 1999; Park et al., 2000; Wampler et al., 2004). Following internalization, bacteria are transiently (~30 min) entrapped in a primary single membrane

FIG. 1-1. Schematic representation of the infection life cycle for *L. monocytogenes*. The life cycle begins with the adherence of *L. monocytogenes* to the cell surface of eukaryotic cells (1). *L. monocytogenes* is capable of entry into both professional phagocytes via phagocytosis and nonprofessional phagocytic cells through induced phagocytosis. Several bacterial factors (e.g., InlA, InlB, Ami, Auto, ActA, p60, and p104) are involved in bacterial invasion into various types of nonprofessional phagocytic cells. Following internalization, bacteria are transiently entrapped in a primary single membrane phagocytic vacuole or phagosome, an adverse, growth-limiting, low-pH compartment (2). The membrane of the phagosome is lysed by the pore forming toxin listeriolysin O (LLO) along with two phospholipases C (PlcA and PlcB) (3), thereby allowing bacteria to escape into the growth-permissive host cytosol. Once in the cytosol, the surviving bacteria begin to rapidly replicate (4). Concomitantly, the bacterial surface protein ActA recruits and polymerizes host cell actin molecules and other cytoskeletal proteins to form a comet-like tail at one pole of the bacterium which propels bacterial intracellular movement and intercellular spread (5). A randomly moving bacterium reaches the cytoplasmic membrane and induces the formation of a finger-like protrusion or filopodia with the bacterium at the tip and the actin tail behind (6), which is subsequently engulfed by a neighboring cell giving rise to a secondary double membrane phagosome, with the inner membrane originating from the previously infected cell and the outer one from the newly infected cell (7). Bacteria rapidly escape into the host cell cytosol after dissolution of the newly formed double membrane phagosome mediated by LLO, PlcA, and PlcB (8) and then initiate a new round of infectious cycle. The virulence factors involved are indicated at each step.

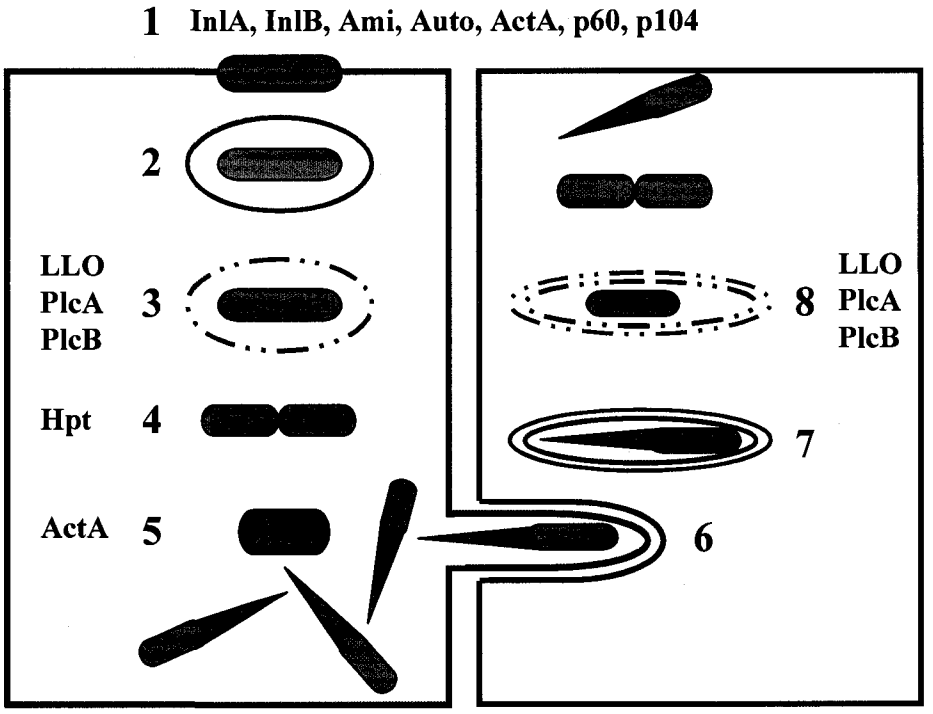
1 InlA, InlB, Ami, Auto, ActA, p60, p104
2
LLO
PlcA
PlcB
3
Hpt
4
ActA
5
6
7
8
LLO
PlcA
PlcB

phagocytic vacuole or phagosome, an adverse, growth-limiting, low-pH compartment (de Chastellier and Berche, 1994). Escape into the growth-permissive cytosol requires the lysis of the membrane by the pore-forming toxin listeriolysin O (LLO) together with two phospholipases C (PlcA and PlcB) (Alberti-Segui et al., 2007; Armstrong and Sword, 1966; Camilli et al., 1993; Gaillard et al., 1987; Grundling et al., 2003; Marquis et al., 1997; Portnoy et al., 1988; Raveneau et al., 1992; Vazquez-Boland et al., 1992). Once in the cytosol, surviving bacteria begin to rapidly replicate. Hpt, a hexose phosphate translocase is required for efficient intracytosolic proliferation of *L. monocytogenes* (Chico-Calero et al., 2002). Concomitantly, the bacterial surface protein ActA recruits and polymerizes host cell actin molecules and other cytoskeletal proteins to form a comet-like tail at one pole of the bacterium, which propels bacterial intracellular movement and intercellular spread (Dabiri et al., 1990; Pistor et al., 1995; Temm-Grove et al., 1994; Tilney and Portnoy, 1989). A randomly moving bacterium reaches the cytoplasmic membrane and induces the formation of a finger-like protrusion or filopodia with the bacterium at the tip and the actin tail behind, which is subsequently engulfed by a neighboring cell giving rise to a secondary double membrane phagosome, with the inner membrane originating from the previously infected cell and the outer one from the newly infected cell (Monack and Theriot, 2001; Tilney and Portnoy, 1989). Bacteria rapidly (within 5 min) escape into the host cell cytosol after dissolution of the newly formed double membrane phagosome mediated by LLO, PlcA, and PlcB and then initiate a new round of infectious cycle (Cossart et al., 2003; Greiffenberg et al., 2000). Thus, once *Listeria* has entered the host cytosol, it can spread directly from cell to cell without entry into the extracellular environment in which host defense factors such as antibodies, complements and immune cells (e.g., neutrophils) are present.

1.3 Virulence Factors

Several surface-exposed or secreted proteins of *L. monocytogenes* have been identified to be important for virulence and are involved in the intracellular life cycle at different steps (Cabanes et al., 2002; Dussurget et al., 2004; Vazquez-Boland et al., 2001). The genes coding for all known major virulence factors including *inlA, inlB, prfA, plcA, hly, mpl, actA, plcB*, and *hpt* are absent from the nonpathogenic *L. innocua* and *L. welshimeri* (Buchrieser, 2007).

1.3.1 InlA and InlB

The genetic locus (i.e., the *inlAB* operon) coding for two major internalins InlA and InlB was originally identified by screening a bank of transposon mutants of *L. monocytogenes* defective in invasiveness into the human enterocyte-like epithelial cell line Caco-2 (Dramsi et al., 1995; Gaillard et al., 1991). InlA and InlB belong to a large internalin family characterized by the presence of tandem leucine-rich repeats (LRRs), a domain involved in protein-protein interactions (Cabanes et al., 2002; Glaser et al., 2001; Vazquez-Boland et al., 2001). Several lines of evidence indicate that InlA and InlB are necessary and sufficient for bacterial internalization into host specific cells (Dramsi et al., 1995; Gaillard et al., 1991): (i) Mutants lacking InlA or InlB are almost noninvasive and complementation with the wild type allele restores the invasiveness (Dramsi et al., 1995; Gaillard et al., 1991), (ii) Heterologous expression of InlA or InlB confers invasive phenotype to normally noninvasive bacteria such as *L. innocua* (InlA and InlB), *Enterococcus faecalis* (InlA) or *Staphylococcus carnosus* (InlB) (Braun et al., 1998; Gaillard et al., 1991; Lecuit et al., 1997), and (iii) Coating of noninvasive bacteria or inert latex beads with purified InlA or InlB lead to internalization into mammalian cells (Braun et al., 1998; Lecuit et al., 1997). By infection of different eukaryotic cells with *inlA* or *inlB* deletion mutants, Dramsi *et al.* (1995) first demonstrated that InlA and InlB had different cell tropism, i.e., InlA but not InlB was

necessary and sufficient to trigger entry of *L. monocytogenes* into Caco-2 cells, whereas InlB but not InlA was required for entry into cultured murine hepatocyte ATCC T1B73. In the human hepatocye cell line HepG-2, both InlA and InlB are required for internalization (Dramsi et al., 1995). Invasion of human brain microvascular endothelial cells (HBMEC) by *L. monocytogenes* is dependent on InlB but not InlA (Greiffenberg et al., 1998). Increasing evidence shows that InlA has a restricted cell tropism in that it triggers entry into epithelial cells expressing the receptor E-cadherin (Vazquez-Boland et al., 2001). In contrast, InlB has a much broader host cell spectrum including hepatocytes, fibroblasts, certain epithelial cells, and endothelial cells (Braun et al., 1998; Braun et al., 1999; Dramsi et al., 1995; Greiffenberg et al., 1998; Shen et al., 2000). Although many studies have provided clear evidence that InlA and InlB play an essential role in bacterial entry into host cells, *L. monocytogenes* mutants lacking InlA and/or InlB still retain significant residual level of invasiveness in both *in vitro* cultured cells and *in vivo* animal models (Domann et al., 1997; Dramsi et al., 1995; Drevets et al., 1995; Gaillard and Finlay, 1996; Gaillard et al., 1996; Gregory et al., 1996; Greiffenberg et al., 1998; Lingnau et al., 1995; Mengaud et al., 1996). This suggests that other virulence factors are also important in invasion of host cells by *L. monocytogenes*.

InlA is an 80-kDa surface protein of 744 amino acid (Gaillard et al., 1991). It possesses an N-terminal Cap region followed by two repeat regions which are separated by an inter-repeat region (IR). The first, designated region A, consists of a succession of fifteen 22-amino acid LRRs. The second, designated region B, is made up of three repeats, two of 70 amino acids and one of 49 amino acids. InlA has a conserved cell wall anchoring LPXTG motif at the C-terminus preceeding a hydrophobic membrane spanning region of ~ 20 amino acids and a short positively charged tail of 7 amino acids (Gaillard et al., 1991). The sortase

SrtA of *L. monocytogenes* is responsible for covalent anchoring of InlA to cell wall peptidoglycan (Bierne et al., 2002; Dhar et al., 2000; Garandeau et al., 2002).

E-cadherin, the host receptor for InlA, is a transmembrane glycoprotein which was identified from Caco-2 cell extracts by InlA-coupled affinity chromatography (Cossart and Lecuit, 1998; Geiger and Ayalon, 1992; Lecuit et al., 1997; Mengaud et al., 1996). In polarized epithelial cells, E-cadherin is mainly expressed at the adhesion junctions and on the basolateral face and mediates calcium-dependent intercellular adhesion through homophilic interactions between extracellular domains (Cossart and Lecuit, 1998). E-cadherin contains five extracellular, immunoglobulin (Ig)-like domains (EC1-5), a transmembrane domain, and a cytoplasmic domain (Lecuit et al., 1999). Upon binding of InlA to the first ectodomain of human E-cadherin (hEC1), the cytoplasmic domain of E-cadherin interacts with cytoplasmic catenins, which in turn link to the host actin cytoskeleton leading to actin cytoskeleton rearrangements and ultimate internalization of *L. monocytogenes* (Lecuit et al., 2000; Schubert et al., 2002). Functional studies showed that the N-terminal LRR and IR regions were necessary and sufficient for InA-mediated entry (Lecuit et al., 1997). The InlA-E-cadherin interaction is species specific; InlA recognizes and activates human and guinea pig E-cadherins but not mouse and rat E-cadherins (Lecuit et al., 1999; Mengaud et al., 1996). Studies using transgenic mice expressing the human E-cadherin in intestine and guinea pigs expressing a functional E-cadherin established the role of InlA in crossing of the intestinal epithelial barrier *in vivo* (Lecuit et al., 2001). Epidemiological findings by Jacquet *et al.* (2004) suggested a role of InlA-E-cadherin interaction in maternofetal listeriosis. Further experimental studies, including immunohistopathological studies of placentas from woman with listeriosis and infection of human trophoblast cell line (BeWo), primary cultures of human cytotrophoblasts, and human placental villous explants with WT and *inlA*⁻ mutant

strains of *L. monocytogenes* and WT and InlA-expressing strains of *L. innocua*, established that the interaction of InlA and E-cadherin at the trophoblast barrier level conferred the ability of *L. monocytogenes* to target and cross the human maternofetal barrier (Lecuit et al., 2004). Lecuit *et al.* (1999) using domain swapping and mutagenesis experiments identified a key residue at position 16 in E-cadherin that is responsible for such host specificity: a proline in functional human and guinea pig E-cadherins in contrast to a glutamic acid in nonfunctional mouse and rat E-cadherins. Mutagenesis and analytical ultracentrifugation analyses have shown that the Pro 16 of hEC1 is essential for intermolecular recognition and *in silico* structural analysis indicated that a substitution of a Glu residue for Pro16 would both sterically and by hydrophilic/charge effects prevent a close approach of InlA and E-cadherin (Schubert et al., 2002).

InlB is a 67-kDa surface protein of 630 amino acids with the N-terminal part containing a domain organization similar to that of InlA. An N-terminal signal peptide, an N-terminal Cap region, eight LRRs, an IR region, and one B repeat are present in the N-terminal part of InlB (Dramsi et al., 1995; Gaillard et al., 1991). Unlike InlA, InlB has a C-terminal 232-amino acid cell wall binding domain (CWBD) comprising three tandem repeats (GW modules) of ~80 amino acids each beginning with a conserved glycine-tryptophan (GW) dipeptide, which dissociably anchors the protein to the surface by binding the cell wall component lipoteichoic acid (LTA) (Braun et al., 1997; Jonquieres et al., 1999).

Three mammalian host receptors have been identified for InlB, the Met receptor protein tyrosine kinase whose endogenous ligand is hepatocyte growth receptor/scatter factor (HGF/SF) (Braun et al., 1998; Braun et al., 1999; Dramsi et al., 1995; Greiffenberg et al., 1998; Shen et al., 2000), glycosaminoglycans (GAGs) (Jonquieres et al., 2001) and the receptor of the globular part of the complement component C1q (gC1q-R) (Braun et al.,

2000). InlB-Met interaction stimulates protein tyrosine phosphorylation and phosphoinositide (PI) 3-kinase activity and ultimately induces actin cytoskeleton rearrangements required for invasion into target mammalian cells such as Vero, Hep-2, and Hela by *L. monocytogenes* (Braun et al., 1998; Gaillard et al., 1987; Ireton et al., 1996; Ireton et al., 1999; Tang et al., 1994; Velge et al., 1994). InlB activates the Met receptor through its LRR and IR domains binding to the receptor (Braun et al., 1999; Freiberg et al., 2004). Like InlA, InlB exhibits host receptor tropism, as InlB interacts with the Met isoforms from humans and mice but not with those from guinea pigs or rabbits (Khelef et al., 2006; Lecuit et al., 1999). Inhibition experiments show that invasion of HBMEC by *L. monocytogenes* is independent of PI 3-kinase, although InlB is required for efficient infection of this cell line (Greiffenberg et al., 1998). This suggests that there are other invasion mechanisms by which InlB mediates bacterial entry. InlB is able to interact with the receptors GAG and gC1q-R through its C-terminal GW modules, further facilitating bacterial internalization mediated by InlB-Met interaction (Braun et al., 2000; Jonquieres et al., 2001).

The crystal structures of the Cap/LRR/IR-domain of InlA in a functional complex with hEC1 (Schubert et al., 2002), the Cap/LRR-domain of InlB (Marino et al., 1999), the Cap/LRR/IR-domains of InlB and InlH (Schubert et al., 2001) reveal a common structure in the N-terminal parts of InlA, InlB and InlH. Three distinct contiguous N-terminal domains in InlA, InlB, and InlH, the N-terminal truncated EF-hand-like cap, the central LRR region, and the immunoglobulin (Ig)-like IR region, constitute a single structural domain referred to as "internalin" domain (Schubert et al., 2002). Each LRR begins with a β strand of five residues followed by a seven-residue loop, a five-residue 3_{10}-helix, and a second five-residue loop (Marino et al., 1999; Schubert et al., 2001; Schubert et al., 2002). The LRR repeats fold into an arc shape with a parallel β-sheet on the concave face and with a 3_{10}-helix on the convex

face (Marino et al., 1999; Schubert et al., 2001; Schubert et al., 2002). The concave face of LRR domain forms the interaction interface with the hEC1 of human E-cadherin for InlA (Schubert et al., 2002) and with the first Ig-like domain (this domain does not bind HGF/SF) of the Met receptor for InlB (Niemann et al., 2007). Obviously, InlB is not a structural mimic of the endogenous ligand HGF/SF for Met. The IR region of InlA is proposed to be involved in folding of the LRR domain, which has been shown to be essential for InlA-directed invasion (Lecuit et al., 1997). The IR region plays a role in providing the *in vivo* stability of InlB (Freiberg et al., 2004).

The crystal structure of the full-length InlB has been solved. It is an elongated molecule of "L" shape in which the N-terminal Cap and LRR domain form the short arm of the "L" and the IR region projects at nearly a right angle from the base of the LRR (Marino et al., 2002). The C-terminal three GW modules form the long arm which are mainly composed of β-strands (Marino et al., 2002; Schubert et al., 2001). The surface of the GW domains is primarily basic and may thus partially account for binding of InlB to its three acidic receptors (i.e., LTA, GAG heparin, and gC1q-R) through ionic interactions (Marino et al., 2002). A small hydrophobic groove located between the first and second GW modules is thought to likely contribute to the binding specificity of InlB with gC1q-R (Marino et al., 2002). The second and third GW modules pair with an interface involving several conserved hydrophobic residues and one conserved hydrogen bond (Marino et al., 2002). However, the first GW module of InlB does not pair with the other two GW modules, which may explain its susceptibility to proteolysis (Marino et al., 2002).

1.3.2 p104/LAP

A 104-kDa surface protein (p104 or LAP) of *L. monocytogenes* is capable of mediating bacterial adherence to Caco-2 cells, as demonstrated by transposon insertion mutagenesis

and antibody inhibition studies (Jaradat et al., 2003; Pandiripally et al., 1999). Proteins cross reactive with anti-p104 antibody are present in all *Listeria* spp. except *L. grayi*. Sequence analysis reveals that LAP is a putative alcohol acetaldehyde dehydrogenase (Aad) (Kim et al., 2006). Using a LAP-deficient transposon mutant, Jaradat *et al.* (2003) further showed that LAP-mediated attachment is restricted to specific intestinal epithelial cells. The mutant showed significantly reduced adherence to human intestinal cells originating from the lower part of small intestine (ileum-cecum, HCT-8) and the upper part of the large intestine (colon, Caco-2 and HT-29) but not to other intestinal cell lines stemming from the upper part of the small intestine (duodenum, HuTu-80 or jejunum, Int-407) nor to a variety of nonintestinal cell lines derived from liver, kidney, bladder, ovary, cervix, breast, larynx, or skin (Jaradat et al., 2003). The LAP-deficient mutant was unable to translocate to the liver in a mouse model of oral inoculation, contrasting the results obtained with intraperitoneal administration that bypassed the intestinal barrier (Jaradat et al., 2003). These data indicate that LAP is an additional adhesion factor that is specifically involved in intestinal phase of *L. monocytogenes* infection. Hsp60 (heat shock protein 60), a chaperonin assisting in protein folding and being constitutively expressed in many normal cells and upregulated under stressful conditions, was identified as a host receptor for LAP in Caco-2 cells by using a ligand overlay assay (Wampler et al., 2004).

1.3.3 Listeriolysin O and two phospholipases C

L. monocytogenes is entrapped in two distinct phagosomes during the entire intracellular life cycle: the primary single membrane phagosome formed upon entry and the secondary double membrane phagosome formed upon spreading into neighbouring cells. Disruption of the phagosomal membrane is essential for bacterial intracellular survival and replication and is mediated by three bacterial secreted proteins LLO, PlcA and PlcB. These proteins are

encoded by the corresponding genes *hly*, *plcA* and *plcB* residing in the *Listeria* pathogenicity island 1 (LIPI-1), respectively. The relative importance of LLO, PlcA and PlcB for primary and secondary phagosomal lysis is dependent on cell types and origin of cells.

The 58-kDa LLO (Geoffroy et al., 1987) is the first identified virulent factor in *L. monocytogenes* belonging to a family of pore-forming, cholesterol-dependent cytolysins (CDCs) produced by diverse species of pathogenic Gram-positive bacteria, including pneumolysin (PLY) from *Streptococcus pneumoniae*, streptolysin from *S. pyogenes*, and perfringolysin O (PFO) from *Clostridium perfringens* (Goebel et al., 1988; Kathariou et al., 1987). LLO has unique biochemical properties in comparison to other known non-*Listeria* CDCs. *Listeria* LLO is active at acidic pH with an optimum pH of 5.5 and nearly inactive at neutral or alkaline pH, in contrast to other cholesterol-dependent cytolysins of extracellular bacterial pathogens that are active over a broad pH range from 4.5 to 8.5 (Geoffroy et al., 1987; Nomura et al., 2007). By swapping dissimilar residues from a pH-insensitive orthologue PFO, Glomski *et al.* (2003) identified Leu 461 as being unique to LLO and responsible for the acidic pH optimum of LLO. As typically found in CDCs, a highly conserved Trp-rich undecapeptide sequence, 483ECTGLAWEWWR493, was present at the C-terminus of LLO. Conversion of Cys 484 in this undecapeptide to alanine by site-directed mutagenesis resulted only in minor (25%) loss of hemolytic activity (Michel et al., 1990). In contrast, replacement of the hydrophobic residues Trp 491 and Trp 492 dramatically decreased hemolytic activity by 95% and 99.9%, respectively, indicating tryptophan residues in this undecapeptide are more critical for the hemolytic activity of LLO (Michel et al., 1990). There is a high degree of sequence identity (40-70%) between CDCs which have a common mode of action, i.e., binding to their receptor cholesterol present in the lipid membranes and then forming via oligomerization ring-shaped transmembrane pores with a diameter of 30-35

nm comprising 30-50 subunits; this leads to membrane disruption (Jacobs et al., 1998; Rossjohn et al., 1997; Tilley et al., 2005). Electron microscopy of erythrocyte ghosts treated with LLO showed characteristic arc- and ring-shaped structures as described for other toxins of this family (Jacobs 1998). The crystal structure of PFO in water-soluble, monomeric state reveals that the protein is an elongated, rod-shape molecule rich in β-sheet (Rossjohn et al., 1997). PFO is comprised of four discontinuous domains with domain 4 responsible for cholesterol binding which induces conformational changes, oligomerization and pore formation (Czajkowsky et al., 2004; Heuck et al., 2007; Ramachandran et al., 2005; Rossjohn et al., 1997). There are no significant hydrophobic patches on the surface or in the domain interfacial regions (Rossjohn et al., 1997). Given that there is high similarity in amino acid sequence and function between LLO and PFO (Rossjohn et al., 1997), LLO may be similar in structure to PFO.

The role of LLO in virulence has long been suggested and established by a number of studies. There is a strong correlation between hemolytic activity and pathogenicity, i.e., virtually all virulent strains of *L. monocytogenes* from natural infections are hemolytic whereas nonhemolytic *Listeria* strains are avirulent (Groves and Welshimer, 1977; Rocourt et al., 1983; Skalka et al., 1982). *L. monocytogenes* LLO injected intravenously into mice caused rapid lethality (Geoffroy et al., 1987; Kingdon and Sword, 1970) and exhibited cytotoxicity toward various mammalian cells *in vitro* (Groves and Welshimer, 1977; Kingdon and Sword, 1970; Siddique, 1969; Watson and Lavizzo, 1973). Direct evidence for the involvement of LLO in *L. monocytogenes* virulence was obtained from transposon mutagenesis and complementation studies. Nonhemolytic mutants were unable to grow in host tissues and rapidly eliminated from infected mice and the revertant strains regained hemolytic activity and virulence (Berche et al., 1987; Cossart et al., 1989; Dabiri et al., 1990;

Gaillard et al., 1986; Goebel et al., 1988; Kathariou et al., 1987; Kuhn et al., 1988; Mengaud et al., 1989; Portnoy et al., 1988). Armstrong and Sword (1966) observed with electron microscopy the breakdown of bacteria-containing vacuolar membrane in splenic tissues from mice infected with *L. monocytogenes* and proposed that this membrane dissolution was associated with LLO production. Subsequent studies using various cultured eukaryotic cells demonstrated that LLO was absolutely required for escape from both primary and secondary phagosomes in murine-derived cells, but was dispensable in some human cell lines (Alberti-Segui et al., 2007; Grundling et al., 2003; Portnoy et al., 1988; Vazquez-Boland et al., 2001). Studies with LLO^- mutants showed that bacteria were retained in the intact primary phagosome and unable to replicate in various cultured murine cells (Berche et al., 1987; Cossart et al., 1989; Gaillard et al., 1986; Kuhn et al., 1988; Portnoy et al., 1988). Phagosomal escape of the wild type *L. monocytogenes* within macrophages was inhibited by neutralizing monoclonal antibody to LLO (Edelson and Unanue, 2001). Interestingly, heterologous expression of LLO conferred upon the extracellular bacteria *Bacillus subtilis* and *E. coli* the ability to escape from phagosome (Bielecki et al., 1990; Monack and Theriot, 2001). Recently Alberti-Segui *et al.* (2007) investigated the role of LLO in the disruption of secondary spreading vacuoles using an LLO-inducible strain that was constructed by integrating the *hly* gene under the transcriptional control of an IPTG-inducible promoter into the chromosome of an LLO-negative *L. monocytogenes* mutant. Based on the findings from that study, they identified LLO as a key factor in the disruption of the outer membrane of the spreading vacuole and proposed that the two extracellular phospholipases C (PLC), PlcA and PlcB, were involved in the dissolution of the inner membrane (Alberti-Segui et al., 2007). The acidic pH within the vacuolar environment permits effective LLO dissolution of the phagosomal membrane for release of *L. monocytogenes* to the host cytosol, where the neutral

pH prevents the host cytoplasmic membrane from being damaged by LLO and thus bacteria from losing the replicative and protective niche.

PlcA is a 36-kDa phosphatidylinositol-specific PLC (PI-PLC) (Mengaud et al., 1991a; Vazquez-Boland et al., 1992). PlcB is a 29-kDa PLC (also known as PC-PLC and lecithinase) with a broad spectrum of substrates including phosphatidylcholine, phosphatidylethanolamine, phosphatidylserine, and sphingomyelin, but not phosphatidylinositol (Geoffroy et al., 1991). PlcB is synthesized as an inactive proenzyme that prevents bacterial membrane damage and is proteolytically activated by a secreted zinc metalloprotease encoded by *mpl* (Geoffroy et al., 1991; Raveneau et al., 1992). PlcA and PlcB are active over a broad pH range from pH 5.5 to 8.0 with a pH optimum of 5.5-7.0 and 6.0-7.0, respectively (Geoffroy et al., 1991; Goldfine and Knob, 1992). Evidence accumulated to date indicated that PlcA and PlcB are virulence factors required for phagosomal lysis (Camilli et al., 1993; Marquis et al., 1995; Smith et al., 1995; Vazquez-Boland et al., 1992). The egg yolk agar opacification (lecithinase activity) phenotype is closely associated with *L. monocytogenes* virulence (Coffey et al., 1996; Geoffroy et al., 1991). The role of PlcB in the lysis of secondary double membrane phagosomes was first established using a cultured cell model of infection with a *plcB* deficient mutant created by transposon mutagenesis (Vazquez-Boland et al., 1992). Smaller plaques are formed in fibroblast cell monolayers infected with PlcB-negative mutant bacteria (reflecting the impaired ability of bacteria to replicate intracellularly and to spread within the cell monolayer), many of which are sequestrated in the double-membrane vacuoles (Smith et al., 1995; Vazquez-Boland et al., 1992). The *plcA* gene was initially identified by screening of *L. monocytogenes* transposon mutants that produced small plaques in cell monolayers (Camilli et al., 1991; Sun et al., 1990). A *plcA* in-frame deletion mutant

exhibited a minor reduction in virulence and a delay in bacterial escape from the primary phagosome of bone marrow-derived macrophages but not from the secondary phagosome (Camilli et al., 1993; Smith et al., 1995). Furthermore, PlcA and PlcB appear to function synergistically since a double mutant lacking both phospholipases shows more deficiency in virulence in mice and more severe effect on escape from both the primary and the secondary phagosomes than the sum of the defects observed with the individual mutants (Smith et al., 1995). PlcB is necessary for phagosomal lysis in the human-derived Henle 407 epithelial cells while PlcA, like LLO, is dispensable, indicating that PlcB also mediates the lysis of the primary phagosome in these cells (Marquis et al., 1995). Data from these previous studies suggest that PlcA plays an accessory role independently of its catalytic function and acts in concert with LLO (Goldfine et al., 1995) and/or PlcB to achieve efficient escape from primary and secondary phagosomes.

1.3.4 ActA

The surface protein ActA, a virulence factor involved in actin-based intracellular motility of *L. monocytogenes*, was identified by searching for transposon mutants defective in actin polymerization (Kocks et al., 1992). The *actA*-deficient mutant was avirulent in a mouse infection model, consistent with the phenotypic observations that mutant bacteria grew locally as microcolonies in host cytosol and were unable to form actin tails and plaques on a fibroblast monolayer (Dabiri et al., 1990; Domann et al., 1992; Kocks et al., 1992; Mounier et al., 1990; Tilney and Portnoy, 1989).

The mature ActA of *L. monocytogenes* is a 610-amino acid protein with an apparent molecular mass of 90 kDa that is formed following the cleavage of a 29-amino acid N-terminal signal peptide from the 639-amino acid protein precursor (Kocks et al., 1993). The mature protein has three domains: a positively charged residue-rich N-terminal domain

(aa 1-234), a central region of proline-rich repeats (aa 235-396), and C-terminal domain (aa 395 to 610) with a highly hydrophobic region (aa 585-610) responsible for anchoring of the protein to the bacterial surface (Vazquez-Boland et al., 2001). ActA functionally mimics the eukaryotic Wiskott-Aldrich syndrome protein (WASP)-family of proteins that activate the actin filament nucleation function of the Arp2/3 complex (Cossart, 2000; Welch et al., 1998). Functional studies with various *actA* deletion constructs revealed that all the elements necessary for actin tail formation are located in the N-terminal and central regions (Lasa et al., 1995; Lasa et al., 1997; Marchand et al., 1995; Niebuhr et al., 1997; Smith et al., 1996; Vazquez-Boland et al., 2001). The N-terminal region (aa 129-153) is strictly required for actin assembly (Vazquez-Boland et al., 2001) while the other two N-terminal regions (aa 21-97 and aa 117-121) are crucial for the continuity of the actin tail formation and filament elongation, respectively (Lasa et al., 1997). The proline-rich repeats (aa 265-396) bind members of the Ena (Drosophila Enabled)/VASP (vasodilator-stimulated phosphoprotein) family that are dispensable for the initiation of actin assembly but required for the efficiency of the process (Chakraborty et al., 1995; Lasa et al., 1997; Laurent et al., 1999; Machner et al., 2001; Niebuhr et al., 1997; Pistor et al., 1995; Portnoy et al., 2002). Polar distribution of ActA on the bacterial surface is critical for actin tail formation, which requires an optimal balance between protein secretion, protein degradation, and bacterial cell wall growth (Rafelski and Theriot, 2005; Rafelski and Theriot, 2006).

Extracellularly, ActA also promotes attachment and entry of *L. monocytogenes* into host cells, evidenced by the fact that an ActA-deficient mutant was significantly impaired in attaching to and entering IC-21 murine macrophages and CHO epithelial-like cells (Alvarez-Dominguez et al., 1997). Work by Alvarez-Dominguez *et al.* (1997) demonstrated that attachment and entry of *L. monocytogenes* involves specific interaction with a GAG

heparan sulphate (HS) receptor on the surface of host cells and suggested that ActA is the bacterial surface protein mediating GAG receptor recognition (Alvarez-Dominguez et al., 1997). Suarez *et al.* (2001) further assessed the role of ActA in host cell invasion by constructing an *actA* in-frame deletion mutant strain from a *prfA** derivative of a *L. monocytogenes* serotype 4b strain in which a G145S substitution was introduced into PrfA, a transcriptional activator for a number of known virulence genes. The *prfA** strain locks the regulatory protein in its transcriptionally constitutively active form, leading to constitutive expression *in vitro* of all the PrfA-dependent genes or operons, including *actA* (Suarez et al., 2001). Studies with these strains showed that ActA contributed to bacterial internalization into epithelial cells (Caco-2, HeLa, MDCK and Vero) but not fibroblasts (COS-1) or hepatocytes (Hepa 1-6) (Suarez et al., 2001). Heterologous expression of ActA conferred invasiveness to the noninvasive *L. innocua* leading to bacterial internalization into epithelial cell lines but not fibroblasts or hepatocytes, indicating that ActA is a virulence factor involved in invasion and host cell tropism (Suarez et al., 2001). Infection of Caco-2 cells with the *prfA** strain showed evidence that ActA is required for remodeling microvilli on the apical surface to form pseudopods leading to active phagocytosis of the *prfA** strain (Suarez et al., 2001).

1.3.5 Hpt

Rapid cytosolic mutiplication of *L. monocytogenes* after escape from the phagosome allows the increase in the bacterial count within the host and represents a critical stage of the infectious life cycle. Using a gene in-frame deletion mutant, Chico-Calero *et al.* (2002) demonstrated that *L. monocytogenes* possesses a hexose phosphate transporter Hpt that promotes rapid intracellular replication in mammalian cells and that is necessary for full virulence in mice. *L. monocytogenes* Hpt is a bacterial homolog of the mammalian

glucose-6-phosphate translocase that mediates the transport of glucose-6-phosphate from the cytosol to the endoplasmic reticulum in the final step of gluconeogenesis and glycogenolysis. Loss of Hpt in the Δ*hpt* mutant had no effect on the *in vitro* growth of *L. monocytogenes* in broth and prevented the bacterium from utilizing carbon sources such as hexose phosphate (HP) sugars but not nonphosphate sugars (glucose). However, the Δ*hpt* mutant was impaired in intracellular growth in various eukaryotic cell types (Caco-2, HepG2 and J774) and proliferation and survival *in vivo* in mouse organs (liver and spleen). This finding indicates that Hpt is a "metabolic" virulence factor contributing to host tissue colonization (Chico-Calero et al., 2002).

Work by Chico-Calero *et al.* (2002) indicated that Hpt, the product of the *hpt* gene preceded by a PrfA box (the binding site of the transcriptional activator PrfA in target promoters), is responsible for the PrfA-dependent utilization of HP by *L. monocytogenes*. *In vivo* expression of Hpt under the tight control of PrfA allows *L. monocytogenes* to exploit HP from the host cytosol as a carbon source to facilitate intracellular growth (Chico-Calero et al., 2002). Heterologous expression of Hpt in nonpathogenic *L. innocua* did not lead to efficient intracytosolic replication, suggesting other yet unidentified factors are involved in the efficient cytosolic growth in addition to Hpt (Slaghuis et al., 2004). Comparative genomic analysis of *L. welshimeri* and *L. monocytogenes* revealed that 55 genes involved in carbohydrate transport and metabolism are absent from the nonpathogenic *L. welshimeri* (Hain et al., 2006) and may thus be potential determinants important for the efficient cytosolic growth of *L. monocytogenes*.

O'Riordan *et al.* (2003) identified an additional virulence factor lipoate protein ligase LplA1 important for intracellular growth of *L. monocytogenes*, as evidenced by the fact that

the Δ*lpl1* mutant is defective for intracellular replication and is less virulent in an intravenous mouse model of infection. LplA1 is responsible for lipoylation of the E2 subunit of pyruvate dehydrogenase (PDH) using host-derived lipoic acid (LA) (O'Riordan et al., 2003), which is required for the metabolic function of PDH for aerobic growth. Recently, Keeney *et al.* (2007) have further shown that LplA1 enables utilization of host-derived lipoyl peptides by *L. monocytogenes* as a source of lipoate to support the bacterial cytosolic growth and virulence (Keeney et al., 2007).

1.3.6 PrfA

L. monocytogenes infection is a complex process involving multiple key virulence factors (Fig. 1-2A) whose genes (e.g., *hly*, *plcA*, *plcB*, *hpt*, *mpl*, *actA*) are coordinately expressed under the control of the protein PrfA, a pleiotropic transcriptional activator belonging to the Crp (cAMP receptor protein)/Cap (catabolite gene activator protein)-Fnr (fumarate and nitrate reductase regulator) family of bacterial transcription factors (Milohanic et al., 2003; Sheehan et al., 1995). The *inlA-inlB* coding for the internalins InlA and InlB is partially regulated by PrfA (Sheehan et al., 1994). This positive regulatory factor is absolutely required for *L. monocytogenes* virulence, as the mutant carrying a deletion of the *prfA* gene is avirulent (Leimeister-Wachter et al., 1990).

PrfA is a 237-amino acid 27-kDa protein comprising (i) an N-terminal domain that provides most of the interface for PrfA dimerization, (ii) a hinge/interdomain region, and (iii) a C-terminal DNA-binding domain carrying the conserved helix-turn-helix (HTH) motif (Scortti et al., 2007). The PrfA homodimer activates transcription of target genes or operons by binding through its C-terminal HTH motif to a conserved 14-bp palindromic DNA sequence (PrfA box) centered near the position 41 bp 5' upstream of the transcriptional start sites. The PrfA box has a consensus sequence of tTAACanntGTtAa, with 7 invariant

FIG. 1-2. (A) Physical and transcriptional organization of known key virulence genes involved in the intracellular life cycle. These virulence genes are transcribed either individually from their own promoters or together as an operon from a common promoter. The *prfA* gene is the first gene in the LIPI-1 and its gene product is presumed to undergo an allosteric shift from weakly active (●) to highly active (◓) states upon interaction with a putative cofactor. The active form of PrfA binds to the PrfA boxes of the promoters of PrfA-dependent genes or operons and activates their transcription. PrfA-boxes, PrfA-dependent transcripts, and PrfA-independent transcripts are indicated by black rectangles (■), solid and dotted lines, respectively. **(B)** The PrfA boxes are centered near the position 41 bp 5' upstream of the transcriptional start sites and have a consensus sequence of tTAACanntGTtAa, with 7 invariant nucleotides (uppercases) and a two-mismatch tolerance (n, any nucleotides). Adapted from references (Chico-Calero et al., 2002; Scortti et al., 2007; Vazquez-Boland et al., 2001).

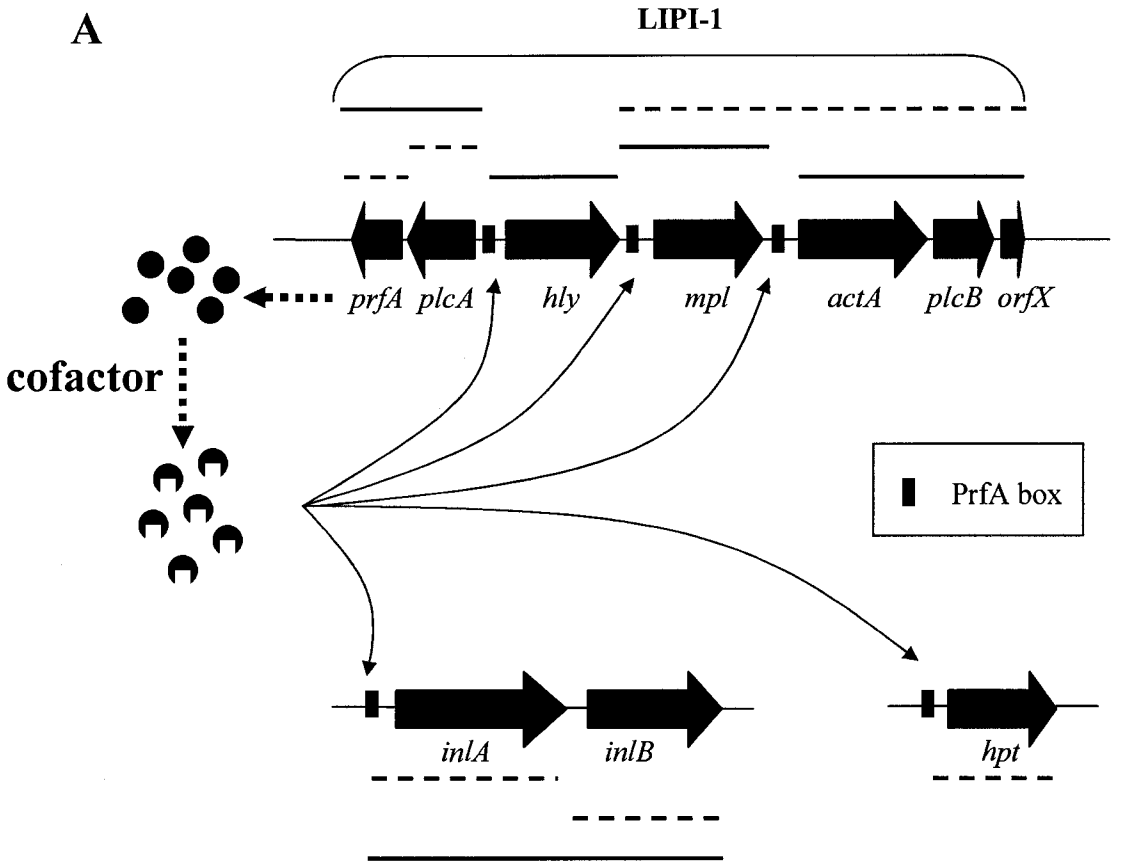

B

PrfA box

TTAACAAATGTTAA	***plcA***
TTAACAttTGTTAA	***hly***
TTAACAAATGTaAA	***mpl***
TTAACAAATGTTAg	***actA***
aTAACAtAaGTTAA	***inlAB***
aTAACAAGTGTTAA	***hpt***
TTAACAnnTGTTAA	**Consensus**

nucleotides (uppercase) and a two-mismatch tolerance (n, any nucleotide) (Bockmann et al., 2000; Bubert et al., 1999; Scortti et al., 2007; Sheehan et al., 1995; Vazquez-Boland et al., 2001) (Fig. 1-2B). The degree of symmetry of the PrfA boxes greatly influences PrfA-binding affinity and thus the efficiency of transcriptional activation, i.e., PrfA binds more strongly to the promoters with perfectly symmetrical palindromes (e.g., P*hly* and P*plcA*) than those having imperfect palindromic PrfA-binding sites (e.g., P*mpl*, P*actA*, and P*inlA*), thus allowing differential regulation of PrfA-dependent gene expression (Vega et al., 2004). In addition to that, the interspace sequences between or flanking sequences adjacent to the PrfA-box and the -10 Pribnow box (an essential consensus site for transcription to occur), two critical elements of PrfA-dependent promoters, have an effect on the functionality and efficiency of PrfA-dependent transcription (Luo et al., 2004; Luo et al., 2005; Mauder et al., 2006).

PrfA can regulate the level of PrfA-dependent gene expression primarily via two control mechanisms, i.e., the allosteric control of the DNA-binding activity of PrfA and the control of PrfA concentration in the bacterial cytosol (Scortti et al., 2007). Studies with the PrfA* mutants provide strong evidence to suggest that upon interaction with a putative cofactor, PrfA undergoes an allosteric shift from weakly active to highly active states (conformations) (Vega et al., 1998; Vega et al., 2004). Negative regulation of the PrfA activity has been suggested as a mechanism responsible for repression of PrfA-dependent gene expression (Scortti et al., 2007). The concentration of the PrfA protein is subjected to regulation at both transcriptional and translational levels. Transcription of the *prfA* gene is driven by three promoters: two promoters (P1*prfA* and P2*prfA*), located in the intergenic region immediately upstream of the *prfA* ORF, promote the synthesis of the monocistronic transcript and the third promoter (P*plcA*), situated upstream of the *plcA* gene, directs the generation of a

bicistronic *plcA-prfA* transcript (Scortti et al., 2007). The promoters P1*prfA* and P2*prfA* play a role in maintaining basal levels of *prfA* transcripts and thus a basal amount of the PrfA protein during normal bacterial growth. Synthesis of the PrfA protein from the P1*prfA*-directed *prfA* mRNA is thermoregulated through the "thermosensor" secondary structure present at the 5'untranslated region (5'-UTR) of the transcript that masks the ribosome binding site at low temperature (30 °C) and prevents PrfA translation. This thermosensor structure is destabilized (melts down) at high temperature (37 °C), allowing protein translation (Johansson et al., 2002). This is consistent with thermoregulated expression of PrfA-dependent virulence genes in *L. monocytogenes* (Leimeister-Wachter et al., 1992). The P*plcA* promoter is dependent on PrfA for generation of the bicistronic *plcA-prfA* transcript through which PrfA can stimulate its own synthesis by positive feedback (Chakraborty et al., 1992; Mengaud et al., 1991b). This suggests that any alteration in PrfA activity may lead to a change in the level of *prfA* expression. Studies with the mutational disruption of *plcA* to *prfA* readthrough transcription have shown evidence that the positive autoregulatory loop is essential for the synthesis of a sufficient amount of the PrfA protein for *L. monocytogenes* virulence (Camilli et al., 1993; Mengaud et al., 1991b).

1.4 Genetic Organization of Major Virulence Factors

All *L. monocytogenes* virulence genes identified to date are located on the chromosome. Figure 1-2A illustrates the physical and transcriptional organization of known key virulence genes involved in the intracellular life cycle. As found in other pathogenic bacteria, most virulence genes of *L. monocytogenes* are organized into discrete genetic units referred to as pathogenicity islands (Vazquez-Boland et al., 2001). Several virulence genes, including *prfA* required for the regulation of virulence gene expression and those involved in key steps of the intracellular life cycle (*plcA*, *hly*, *mpl*, and *plcB* for phagosomal escape, and *actA* for

bacterial intracellular movement and cell-to-cell spread), are physically clustered in a 9.6-kb region of the chromosome referred to as *Listeria* pathogenicity island 1 (LIPI-1) in the order of *prfA-plcA-hly-mpl-actA-plcB* (Gouin et al., 1994; Vazquez-Boland et al., 2001). The *inlAB* operon, encoding the internalins InlA and InlB, is situated at a separate locus outside LIPI-1 in the chromosome. The *hpt* gene, expressed under the tight control of PrfA (Goetz et al., 2001) and involved in bacterial intracellular multiplication, is located individually in the chromosome. Autolysins such as Auto and p60, recognized as virulence factors in *L. monocytogenes* (see Section 1.7.5) and independent of PrfA for their expression (Bubert et al., 1999; Cabanes et al., 2004), are each located in a separate region. Major virulence genes are transcribed either individually from their own promoters (e.g, *prfA*, *plcA*, *mpl*, *hly*, *inlB*) or together as an operon from a common promoter (e.g, the *inlAB* operon, the *plcA-prfA* operon, the *mpl-actA-plcB* operon).

1.5 Experimental Infection Models

Knowledge of *L. monocytogenes* infection and pathogenesis are mostly gained from studies with animal infection models, such as mice and guinea pigs, and cell culture infection models, such as those eukaryotic cell types that are normally encountered during listerial infection.

1.5.1 Animal models

Mouse. The mouse model remains one of the most attractive animal models because they are small, genetically highly similar (~80%) to humans, inexpensive, easily maintained, reproduce quickly, and physiologically and pathophysiologically in many respects comparable to humans. Moreover, a significant advantage of this model is the availability of a diversity of genetically modified transgenic mice, which allows the study of the roles of host factors in infection development and host defenses. Most of our knowledge and

understanding of listeriosis comes from numerous studies in the mouse model of infection. In the early 1960s, pioneering work by Mackaness (1962) revealed that (i) *L. monocytogenes* can survive and proliferate in macrophage in mice, and (ii) the cellular rather than humoral components such as mononuclear phagocytes in infected mice are suggested to be responsible for the acquired resistance to *Listeria* infection. Since then, the murine model of *L. monocytogenes* infection has been used extensively to study both the innate and adaptive components of immunity for about five decades, which has significantly advanced our understanding of T cell-mediated immune response to intracellular pathogens (Bouwer et al., 1997; Finelli et al., 1999; Garifulin and Boyartchuk, 2005; Kaufmann et al., 1997; MacDonald and Carter, 1980; Milon, 1997; Pamer, 2004). It was not until the late 1980s that the murine model was extensively used in the study of the molecular mechanisms of *L. monocytogenes* pathogenesis. These studies have led to the findings that virulent strains of *L. monocytogenes* isolated from clinical samples are also virulent in experimental mouse infection model (Hof, 1984; Rocourt et al., 1983; Rocourt et al., 1983). Most aspects of human listeriosis can be experimentally reproduced in infected mice (Cossart and Mengaud, 1989; Garifulin and Boyartchuk, 2005). The murine listeriosis model, with the aid of bacterial mutants created by using genetic techniques, has resulted in the identification of a number of key virulence factors (e.g., *hly*, *actA*, *plcA*, *plcB*, *prfA*) involved in intracellular life cycle (Gaillard et al., 1996; Kathariou et al., 1987).

Intravenous (iv) route of inoculation of *L. monocytogenes* in mice is most commonly used; this route requires a lower dose of inoculum as compared to oral inoculation and can induce reproducible, dose-dependent lethality in mice (Lecuit, 2005; Lecuit and Cossart, 2002). With the iv route, however, specific targeting of *L. monocytogenes* to brainstem and the fetoplacental unit was not seen as that found in human listeriosis (Cossart and Mengaud,

1989; Lecuit et al., 2001). In contrast to human listeriosis which is primarily acquired orally through the ingestion of contaminated foods, oral inoculation in mice is a very inefficient way to trigger systemic fatal listeriosis, as evidenced by presentation of subclinical features even with high doses of bacteria, small amounts of bacterial antigen, low organ bacterial counts, and insignificant histopathological lesions (Czuprynski and Brown, 1990; MacDonald and Carter, 1980; Marco et al., 1992b; Zachar and Savage, 1979). Many studies using the oral route yield inconsistent and even controversial results (Marco et al., 1992b; Pine et al., 1990). The translocation efficiency of *L. monocytogenes* across the intestinal barrier is very low, at a level similar to that of the nonpathogenic *L. innocua* (Lecuit, 2005; Marco et al., 1992b; Pron et al., 1998). These former observations are no longer surprising because a significant report by Lecuit *et al.* (1999) revealed that a residue of Glu 16 in the first extracellular domain of E-cadherin of mouse (mEcad) and rat renders it unable to interact with the bacterial ligand InlA, which is in contrast to Pro 16 in the functional human and guinea pig E-cadherin receptors. Based on this finding, Lecuit *et al.* (2001) has developed a novel transgenic mouse expressing the human E-cadherin on the surface of enterocytes, thus allowing the study of the *in vivo* function of InlA in crossing the intestinal barrier. With the transgenic mice expressing the human E-cadherin in enterocytes, it is not possible to study the role of InlA in other target tissues such as the fetoplacental barrier (Hamon et al., 2006; Lecuit et al., 2001). In addition, the mouse model of *L. monocytogenes* infection has also been used to evaluate the efficacy and toxicity of antimicrobial agents *in vivo*.

Guinea pig. Guinea pigs are another currently used animal model for studying human listeriosis. Oral inoculation of *L. monocytogenes* in guinea pigs is capable of inducing a gastroenteritis resembling that observed in humans and of inducing a dose-dependent

lethality following dissemination to the systemic circulation (Lecuit and Cossart, 2002). In contrast to the mouse model, guinea pigs express the functional E-cadherin receptor that can recognize and interact with InlA (Lecuit et al., 2001), thereby allowing use of oral route to reproduce listerial infection in this model and the analysis of the *in vivo* function of InlA. However, *L. monocytogenes* is a low-grade pathogen for this species because of the relatively high lethal dose of *L. monocytogenes* which is needed for the guinea pig (Dustoor et al., 1977). *L. monocytogenes* infection of the fetoplacental unit in a pregnant guinea pig model resembled that in humans, suggesting that the pregnant guinea pig is a good model for studying the cellular and molecular mechanism of vertical transmission of *L. monocytogenes* (Bakardjiev et al., 2004; Williams et al., 2007). It should be noted that the Met receptor from guinea pigs does not recognize InlB, and this animal model is thus not appropriate for studying the *in vivo* function of InlB during infection (Khelef et al., 2006).

1.5.2 Cell culture models

Cultured mammalian cells provide several advantages over the animal models in the study of *L. monocytogenes* pathogenesis, including unlimited access to cultured cells, quick and easy growth in the laboratory, and simplified experimentation in the absence of other cell types from complex host tissues. *L. monocytogenes* is able to invade and multiply in a broad spectrum of eukaryotic cells including macrophages, epithelial cells, endothelial cells, hepatocytes and fibroblasts. A variety of cultured eukaryotic cells have been extensively used for the study of *L. monocytogenes* pathogenesis, including Human U937 macrophages (Alberti-Segui et al., 2007), murine J774 macrophages (Inoue et al., 1995), human Hep2 epithelial cells (Alberti-Segui et al., 2007), human cervical epithelial cell line Hela (Francis and Thomas, 1996), African green monkey kidney cell line Vero (Bierne and Cossart, 2002), human colon carcinoma enterocyte-like epithelial cell line Caco-2 (Gaillard et al., 1987),

human hepatocellular carcinoma cell line Hep-G2 (Bierne and Cossart, 2002), mouse hepatocyte cell line TIB73 (Dramsi et al., 1995), murine L2 fibroblasts (O'Riordan et al., 2003), and human brain microvascular endothelial cells (HBMEC) (Greiffenberg et al., 1998).

Cell culture models have greatly advanced our understanding of the cell biology of *L. monocytogenes* during intracellular infection (e.g., entry, intracytosolic growth and replication, actin-based intracellular movement, and cell-to-cell spread) (Gaillard et al., 1987; Tilney and Portnoy, 1989). Since the late 1980s, the availability of genetic techniques (e.g., plasmid transformation, transposons, allelic exchange) and the development of various cell culture infection models (primary or established cells of different origins, such as human, mouse, and monkey) (Portnoy et al., 1992), have led to the identification of a number of important virulence determinants and their function(s) in specific stages of the intracellular life cycle. These include InlA and InlB triggering entry into nonprofessional phagocytes, LLO, along with two phospholipases C (PlcA and PlcB) required for phagasomal lysis, ActA required for actin-based motility and cell-to-cell spread, and PrfA (a positive regulatory factor) involved in activating the transcription of multiple virulence genes (Chakraborty et al., 1992; Gaillard et al., 1987; Gaillard et al., 1991; Gaillard et al., 1996; reviewed by Tilney *et al.* (1993)). The E-cadherin receptor for InlA was identified from human intestinal epithelial Caco-2 cells by affinity chromatography on an InlA column (Mengaud et al., 1996).

In addition, cell culture models of infection with *L. monocytogenes* have enhanced our understanding of the fundamental processes of the host cell biology (e.g., phagocytosis, actin assembly, signalling) (Gaillard et al., 1987; Tilney and Portnoy, 1989). Our knowledge in immunity has been greatly improved by studying the responses of cultured cells to *L. monocytogenes* infection with respect to the expression of immunologically related genes

such as stress genes, MHC I or II genes, cytokine genes, and cytokine receptor genes (Barry et al., 1992; Kuhn and Goebel, 1994; Kuhn and Goebel, 1997; Kuhn and Goebel, 1998). Cell culture models have also been used for determination of the antibacterial efficacy of drugs for controlling listerial infection (Hof et al., 1997).

1.6 Mechanisms for Anchoring *Listeria* Surface Proteins

Gram-positive pathogenic bacteria display on the surface a variety of proteins that not only serve as unique markers for the identification and recognition of a strain but also function in a number of critically important processes, such as protecting bacteria from adverse environments, colonization in a specific environmental niche or interaction with each other to facilitate biofilm formation, nutrient acquisition, cell division and separation, adhesion to and invasion of host cells, and interaction with the host immune system. At least 4.7% of the ORFs or genes (133 versus 2853 genes) from the genome of *L. monocytogenes* EGD-e strain are allocated for surface proteins (Cabanes et al., 2002). Only a small number of these proteins have been experimentally demonstrated to be covalently or noncovalently immobilized on the surface (Bierne and Cossart, 2007; Cabanes et al., 2002). The mechanisms of surface attachment may be summarized into five major categories.

The well studied mechanism responsible for covalent attachment of Gram-positive bacterial surface proteins to the cell wall peptidoglycan requires a C-terminal sorting signal originally characterized in *Staphylococcus aureus* protein A (Navarre and Schneewind, 1999). The characteristics of the sorting signal include a sortase-recognition sequence motif LPXTG (X, any amino acid) followed by a hydrophobic domain and a short tail of positively charged amino acids. The *S. aureus* sortase SrtA, a membrane-bound transpeptidase (Mazmanian et al., 1999), catalyzes the cleavage between the threonine (T) and the glycine (G) of the LPXTG motif and subsequent formation of the amide linkage between the carboxyl group of

threonine and an amine group of the peptide (pentaglycine) crossbridge on the cell wall peptidoglycan precursor, which is then incorporated into the mature cell wall (Scott and Barnett, 2006). The *L. monocytogenes* genome is recognized to encode the largest number of LPXTG proteins among all known sequenced genomes of Gram-positive bacteria. The internalin InlA of *L. monocytogenes*, a LPXTG protein mediating bacterial entry into epithethial cells (Gaillard et al., 1991), has been shown to be covalently anchored by SrtA to the surface through an amide bond between the threonine of the cleaved LPXTG and the amino group of *meso*-diaminopimelic acid (*m*-Dpm) crossbridge within the peptidoglycan (Bierne and Cossart, 2007; Bierne et al., 2002; Dhar et al., 2000; Garandeau et al., 2002). Surface localization of Vip, a LPXTG protein involved in *L. monocytogenes* virulence, is also SrtA-dependent. Thirteen proteins including InlA have been identified to be the substrates of SrtA using a novel nongel proteomic approach (Pucciarelli et al., 2005).

Anchoring of bacterial lipoproteins, characterized by the presence of a lipobox (LXXC) with a conserved cysteine residue within the N-terminal signal peptide sequence of prolipoproteins (Sutcliffe and Harrington, 2002) to the membrane, requires the actions of lipoprotein-processing enzymes, prolipoprotein diacylglycerol transferase (Lgt), specific lipoprotein signal peptidase (SPase) II and in the instance of Gram-negative bacteria phospholipids/apolipoprotein transacylase (Lnt) (Tokuda and Matsuyama, 2004). Following the signal peptide-directed translocation of prolipoproteins, Lgt catalyzes the formation of a thioether linkage between the diacylglycerol moiety from the membrane phosphatidylglycerol and the thiol group of the conserved cysteine residue in the lipobox. Subsequently, SPase II cleaves the signal peptide within the lipobox to form mature lipoproteins with a lipidated cysteine at the N-terminus. Aminoacylation of the N-terminal cysteine is catalyzed by Lnt that is widespread in Gram-negative bacteria but has not been

found in Gram-positive bacteria (Tokuda and Matsuyama, 2004). There are 68 putative lipoproteins encoded by the *L. monocytogenes* genome (Glaser et al., 2001), which constitute the largest group of listerial surface proteins. Of these predicted surface proteins, 26 lipoproteins have been experimentally verified and are specifically released into the culture supernatant by a Δ*lgt* strain (Baumgartner et al., 2007).

GW modules are tandem repeats with a conserved Gly-Trp dipeptide responsible for noncovalent attachment of a number of GW module-containing proteins to the surface of Gram-positive bacteria (Bierne and Cossart, 2007; Scott and Barnett, 2006). The C-terminal 232-amino acids region of InlB, a surface protein of the internalin family required for the entry of *L. monocytogenes* into various eukaryotic cell types (Hamon et al., 2006; Vazquez-Boland et al., 2001), is composed of three tandem repeats of ~ 80 amino acids. These GW modules are necessary and sufficient for anchoring InlB to the bacterial cell surface via the interaction with the bacterial cell wall component LTA (Braun et al., 1997; Jonquieres et al., 1999). The GW modules of *L. monocytogenes* InlB show the cell wall binding specificity and determine the strength of cell wall association by the number of GW modules. It has been demonstrated that the GW modules of *L. monocytogenes* InlB do not bind to the cell wall of *L. innocua* or to that of *S. pneumoniae* (Jonquieres et al., 1999), and that an InlB variant with eight GW modules of the autolysin Ami binds more efficiently than InlB to the bacterial surface (Braun et al., 1997). The *L. monocytogenes* EGD-e genome encodes 8 additional GW module-containing proteins, including two known autolysins, Ami and Auto, and five other putative autolysins containing peptidoglycan hydrolase domains (Bierne and Cossart, 2007; Cabanes et al., 2002).

The lysine motif (LysM) domain, a domain of approximately 40 amino acids originally identified in bacterial lysins (Birkeland, 1994), is found in a variety of bacterial proteins

including cell wall hydrolases (Bierne and Cossart, 2007; Scott and Barnett, 2006). The LysM domain, often repeated several times in a LysM-containing protein, is involved in surface attachment of bacterial proteins. Steen *et al.* (2003) showed that the C-terminal region of the *Lactococcus lactis* autolysin AcmA, which contains six LysM domains, is necessary for immobilization on the bacterial surface. The C-terminal region of the *E. faecalis N*-acetylglucosaminidase AtlA, composed of six LysM domains, shows binding activity towards purified peptidoglycan (Eckert et al., 2006). The *L. monocytogenes* EGD-e genome encodes six proteins including the surface autolysin p60 and MurA that contain one to four LysM domains (Bierne and Cossart, 2007). Although p60 and MurA containing two and four LysM domains respectively are found in purified cell wall fractions of *L. monocytogenes* (Calvo et al., 2005), the peptidoglycan binding activity of LysM domains remains to be determined for any listerial proteins. It is not known how and to which moiety LysM domains attach to the cell wall.

The hydrophobic segments present in the N- or C-terminal regions of bacterial proteins can serve as membrane anchors for surface localization. The ActA protein of *L. monocytogenes*, a surface protein crucial for bacterial intracellular motility (Kocks et al., 1992), contains a C-terminal stretch of hydrophobic residues followed by positively charged residues, which is probably used to tether the protein to the cell membrane. In addition to ActA, the *L. monocytogenes* EGD-e genome encodes 9 other proteins with a C-terminal hydrophobic tail (Bierne and Cossart, 2007).

1.7 Bacterial Peptidoglycan Hydrolases

Peptidoglycan hydrolases are a group of enzymes that degrade the cell wall peptidoglycan of bacteria. Excessive degradation of the cell wall by these cell wall hydrolases can potentially lead to the lysis of enzyme-producing bacteria; and these enzymes

are thus named autolysins. Autolysins are ubiquitously found in both Gram-positive and Gram-negative bacteria (Bernadsky et al., 1994; Foster, 1992).

1.7.1 Peptidoglycan

The cell wall peptidoglycan (PG), the substrate of peptidoglycan hydrolases or autolysins, is a biopolymer unique to bacteria (Madigan et al., 2002; Moat and Foster, 2002). PG, also known as murein, is the major component of the Gram-positive bacterial cell wall, accounting for 30-70% of total cell wall. In contrast to the Gram-negative bacterial PG, which is located in the periplasm between the inner and outer membranes and accounts for less than 10% of total cell wall, the Gram-positive bacterial PG forms the outermost layer immediately external to the cytoplasmic membrane (Schleifer and Kandler, 1972). The cell wall of Gram-positive bacteria, in particular the PG, is responsible for providing protection to the protoplast from mechanical and osmotic forces, maintaining the cell shape, and also serving as an attachment site for bacterial surface proteins (Navarre and Schneewind, 1999; Shockman and Barrett, 1983). The cell wall PG is dynamic and undergoes reorganization during bacterial growth, division, separation, *etc.*; various autolysins are involved in these processes (Anantharaman and Aravind, 2003; Nanninga, 1991).

The backbone of PG is composed of a linear glycan chain of alternating *N*-acetylglucosamine (NAG or GlcNAc) and *N*-acetylmuramic acid (NAM or MurNAc) units linked by a β-1, 4 glycosidic bond (Fig. 1-3) (Schleifer and Kandler, 1972). The average length of glycan strands varies between 10 and 65 disaccharide units in different bacterial species (Schleifer and Kandler, 1972). NAM is covalently linked to a short peptide of 3 to 5 residues, which usually contains both the canonical L-amino acids and unusual D-amino acids (e.g., D-Ala, D-Glu, and *m*-Dpm) (Schleifer and Kandler, 1972). Neighboring glycan strands are cross-linked directly by forming a peptide bond between the carboxyl group of a

FIG. 1-3. Diagrammatic representation of the structure of a typical bacterial peptidoglycan. The backbone of PG is composed of a linear glycan chain of alternating *N*-acetylglucosamine (NAG or GlcNAc) and *N*-acetylmuramic acid (NAM or MurNAc) units linked by a β-1, 4 glycosidic bond. The average length of glycan strands varies between 10 and 65 dissacharide units (n = 10~65) in different bacterial species. NAM is covalently linked to a short peptide of 3 to 5 residue, which usually contains both the canonical L-amino acids and unusual D-amino acids. Usually L-alanine (L-Ala) binds the lactic acid residue of the NAM followed by D-glutamic acid (D-Glu), L-diamino acid (L-DA; e.g., *m*-Dpm), and D-alanine (D-Ala) or an additional D-Ala at the C-terminus. Neighboring glycan strands are cross-linked directly by forming a peptide bond between the carboxyl group of a terminal D-Ala residue of one short peptide and the amino group of *m*-Dpm or D-Glu of another short peptide attached to the other glycan strand or through a peptide crossbridge (b), giving rise to a rigid three-dimensional lattice structure of bacterial cell walls. In *L. monocytogenes*, the cell wall PG contains pentapeptides -L-Ala-D-iGlu (iso-glutamate)-*m*-Dpm-D-Ala-D-Ala that are covalently linked to NAM. The cell wall pentapeptides are not cross-linked via a peptide crossbridge but directly via an amide bond between the *m*-Dpm residue at position 3 of one cell wall peptide and the terminal D-Ala residue at position 4 of an adjacent cell wall peptide from the other glycan chain.

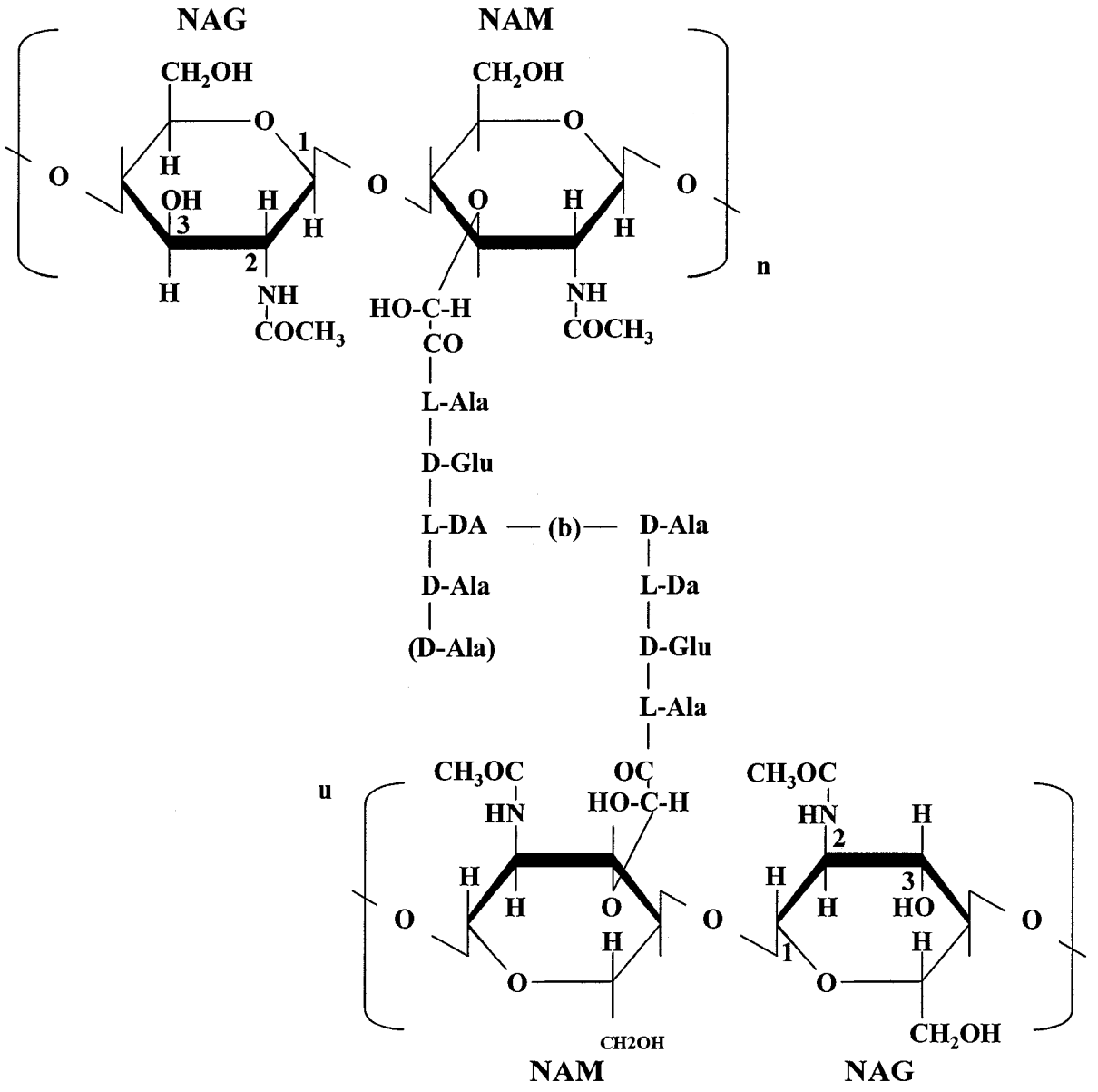
NAG
NAM
CH2OH
O
1
H
OH
3
H
H
2
H
NH
COCH3
n
HO-C-H
CO
L-Ala
D-Glu
L-DA
(b)
D-Ala
D-Ala
(D-Ala)
L-Da
D-Glu
L-Ala
u
CH3OC
HN
OC
HO-C-H
CH2OH
HO
NAM
NAG

terminal D-Ala residue of one short peptide and the amino group of *m*-Dpm or D-Glu of another short peptide attached to the other glycan strand or through a peptide crossbridge (e.g., the pentaglycine -$(Gly)_5$- in *S. aureus*) (Schleifer and Kandler, 1972; Shockman and Barrett, 1983). This covalent cross-linkage gives rise to a rigid three-dimensional lattice structure of bacterial cell walls.

The glycan strands are highly conserved among different bacteria, whereas the chemical composition of the peptide moiety and the peptide crossbridge as well as the extent of cross-linking of glycan strands varies considerably with the species (Schleifer and Kandler, 1972). In *L. monocytogenes*, the cell wall PG contains pentapeptides -L-Ala-D-iGlu (iso-glutamate)-*m*-Dpm-D-Ala-D-Ala that are covalently linked to NAM (Navarre and Schneewind, 1999). The cell wall pentapeptides are not cross-linked via a peptide crossbridge but directly via an amide bond between the *m*-Dpm residue at position 3 of one cell wall peptide and the terminal D-Ala residue at position 4 of an adjacent cell wall peptide from the other glycan chain (Kamisango et al., 1982 ; Navarre and Schneewind, 1999 ; Schleifer and Kandler, 1972). The PG of Gram-positive bacteria is usually covalently complexed with accessory cell wall polymers such as teichoic acids (TAs), teichuronic acids (TUAs), and neutral or other acidic polysaccharides (Shockman and Barrett, 1983).

1.7.2 Classification of Peptidoglycan Hydrolases

Peptidoglycan hydrolases catalyze the cleavage of the covalent bonds within the cell wall peptidoglycan (murein) (Shockman and Holtje, 1994). Based on the covalent bonds they cleave (Fig. 1-4), peptidoglycan hydrolases are classified into five categories: *N*-acetylmuramidase, *N*-acetylglucosaminidase, *N*-acetylmuramyl-L-alanine amidase,

FIG. 1-4. The cleavage sites of the peptidoglycan hydrolases of *E. coli*. The difference in the action between lytic transglycosylase and *N*-acetylmuramidase is that after cleaving the β-1,4-glycosidic bond between the NAM and the NAG residues of the glycan strands, lytic transglycosylase also catalyzes an intramolecular glycosyltransferase reaction, resulting in the formation of an anhydro bond between the C6 and C1 of the NAM residue. Arrows indicate the chemical bonds cleaved by individual peptidoglycan hydrolases. Abbreviations: NAG, *N*-acetylglucosamine; NAM, *N*-acetylmuramic acid.

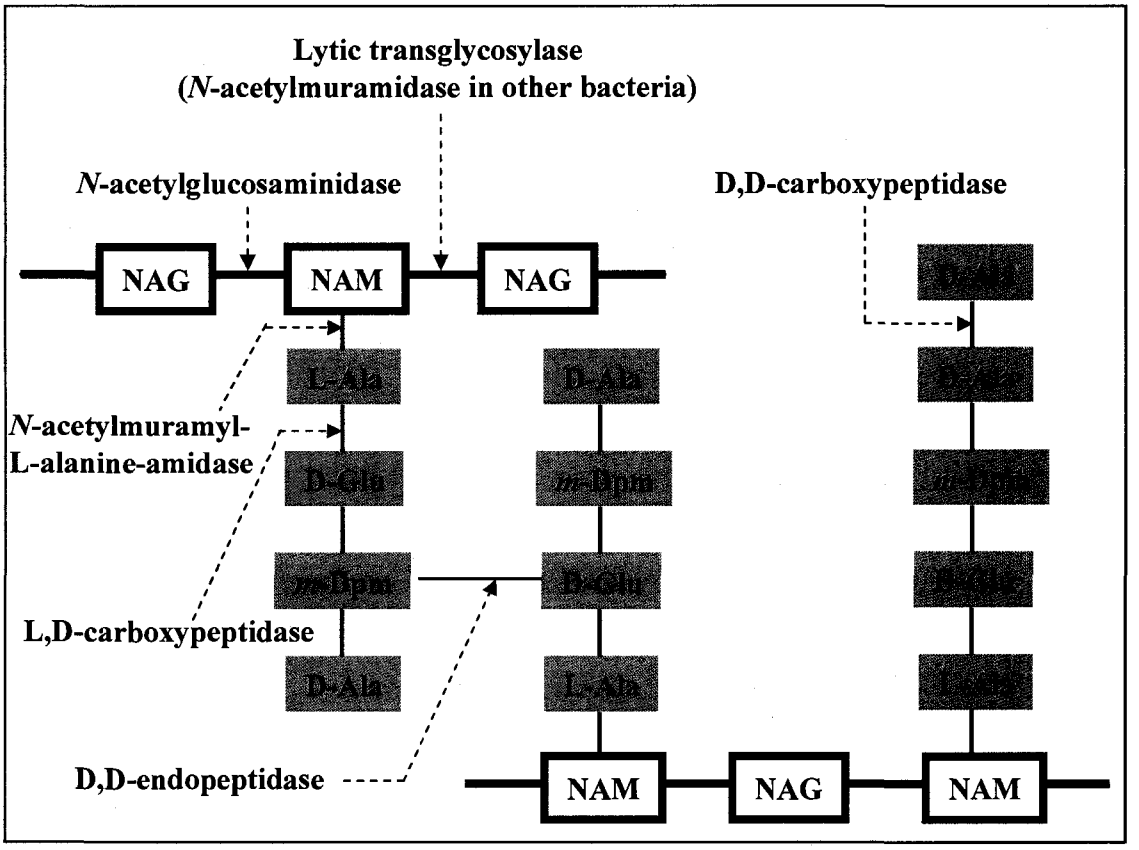
Lytic transglycosylase
(N-acetylmuramidase in other bacteria)
N-acetylglucosaminidase
D,D-carboxypeptidase
NAG
NAM
NAG
L-Ala
D-Ala
D-Glu
m-Dpm
m-Dpm
D-Glu
D-Ala
L-Ala
N-acetylmuramyl-
L-alanine-amidase
L,D-carboxypeptidase
D,D-endopeptidase
NAM
NAG
NAM

endopeptidase (e.g., L,D-carboxypeptidase, D,D-carboxypeptidase, D,D-endopeptidase) and lytic transglycosylase (Tomasz, 1984).

1.7.3 Biological Functions

Bacterial autolysins are involved or implicated in a variety of biological functions including cell wall turnover, cell wall expansion, cell division, cell separation, chemotaxis, biofilm formation, genetic competence, protein secretion, antibiotic-induced lysis, sporulation, and formation of flagella (Shockman et al., 1996; Smith et al., 2000). Multiple autolysins have been demonstrated and studied in various bacterial species (Foster, 1992; Foster, 1995; Heidrich et al., 2002; Oshida et al., 1995; Smith et al., 2000), and the purpose of this functional redundancy (if there is any) is not clear. This functional redundancy may serve as a backup mechanism or reflect a specific function of each individual autolysin.

1.7.4 Role in virulence

Bacterial autolysins have greatly attracted the attention of bacteriologists as an important virulence factor in the past two decades. Experimental studies with autolysin-deficient mutants have revealed the important role of autolysins in bacterial pathogenesis. Autolysin-deficient mutants, such as an LytA mutant of *S. pneumoniae* (Berry and Paton, 2000), an AtlE mutant of *Staphylococcus epidermidis* (Rupp et al., 1999), and Ami, Auto, p60 and MurA mutants of *L. monocytogenes* (Cabanes et al., 2004; Lenz et al., 2003; Milohanic et al., 2001; Pilgrim et al., 2003), are less virulent in animal models than their parental wild type strains.

The mechanisms underlying how autolysins are involved in virulence are not fully understood and remain to be elucidated. The autolytic activity and the cell wall binding

domain of bacterial autolysins have been shown to be involved in virulence. LytA of *S. pneumoniae* and MurA and p60 of *L. monocytogenes* are thought to mediate the release of cytoplasmic toxins or inflammatory degraded cell wall components resulting in subsequent tissue injuries (Jedrzejas, 2001; Lenz et al., 2003; Lock et al., 1992; Tuomanen, 2000). Restoration of virulence in a *L. monocytogenes* p60-defective mutant strain requires expression of the full-length autolysin p60 with an intact catalytic domain (Lenz et al., 2003). Moreover, the direct involvement of the autolysin protein itself in pathogenesis has been revealed by studying the adhesive properties of noncatalytic domains. The cell wall binding domains of the autolysins, made up of repeated GW modules, directly contribute to bacterial virulence by promoting adherence to eukaryotic cells as shown for Ami of *L. monocytogenes* (Milohanic et al., 2001) or to extracellular matrix proteins as shown for Aas of *Staphylococcus saprophyticus* (Hell et al., 1998) and AtlC of *Staphylococcus caprae* (Allignet et al., 2002). The endo-*β*-*N*-Acetylglucosaminidase from *S. aureus* interferes with the response of human lymphocytes to mitogenic stimuli and with antibody production in mice (Valisena et al., 1991).

1.7.5 Autolysins in *L. monocytogenes*

In *L. monocytogenes*, six autolysins have been experimentally demonstrated, including p60 (Wuenscher et al., 1993), P45 (Schubert et al., 2000), Ami (Braun et al., 1997; McLaughlan and Foster, 1998), MurA/NamA (Carroll et al., 2003; Lenz et al., 2003), Auto (Cabanes et al., 2004), and Lmo0327 (Popowska and Markiewicz, 2006) (Fig. 1-5). The flagellin FlaA, a structural component of *L. monocytogenes* flagella responsible for bacterial motility (Dons et al., 1992), has been identified to be a peptidoglycan hydrolase by using renaturing SDS-PAGE analysis of the LiCl surface protein extracts of *L. monocytogenes* EGD-e with the cell wall substrates of *B. subtilis*, *Micrococcus luteus,* and *E. coli*

FIG. 1-5. Schematic diagrams of domain organization of known *L. monocytogenes* autolysins. Six *L. monocytogenes* autolysins including p60, P45, Ami, MurA/NamA, Auto, and Lmo0327 have been experimentally identified.

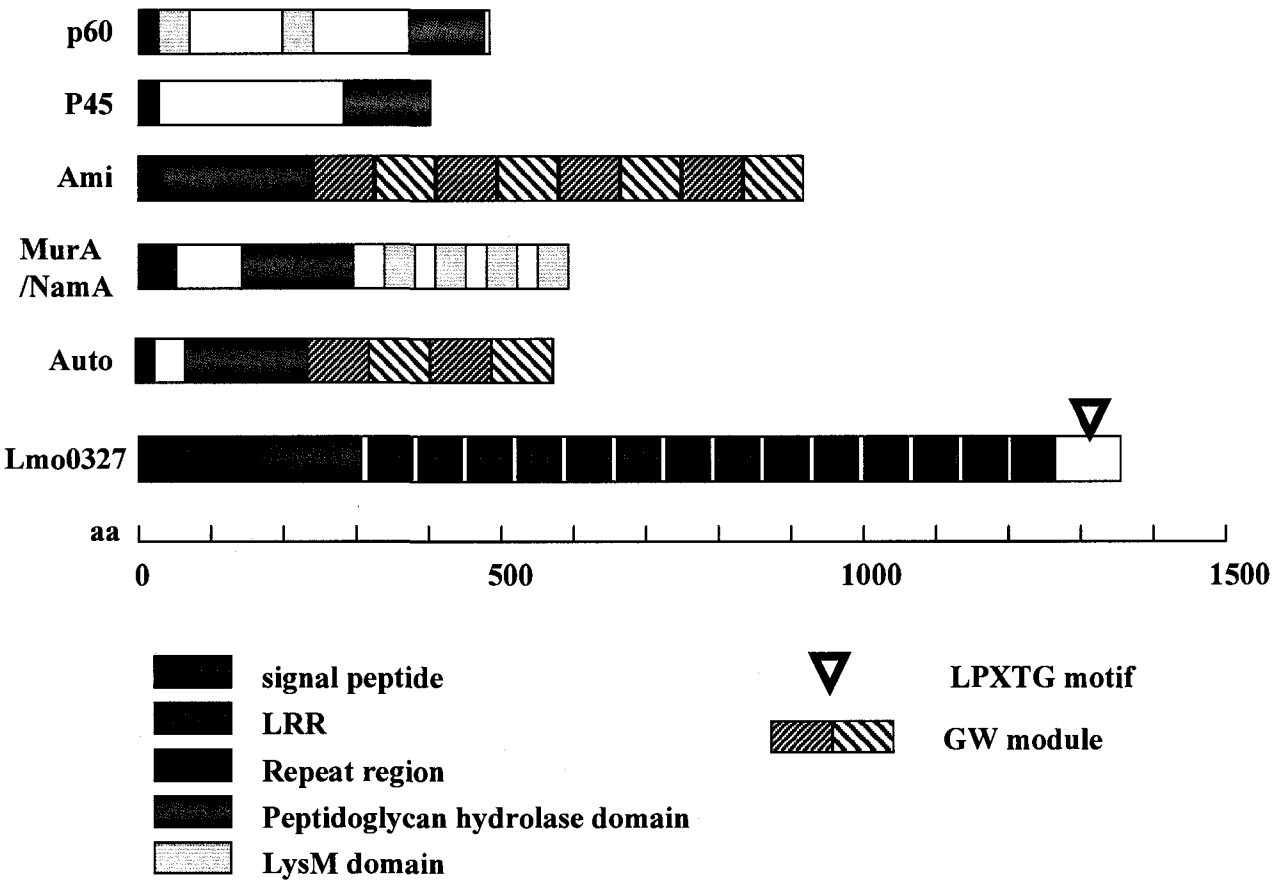
p60
P45
Ami
MurA
/NamA
Auto
Lmo0327
aa
0
500
1000
1500
signal peptide
LRR
Repeat region
Peptidoglycan hydrolase domain
LysM domain
LPXTG motif
GW module

(Popowska and Markiewicz, 2004). The autolytic activity of FlaA is proposed but has not yet been experimentally determined. Further searches in the *L. monocytogenes* genome database reveal the presence of at least five additional proteins containing a putative peptidoglycan hydrolase domain (Popowska and Markiewicz, 2006).

1.7.5.1 p60

p60, a 60-kDa extracellular protein, is the first identified autolysin in *L. monocytogenes* by transposon mutagenesis of *L. monocytogenes* EGD-e (Goebel et al., 1988). The mutant produces a reduced amount of p60 and shows an impaired ability to enter mouse embryo fibroblast (3T6) cells (Goebel et al., 1988). Thus, the p60 gene was named the invasion associated protein (iap) gene, *iap* (Kohler et al., 1990).

The autolysin p60 is a 484-amino acid protein with a high pI of 9.3 comprising an N-terminal putative 27-amino acid signal peptide, a putative cell wall binding domain consisting of two LysM domains (aa 28-70, aa 201-243), and a C-terminal predicted endopeptidase domain (aa 379-481) referred to as the p60 domain (Kuhn and Goebel, 1989; Lenz et al., 2003). p60 has been recognized as a representative of a large NIpC/P60 superfamily of peptidases encompassing members from bacteria, DNA or RNA viruses, eukaryotes, and archaea (Anantharaman and Aravind, 2003), such as *L. monocytogenes* P45 (Schubert et al., 2000), *B. subtilis* autolysins LytE and LytF (Margot et al., 1998; Ohnishi et al., 1999), *Streptococcus* PcsB protein (Reinscheid et al., 2001), and *E. coli* membrane-associated lipoprotein NIpC (Anantharaman and Aravind, 2003). They typically contain in the catalytic domain a characteristic N-terminal region with a conserved cysteine, followed by a C-terminal characteristic region with a conserved histidine (Anantharaman and Aravind, 2003). The conserved cysteine and histidine residues are believed to be essential for the catalytic activity (Mondal et al., 2000).

p60 is found mostly in the culture supernatant and partially cell surface-bound (Lenz et al., 2003; Machata et al., 2005). The secretion of p60, together with the autolysin MurA/NamA, is dependent on the auxiliary protein secretion system (SecA2), which is conserved in several Gram-positive bacterial pathogens including *S. aureus, Mycobacterium tuberculosis, Bacillus anthracis, and S. pneumoniae* (Lenz et al., 2003). The transcription of *p60* gene is independent of PrfA; expression of the p60 protein was suggested to be regulated at the posttranscriptional level (Bubert et al., 1997; Bubert et al., 1999; Kohler et al., 1991). Immunologically cross-reacting proteins that display significant homology to p60 are also present in other nonpathogenic *Listeria* species such as *L. innocua* and *L. seeligeri* (Bubert et al., 1992a; Bubert et al., 1992b; Kohler et al., 1990; Kohler et al., 1991; Kuhn and Goebel, 1989).

Like the *B. subtilis* autolysins LytE and LytF (Margot et al., 1998; Ohnishi et al., 1999), and the *Streptococcus* PcsB protein (Reinscheid et al., 2001), p60 is similarly involved in cell division and separation. The p60 mutants producing a reduced amount of p60 or lacking p60, form abnormal septa and long cell chains in broth culture; treatment of the mutants with the p60 protein can disaggregate long cell chains into individual cells (Kohler et al., 1991; Kuhn and Goebel, 1989; Pilgrim et al., 2003). However, p60 is not essential for growth extracellularly in broth medium or intracellularly in mouse bone marrow macrophages (Kuhn and Goebel, 1989; Lenz et al., 2003; Pilgrim et al., 2003).

p60 is required for *L. monocytogenes* virulence *in vivo* since p60 deficient mutants show reduced virulence in a mouse model (Bubert et al., 1992b; Gutekunst et al., 1992; Kohler et al., 1991; Kuhn and Goebel, 1989; Lenz et al., 2003; Pilgrim et al., 2003). The direct involvement of p60 itself extracellularly in bacterial invasion is supported by several lines of evidence. The long cell chains of the p60 deficient mutant disaggregates into individual cells

after addition of the p60 protein and restores bacterial invasion into 3T6 cells (Kohler et al., 1991; Kuhn and Goebel, 1989). The single cell morphology is not critical for the restoration of such invasiveness since physically disrupted single cells by ultrasonication do not restore the ability of the mutant to invade 3T6 cells. Heterologous expression of p60 in the Gram-negative bacterium *Salmonella* Typhimurium enhances bacterial survival in mice and promotes bacterial invasion into murine hepatocytes and macrophages (Hess et al., 1995). Anti-p60 antibody can partially block the invasion of *L. monocytogenes* into murine hepatocytes (Hess et al., 1995). Recombinant p60 protein can directly bind to the Caco-2 cell membrane, although the potential cellular receptor for p60 has not been defined (Kuhn and Goebel, 1989; Park et al., 2000). However, p60 is necessary but not sufficient to induce uptake since treatment of a noninvasive *L. innocua* strain with p60 does not render this bacterium invasive for 3T6 cells (Kuhn and Goebel, 1989). By successful construction of a p60 in-frame deletion mutant, Pilgrim *et al.* (2003) clearly demonstrated the influence of p60 on virulence intracellularly. Lack of the p60 protein results in abnormal cell division which causes uneven, nonpolar distribution of ActA and loss of actin tail formation, thus affecting bacterial capacity for actin-based intracellular movement and cell-to-cell spread, while the p60 deficiency does not alter the expression of several other important virulence factors and bacteriolytic enzymes, i.e., ActA, LLO, InlA, InlB, PlcB, and P45 (Pilgrim et al., 2003). The importance of the autolytic activity of p60 in virulence is highlighted in the studies showing that the virulence of the p60 deletion strain can be restored only by expression of a full-length, catalytically active p60 and a possible role of p60 in bacterial infection was proposed by producing proinflammatory degraded cell wall components *in vivo* (Humann et al., 2007; Lenz et al., 2003).

1.7.5.2 P45

P45, a protein with an apparent molecular mass of 45 kDa identified initially using a monoclonal antibody developed by immunization of mice with heat-killed cells of *L. monocytogenes* serotype 4d (Schubert et al., 2000), was shown to possess peptidoglycan hydrolase activity towards SDS-treated cells of *L. monocytogenes*. Like p60, this protein is associated with the cell surface and also present in the culture supernatant (Schubert et al., 2000). Proteins cross-reacting with the monoclonal antibody to P45 are present in other *L. monocytogenes* strains (45 kDa), *L. innocua* (45 kDa), and *L. ivanovii* (47 kDa) but not in *L. seeligeri*, *L. welshimeri,* or *L. grayi* (Schubert et al., 2000). In contrast to p60, P45 has narrow substrate specificity as it is capable of hydrolyzing the listerial cell wall but not that of *M. luteus* (Schubert et al., 2000). The role of P45 in *L. monocytogenes* virulence is not known.

P45 is a 402-amino acid protein, which contains a 27-amino acid signal peptide and a C-terminal region of approximately 120 amino acids with significant homology to the C-terminal catalytic domain of p60 (Schubert et al., 2000). Although P45 exhibits homology (38% identity) to p60, the anti-p60 polyclonal antibody did not cross react with P45 and P45 immunologically-related proteins (Schubert et al., 2000).

P45 is also a member of the large NlpC/P60 superfamily. Protein database searches show that P45 exhibits significant sequence similarities to several proteins of Gram-positive bacteria, e.g., p54 from *Enterococcus faecium*, Usp45 from *Lactococcus lactis*, PcsB from *Streptococcus agalactiae*, and YvcE from *B. subtilis* (Reinscheid et al., 2001; Schubert et al., 2000). A C-terminal short stretch of amino acids (FDCSG) of P45 is similarly found in p60, P54 and YcvE (Reinscheid et al., 2001).

1.7.5.3 Ami

Ami, a major 102-kDa surface autolysin accounting for up to 66% of total lytic enzyme activity in *L. monocytogenes* EGD-e, was identified by three different approaches, (i) Southern blotting analysis of *L. monocytogenes* EGD-e chromosomal DNA using the 3'-end of the *inlB* gene as a probe (Braun et al., 1997; Milohanic et al., 2001), (ii) screening a genomic expression library of *L. monocytogenes* EGD-e for lytic enzyme-producing clones (McLaughlan and Foster, 1998), and (iii) genetic screening for transposon insertional mutants defective in adherence to eukaryotic cells in the *inlAB* deletion genetic background (Milohanic et al., 2000).

The autolysin Ami of *L. monocytogenes* EGD-e strain is a 917-amino acid protein with a cell wall binding domain (CWBD) (aa 262 to 917) consisting of eight GW modules of ~ 80 amino acids (Milohanic et al., 2004), a domain structure similar to the three GW modules of InlB responsible for noncovalent anchoring of InlB to the cell wall (Braun et al., 1997). The CWBD of Ami displays the cell wall binding specificity towards *Listeria* strains, as shown by the finding that the purified CWBD of *L. monocytogenes* serotype 4b binds more efficiently to the homologous strain than to the serotype 1/2a (Milohanic et al., 2004). This specificity is consistent with the observation that the amino acid sequence is poorly conserved in the CWBD of different *Listeria* serotypes (Milohanic et al., 2004). The N-terminal region (aa 31-261) of Ami contains a putative 179-amino acid peptidoglycan hydrolase similar to the *N*-acetylmuramyl-L-alanine amidase domain of the Atl autolysin of *S. aureus* (Braun et al., 1997).

Ami is not important for bacterial growth, cell division, cell separation, or cell wall morphology since inactivation of Ami has no effect on these phenotypic characteristics (McLaughlan and Foster, 1998). Ami is necessary for *L. monocytogenes* virulence *in vivo* as the *ami* deletion mutant has the reduced capacity to colonize the liver of mice following an iv

challenge (Milohanic et al., 2001). *In vitro* analysis of the Δ*ami* using cultured eukaryotic cells has showed that Ami contributes to bacterial adherence to eukaryotic cells but is not important for invasion, bacterial intracellular replication or actin tail formation (Milohanic et al., 2001). The role of Ami in adherence of bacteria to eukaryotic cells (i.e., SK-MEL 28, Caco-2, and Hep-G2) is more evident in the *inlA*-, *inlB*- and *inlAB*-deletion backgrounds than in the wild type EGD-e background (Milohanic et al., 2001). The *ami* mutants generated from these gene deletion backgrounds retain the ability to trigger their uptake by eukaryotic cells, indicating that other factors are involved in invasion (Milohanic et al., 2001). Adhesion of Ami to eukaryotic cells is mediated by its C-terminal CWBD comprising eight GW modules (Braun et al., 1997; Milohanic et al., 2001) presumably through the interaction with an as yet unknown host cell receptor(s). The efficacy of binding to eukaryotic cells varies with the CWBD of Ami from different *L. monocytogenes* serotypes (Milohanic et al., 2004).

1.7.5.4 MurA/NamA

MurA/NamA of *L. monocytogenes* EGD-e is a 66-kDa surface autolysin, which was identified by Western blotting using a *L. monocytogenes*-specific monoclonal antibody that also cross reacted with p60 (Carroll et al., 2003) and by a proteomic approach as one of the SecA2-dependent secreted and surface proteins (Lenz et al., 2003). MurA/NamA is a protein of 590 amino acids with a predicted molecular mass of 63.571 kDa (Carroll et al., 2003). This protein contains an N-terminal putative 52-amino acid signal peptide and a C-terminal cell wall binding domain consisting of four copies of LysM repeats of ~ 40 amino acids (aa 332-590) with homology to the two LysM repeats in the N-terminus of p60 (Carroll et al., 2003; Lenz et al., 2003). In contrast to the predicted endopeptidase domain within the p60, a putative muramidase domain similar to the amidase_4 domain (mannosyl glycoprotein

endo-*β*-*N*-acetylglucosamidase; accession number PF01832) is found in the N-terminal region (aa 149-301) of MurA/NamA (Carroll et al., 2003). The MurA homologs are present in *L. monocytogenes* serotype 4b and *L. innocua* CLIP11262 with 96% and 84% amino acid sequence identity, respectively, to the MurA protein of *L. monocytogenes* EGD-e (Carroll et al., 2003).

Like p60, MurA/NamA is involved in cell separation since the gene deletion mutant Δ*murA* grows as long chains in broth culture (Carroll et al., 2003). This autolysin, however, is not essential for bacterial growth rate (Carroll et al., 2003; Lenz et al., 2003). Both NamA and p60 are required for virulence *in vivo* in mice but p60 plays a more important role in virulence than NamA as the Δ*p60* mutant is more severely attenuated in mice as compared to the Δ*namA* mutant (Lenz et al., 2003). Since the NamA deficient mutant shows no defect in the ability to infect and intracellularly replicate in cultured eukaryotic cells *in vitro*, it is hypothesized that NamA might be involved in the release of inflammatory degraded cell wall components affecting host immune responses (Lenz et al., 2003).

1.7.5.5 Auto

Auto encoded by *aut* (*lmo1076*) was discovered and experimentally confirmed to possess PG hydrolase activity against the cell wall of *L. monocytogenes* using the recombinant protein during the search for new genes of *L. monocytogenes* EGD-e encoding surface proteins absent from the genome of the nonpathogenic species *L. innocua* (Cabanes et al., 2004). Auto is a 64-kDa protein of 572 amino acids sharing a common modular domain structure with Ami, i.e., a putative N-terminal 26-amino acid signal peptide, a N-terminal putative PG hydrolase domain (aa 75-243), and a C-terminal region (aa 244-572) containing four GW modules similar to the CWBD of InlB and Ami. Like the *p60* gene,

transcription of the *auto* gene is independent of the positive transcriptional regulator PrfA (Cabanes et al., 2004).

Auto is not important for cell division and separation as deletion of the *aut* gene from the *L. monocytogenes* chromosome does not result in a physiological defect in these processes; the Δ*aut* mutant shows no alteration in the expression of other major virulence factors (e.g., InlA, InlB, ActA, and LLO) (Cabanes et al., 2004). Auto, however, is required for *L. monocytogenes* virulence as the Δ*aut* mutant exhibits a significant defect in colonization in the target organs (i.e., brain, liver and spleen) of mice following iv inoculation and those (i.e., small intestine, mesenteric lymph nodes, liver, and spleen) of guinea pigs following an oral administration (Cabanes et al., 2004). *In vitro* analysis of the mutant using various cultured eukaryotic cells reveals that unlike Ami, Auto is not essential for bacterial adherence to eukaryotic cells (e.g., Vero, the Caco-2 or Hep-2). It is required for entry into nonprofessional phagocytic cells (e.g., Vero, Caco-2, Hep-2, guinea-pig epithelial cell line GPC16, and the murine fibroblast cell line L2) but not murine macrophage J774 (Cabanes et al., 2004). Auto is also not important for intracellular growth, actin-tail formation or cell-to-cell spread during infection of J774 macrophages (Cabanes et al., 2004). In contrast to the internalins InlA and InlB, Auto alone is not sufficient to confer invasiveness to the noninvasive *L. innocua* for cultured eukaryotic cells (Cabanes et al., 2004).

1.7.5.6 Lmo0327

Recently, Popowska and Makievicz (2006) have identified a new 144-kDa surface autolysin to be Lmo0327 by screening for lytic enzyme-producing clones from a lambda Zap expression library of *L. monocytogenes* EGD-e genomic DNA. Lmo0327, originally annotated as a hypothetical protein of 1348 amino acids encoded by *L. monocytogenes*

EGD-e genome (Glaser et al., 2001), contains an N-terminal putative signal sequence and a C-terminal cell wall anchoring motif LPXTG, suggesting that surface localization of this autolysin is achieved through covalent attachment to the cell wall peptidoglycan in a manner similar to InlA. As similarly found in the internalins InlA and InlB, a LRR domain (aa 25-176) comprising five tandem repeats of 20–22 amino acids is present in the N-terminal part of Lmo0327. The central part (aa 315-1273) of Lmo0327 is an extensive repeat region consisting of 14 repeats of 64 amino acids, revealed by the sequence analysis with Interproscan (http://www.ebi.ac.uk/InterProScan/, 2007/10/27). The functionality of the LRR domain and the central repeat region (domain) is not clear and requires experimental studies. *In silico* modeling of the tertiary structure of the N-terminal 152-amino acid LRR domain reveals a structure (i.e., a right-handed β-helix with a turn after each repeat) similar to those of the LRR domains described for InlA, InlB and InlH (Popowska and Markiewicz, 2006). A similarity search against the protein database reveals that NP469697 is a highly conserved homolog of Lmo0327 in the nonpathogenic species *L. innocua* with a 95% amino acid identity (Popowska and Markiewicz, 2006).

By insertional inactivation of the *lmo0327* gene, Popowska and Mariewicz (2006) demonstrated that Lmo0327 is involved in cell separation and PG turnover. The insertionnal mutant shows no polar effects and grows in the form of long cell chains in broth culture (Popowska and Markiewicz, 2006), similar to what was found with Δ*murA* and Δ*p60* mutants (Machata et al., 2005). In contrast to the p60 deficient mutant that produces an abnormal septum, the *lmo0327* mutant forms a complete septum during cell division but cell separation does not occur. Furthermore, the *lmo0327* mutant shows a slower turnover of PG as compared to the wild type (Popowska and Markiewicz, 2006). It is not known whether

Lmo0327 plays a role in *L. monocytogenes* virulence, although such a role is strongly suggested by the autolysin nature of Lmo0327 along with its internalin-like sequence characteristics.

1.7.5.7 FlaA

Peptidoglycan hydrolase activity has been shown for the 29-kDa flagellin, FlaA (Popowska and Markiewicz, 2004), a structural component of *L. monocytogenes* flagella responsible for bacterial motility (Dons et al., 1992). It is not known whether FlaA can degrade the cell wall of *L. monocytogenes*. Flagellar motility is essential for bacterial adherence to environmental surfaces and biofilm formation (Lemon et al., 2007; Vatanyoopaisarn et al., 2000). FlaA plays a role in *L. monocytogenes* pathogenesis, as evidenced by the fact that this protein facilitates bacterial adhesion to and entry into cultured Caco-2 cells and promotes early-stage bacterial intestinal colonization *in vivo* in mice (Dons et al., 2004; O'Neil and Marquis, 2006; Shen and Higgins, 2006).

CHAPTER II

Rationale, Hypothesis, and Objectives

2.1 Previous Study

Dr. M Lin's group has been interested in immunogenic surface proteins (Isp) of *L. monocytogenes*, which are less characterized and understood. Study of such proteins may provide new insights into the mechanism of *Listeria* pathogenesis, immunity, and bacterial *in vivo* survival and growth. A recent study with differential immunoscreening of a *L. monocytogenes* serotype 4b genomic expression library was conducted by this group to identify genes coding for proteins that reacted with serum antibodies (RαL) from rabbits infected with live *L. monocytogenes* serotype 4b but not with antibodies (RαK) from animals immunized with heat-killed bacteria (Fig. 2-1; Yu et al., 2007). That study led to the identification of 8 *L. monocytogenes* proteins as the targets of humoral immune response to listerial infection; three internalin proteins (InlA, InlD, InlC2) and 5 novel proteins of unknown function (designated IspA, IspB, IspC, IspD, and IspE, respectively). Putative proteins highly homologous to some of these novel proteins have not been characterized in *Listeria*. Demonstration of humoral immune responses to these proteins only in actively infected rabbits but not in animals receiving heat-killed *L. monocytogenes*, suggests that they are induced only or significantly upregulated *in vivo* during infection and thus are likely important in *Listeria* pathogenesis. In fact, InlA is a known virulence factor (Gaillard et al., 1991).

Analysis of the genome sequence of pathogenic *L. monocytogenes* serotypes 1/2a and 4b strains revealed that almost 40% of ~2800 ORFs have not been assigned any functions and putative functions assigned to proteins encoded by a significant proportion of ORFs remain to be confirmed with experimental data (Nelson et al., 2004). My Ph.D research will focus on biochemical, molecular and functional characterization of IspC, one of five novel immunogenic proteins of unknown function identified earlier (Yu et al., 2007).

FIG. 2-1. Schematic representation of the construction and differential immunoscreening of a *L. monocytogenes* serotype 4b genomic expression library. (A) The *L. monocytogenes* serotype 4b genomic expression library was constructed by cloning the digested genomic DNA of *L. monocytogenes* serotype 4b into *E. coli* expression vector followed by transformation into *E. coli* host cells. The genomic DNA of *L. monocytogenes* was partially digested with Sau3AI and the DNA fragments of 1.5-2.5 kb were separated by gel electrophoresis, purified, partially filled-in with dGTP and dATP and cloned into the expression vector pScreen 1b+ΔecoRV that had been digested with XhoI and partially filled-in with dCTP and dTTP resulting in the genomic expression library. **(B)** The genomic expression library was differentially screened with two kinds of serum antibodies, one (RαL) from rabbits infected with live *L. monocytogenes* serotype 4b and the other (RαK) from animals immunized with heat-killed bacteria. The clones that reacted with RαL but not RαK were identified as positive clones, the inserts were sequenced and the corresponding ORFs were identified. Detailed procedures are described (W. Yu, MSc. Thesis, 2004; Yu et al., 2007).

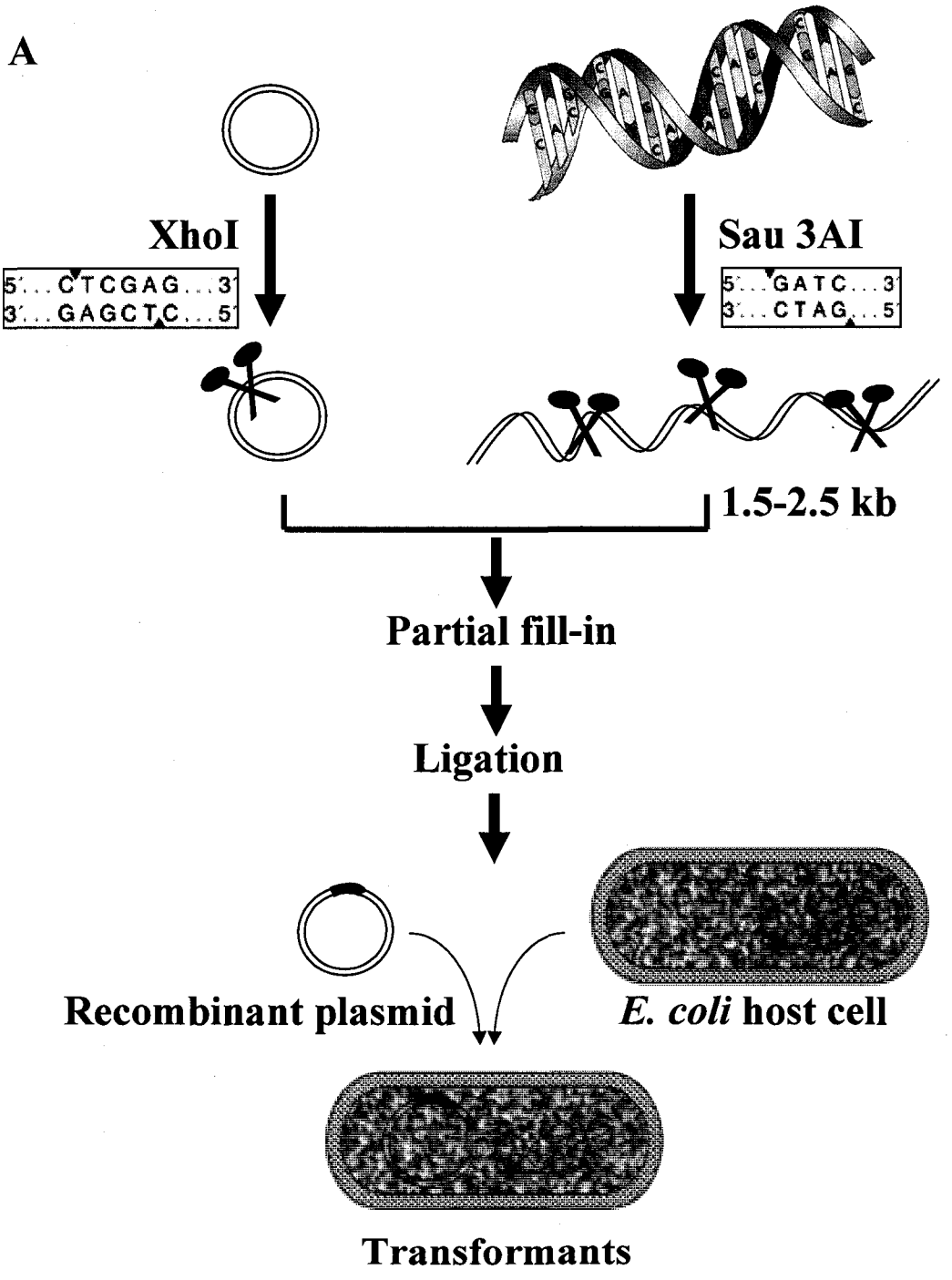
A
XhoI
5′...CTCGAG...3′
3′...GAGCTC...5′
Sau 3AI
5′...GATC...3′
3′...CTAG...5′
1.5-2.5 kb
Partial fill-in
Ligation
Recombinant plasmid
E. coli host cell
Transformants

B

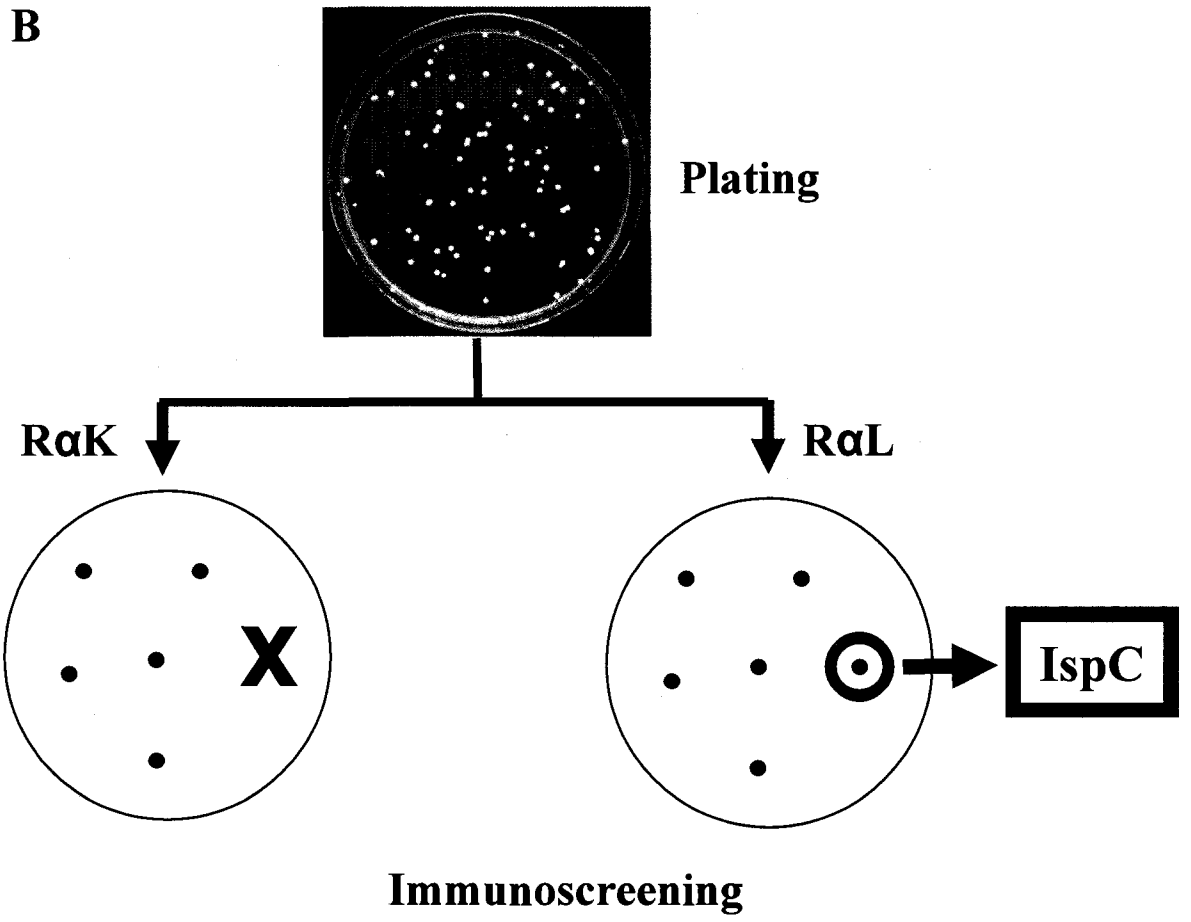

2.2 Sequence Analysis of IspC

L. monocytogenes IspC is a protein of 774 amino acids in length deduced from its ORF (Yu et al., 2007; H. Dan and M. Lin, unpublished data; Genbank access no. EF409982; Appendix I) with a calculated molecular mass of 86 kDa and a theoretical pI of 9.4. Sequence characteristics of IspC include (i) a 29-amino acid N-terminal signal peptide predicted by SignalP 3.0 (http://www.cbs.dtu.dk/services/SignalP/), (ii) an N-terminal region (aa 58-197) sharing significant homology (35% identity) to the muramidase domain in the C-terminal region (aa 151-316) of the flagellar protein FlgJ, of *Salmonella* Typhimurium (Nambu et al., 1999), and (iii) a putative C-terminal CWBD (aa 198-774) made up of 7 GW (glycine-tryptophan) modules of 81-82 amino acids each containing a conserved GW dipeptide, which is similarly found in the C-terminal region of *L. monocytogenes* InlB (Braun et al., 1997), Ami (Milohanic et al., 2001), and Auto (Cabanes et al., 2004).

As shown by the results of a protein database similarity search with BLAST, IspC of *L. monocytogenes* serotype 4b is highly similar to Lin1064 of the nonpathogenic *L. innocua* Clip11262 (Glaser et al., 2001), with 83% amino acid identity. Comparison of the regions surrounding the *ispC* gene homologue *LMOf2365_1093* from *L. monocytogenes* serotype 4b strain F2365 (Nelson et al., 2004) with those surrounding the *Lin1064* gene of *L. innocua* Clip11262 (Glaser et al., 2001) revealed a highly conserved genome organization between the two species (Fig. 2-2), suggesting these two genes may have a common evolutionary ancestor or may arise by flowing from one species to another through a horizontal gene transfer mechanism. Interestingly, the IspC homologue is absent in *L. monocytogenes* EGDe (serotype 1/2a) (Glaser et al., 2001). The genetic diversity in *Listeria* strains may be an important factor accounting for the epidemiological observation that not all strains in all 13 serotypes of *Listeria* are equally important in human listeriosis, with serotypes 4b, 1/2a, and

FIG. 2-2. Genetic organization of the *ispC* gene homologue and its neighboring putative genes on the chromosomes of *L. monocytogenes* F2365 (serotype 4b) and nonpathogenic *L. innocua* Clip11262. LMOf2365_1093 and Lin1064 are the IspC homologue in *L. monocytogenes* serotype 4b strain F2365 and *L. innocua* Clip11262, respectively. Arrows and hairpins indicate the direction of transcription of putative genes and putative transcription terminators, respectively.

***L. monocytogenes* 4b F2365**

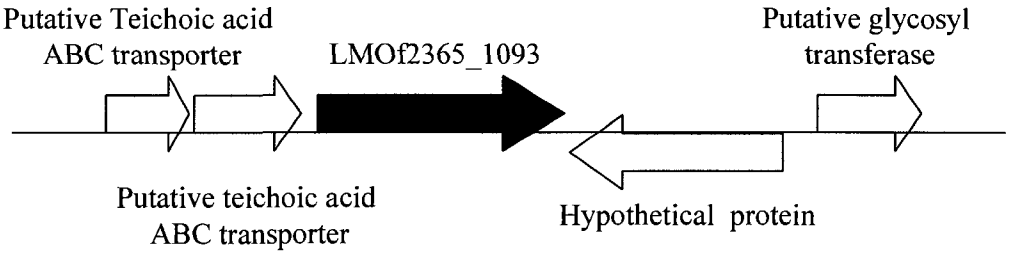

***L. innocua* Clip11262**

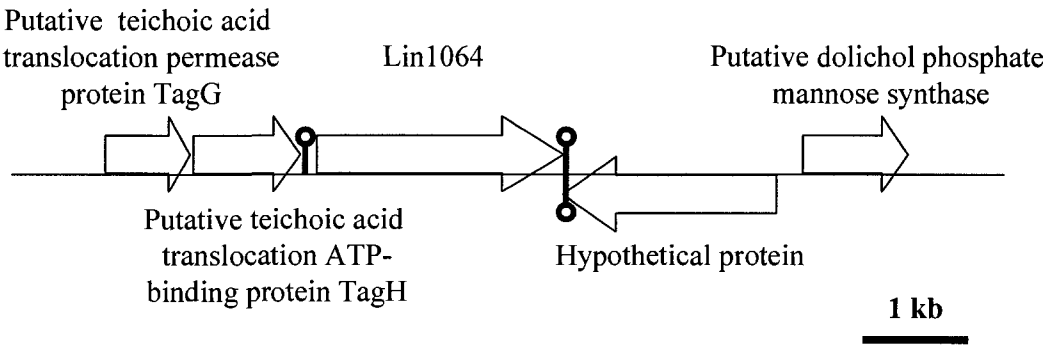

1/2b responsible for almost all human infection and with serotype 4b strains accounting for almost all major outbreaks and a large portion of sporadic cases (Donnelly, 2001; Lorber, 1997; Vines and Swaminathan, 1998).

2.3 Research Rationales and Hypotheses

The 86-kDa protein IspC of *L. monocytogenes* serotype 4b is targeted for study for several reasons. The recent study by Yu *et al.* (2007) concluded that IspC is one of several novel protein targets of the humoral immune response to infection with *L. monocytogenes* serotype 4b. Besides that knowledge, nothing is known about IspC. Further experimental studies on the biochemical, molecular and structural properties of IspC are necessary to expand our knowledge about the functionality of this novel protein. The observation that antibodies to IspC were present in RαL antisera from rabbits infected with live *L. monocytogenes* serotype 4b but not in RαK antisera from animals receiving heat-killed bacteria (Yu et al., 2007) leads to hypothesizing about lack or a low level of IspC expression in *in vitro* cultured *L. monocytogenes*. To test this, experiments are proposed to be conducted for the analysis of expression of IspC in bacteria during *in vitro* growth at the transcriptional and translational levels. The results of such experiments would provide additional information about regulated expression of IspC *in vivo* during infection.

Surface proteins of pathogenic bacteria are most likely the candidates targeted by the host immune response during infection. Given the fact that an antibody response to IspC was demonstrated in infected host (Yu et al., 2007) and that a putative peptidoglycan hydrolase domain and a putative cell wall binding domain were detected in the deduced amino acid sequence of IspC, it is hypothesized that IspC is a surface protein with peptidoglycan hydrolase activity (i.e., a surface autolysin). To test this hypothesis, immunological and biochemical experiments are proposed to localize IspC in *L. monocytogenes* and to analyze

the cell wall-hydrolyzing or –binding activity of the full-length protein or putative domains using various recombinant forms of IspC. These experiments would potentially lead to demonstration of IspC as a surface autolysin and would provide new insights into the biological function(s) of this protein.

Bacterial autolysins are involved in pathogenesis (Berry et al., 1989; Canvin et al., 1995; Lock et al., 1992; Mani et al., 1994), including p60 (Pilgrim et al., 2003), MurA (Lenz et al., 2003), Ami (Milohanic et al., 2001) and Auto (Cabanes et al., 2004) of *L. monocytogenes*. IspC is likely a surface autolysin with putative domain structures similar to that found in Ami and Auto. Furthermore, *L. monocytogenes* InlB is a well characterized virulence factor with its C-terminal CWBD made up of three GW modules involved in interaction with the host specific receptors GAGs and gC1q-R (Braun et al., 2000; Jonquieres et al., 2001). Similarly, the GW modules of Ami have been shown to be directly involved in pathogenesis through binding to unidentified host cell components (Milohanic et al., 2001). Based on these findings reported in the literature, it is hypothesized that IspC is a protein factor involved in *L. monocytogenes* virulence. To test this hypothesis, a genetic approach is proposed to generate an *ispC* knockout mutant with which virulence studies can be performed in mouse and cell culture infection models and with which proteomic and immunological analyses can be conducted to assess the effects of IspC deficiency on the display of surface proteins in *L. monocytogenes*. As well, purified recombinant IspC and its putative C-terminal CWBD would be tested *in vitro* for binding to selected eukaryotic cells, GAG heparin and gC1q-R. The results obtained from such studies would establish the role of IspC in *L. monocytogenes* pathogenesis. Given that (i) Ami contributes to bacterial adhesion to eukaryotic cells, whereas Auto is not involved in adhesion but contributes to the entry of *L. monocytogenes* into eukaryotic cells (Cabanes et al., 2004; Milohanic et al., 2001) and (ii) the homologue of

IspC is found in the nonpathogenic species *L. innocua* Clip11262 but absent in *L. monocytogenes* EGDe (serotype 1/2a) (Glaser et al., 2001), the present study may provide a better understanding of listerial autolysins in virulence.

2.4 Objectives

This present research focused on the biochemical, molecular and genetic characterization of the *ispC* gene and its gene product in an attempt to understand the biological function(s) of IspC and its role in *L. monocytogenes* pathogenesis. The specific aims are to (i) produce various recombinant forms of IspC (full-length and truncated) using molecular cloning techniques and raise rabbit polyclonal antibody to IspC, (ii) characterize the full length recombinant IspC (rIspC) using biochemical, molecular, mass spectrometry, CD and Raman spectroscopy approaches, (iii) localize IspC by immunofluorescence and immunogold transmission electron microscopy, (iv) determine if IspC functions as an autolysin and define its catalytic domain and cell wall binding domain, (v) study the *in vitro* expression of IspC in *L. monocytogenes* by time course RT-PCR and Western blots, (vi) create an isogenic in-frame *ispC* gene deletion mutant (Δ*ispC*) and investigate the biological functions of *ispC* and its role in virulence with the Δ*ispC* mutant in a mouse and cultured eukaryotic cell culture model, and (vii) analyze the interaction of rIspC and its C-terminal CWBD with selected eukaryotic cells, GAG heparin or cellular gC1q-R.

CHAPTER III

Materials and Methods

3.1 Bioinformatic Analysis of IspC

The secondary structure of IspC was analyzed by using the PSIPRED server (http://bioinf.cs.ucl.ac.uk/psipred/, accessed date 07/26/2007) and formation of disulfide bonds within the protein using DIpro (http://www.ics.uci.edu/%7Ebaldig/scratch/, accessed date 07/26/2007).

3.2 Bacterial Strains, Plasmids, and Growth Conditions

L. monocytogenes LI0521 (serotype 4b) and five *Escherichia coli* strains, DH5α, Rosetta (DE3)/pLysS, BL21 (DE3), BL21 (DE3)/pLysS, and ATCC 25922, were used in this study. *E. coli* strains were grown in Luria-Bertani (LB) broth or LB agar plates at 37 °C. *L. monocytogenes* was cultured in tryptic soy sheep blood agar (TSBA) plates, LB broth or agar plates containing 50 mM MOPS (morpholinepropanesulfonic acid) (pH 7.5) (LBMOPS) or brain heart infusion (BHI) broth or agar plates (Appendix 2). Antibiotics were added in broth or agar plates as required. For *E. coli* strains containing the plasmids pCR2.1 (Invitrogen, Burlington, Ontario, Canada) or pET-30a (Novagen, Madison, Wis.) or their derivatives, 30 μg/ml kanamycin was added to broth and 50 μg/ml kanamycin to agar plates; for *E. coli* strains containing pUC118 or its derivatives, 100 μg/ml carbenicillin was added to both broth and agar plates; for *E. coli* strains containing pAUL-A or its derivatives, 300 μg/ml erythromycin was added to both broth and agar plates. For *L. monocytogenes* containing pAUL-A derivatives, 5 μg/ml erythromycin was added to agar plates. Bacterial growth and cell number were determined by measuring the optical density (OD) at 590 nm (OD_{590}) for *E. coli* and the OD_{620} for *L. monocytogenes* with an OD_{620} of 0.61 equivalent to 1×10^9 bacteria/ml (Schlech, 1993). The cell number of *L. monocytogenes* was also estimated by plating of serial dilutions of bacteria.

3.3 Generation of Expression Constructs

All DNA manipulations were essentially performed according to established procedures (Sambrook and Russel, 2000).

3.3.1 pIspC

The *ispC* open reading frame (ORF) was amplified from the *L. monocytogenes* serotype 4b genomic DNA prepared as described in Appendix 2 by PCR with primer pair P398/P399 (Table 1; Wang and Lin, 2007) and Platinum Pfx DNA polymerase (Invitrogen) and then blunt-end cloned into the NdeI and XhoI sites of pET30a (Novagen). The resultant construct was designated pIspC.

3.3.2 pEAD1, pEAD2, and pEAD3

The constructs pEAD1, pEAD2, and pEAD3, coding for putative N-terminal catalytic domains (EAD1 [aa 58 to 197], EAD2 [aa 58 to 263], and EAD3 [aa 1 to 197], respectively) of IspC, were similarly generated by cloning into pET30a the coding sequences derived from pIspC by PCR with gene-specific primers (Table 1).

3.3.3 pGFPuv-CBD1, pGFPuv-CBD2, pGFPuv-CBD3, pGFPuv-CBD4, and pETGFPuv

The constructs pGFPuv-CBD1, pGFPuv-CBD2, pGFPuv-CBD3, and pGFPuv-CBD4, coding for putative cell wall binding domains (CBD1 [aa 198 to 774], CBD2 [aa 234 to 774], CBD3 [aa 249 to 774], and CBD4 [aa 264 to 774], respectively) of IspC fused to the C terminus of GFPuv, were generated using a two-step PCR strategy (Lin et al., 2004).

The CBD and GFPuv coding sequences derived from pIspC and pGFPuv (Clontech, Palo Alto, CA), respectively, were first amplified by primary PCR using Platinum Pfx DNA Polymerase System (Invitrogen) with gene-specific primers (Table 1). The PCR products purified from agarose gels using Wizard™ PCR Preps DNA Purification System (Promega, Madison, WI) were pieced together by a secondary PCR using primers P455 and P399. The fused DNA fragments and the GFPuv coding sequence derived from pGFPuv by PCR with

TABLE 1. List of primers used for the generation of various expression constructs, the Δ*ispC* mutant strain, and for RT-PCR.

Plasmid Constructs	**Primers used (5' to 3')[e]**
pIspC	P398 (F[a]): TGATAAATAAAAAGTGGATGA P399 (R[b]): **G**TTTAACGTTTGTAAAAGCTC
pETGFPuv	P455 (F): TGAGTAAAGGAGAAGAAC P456 (R): **G**TTTGTAGAGCTCATCCATG
pGFPuv-CBD1	P455 (F): TGAGTAAAGGAGAAGAAC P457 (R): CATATTTGGCTTTGTAGAGCTCATCCATG P458 (F): GCTCTACAAAGCCAAATATGATGTTTTATACG P399 (R): **G**TTTAACGTTTGTAAAAGCTC
pGFPuv-CBD2	P455 (F): TGAGTAAAGGAGAAGAAC P459 (R): CTCCTTTTACTTTGTAGAGCTCATCCATG P460 (F): GCTCTACAAAGTAAAAGGAGTGCAATCTG P399 (R): **G**TTTAACGTTTGTAAAAGCTC
pGFPuv-CBD3	P455 (F): TGAGTAAAGGAGAAGAAC P461 (R): CGATATCCTTTTTGTAGAGCTCATCCATG P462 (F): GCTCTACAAAAAGGATATCGATTTAGTATCTG P399 (R): **G**TTTAACGTTTGTAAAAGCTC
pGFPuv-CBD4	P455 (F): TGAGTAAAGGAGAAGAAC P463 (R): ATTGATAGTATTTGTAGAGCTCATCCATG P464 (F): GCTCTACAAATACTATCAATTTAAATATAATGG P399 (R): **G**TTTAACGTTTGTAAAAGCTC
pEAD1	P465 (F): **TG**ATAGCACCTGCTGCCCAG P466 (R): **G**TAAATCATAATTCTCAATTAC
pEAD2	P465 (F): **TG**ATAGCACCTGCTGCCCAG P467 (R): **G**CGTACCTCTCTTTGTTG
pEAD3	P398 (F): TGATAAATAAAAAGTGGATGA P466 (R): **G**TAAATCATAATTCTCAATTAC
RT-PCR Targets	
16S rRNA	P394 (F): TTAGCTAGTTGGTAGGGT P395 (R): AATCCGGACAACGCTTGC
ispC mRNA	P304 (F): GATGGTAAAGTCATTGGCTG P285 (R): TTAGCCTCGCGTATCAACTG

Construction of the Δ*ispC* mutant strain	
pAUL-A-517/518	P517 (F): **ATC*GAGCTC***AGGAAAATCAAAAAGCTCCTCA P496 (R): TAAAAGCTCGATTTATCATTATTCTCCAACCA P495 (F): AATGATAAATCGAGCTTTTACAAACGTTAAATAGAC P518 (R): **AAA*GTCGAC***TGAGTGGAAAGGCTATGCTG[d]
Confirmation of the deletion of *ispC* in the Δ*ispC* mutant genome by PCR	P304 (F): (see above) P285 (R): (see above) P481 (F): CAGCACAAGAAGTTGCTCAAAA P518 (R): (see above)

[a] F, forward primers.

[b] R, reverse primers.

[c] SacI restriction enzyme site (bold, italic, and solid-underlined).

[d] SalI restriction enzyme site (bold, italic, and solid-underlined).

[e] Additional nucleotides have been included at the 5' ends of several primers to generate fusions by overlap PCR (solid-underlined) or to ensure in-frame cloning (bold and underlined) into the NdeI and XhoI sites of pET30a, or to ensure the cleavage efficiency of restriction enzymes (bold).

the primers P455 and P456 were blunt-end cloned into the *Nde*I and *Xho*I sites of pET30a. The resultant constructs were designated pGFPuv-CBD1, pGFPuv-CBD2, pGFPuv-CBD3, pGFPuv-CBD4 and pETGFPuv.

3.4 Expression of Recombinant Proteins in *E. coli*

The expression constructs were introduced using an established transformation procedure into *E. coli* Rosetta (DE3)/pLysS for the expression of IspC, BL21 (DE3)/pLysS for the expression of EADs, or BL21 (DE3) for the expression of GFPuv-CBD fusions and GFPuv, respectively. The overnight cultures of *E. coli* harboring one of the expression constructs were diluted 1:100 into 250 ml of fresh LB broth supplemented with kanamycin (30 μg/ml) and incubated at 37 °C with vigorous shaking until the culture reached an OD_{590} of 0.45 ± 0.05 (IspC) or 0.6 ± 0.1 (EADs, GFPuv-CBDs, and GFPuv). IPTG (isopropyl-β-D-thiogalactopyranoside) (1 mM) was added to induce expression of recombinant proteins under predetermined optimal conditions: for IspC, induction was carried out at 37 °C for 2 h and then at 4 °C overnight; for EADs, induction was performed at 37 °C for 3 h; for GFPuv-CBD fusions and GFPuv, the culture was induced at room temperature for 4 h and then at 4 °C overnight. The cells were harvested by centrifugation at 16,900 × g at 4 °C for 10 min and frozen at -80 °C for protein purification.

3.5 Recombinant Protein Purification

All the recombinant proteins were found to be expressed in soluble form in *E. coli* and were thus purified under native conditions. The -80 °C frozen cell pellets from 2 L of culture were resuspended in a minimum volume of phosphate-buffered saline (PBS) (pH 7.2) containing 1 mM PMSF (phenylmethylsulfonyl fluoride) and lysed by passage through a French press at 1500 lb/in^2. The homogenates were spun at 27,000 × *g* at 4 °C for 20 min.

The supernatant, mixed with an equal volume of buffer A (50 mM NaH_2PO_4, pH 8.0, 300 mM NaCl, 20 mM imidazole), were applied at 1 ml/min to a column (1 by 1.5 cm) of Ni-nitrilotriacetic acid (Ni-NTA) superflow (Qiagen, Mississauga, Ontario, Canada) that had been attached to a BioRad Econo System and pre-equilibrated with buffer A. The column was washed with 30 ml of buffer A, and the proteins were eluted in 1 ml per fraction with 30 ml of buffer B (25 mM NaH_2PO_4–NaOH, 250 mM imidazole, pH 8.0). The absorbance at 280 nm was monitored online for eluted proteins. The concentrations of purified proteins were determined by using the Bradford method (Bradford, 1976) with bovine serum albumin (BSA) as a standard.

For further purification of recombinant IspC (rIspC), the A_{280} peak fractions containing the target protein, judged by SDS–PAGE and Western blot analysis, were pooled and loaded at 1 ml/min into a column (1 by 2 cm) of SP Sepharose Fast Flow (Amersham, Baie d'Urfe, Quebec, Canada) which had been pre-equilibrated with buffer C (10 mM phosphate buffer, pH 8.0, 5% glycerol). After washing with at least 10 times bed volume of buffer C, the rIspC was eluted in a sharp A_{280} peak following a linear 0–500 mM NaCl gradient in buffer C (30 ml; fraction size, 1 ml). The fractions containing rIspC were assessed for its purity by SDS–PAGE, pooled, and determined for protein concentration as above.

Purified proteins were concentrated and stored in 40% glycerol at -20 °C. Prior to use, when required, the stored proteins were dialyzed against appropriate solutions as described in separate experiments and sterilized using a 0.2 μm filter.

3.6 SDS-PAGE and Western blots

Sodium dodecyl sulfate-polyacrylamide gel electrophoresis (SDS-PAGE) was performed as described by Laemmli (Laemmli, 1970), using a 4% stacking gel and a 12% resolving gel in a BioRad minigel apparatus or BioRad Protein® II xi Cell (Bio-Rad,

Mississauga, Ontario, Canada). Following electrophoresis, the separated proteins were either stained with Coomassie blue or electrotransferred onto a nitrocellulose membrane by using a Trans-Blot SD semidry transfer cell (Bio-Rad) according to the manufacturer's instructions. The Western blot procedure for analysis of the target proteins with specific primary antibodies followed by peroxidase-conjugated goat anti-mouse or –rabbit immunoglobulin G (IgG) (Jackson ImmunoResearch Laboratories, West Grove, Pa.) was performed essentially as described previously (Lin et al., 2006).

3.7 Production of Polyclonal Anti-IspC Antibody

After collection of preimmune sera, two New Zealand female rabbits at the age of 2 to 3 months were immunized intramuscularly with the purified rIspC (~100 μg) emulsified with an equal volume of complete Freund's adjuvant on day 0. Booster injections with the same immunogen (~50 μg per rabbit) emulsified in incomplete Freund's adjuvant were subcutaneously administered on days 14 and 28. Two weeks after the final injection, both animals were sacrificed to obtain a maximal volume of blood through cardiac puncture. Following removal of the clotted blood cells by centrifugation, anti-IspC immune sera (designated RαIspC) were collected and stored at –20 °C until use.

3.8 Estimation of rIspC Extinction Coefficient

The molar extinction coefficient (ε) of rIspC at 280 nm was calculated from its amino acid sequence (i.e., the number of tryptophan, tyrosine, and cysteine residues within the protein) (Wang and Lin, 2007; Yu et al., 2007) according to the method of Gill and von Hippel (Gill and von Hippel, 1989).

3.9 N-terminal Sequencing

The N-terminal sequence of purified rIspC was determined using Edman degradation chemistry. Following separation of the purified protein by SDS-PAGE and electrotransfer

onto a PVDF membrane as described (Lin et al., 1997), the protein band was visualized by staining with 0.1% (w/v) Ponsceau S and excised for N-terminal sequencing performed at the Biotechnology Research Institute, National Research Council Canada (Montreal, Quebec, Canada).

3.10 Mass Spectrometry Analysis

Electrospray ionization (ESI) mass spectrum was acquired on Waters Micromass Global Q-TOF mass spectrometer coupled to a Waters capillary HPLC (Milford, Massachusetts, USA). The mass spectrometer was calibrated with a mixture of proteins: [glu^1]-fibrinopeptide B human, horse heart myoglobin, and chicken lysozyme (Sigma, St. Louis, MO). The calibration for intact protein analysis was checked by running Cytochrome C, which resulted in a mass accuracy of ± 1 amu. The purified IspC at a concentration of 1 pmol/μL in water was loaded onto an Atlantis dC18 trap with a 50 μm ID silica tubing in the place of a column. The autosampler parameters included a sample loading flow rate of 15 μL/min for 3 min, which was reduced to 5 μL/min for the remainder of the run. The gradient was delivered at a flow rate of 7 μL/min, which was split to a flow rate through the column of 300 nL/min. The linear binary gradient was formed from A: 2% (v/v) acetonitrile + 0.2% (v/v) formic acid (FA) and B: 90% (v/v) methanol + 0.5% (v/v) acetic acid. The gradient profile was 2% B for 3 min, increased to 100% over the time interval 3.0 to 12.0 min. The system was maintained at 100% B for 1.5 min, then returned to 2% B in 0.5 min and allowed to re-equilibrate for 15.4 min. The concentrated sample was also infused directly after dilution 1:4 with the injection buffer (0.2% [v/v] FA + 0.5% [v/v] trifluoroacetic acid) and run on the mass spectrometer operated in the positive ion electrospray mode over the mass range 500 to 2000 amu in the continuum mode, with a scan time of 5.0 sec and an interscan time 0.1 sec. Other instrument parameters include a capillary voltage of 3.5 kV and a cone

voltage of 100 V. Data acquisition and analysis were accomplished using the MassLynx version 4.1 software. Deconvolution of the positive ESI mass spectra was accomplished using MaxEnt1®.

3.11 Circular Dichroism Spetroscopy

The circular dichroism (CD) spectra of purified rIspC in PBS was recorded on a JASCO J-600 Spectropolarimeter (JASCO Co. Ltd., Victoria, BC, Canada) in a 0.5 mm quartz cuvette at ambient temperature (20–22 °C) with a scanning speed of 20 nm/min in the far UV spectral region (190.0 – 260.0 nm). The rIspC was used at a concentration of 1.6×10^{-6} M, calculated from an absorption at 280 nm (OD_{280}) of 0.285 using an extinction coefficient of 1.7851×10^{5} M^{-1} cm^{-1} (Wang et al., 2007). Four CD scans were collected and averaged, and the data were smoothed by the JASCO software. Data were expressed as mean residue ellipticity $[\theta] \times 10^{-3}$ (deg cm^2 $dmol^{-1}$).

3.12 Raman Spectroscopy

The purified rIspC (2 µl) in PBS at a concentration of 5.6×10^{-6} M (OD_{280} 1.0) was spotted onto a piece of clean CaF_2 substrate and allowed to dry. PBS (2 µl) was used as a control. Raman spectra were acquired on a LabRAM HR VIS-NIR microRaman spectrometer (Horiba Jobin Yvon, Edison, NJ) equipped with a software controlled XY stage and a thermal-electric cooled CCD detector, with an excitation at 633 nm and a power of 3 mW focused down to 1 mm diameter spot with a 100 × objective. Raman spectra of rIspC were acquired with the parameter, 15 sec × 4 accumulation. Raman spectra of CaF_2 substrate and PBS (2 µl) spotted on the substrate were acquired similarly.

3.13 Renaturing SDS-PAGE Analysis

Full-length rIspC, its putative catalytic domains, or bacterial surface protein extracts

from an early-log growth phase culture were analyzed for the peptidoglycan hydrolase activity by using a renaturing SDS-PAGE procedure modified from that described by Potvin *et al.* (Potvin et al., 1988). Briefly, the proteins were electrophoretically separated on 12% SDS-polyacrylamide gels containing one of the following autoclaved, lyophilized bacteria: 0.2% (w/v) *Micrococcus lysodeikticus* ATCC 4698 (Sigma), 0.2% (w/v) *E. coli* ATCC 25922, or 0.1% (w/v) *L. monocytogenes* serotype 4b. Following electrophoresis, gels were rinsed with deionized H_2O (dH_2O) and incubated in a renaturing buffer at room temperature for 16 to 48 h with gentle shaking. For routine analysis, proteins were renatured in gels with 25 mM Tris-HCl (pH 7.5) containing 1% (v/v) Triton X-100. To determine the pH optimum for the hydrolytic activities of IspC or its EADs, various renaturing buffers (50 mM sodium citrate-citric acid buffer, 1% [v/v] Triton X-100, pH 3 to 6; 10 mM Tris-HCl, 1% [v/v] Triton X-100, pH 7.5 to 9.0; and 50 mM glycine-NaOH buffer, 1% [v/v] Triton X-100, pH 10) were used. After renaturing, the gels were rinsed with dH_2O, stained with 0.1% (w/v) methylene blue (Fisher, Ottawa, Ontario, Canada) in 0.01% (w/v) KOH for 1 h at room temperature with gentle shaking, and destained with dH_2O. The appearance of clear bands on a blue background gel indicates hydrolytic activity.

3.14 Detection of IspC Expression in *in vitro* Cultured *L. monocytogenes*

Expression of *ispC* in *L. monocytogenes* was analyzed during *in vitro* growth over a 22 h time course, at the transcriptional level by reverse transcription-PCR (RT-PCR) and at the translational level by Western blotting. An overnight culture of *L. monocytogenes* was subcultured at a dilution of 1:100 in 2 L of LBMOPS at 37°C. Bacterial samples (total RNA extraction, 4 ml; total cell protein preparation, a volume containing cells equivalent to 50 ml of culture with an OD_{620} of 0.5) were harvested by centrifugation at different time points of the growth curve (i.e., different OD_{620} values) and stored at –80 °C until use. Total RNA was

isolated from each frozen sample by using an RNeasy minikit (Qiagen) according to the supplier's protocol for the isolation of total RNA from bacteria and quantified on a UV-Visible Thermo Spectronic BioMate 3 spectrophotometer (Thermo Spectronic, Rochester, NY). Prior to RT-PCR, RNA samples were treated with RQ1 RNase-free DNase (Promega) as per the manufacturer's instructions. cDNA, synthesized from 100 ng total RNA by reverse transcription with random hexamers and a ThermoScript RT-PCR system (Invitrogen), was used for PCR detection of the *ispC* transcript in each sample with gene-specific primers P285 and P304 (Table 1) in a 100 µl of reaction mixture: 1 × PCR minus Mg buffer (Invitrogen), 0.2 mM dNTPs, 3 mM $MgCl_2$, 0.25 µM of each primer, cDNA, and 0.05 U/µl of Taq DNA polymerase. The reaction mixtures were incubated in a thermocycler for 2 min at 94 °C, followed by 35 cycles of 30 sec at 94 °C, 45 sec at 55 °C, and 2 min at 72 °C, with a final extension at 72 °C for 10 min. The PCR products were analyzed by electrophoresis in a 1% agarose gel. DNase-treated RNA before the RT step was analyzed by PCR as a control to ensure that there was no genomic DNA contamination. The level of 16S rRNA in each RNA sample, as determined by RT-PCR with primers P394 and P395 (Table 1), was used as an internal control. For Western blot analysis of IspC, frozen cells of each sample were resuspended in 1 ml of extraction buffer (62.5 mM Tris-HCl [pH 6.8], 2% [w/v] SDS, 1 mM phenylmethylsulfonyl fluoride), sonicated 10 times on ice for 30 sec each with 1-min intervals, mixed with an equal volume of 2 × SDS-PAGE sample buffer (Appendix 2), and boiled for 10 min. After removal of cell debris by centrifugation at 14,100 × g for 1 min, the supernatant was analyzed by Western blotting probed with RαIspC.

3.15 Immunofluorecence and Immunogold Transmission Electron Microscopy

Surface proteins of *L. monocytogenes* were detected by immunofluorecence and

immunogold transmission electron microscopy. Briefly, one colony of *L. monocytogenes* from TSBA plate was inoculated into LBMOPS broth (for IspC) or BHI (for ActA) and incubated overnight at 37°C with shaking. The overnight culture was subcultured at a dilution of 1:100 at 37°C with shaking. Live bacteria (3.6×10^8) from the mid-log growth phase were harvested by centrifugation at 10,000 × g for 3 min and washed three times with PBS, blocked with PBS containing 3% BSA for 0.5 h. Bacteria were incubated with anti-IspC or -ActA rabbit antiserum at 1:500 in PBS containing 3% BSA for 1 h. Rabbit pre-immune serum was used at the same dilution as negative control. Following three times washing, bacteria were stained with FITC (fluorescein isothiocyanate)-conjugated goat anti-rabbit IgG at 1: 500 (ICN Biomedicals, Costa Mesa, CA) or at 1:50 (Zymed Laboratories, S. San Francisco, CA) in PBS containing 3% BSA for 0.5 h. Bacteria were washed with PBS and resuspended in 200 µl of PBS. The bacterial suspension (9 µl) was spotted to a glass slide, covered with a glass (20 mm × 20 mm), and sealed with cytoseal (Richard-Allan Scientific, Kalamazoo, MI). Fluorescence images of bacteria were viewed and captured using a Leica DMRXA digital microscope (Leica Microsystems, Richmond Hill, Ontario, Canada).

The procedures of immunogold transmission electron microscopy analysis were almost the same as above except that following primary antibody incubation, bacteria were stained with 12-nm colloidal gold-conjugated goat anti-rabbit IgG (Jackson ImmunoResearch Laboratories) at 1:30 dilution in PBS containing 3% BSA for 0.5 h. Bacteria were washed three times with PBS followed by washing once with water, and then resuspended in 50 µl of water. Carbon-stabilized Nickel grids were placed into one drop (20 µl) of bacteria suspension for 10 min and the excessive liquid was removed using filter paper. Then bacteria

were stained with 0.5% uranyl acetate for 5 sec and viewed on a transmission electron microscope (TEM; Hitachi H-7000 Electron Microsope).

3.16 TCA Precipitation of Culture Supernatant Proteins

Proteins were recovered by trichloroacetic acid (TCA) precipitation from the culture supernatant of *L. monocytogenes* grown overnight in LBMOPS broth for analysis of the presence of IspC. To each 1.2 ml of the chilled supernatant, bovine serum albumin (20 μg, heat treated at 100 °C for 5 min) and ice-cold TCA (250 μl, 100% [w/v]) were added, and the supernatant was incubated on ice for 4 h. The precipitated proteins from 4.8 ml of the culture supernatant were collected by centrifugation at room temperature at 14,100 × g for 10 min, washed with ice-cold acetone (500 μl), and air dried. The protein pellets were dissolved in 60 μl of 2 × SDS-PAGE sample buffer and subjected to Western blot analysis, with probing with RαIspC.

3.17 Cell Wall Binding Domain Analysis

Binding of GFPuv-CBDs to the cell wall (surface) of *L. monocytogenes* was investigated by using a modification of the method of Loessner *et al.* (2002). Briefly, live bacteria (6×10^8 cells) were harvested from the late exponential growth phase by centrifugation, washed twice with PBS (pH 8.0) containing 0.01% (v/v) Tween 20 (PBS-T), and resuspended in 1 ml of PBS-T. Purified GFPuv-CBD fusion proteins were normalized by measurement of fluorescence at 512 nm with excitation at 396 nm on a LS50B luminescence spectrometer (Perkin-Elmer, Montreal, Quebec, Canada), using purified GFPuv as a standard. GFPuv-CBD fusions and GFPuv (control), each at an equal molar concentration (0.564 nM), were added into 100 μl of the above-described cell suspension, incubated for 5 min at room temperature, washed three times with PBS-T, and resuspended in 250 μl of PBS.

Fluorescence images of bacterial cells complexed with GFPuv-CBD fusions were viewed and captured as described above.

3.18 Construction of an *ispC* in-frame Deletion Mutant

A Δ*ispC* mutant was constructed by homologous recombination using a *L. monocytogenes* serotype 4b strain LI0521 as the parental strain (Fig. 3-1). Briefly, a DNA fragment composed of the 453-bp sequence upstream of the *ispC* ORF and the first 3 codons was derived by PCR from the *L. monocytogenes* genomic DNA with the primer pair P517 and P496 (Table 1). A DNA fragment containing the 405-bp sequence downstream of the *ispC* ORF and the last 8 C-terminal codons was similarly obtained by PCR with the primer pair P495 and P518 (Table 1). The two PCR fragments were spliced together using the sequence complimentarity between the primers P495 and P496 as described (Wang and Lin, 2007), resulting in an internal deletion of a 764-amino acid coding sequence within *ispC*. The fused DNA fragment was inserted into the SacI and SalI sites of pAUL-A. The resulting recombinant plasmid was introduced by electroporation into competent *L. monocytogenes* that had been prepared as described (Park and Stewart, 1990). The generation of the Δ*ispC* mutants was performed as described (Schaferkordt et al., 1998; also see the detailed procedures in Appendix 2). The mutants were confirmed by PCR analysis of the genomic DNA using the primer pair internal to the deletion region P304 and P285 and the primer pair external to the deletion region P481 (Table 1) and P518 and by sequencing the PCR products.

3.19 Extraction of Total Bacterial Proteins

The Δ*ispC* mutant and WT strains of early-log growth phase equivalent to 5 ml of culture with an OD_{620} of 1.0 were collected and treated with chloramphenol at 20 μg/ml to inhibit protein synthesis. Bacterial pellets were washed twice with ice-cold PBS containing

FIG. 3-1. Schematic representation of the construction of an *ispC* in-frame deletion mutant strain (Δ*ispC*). **(A)** Generation of the recombinant plasmid pAUL-A-517/518 carrying an in-frame deleted *ispC* version. A DNA fragment composed of the 453-bp sequence upstream of the *ispC* ORF and the first 3 codons was derived by PCR from the *L. monocytogenes* serotype 4b genomic DNA with the primer pair P517 and P496. A DNA fragment containing the 405-bp sequence downstream of the *ispC* ORF and the last 8 C-terminal codons was similarly obtained by PCR with the primer pair P495 and P518. The two PCR fragments were spliced together by a second PCR using the sequence complimentarity between the primers P495 and P496, resulting in an internal deletion of 764-amino acid coding sequence within *ispC*. The fused DNA fragment was inserted into the SacI and SalI sites of pAUL-A, thus giving rise to the recombinant plasmid pAUL-A-517/518. **(B)** Construction of a Δ*ispC* mutant by homologous recombination using a *L. monocytogenes* serotype 4b strain as the parental strain. The resulting plasmid pAUL-A-517/518 was next introduced by electroporation into the competent wild type *L. monocytogenes* serotype 4b. Integration of the recombinant plasmid into bacterial chromosome was achieved by incubation of the transformant at 42 °C in the presence of erythromycin (Em). A second intracellular homologous recombination was obtained by incubation of the integrated bacteria in broth at 30 °C in the absence of Em. The excised plasmid was removed by incubation at 42 °C in the absence of Em. Bacteria were then screened for Em-sensitive clones by inoculation of bacteria on agar plates with or without Em. Lastly, the mutants were confirmed by PCR analysis of the genomic DNA using the primer pair P304 and P285 internal to the deletion region and the primer pair P481 and P518 external to the deletion region and by sequencing the PCR products.

A

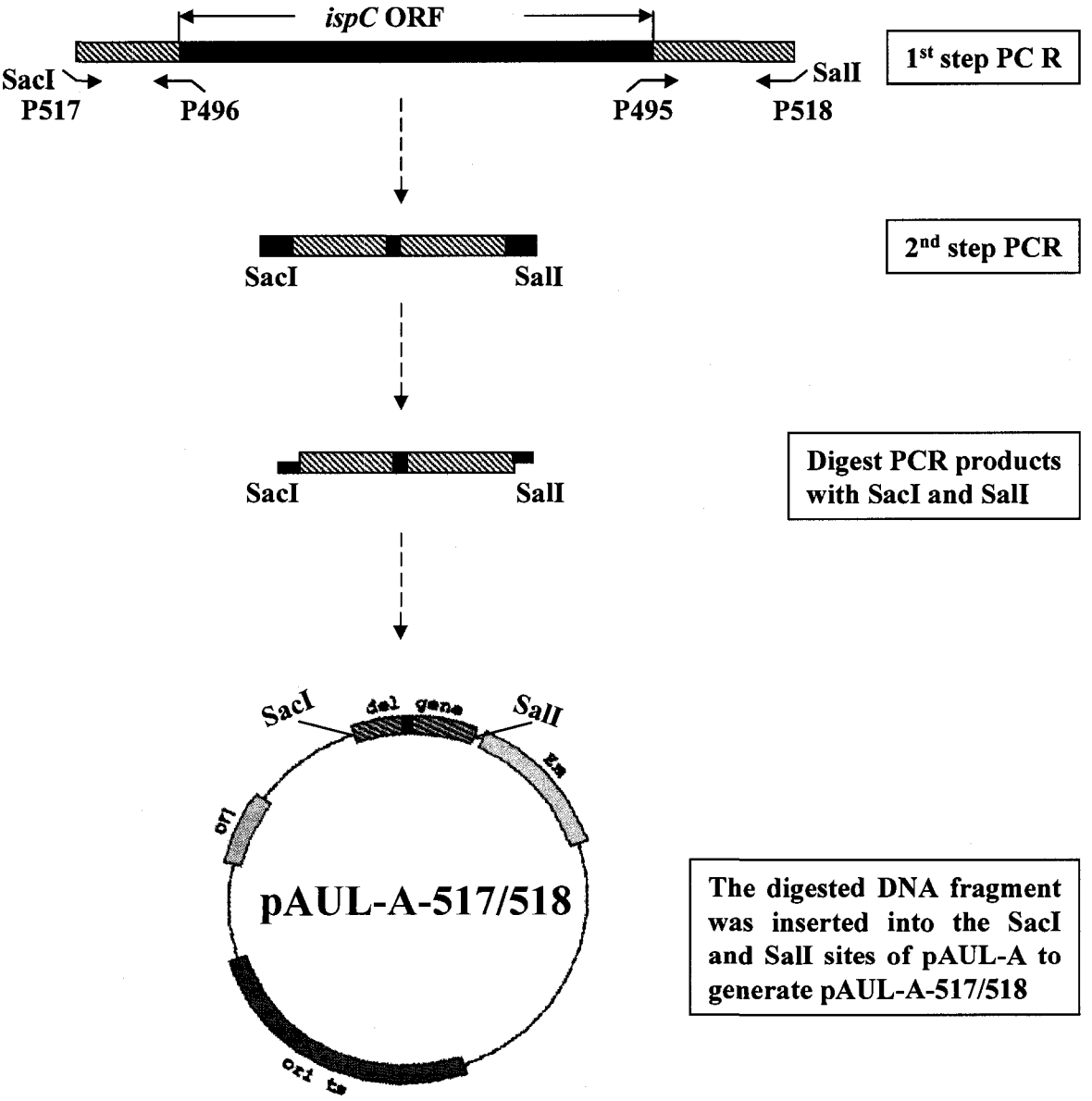
ispC ORF
SacI
P517
P496
P495
SalI
P518
1st step PC R
SacI
SalI
2nd step PCR
SacI
SalI
Digest PCR products with SacI and SalI
SacI
del gene
SalI
ori
pAUL-A-517/518
ori te
The digested DNA fragment was inserted into the SacI and SalI sites of pAUL-A to generate pAUL-A-517/518

B

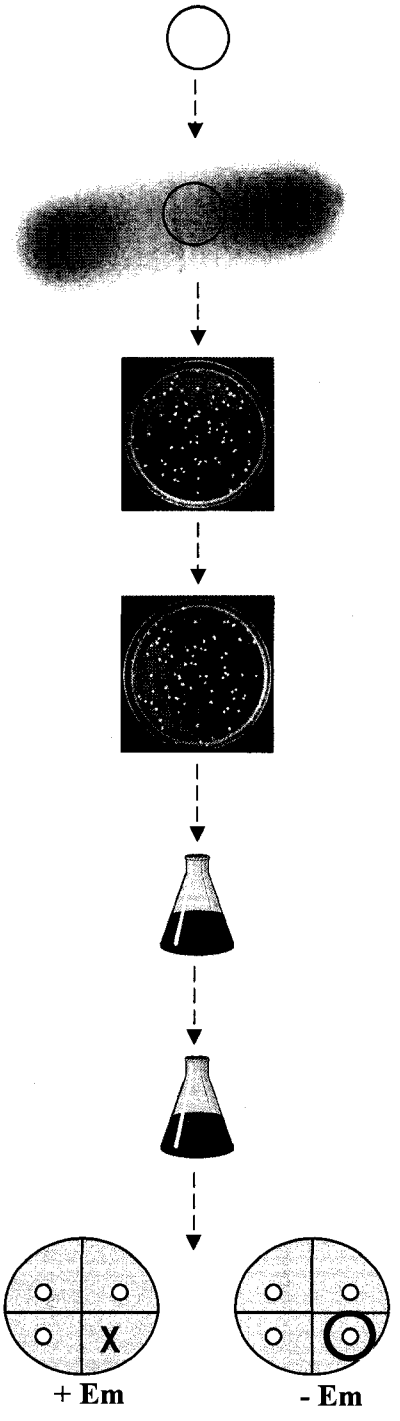

pAUL-A-517/518

Transformation of pAUL-A-517/518 into competent *L. monocytogenes* serotype 4b

Grow transformants (30 °C, Em)

Integration (42 °C, Em)

A second intracellular homologous recombination (30 °C)

Remove the excised plasmid (42 °C)

Screen for Em-sensitive clones

proteinase inhibitor cocktail (Roche, Laval, Québec, Canada) and 20 μg/ml chloramphenicol (PBS-CC), resuspended in 500 μl of PBS-CC, and stored at -80 °C. Frozen cells were thawed on ice, transferred into FastProtein Blue tubes (Q-BIOgene, Carlsbad, CA) and lysed on a FastPrep apparatus FP120 (Q-BIOgene) with 5 bursts of 45 sec on setting 6.5. Tubes were chilled on ice between bursts and the cell lysates were boiled for 10 min after addition of 500 μl of 2 × SDS-PAGE sample buffer. Supernatant was collected by centrifugation at 14,100 × g for 3 min at room temperature and stored at -20 °C until use.

3.20 Extraction of Bacterial Surface Proteins

The Δ*ispC* mutant and WT strains equivalent to 50 ml of culture with an OD_{620} of 0.5 were collected at various growth phases (early-log, mid-log, late-log and stationary) and washed with PBS-CC. Cell pellets were resuspended in 1 ml of 2 × SDS-PAGE sample buffer and boiled for 10 min. The supernatant containing surface-extracted proteins were collected by centrifugation at 14,100 × g for 5 min and stored at -20 °C until use.

3.21 Confirmation of the Δ*ispC* Mutant at the Protein Level

Surface expression of IspC was examined by immuofluorescence microscopy analysis of live bacteria (the Δ*ispC* mutant and the WT) probed with RαIspC as described above. The total protein extracts (see below) from the mutant and WT strains were analyzed for the presence of IspC by Western blot using RαIspC. The bacteriolytic activity of the WT and the Δ*ispC* mutant was assessed by analysis of the cell surface protein extracts (see below) equivalent to 1 ml of culture with an OD_{620} of 1.0 in a 12% renaturing SDS-PAGE gel containing 0.2% (w/v) autoclaved *M. lysodeikticus* ATCC 4698.

3.22 Passage of *L. monocytogenes* in Mice

The Δ*ispC* mutant and WT strains were passed *in vivo* in mice to eliminate the

possibility that *in vitro* growth may reduce the bacterial virulence. Both strains (100 µl) at a concentration of 2×10^5 cells/ml in PBS were intravenously inoculated into 6- to 8-week-old female specific pathogen-free BALB/c mice. At day 3, the mice were euthanized to remove livers, which were then homogenized in 1% (w/v) buffered peptone water (BPW) and plated at various dilutions onto BHI agar plates. A single colony of each strain was inoculated into BHI broth, grown overnight, and subcultured at a 1:100 dilution to reach an OD_{620} of 0.8. Bacteria were washed once, resuspended in PBS at appropriate concentrations, and stored in 1-ml aliquots in PBS containing 15% glycerol at -80 °C until use.

3.23 Phenotypic Analysis

Comparative phenotypic analysis of the Δ*ispC* mutant and the WT with respect to their *in vitro* growth, and biochemical and morphological characteristics was performed. (i) The growth curve was established by subculturing each strain at the same starting concentration from the overnight culture in triplicates in 50 ml of BHI broth (pH 7.2), BHI broth (pH 7.2) containing 0.3 M NaCl (osmotic stress), and BHI broth (pH 4.5, acidic stress). Samples of cultures were taken at various time points for 48 h for measuring the OD_{620}. (ii) Catalase test, CAMP test (*S. aureus* and *Rhodococcus equi*), H_2S test, oxidase test, nitrate reduction test, and motility test (25 °C and 35 °C) were conducted according to established methods (MacFaddin, 2000). Carbohydrate utilization under fermentation and oxidative conditions was tested by using API 50 CH strips (BioMérieus, La Balme les Grottes, France) using CHB/E medium according to the manufacturer's instructions. (iii) Colony morphology of the mutant was examined by culturing bacteria on TSBA plates. Microscopic morphology of bacterial cells was examined at various phases of growth (i.e., early-log, mid-log, late-log, and stationary phases) using phase contrast light microscopy and TEM. For sectional TEM, 1

ml of bacteria were harvested at the mid-log phase (OD_{620} of 0.83), washed with PBS, and fixed in 2.5% glutaraldehyde in 0.1 M sodium phosphate buffer (pH 7.4). Bacteria were then embedded in 4% low melting agarose, cut into ~1 mm^3 blocks, and postfixed in 1% osmium tetroxide in the same buffer at room temperature for 1 h. Following washing with dH_2O and en bloc staining with 3% (w/v) aqueous uranyl acetate for 2 h, bacteria were dehydrated through a graded ethanol series and embedded in epon. Thin sections were stained with 3% (w/v) uranyl acetate for 20 min followed by 0.4% (w/v) lead acetate for 10 min. Electron micrographs were obtained on a Hitachi H-7000 transmission electron microscope at an accelerating voltage of 75 kV.

3.24 Analysis of Cell Surface Proteins by Mass Spectrometry and Western Blots

Bacterial surface proteins (150 µl) from each of the Δ*ispC* mutant and WT strains were separated by SDS-PAGE using a 4% stacking gel and a 12% resolving gel on a Protein® II xi system (Bio-Rad) and stained with Coomassie brilliant blue. Resolved protein bands of interest were excised from the WT samples and subjected to in-gel tryptic digestion for LC-MS/MS analysis as described (Vasilescu et al., 2005). The MS/MS data was then analyzed against the NCBI database using the Mascot search engine. Western blot analysis of surface proteins was performed using rabbit anti-InlA, anti-InlB, anti-ActA, and anti-InlC2 antibodies.

3.25 *In Vivo* Virulence Assay

Six- to 8-week-old specific pathogen-free female BALB/c mice were used for *in vivo* infection experiments with the Δ*ispC* mutant and the WT. For each bacterial strain, four groups of six mice each were intravenously inoculated with 5×10^4 bacteria in 100 µl of PBS. Brains, livers, and spleens were aseptically removed from one particular group (n = 6) after

euthanization for the determination of bacterial number in the organs at 6, 24, 48 and 72 h post infection. The organs were homogenized in 5 ml of 1% (w/v) BPW using a Stomacher Lab Blender Model 80 (VWR, Montreal, Québec, Canada) and plated on BHI agar plates with 0.1 ml of homogenates at 10-fold serial dilutions. Bacteria were enumerated after incubation at 37 °C for 24 h.

3.26 Cell Lines and Cell Culture

Both normally nonprofessional phagocytic cells (human colon carcinoma enterocyte-like epithelial cell line Caco-2, human hepatocellular carcinoma cell line Hep-G2, African green monkey kidney cell line Vero, human embryonic lung fibroblast L132, murine fibroblast L2, human cervical epithelial cell line Hela, sheep choroid plexus (SCP) epithelial cells, and human brain microvascular endothelial cells (HBMEC) and professional phagocytic cells (murine macrophage cell line J774), were used in this study and passed in tissue culture flasks. Eukaryotic cells except HBMEC were grown in MEM complete medium (1 × Minimal Essential Medium supplemented with 10% (v/v) heat-inactivated fetal bovine serum (FBS) or 5% (v/v) horse serum for SCP, 0.1 mM nonessential amino acids, 2 mM L-glutamine, and 0.15% (w/v) sodium bicarbonate). Sodium pyruvate was added at 1 mM into the MEM complete medium for Hep-G2 cell line only. HBMEC (Cell Systems Corp., Kirkland, WA) was cultured on gelatin-coated surface in CS-C complete medium according to the manufacturer's instructions. Cells were grown at 37 °C and 5% CO_2 in a humid CO_2 incubator.

3.27 Adhesion, Invasion, and Intracellular Growth Assays

The ability of bacteria to adhere to, invade and grow within eukaryotic cells was assessed basically as described (Bergmann et al., 2002; Rowan et al., 2000), with some minor modifications. The nonprofessional phagocytic cells were used in adhesion and

invasion assays, while J774 was used only in the adhesion assay. Vero, Hela and J774, nonprofessional or professional phagocytic cells, were used in an intracellular growth assay. Briefly, 2×10^5 cells (1×10^5 for HBMEC cells) were seeded in 24-well tissue culture plates (VWR) and grown for 48 h. Prior to infection, the medium was replaced with fresh medium. Cells were then infected with 0.5 ml of bacterial suspension (the Δ*ispC* mutant or the WT) in the MEM complete medium (for HBMEC, 25 mM HEPES and 1 mM sodium pyruvate was added to the medium) at 37 °C for 1 h at a desired multiplicity of infection (MOI) for each cell line, MOI 50 for Hela and L132, MOI 100 for Vero, MOI 20 for Caco-2, Hep-G2, SCP and HBMEC, and 2×10^5 bacteria for J774. For the adhesion assay, nonadherent bacteria were removed after infection by washing with 5×3 ml of PBS. The cells were lysed with 1 ml of 1% (v/v) Triton X-100 in H_2O at 37 °C for 5 min, and 0.1 ml of lysates at 10-fold serial dilution plated on BHI agar plates. Bacteria were enumerated after incubation at 37 °C for 24 h. For the invasion assay, cells were washed with 3×3 ml of PBS after infection and further incubated in 1 ml of the medium containing 100 μg/ml gentamicin for 1.5 h to kill extracellular bacteria. After washing with 2×3 ml of PBS, surviving intracellular bacteria that were protected from killing with gentamicin by the cytoplasmic membrane were quantified as above. For intracellular growth assay, cells were washed after infection and incubated in the medium containing 100 μg/ml gentamicin. Surviving bacteria were quantified as above at 2, 4, 6, and 8 h after the addition of gentamicin. For washing HBMEC, Dulbecco's Modified Eagle Medium (DMEM, high glucose) at 37 °C was used instead of PBS. All cellular adhesion, invasion and growth assays were performed in triplicate.

3.28 Actin Tail Formation

Formation of actin tails following infection with the Δ*ispC* mutant and the WT was

examined in J774. Cells (2×10^5 per well) were seeded into 2-well Lab-Tek®II chamber slides (Fisher) and grown to ~90% confluence. The medium was replaced with fresh medium one day before infection. After washing with DMEM minus FBS (37 °C), cells were infected with 10^7 bacteria in 1 ml of the same medium for 1 h. Cells were washed and then incubated in complete MEM containing 100 μg/ml gentamicin for additional 3 h or 6 h. After washing with PBS, cells were fixed in 4% (w/v) paraformaldehyde in PBS at room temperature for 12 min and permeabilized in 0.2% (v/v) Triton X-100 in PBS at room temperature for 8 min. Cells were blocked in 3% (w/v) BSA in PBS for 30 min. Bacteria were stained with rabbit antiserum to ActA for 1 h followed by incubation with Alexa Fluor 647 goat anti-rabbit secondary antibody (Invitrogen) in the dark for 1 h. Actin tails were stained with Alexa Fluor 488 Phalloidin (Invitrogen) in the dark for 30 min. The primary antibody, the secondary antibody conjugate and the phalloidin dye were used at a 1:250 dilution in 3% BSA in PBS. Nuclei were stained with DAPI (Sigma) at 10 μM in PBS at room temperature in the dark for 3 min. After washing with PBS, the slide was air dried, mounted with Vectashield mounting medium (Vector Laboratories, Inc., Burlington, Ontario, Canada) and examined on an Olympus BX51 fluorescence microscope (Olympus Canada Inc., Ontario, Canada).

3.29 Plaque Assay

Plaque assay was performed in murine L2 fibroblast cells infected with the Δ*ispC* mutant or the WT. L2 cells (3×10^5 per well) were seeded into 6-well plates (VWR) and grown to confluence. After washing with DMEM minus FBS (37 °C), the cells were infected with 10^6 bacteria in 1 ml of DMEM minus FBS for 1 h. After washing with the complete MEM medium (37 °C) containing 10 μg/ml gentamicin, 3 ml of agar overlay (42 °C) containing 1 × DMEM, 10% FBS, 10 μg/ml gentamicin and 0.7% agarose were added to

each well, incubated for 4 days at 37 °C and visualized on a Zeiss Axiovert-10 inverted microscope equipped with a Nikon digital camera at a total magnification of 45. The diameters of more than 20 plaques for each bacterial strain were measured using the software ImageJ version 1.37a (National Institutes of Health, Bethesda, MD) and expressed as relative values.

3.30 Cell Binding Assay

Binding of purified recombinant IspC and GFPuv-CBD1 to the surface of SCP and Vero cells was examined by fluorescence microscopy. Cells (1.7×10^5 for SCP, 1×10^5 for Vero) were seeded into 2- or 4-well chamber slides and grown to ~70% confluence. Cells were washed and fixed as described for the actin tail formation assay. Fixation followed by permeabilization treatment was used as a control for surface binding. Cells were blocked in 3% (w/v) BSA in PBS for 30 min and incubated with either IspC (3.5 μg/ml) or GFPuv-CBD1 (1.14 μM) at room temperature for 2.5 h with gentle shaking. For GFPuv-CBD1, cells were air-dried after washing with PBS and loaded with the mounting medium for fluorescence microscopy. For IspC binding, cells were further incubated with RαIspC at 1:250 in 3% (w/v) BSA in PBS at room temperature for 1 h with shaking followed by incubation with FITC-conjugated goat anti-rabbit IgG (Zymed) at 1:50 at room temperature for 30 min. After washing, slides were processed for fluorescence microscopy as above. Fluorescence and phase contrast images were taken on an Olympus BX51 fluorescence microscope (Olympus). Preimmune serum and purified GFPuv were used as negative controls.

3.31 Heparin-Agarose Binding Assay

Binding of purified rIspC and its C-terminal CWBD fused to GFPuv to

glycosaminoglycans (GAGs) was examined using Heparin-agarose beads (Sigma). The rIspC (22 μg) in 0.3 ml of binding buffer (10 mM phosphate buffer, pH 7.5) was incubated with 100 μl of Heparin-agarose beads at room temperature for 1 h with rotating. Agarose beads without heparin conjugation were used as a negative control to ensure that rIspC did not bind to the agarose beads. The supernatant was collected by filtration on a Handee Mini-Spin column (Pierce, Brockville, Ontario, Canada) and the agarose beads complexed with rIspC were washed with 5 × 0.3 ml of binding buffer. The washing flow-throughs were collected. The bound rIspC was eluted with 5 × 0.3 ml of elution buffer (50 mM Tris-HCl, pH 7.5, 2 M NaCl). The CWBD (aa 198-774) of IspC C-terminally fused to GFPuv (i.e., GFPuv-CBD1) and GFPuv (negative control) were used at 11.3 nM for binding assay basically as above except that elution was carried out with 5 × 0.15 ml of elution buffer.

The supernatant, washing flow-throughs and eluted samples were analyzed by SDS-PAGE with staining with Coomassie blue for IspC or imaging under UV illumination for GFPuv-CBD1.

3.32 Preparation of Vero and SCP Cell Lysates

Approximately 8×10^5 Vero or SCP cells were seeded in a 75-cm^2 tissue culture flask and grown for 48 h. Cells were washed 3 × 10 ml of cold PBS, and then scraped into 1.0 ml of cell lysis buffer (50 mM Tris-HCl pH 7.5, 1% [v/v] IGEPAL CA-630, proteinase inhibitor cocktail at 1:100 dilution (Sigma)). The cell suspension was incubated at 4 °C for 45 min, spun at 14,100 × g for 5 min to collect the supernatant (soluble cell lysates) and stored at –80 °C until use.

3.33 Co-Immunoprecipitation

The cellular components recognized by IspC were examined in Vero or SCP by Co-

immunoprecipitation. The soluble cell lysates (1 ml) were precleared at 4 °C for 15 min on a rotator by adaption onto Protein A agarose (Invitrogen) (100 µl of 50% slurry) that had been washed 3 × 1 ml of PBS, blocked in 330 µl of blocking buffer (PBS containing 3% [w/v] IgG-free, proteinase-free BSA (Jackson) at 4 °C for 30 min with rocking, then coated with rabbit preimmune serum (50 µl) in 125 µl of blocking buffer at room temperature for 20 min, and washed 3 × 1 ml of PBS. The protein concentration in the precleared samples was determined using a BCA protein assay kit (Pierce) as per manufacturer's instruction. Agarose beads used for immunoprecipitation (60 µl of 50% slurry) or none were similarly blocked, and coated with 40 µl of RαIspC or rabbit preimmune serum in 100 µl of blocking buffer. After washing, the beads were treated with 1 × SDS-PAGE sample buffer containing 6 M urea at room temperature for 1 h or incubated with 25 µg (80 µl) rIspC in equal volume of blocking buffer at 4 °C for 1 h with rotating (minus rIspC was used as negative control). After washing, the beads were mixed with precleared cell lysates (1 ml, 2 mg/ml) and incubated at 4 °C overnight with rocking. After washing, the immunocomplex was eluted by incubation with 120 µl of 1 × SDS-PAGE sample buffer containing 6 M urea at room temperature for 1 h, and then stored at -20 °C until use for SDS-PAGE analysis with Coomassie blue staining and for Western blot analysis using mouse anti-gC1q-R (Millipore, Mississauga, Ontario, Canada) at a 1:2000 dilution. Bound antibodies were probed with HRP-conjugated goat anti-mouse IgG (Jackson) at a 1:5000 dilution and detected using SuperSignal® West Pico Chemiluminescent Substrate kit (Pierce). The recombinant InlB protein expressed from pKI22 (Ireton et al., 1999) was used as a positive control.

3.34 Ligand Overlay Assay

Cellular proteins of Vero or SCP cells that are potentially recognized by IspC were

confirmed by a ligand overlay assay. Briefly, co-immunoprecipitates, negative control samples (preimmune or minus rIspC), and soluble cell lysates (40 μg) were separated by SDS–PAGE in a 12% gel, electroblotted onto a nitrocellulose membrane and then blocked with 3% (w/v) BSA in 10 mM phosphate buffer pH 7.3 containing 0.2% (v/v) Triton X-100, 0.05% (v/v) Tween-20 (PBS-TT) at room temperature for 1 h. The membrane was then incubated with purified rIspC (25 μg/ml) in 10 ml of 3% (w/v) BSA in PBS-TT at room temperature for 1 h with rocking. Following washing 3 × 10 ml of washing buffer PBS-TT, the membrane was incubated with mouse anti-his monoclonal antibody (Qiagen) at a 1:1000 dilution followed by interaction with HRP-conjugated goat anti-mouse IgG (Jackson) at a 1:5000 dilution. Immunostaining were performed using the SuperSignal West Pico Chemiluminescent Substrate kit (Pierce) as per manufacturer's instruction. The purified recombinant InlB protein was used as a positive control.

3.35 Immunoprecipitation of Tyrosine Phosphorylated Proteins and PI 3-Kinase

The effect of IspC on host cell signalling transduction was examined in Vero by analysis of the overall protein tyrosine phosphorylation, tyrosine phosphorylated adaptor proteins (Gab1 and Shc) and their association with the p85 regulatory subunit of phosphoinositide (PI) 3-kinase. Briefly, Vero cells (confluent) grown in 75-cm^2 tissue culture flasks were washed with 3 × 10 ml of PBS and starved in 10 ml of DMEM (Invitrogen) at 37 °C for 6.5 h. Starved cells were treated in triplicates with rIspC (3 nM) in 5 ml of DMEM for 1 min, human recombinant epidermal growth factor (EGF) (Invitrogen) at100 ng/ml, or DMEM alone, a treatment condition similar to that used for InlB (Ireton et al., 1999). Three independent experiments were performed for each treatment conditions. After washing with 3 × 10 ml of cold PBS, cells were scraped into 1.0 ml of ice-cold lysis buffer (1% [v/v]

IGEPAL CA-630, 50 mM Tris-HCl pH 7.5, 150 mM NaCl, Tyrosine/Alkaline Phosphatase Inhibitor Cocktail (Sigma) at 1:100 dilution, Proteinase Inhibitor Cocktail (Sigma) at 1:100 dilution) and incubated at 4 °C for 45 min. The supernatant was collected by spinning at 14, 100 × g for 5 min and stored at –80 °C until use. For immunoprecipitation, solubilized cell lysates were first precleared using GammaBind® G Sepharose (Amersham) and determined for protein concentration using BCA as above. Precleared cell lysates (1 ml, 2.5 mg/ml) were incubated with the Sepharose beads that had been blocked and coated as above with Catch and Release® Phosphotyrosine, Clone 4G10® (Millipore, 10 µl) or rabbit polyclonal anti-p85 subunit of PI 3-kinase (Millipore, 5 µl) at 4 °C for 2 h with rotating. After incubation, the beads were washed with 3 × 1 ml of 1 × Catch and Release® washing buffer (Millipore) and proteins eluted with 1 × SDS-PAGE sample buffer containing 6 M Urea (160 µl) as above. The eluted protein samples (20 µl) were analyzed for overall protein tyrosine phosphorylation, the tyrosine phosphorylated adaptor proteins Gab1 and Shc, their association with the p85 subunit of PI 3-kinase by Western blots using anti-Phosphotyrosine, recombinant 4G10™ at a dilution of 1:2000, anti-PI 3-Kinase p85 rabbit polyclonal antibody at a 1:2000 dilution, anti-phospho-Gab1 (Tyr627) (Millipore) at a 1:1000 dilution, and anti-phospho-SHC (Tyr317) (Millipore) at a 1:1000 dilution followed by detection with HRP-conjugated goat anti-mouse or rabbit IgG (Jackson) at a 1:5000 dilution and SuperSignal® West Pico Chemiluminescent Substrate (Pierce).

3.36 Detection of Actin Rearrangement

The effects of purified recombinant IspC on actin cytoskeletal changes, i.e, the presence of membrane ruffles (actin-rich membrane folds) (Ireton et al., 1999) were examined in Vero cells. Vero cells (1×10^5) in 1 ml of complete MEM medium were seeded per well on 4-well

Lab-Tek®II chamber slides (Fisher) and grown overnight. Cells were starved in DMEM at 37 °C for 6.5 h after washing with 3 × 1 ml of PBS and incubated with purified recombinant IspC (3 nM) or EGF (100 ng/ml) suspended in 0.5 ml of warm DMEM for 1 min and 5 min, a treatment condition similar to that used for InlB-induced actin rearrangement (Ireton et al., 1999). Untreated starved cells were used as negative control. After washes with 3 × 1 ml of cold PBS, cells were fixed in 4% (w/v) paraformaldehyde in PBS at room temperature for 12 min and permeabilized in 0.2% (v/v) Triton X-100 in PBS at room temperature for 8 min. Cells were then stained with 0.5 ml of Alexa Fluor 488 Phalloidin (Invitrogen) in PBS at a 1:250 dilution at room temperature in the dark for 30 min with rocking. After washing with PBS, the slides were air dried, mounted with Vectashield mounting medium (Vector) and viewed on an Olympus BX51 fluorescence microscope (Olympus) at 40 × magnification. One hundred cells under each treatment condition were examined for actin-rich ruffles: cells with no actin-rich ruffles were scored as negative, whereas cells that had one or more ruffles were considered to be "ruffle-positive".

3.37 Preparation of Peptidoglycan of *L. monocytogenes*

Bacterial cell wall peptidoglycan was prepared from a mid-log growth phase culture of the wild type *L. monocytogenes* serotype 4b or the Δ*ispC* mutant strain grown at 37 °C in BHI broth. Bacteria were harvested by centrifugation, boiled in 4% (w/v) SDS for 30 min, washed six times with room temperature water, and stored at -80 °C until use. Frozen bacteria were broken by passing three times through a French press at 1500 lb/in^2. Unbroken cells were removed by centrifugation at 3000 × g for 5 min. The cell wall materials were collected by centrifugation from the supernatant at 10,000 × g for 20 min, resuspended in 13 ml of 100 mM Tris·HCl (pH 7.5), treated with 0.7 mg α-amylase (Sigma) at 37 °C for 2 h,

100 µg DNase I (Roche) and 500 µg RNase A (Qiagen) in the presence of 20 mM $MgSO_4$ at 37 °C for 2 h, and 1000 µg trypsin (Sigma) in the presence of 10 mM $CaCl_2$ at 37 °C overnight. After inactivation of trypsin by boiling in 1% (w/v) SDS for 15 min, the cell wall materials were washed twice with water, once with 8 M LiCl, and three times with water and resuspended in 10 ml of 49% hydrofluoric acid and rocked for 48 h at 4 °C to remove teichoic acids. The cell wall materials were washed (three times with water, once with 100 mM Tris·HCl (pH 7.5), and three times with water) and treated with 50 U calf intestine alkaline phosphatase (New England Biolabs) in 10 ml supplied 1 × reaction buffer at 37 °C overnight. Finally, the cell wall material (peptidoglycan) was boiled for 5 min, washed with water and lyophilized.

3.38 Statistics

The data from *in vivo* virulence, adhesion, invasion, intracellular growth, and plaque assays with the Δ*ispC* mutant and the WT were statistically analyzed using the Student's *t*-test (SigmaStat software, version 2.03; Systat Software, Point Richmond, California) software and *P*-values of < 0.05 were considered statistically significant.

CHAPTER IV

Expression, Purification and Structural Characterization of IspC

Some of the data from Chapter IV has been published in:
Wang, L., Walrond, L., Cyr, T.D., and Lin, M. (2007). A novel surface autolysin of *Listeria monocytogenes* serotype 4b, IspC, contains a 23-residue N-terminal signal peptide being processed in *E. coli*. Biochem. Biophys. Res. Commun. *354*, 403-408.

4.1 Introduction

IspC is known as a novel 86-kDa protein target of humoral immune response to infection with *L. monocytogenes* from a previous study that aimed to identify genes coding for proteins that reacted with RαL from rabbits infected with live bacteria but not with RαK from animals immunized with heat-killed bacteria through differential immunoscreening of a *L. monocytogenes* serotype 4b genomic expression library (Yu et al., 2007). That study suggested that IspC is not expressed or is expressed at a low level in *in vitro* growth and induced specifically or upregulated *in vivo* during infection. These possibilities indicate the need for research on IspC expression in *in vitro* cultured *L. monocytogenes*. More importantly, the function of this protein remains unknown and requires further study. Investigation into the biochemical and structural properties, and *in vitro* expression of IspC in *L. monocytogenes* may provide some functional insights into the protein. As the first step towards such investigation, an expression construct was generated in this part of the study by cloning the *ispC* ORF into pET30a, which was used to produce the full length recombinant IspC (rIspC) in *E. coli*. By optimizing the conditions for heterologous expression of IspC and using the combination of Ni-NTA affinity and cation-exchange chromatography, sufficient quantity of highly purified rIspC was obtained. This allowed for biochemical and structural characterization of IspC with various techniques including circular dichroism (CD) analysis, Raman spectroscopy, N-terminal sequencing analysis and mass spectrometry and for raising IspC-specific polyclonal antibodies to be used in studies on localization and expression of IspC.

4.2 Results

4.2.1 Expression of recombinant IspC in *E. coli*

Part of this study aimed to develop a protocol for the generation of sufficient amount of homogeneous recombinant IspC (rIspC) from an *E. coli* expression host, which was needed for biochemical analysis (e.g., cleavage site on peptidoglycan substrate), structural analysis (e.g., CD spectroscopy), production of specific polyclonal antibody to IspC, *etc.* The expression construct pIspC was generated by cloning the IspC ORF into the NdeI and XhoI sites of pET30a for expression of rIspC fused with a 6 × his tag. rIspC was initially expressed in *E. coli* BL21(DE3)/pLysS cells harboring pIspC under the control of the T7 promoter. However, induction with 1 mM IPTG added to the culture (OD_{590} = 0.6 to 1.0) at 37 °C for 3 h led to an apparent cell lysis as indicated by an initial increase followed by a decrease in the OD_{590} of the induced culture. An indication of cell lysis was also observed by the formation of fibrous materials in the culture. This is consistent with the putative peptidoglycan hydrolytic nature of IspC, which may have resulted in the production of limited amount of rIspC. To overcome this problem, the protein was induced to express in *E. coli* Rosetta (DE3)/pLysS and allowed the induction earlier (OD_{590} = 0.45 ± 0.05) with IPTG at 37 °C for a shorter period (2 h only) followed by incubation of the cell culture at 4 °C overnight (16 to 18 h). Under these conditions, the level of IspC expression in *E. coli* was significantly increased by at least 4-fold, as judged by comparison to the yield of purified protein under the initial expression conditions, and the recombinant protein remained in a soluble form. Most likely during the expression at low temperature, the

hydrolytic activity of IspC was minimized to prevent the cell lysis and thus improve the protein yield over a longer period of induction.

4.2.2 Purification of rIspC

The rIspC protein was fused with a six-histidine tag at its C-terminus which is specifically designed for the ease of protein purification by metal-chelate affinity chromatography (Hochuli et al., 1987; Porath et al., 1975). The purity of rIspC following chromatography on a column of Ni-NTA superflow was at least 80%, as estimated by SDS-PAGE (see Fig. 4-1A, lane 5) with one major contaminating protein of ~ 33 kDa. IspC has an alkaline pI of 9.4 calculated from its amino acid sequence. Based on this property, cation-exchange chromatography was explored to further purify the protein using a column of SP Sepharose Fast Flow. The protein was eluted in a sharp peak at ~ 300 mM NaCl following a 0 to 500 mM NaCl linear gradient (Fig. 4-1B) and showed electrophoretic homogeneity on SDS-PAGE (Fig. 4-1A, lane 6). The yield of the homogeneous IspC was estimated to be approximately 6 mg from 10 L of culture.

4.2.3 Characterization of rIspC by N-terminal sequencing and mass spectrometry

N-terminal sequencing showed that the sequence of the first 12 N-terminal residues of purified rIspC was NH2-TVGGQLQDSLTG. This sequence matched exactly with that of residues 24 to 35 of the deduced amino acid sequence of IspC (Yu et al., 2007) (Fig. 4-2). This result further confirmed the identity of the purified protein and indicted that the *L. monocytogenes* IspC contained an N-terminal signal peptide of 23 residues which had been removed by an *E. coli* signal peptidase-mediated cleavage between Thr 23 and Thr 24. This

FIG. 4-1. Expression and purification of recombinant IspC (rIspC). (A) SDS-PAGE analysis of the rIspC protein preparations by chromatographic procedures. Lane 1, protein standards with their molecular mass in kDa (left); Lane 2, total proteins from non-induced *E. coli*/pIspC equivalent to 1 ml of culture with an A_{590} of 0.2; Lane 3, total proteins from IPTG-induced *E. coli*/pIspC equivalent to 1 ml of culture with an A_{590} of 0.2; lane 4, the crude soluble protein extract from 1 ml of culture with an A_{590} of 0.3; Lane 5, the protein preparation (6 μg) from Ni-NTA Superflow; Lane 6, protein preparation (3 μg) from SP Sepharose Fast Flow. **(B)** SP Sepharose Fast Flow chromatography of the partially purified rIspC preparation. The rIspC protein, after partial purification by Ni-NTA Superflow affinity chromatography, was applied onto a column of SP Sepharose Fast Flow (1 × 2 cm) and eluted with a 0 to 500 mM NaCl linear gradient in 30 ml of 10 mM phosphate buffer (pH 8.0) containing 5% glycerol.

A

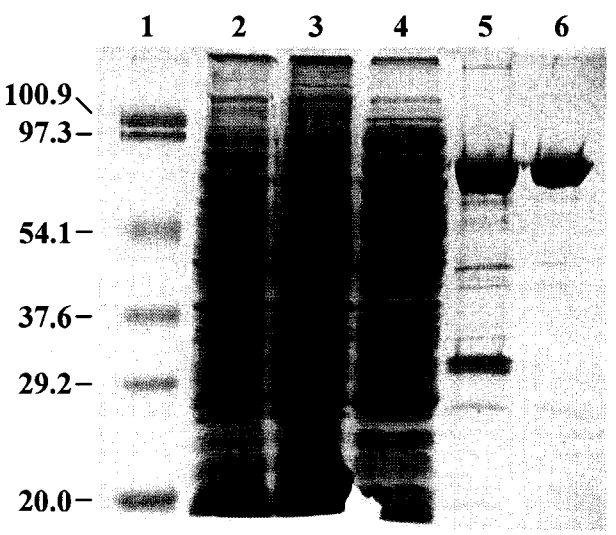
1
2
3
4
5
6
100.9
97.3
54.1
37.6
29.2
20.0

B

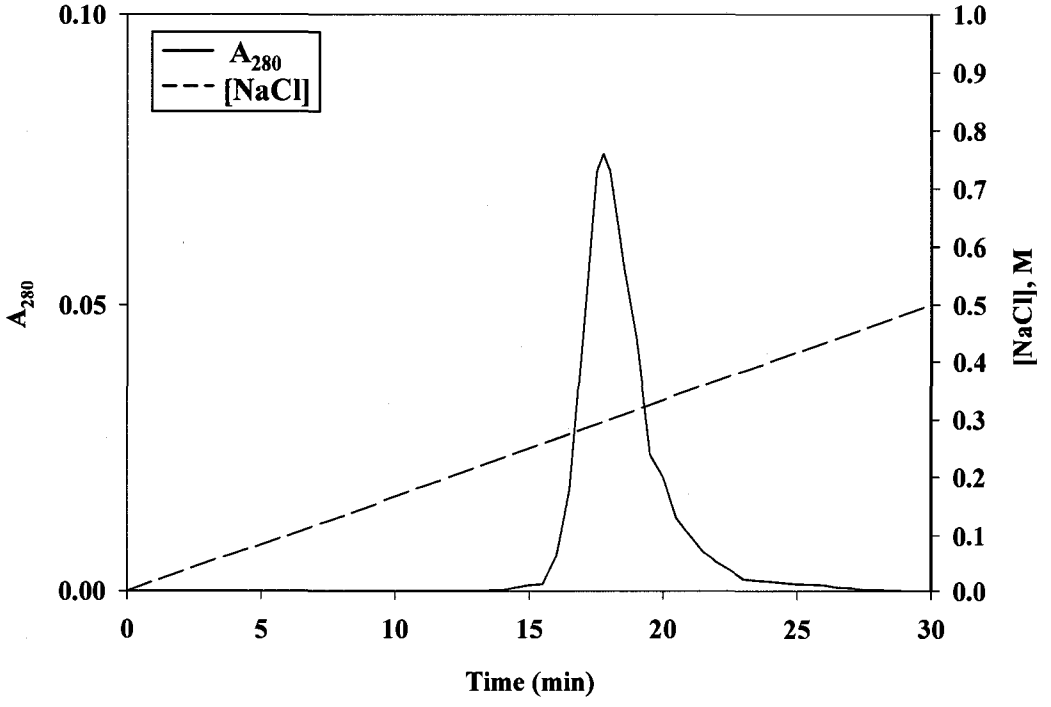
A280
[NaCl]
0.10
0.05
0.00
1.0
0.9
0.8
0.7
0.6
0.5
0.4
0.3
0.2
0.1
0.0
0
5
10
15
20
25
30
Time (min)
[NaCl], M

FIG. 4-2. Alignment of the determined N-terminal sequence of purified rIspC with the deduced N-terminal sequence of IspC precursor. The sequence of the first 12 N-terminal residues (bold) of purified rIspC was experimentally determined as described in Materials and Methods. The IspC precursor sequence was from a previous study (Yu et al., 2007). Cleavage between Thr 23 and Thr 24 by a signal peptidase leading to formation of the mature IspC is indicated by an arrow.

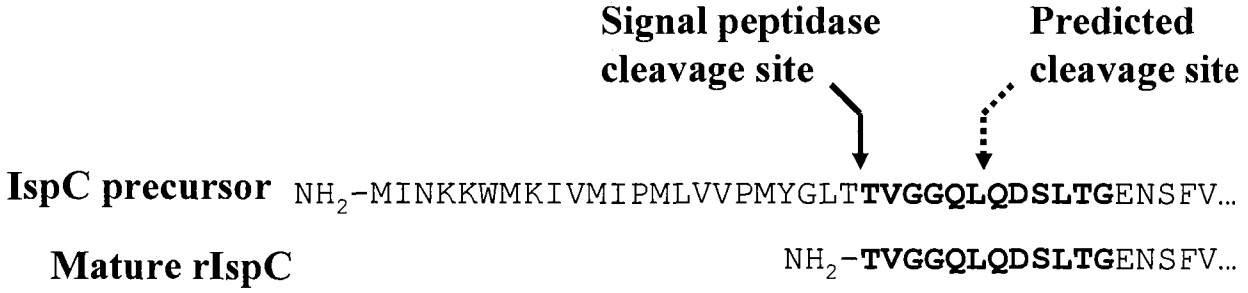
Signal peptidase cleavage site
Predicted cleavage site
IspC precursor NH2-MINKKWMKIVMIPMLVVPMYGLTTVGGQLQDSLTGENSFV...
Mature rIspC
NH2-TVGGQLQDSLTGENSFV...

is in contrast to the predicted cleavage site for the N-terminal signal peptide between Leu 29 and Gln 30 (Fig. 4-2) and illustrates that knowledge of a cleavage site requires experimental determination.

The IspC protein was expressed as a product with a C-terminal fusion of 8 residues including a 6 histidine tag. Mass spectrometry analysis of the purified rIspC revealed its molecular weight of 84.186 kDa (Fig. 4-3), which is essentially the same as the deduced molecular weight of 84.219 kDa after the removal of the N-terminal signal peptide and the addition of 8 C-terminal residues have been taken into consideration. The mass spectral data is in good agreement with the N-terminal sequencing result.

Biochemical and structural analysis of rIspC requires accurate determination of protein concentration in solution. One simple and rapid means to measure the concentration is to use UV-visible spectrophotometry in combination with knowledge of the extinction coefficient (ε) of rIspC. Gill and von Hippel (1989) described a method of calculating ε from the amino acid sequence with very acceptable limits of errors (to ± 5% in most cases) by which the molar extinction coefficient of rIspC was calculated to be 1.7851×10^5 $M^{-1}cm^{-1}$ at 280 nm.

4.2.4 Immunogenic characteristics of the rIspC protein

The purified rIspC reacted only with rabbit antisera (RαL) (Fig. 4-4b) but not with rabbit antisera (RαK) (Fig. 4-4c). This immunological property is consistent with the recent identification of *ispC* as one of several genes coding for the proteins reactive exclusively to RαL by differential immunoscreening of a *L. monocytogenes* serotype 4b genomic

FIG. 4-3. Electrospray ionization (ESI) mass spectrum of the purified rIspC protein at a concentration of 10 pmol/µl. The ESI mass spectral data (top panel) was deconvoluted using MaxEnt1® algorithm to derive the zero charge state spectrum which provided a molecular weight of 84.187 kDa for the purified rIspC (bottom panel)

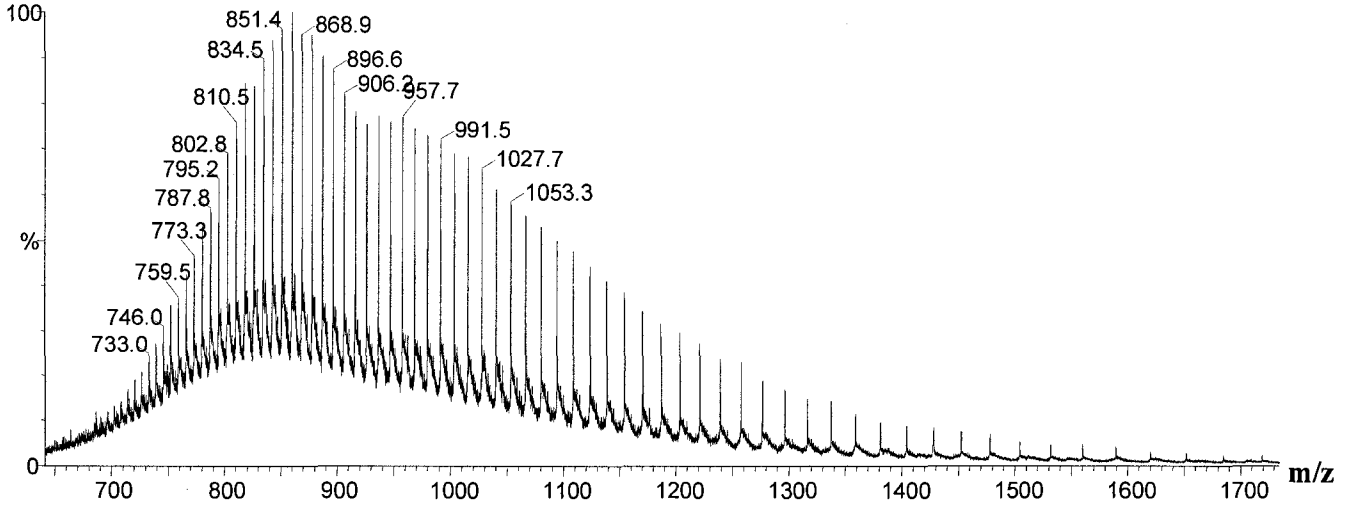
100
%
0
851.4
868.9
834.5
896.6
906.2
957.7
810.5
991.5
802.8
1027.7
795.2
1053.3
787.8
773.3
759.5
746.0
733.0
700
800
900
1000
1100
1200
1300
1400
1500
1600
1700
m/z

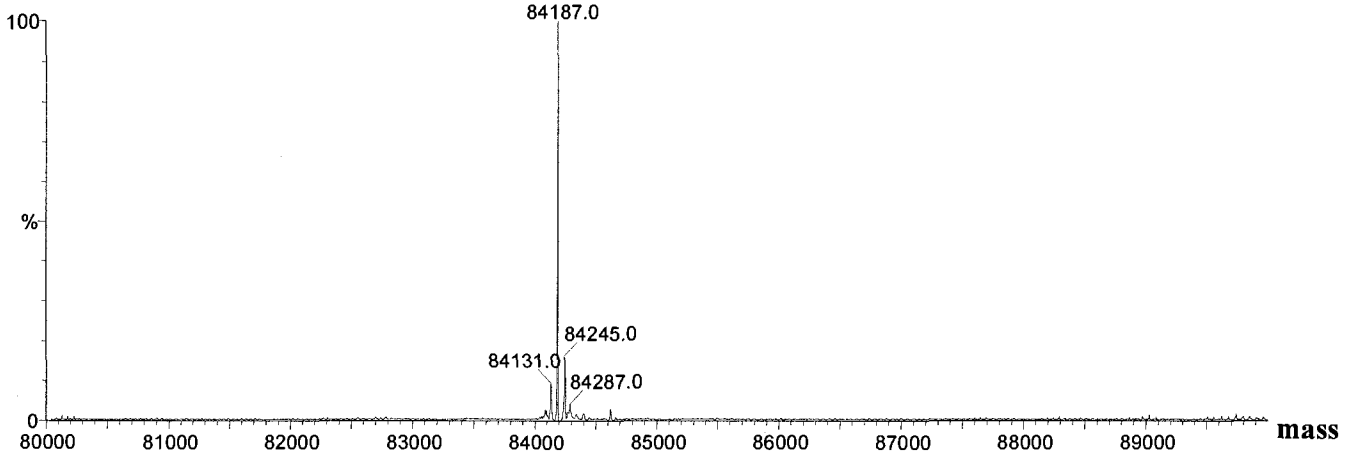
100
%
0
84187.0
84245.0
84131.0
84287.0
80000
81000
82000
83000
84000
85000
86000
87000
88000
89000
mass

FIG. 4-4. The immunogenic characteristics of rIspC. The purified recombinant IspC (1 μg) was analyzed by Western blots probed with anti-His mAb (a) at 0.1 μg/ml, rabbit antisera RαL (b), RαK (c), RαIspC (d) and preimmune sera (e) at a dilution of 1:1000. Protein standards (Std) with their molecular masses in kDa are shown on the left of the blots. The arrow indicates the position of purified recombinant IspC.

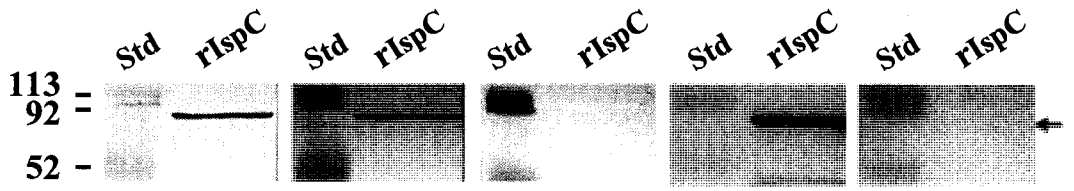
Std
rIspC
Std
rIspC
Std
rIspC
Std
rIspC
Std
rIspC
113
92
52
(a) Anti-His
(b) RαL
(c) RαK
(d) RαIspC
(e) Pre

expression library (Yu et al., 2007). Polyclonal antibodies were raised against the purified rIspC protein and showed at a 1:1000 dilution immunological reaction with rIspC on Western blot (Fig. 4-4d). In contrast, the preimmune serum at the same dilution did not detect any rIspC protein (Fig. 4-4e).

4.2.5 Secondary structure analysis of rIspC

The CD spectral analysis of rIspC revealed that IspC was a predominantly β-sheet protein (Fig. 4-5). This result was further confirmed by Raman spectra of rIspC that exhibited two peaks in the amide I (1665 cm^{-1}) and III (1235 cm^{-1}) regions characteristic of β-sheet (Fig. 4-6). Secondary structure of IspC predicted by PSIPRED revealed that the N-terminal region (aa 1-197) and C-terminal part (aa 198-774) are predominant in α-helix and β-sheet structures, respectively (Fig. 4-7).

4.3 Discussion

A strategy has been developed for efficient expression and purification of rIspC in this part of the study, involving a combination of altered expression conditions (i.e., different *E. coli* host, earlier IPTG induction, shorter period of induction at a high temperature, longer period of induction at a low temperature), metal-chelate affinity chromatography, and cation-exchange chromatography. This procedure resulted in a sufficient quantity of a highly purified recombinant form of IspC required for the biochemical, structural and functional characterization of IspC.

A signal peptidase cleavage site was experimentally identified between Thr 23 and Thr 24 of IspC, giving rise to a mature product of rIspC produced in *E. coli* as a ~84 kDa protein

FIG. 4-5. Analysis of rIspC by Circular Dichroism (CD) spectroscopy. The purified rIspC was prepared in PBS (pH 7.2) at a final concentration of 1.6×10^{-6} M ($OD_{280} = 0.285$) and used to determine its CD spectrum in the far UV spectral region (190.0 – 260.0 nm). The spectra from four CD scans were collected, averaged, and smoothed by the JASCO software.

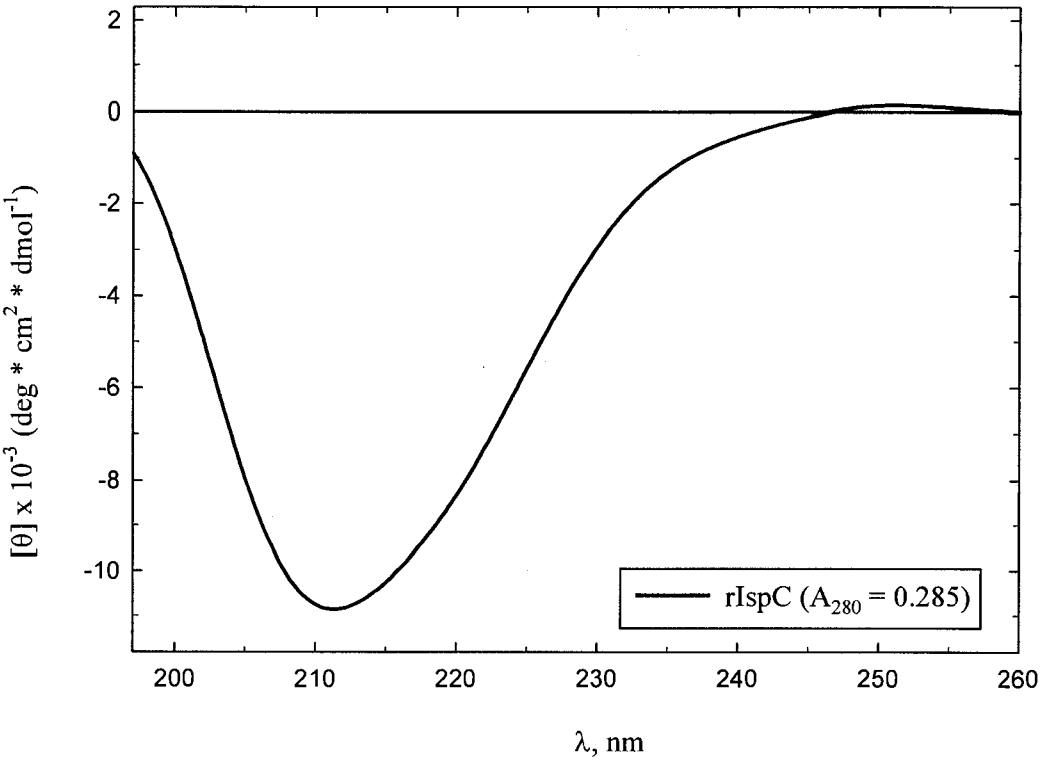
2
0
-2
-4
-6
-8
-10
200
210
220
230
240
250
260
[θ] x 10^-3 (deg * cm^2 * dmol^-1)
λ, nm
rIspC (A280 = 0.285)

FIG. 4-6. Analysis of rIspC by Raman spectroscopy. The purified rIspC at a concentration of 5.6×10^{-6} M (OD_{280} = 1.0, 2 μl) in PBS (pH 7.2) were spotted on a CaF_2 optical window and air dried prior to being analyzed. The Raman spectrum of rIspC (4 scans, 3 mW power) showed two peaks in the amide I (1665 cm^{-1}) and III (1235 cm^{-1}) regions characteristic of β-sheet structure.

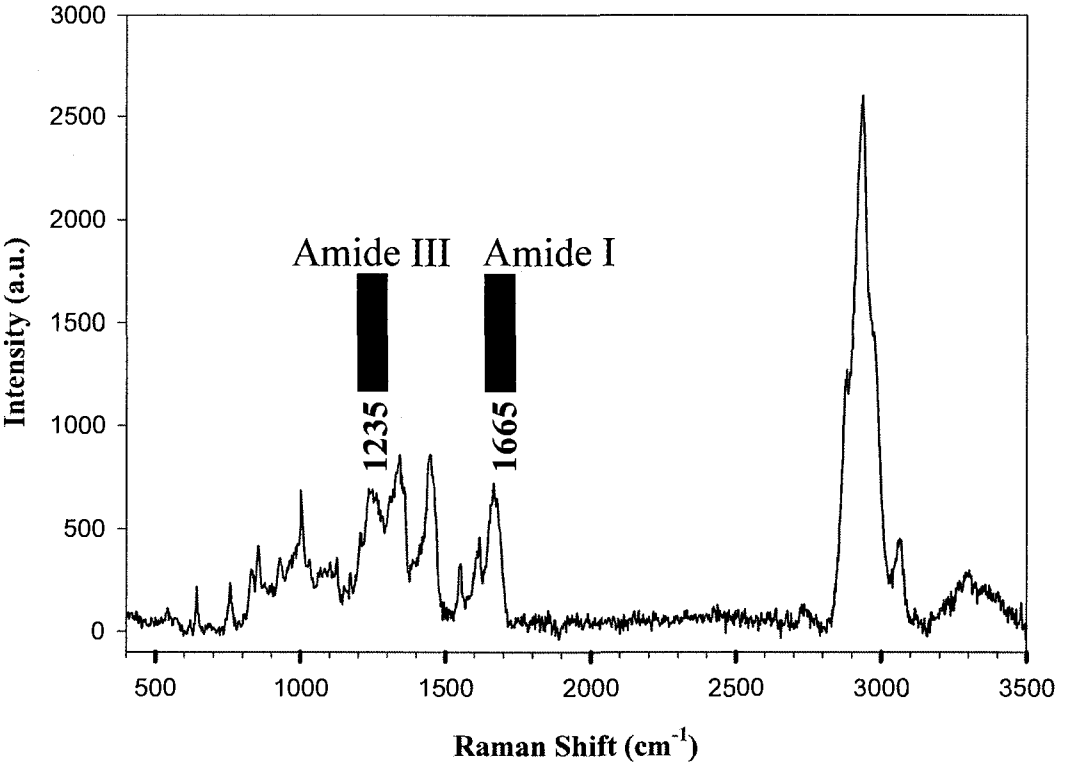
Amide III
Amide I
1235
1665
Intensity (a.u.)
Raman Shift (cm-1)
0
500
1000
1500
2000
2500
3000
3500

FIG. 4-7. The predicted secondary structure of IspC. The secondary structure of IspC was predicted by using the PSIPRED method on the server (http://bioinf.cs.ucl.ac.uk/psipred/). The amino acid regions before and after the red arrow contain an N-terminal putative catalytic domain (aa 58-197) and a C-terminal putative cell wall binding domain (aa 198-774), respectively.

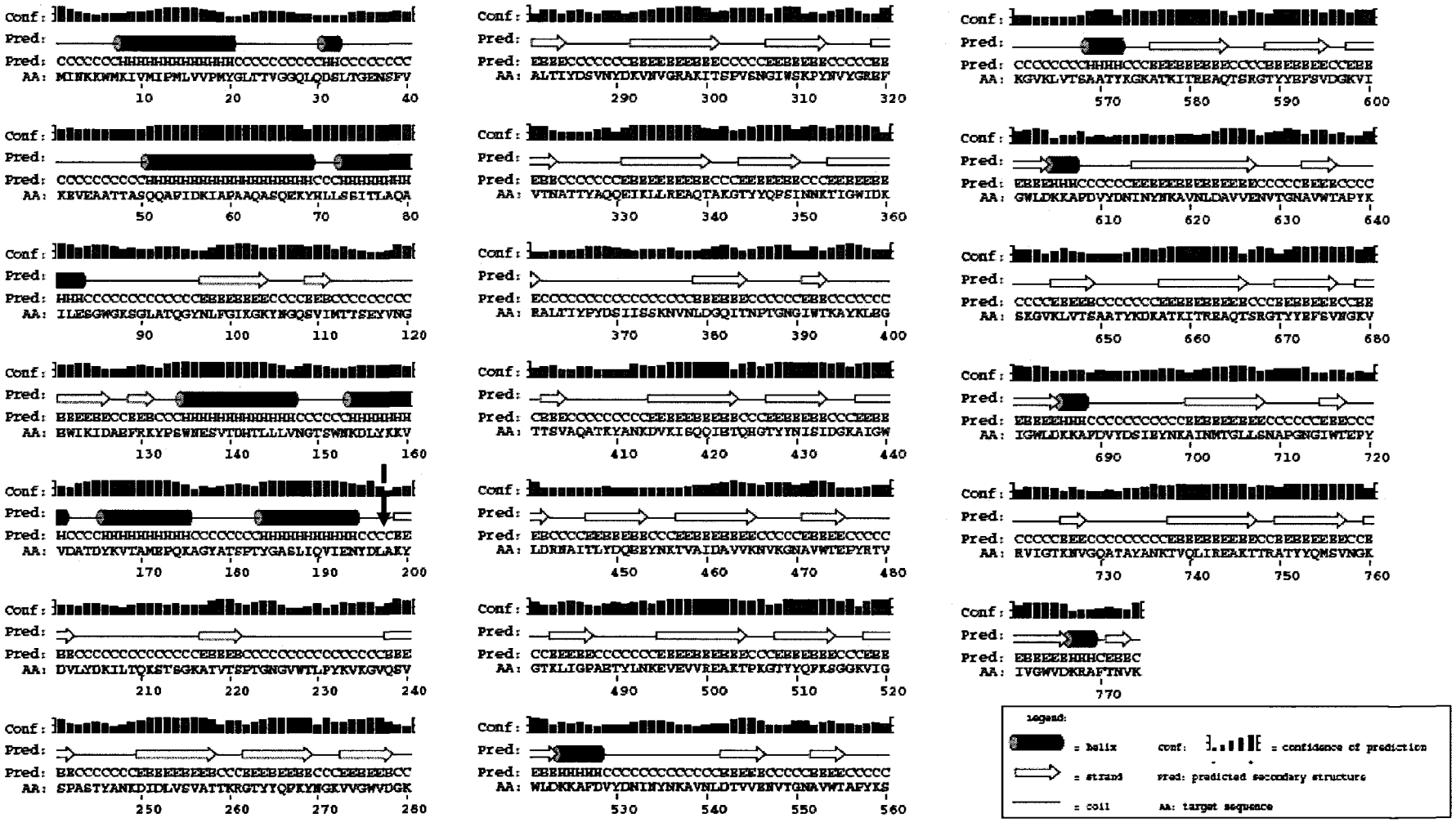
Conf:
Pred:
AA:
10 20 30 40
50 60 70 80
90 100 110 120
130 140 150 160
170 180 190 200
210 220 230 240
250 260 270 280
290 300 310 320
330 340 350 360
370 380 390 400
410 420 430 440
450 460 470 480
490 500 510 520
530 540 550 560
570 580 590 600
610 620 630 640
650 660 670 680
690 700 710 720
730 740 750 760
770
legend:
= helix
= strand
= coil
conf: = confidence of prediction
pred: predicted secondary structure
AA: target sequence

containing the amino acids 24-774 of IspC at the N-terminus and 8 additional residues LEHHHHHH (underlined is a 6 histidine tag) at the C-terminus (Fig. 4-8). Hydrophobicity analysis by ProtScale (http://www.expasy.ch/tools/protscale.html, accessed date 2007/12/22) revealed that the N-terminal 23-amino-acid signal peptide of IspC possessed an overall structural feature (an N-terminal positively charged region, a central highly hydrophobic region, and a C-terminal less hydrophobic region) typical of the Sec-dependent secretion pathway, a main secretion pathway used by secretory proteins to reach their final destinations such as the periplasm, the outer membrane, or the extracellular environment (Choi and Lee, 2004; Mergulhao et al., 2005; Pugsley, 1993; Rusch and Kendall, 2007; Scott and Barnett, 2006; Simonen and Palva, 1993; van Roosmalen et al., 2004; Yamabhai et al., 2008). The Sec-dependent secretion pathways are also found in *L. monocytogenes* (Scott and Barnett, 2006). Moreover, the residues glycine at -3 and threonine at -1 positions are small and neutral, which agrees with the rule of the recognition site for the type I signal peptidase (SPase I), a membrane-bound endopeptidase (Tuteja, 2005). SPase I responsible for processing most exported proteins (March and Inouye, 1985; Stathopoulos et al., 2000; Wolfe et al., 1982) might also cleave the signal peptide of the heterologously expressed *L. monocytogenes* IspC protein in *E. coli*. The observed bacterial lysis during the induction of IspC expression suggests that the synthesized recombinant IspC is exported to the periplasmic space where degradation of the peptidoglycan substrate by IspC (the peptidoglycan hydrolase activity of IspC is demonstrated in Chapter V) occurs. A locus encoding three contiguous Spases I genes, *sipX*, *sipY* and *sipZ* were identified in the genome

FIG. 4-8. Schematic representation of the protein sequence encoded by the pIspC construct. The *ispC* ORF was cloned into the NdeI and XhoI sites of pET30a to create pIspC (top) which codes for the recombinant IspC fused with a 6 histidine residues at the C-terminus (bottom). The internal nucleotide and amino acid sequences were not drawn to scale and labeled with dots.

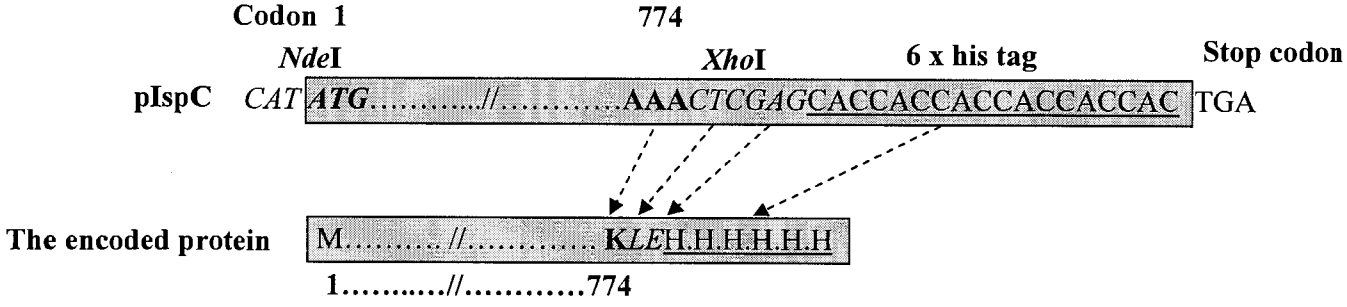
Codon 1
774
NdeI
XhoI
6 x his tag
Stop codon
pIspC
CAT ATG.....//.....AAACTCGAGCACCACCACCACCACCAC TGA
The encoded protein
M.....//.....KLEH.H.H.H.H.H.H
1.....//.....774

of *L. monocytogenes* (Bonnemain et al., 2004). Inactivation of *sipX* results in a significant attenuation in bacterial virulence (~100-fold); deletion of *sipZ* impairs the secretion of PlcB and LLO, restricts intracellular multiplication and almost abolishes the virulence (Bonnemain et al., 2004). Most likely, IspC is the substrate for these Spase I enzymes encoded by the *L. monocytogenes* genome. This needs to be demonstrated experimentally in further studies.

IspC has a C-terminal region composed of seven GW modules which has been demonstrated to be a CWBD responsible for anchoring IspC to the cell wall of *L. monocytogenes* (see Chapter V for more detail). This, together with the findings described here, leads to the hypothesis that the IspC, synthesized as a preprotein in the cytoplasm, is anchored onto the cell surface in a two-step process. The N-terminal signal peptide directs the targeting of the preprotein to the cytoplasmic membrane and then translocation across the membrane occurs via a Sec-dependent secretion pathway. Following the cleavage of the N-terminal signal peptide by a membrane-bound Spase I, IspC is released from the membrane as a mature protein and subsequently retained on the cell surface by its C-terminal CWBD.

Demonstration of antibodies to IspC in the antiserum RαL from rabbits infected with live *L. monocytogenes* but not in the antiserum RαK from rabbits receiving heat-killed bacteria in a previous study (Yu et al., 2007) and the reactivity of purified rIspC exclusively to RαL suggest that IspC is induced or significantly upregulated *in vivo* during infection and thus is likely important in *Listeria* pathogenesis. The availability of rabbit polyclonal

antibodies raised against the purified rIspC (RαIspC) makes it possible to probe the expression of IspC in *L. monocytogenes*.

Both CD and Raman spectral data of rIspC revealed that rIspC is a β-sheet-predominant protein. These experimental data are in good agreement with the predicted secondary structure of IspC showing the N-terminal putative catalytic domain (aa 58-197) and C-terminal putative CWBD (aa 198-774) made up of seven GW modules are predominant in α-helix and β-sheet structures, respectively. Similarly, structure determination by X-ray crystallography revealed that the C-terminal CWBD of InlB comprising three GW modules is primarily composed of β-strands (Marino et al., 2002), suggesting the C-terminal CWBD of IspC may share certain similar functions to that of InlB.

CHAPTER V

Identification of *L. monocytogenes* IspC as a Surface Peptidoglycan Hydrolase (Autolysin): Biochemical and Molecular Characterization

Some of the data from Chapter V has been published in:
Wang, L., and Lin, M. (2007). Identification of IspC, an 86-kilodalton protein target of humoral immune response to infection with *Listeria monocytogenes* serotype 4b, as a novel surface autolysin. J. Bacteriol. *189*, 2046-2054.

5.1 Introduction

Functional clues for hypothetical proteins derived from their ORFs may be found from the analysis of potential domains or motifs within deduced amino acid sequences using bioinformatic tools and is particularly useful in designing experiments for functional study of proteins. *L. monocytogenes* IspC is a novel immunogenic protein of 774 amino acids deduced from the ORF determined earlier (Yu et al., 2007; H. Dan and M. Lin, unpublished data; GenBank access no. EF409982). It possesses a 23-residue N-terminal signal peptide that was shown to be cleaved in an *E. coli* expression host (Chapter IV), in contrast to the 29-amino-acid N-terminal signal peptide predicted by SignalP 3.0 (http://www.cbs.dtu.dk/services/SignalP/). Sequence analysis reveals that IspC contains, in addition to an N-terminal signal peptide, a region (aa 58-197) near the signal peptide sharing significant homology to the muramidase domain of the flagellar protein FlgJ, of *S.* Typhimurium (Nambu et al., 1999), and a C-terminal putative cell wall binding domain (aa 198-774) made up of 7 GW modules, which are similarly found in the cell wall binding domain of InlB (Braun et al., 1997), Ami (Milohanic et al., 2001), and Auto (Cabanes et al., 2004) of *L. monocytogenes*. InlB, Ami and Auto are involved in the virulence of *L. monocytogenes* (Seveau et al., 2007). The presence of these putative domains suggests that IspC is a cell wall-anchored peptidoglycan hydrolase, likely possessing autolytic activity. Demonstration of the enzymatic activity, localization, and the domain functionality for IspC with experimental data would be necessary to elucidate the biological function (s) of IspC and its potential role in pathogenesis.

In this part of the study, experiments were undertaken with various forms of rIspC (full-length ad N- or C-terminal truncation) to show that this immunogenic protein is a cell surface protein with autolytic (peptidoglycan hydrolase) activity and cell wall binding

activity attributed, respectively, to its N- and C-terminal regions.

5.2 Results

5.2.1 Peptidoglycan hydrolase activity of IspC

IspC was assessed for its peptidoglycan hydrolysis activity by renaturing SDS-PAGE analysis of the purified rIspC using cell wall substrates from several bacteria. Hydrolysis of *M. lysodeikticus* ATCC 4698, *E. coli* ATCC 25922 or *L. monocytogenes* serotype 4b present in the renaturing gel resulted in clear bands corresponding to the position to which IspC had migrated on SDS-PAGE and Western blotting (Fig. 5-1A). The recombinant IspC is not only capable of hydrolyzing the cell walls of the Gram-positive bacterium *M. lysodeikticus* and the Gram-negative bacterium *E. coli* but also that of the IspC-producing strain of *L. monocytogenes* serotype 4b. These results indicate that IspC is an autolysin.

5.2.2 Effect of pH on the peptidoglycan hydrolase activity of IspC

The effect of pH on the hydrolase activity of IspC was investigated at various pH values from 3 to 10 using renaturing SDS-PAGE analysis (Fig. 5-1B). IspC is capable of hydrolyzing peptidoglycan in a wide range of pH values from 3 to 9 with a broad pH optimum from 7.5 to 9. Very weak activity was detected at pH 10. Interestingly, IspC exhibited a second pH optimum around 4 with less hydrolytic activity than that at the alkaline pH optimum.

5.2.3 Expression of IspC in *in vitro* cultured *L. monocytogenes*

The reaction of IspC with RαL but not with RαK, as demonstrated previously (Yu et al., 2007) and herein, suggested that IspC was either not expressed or expressed at a low level during *in vitro* growth. To differentiate these possibilities, the expression of *ispC* was monitored at both transcriptional and translational levels over a 22 h growth period (Fig. 5-2). RT-PCR revealed that the *ispC* gene was transiently transcribed during the early exponential

FIG. 5-1. (A) Analysis of the peptidoglycan hydrolase activity of IspC by renaturing SDS-PAGE. The purified recombinant IspC (1.5 μg) was resolved on 12 % gels containing 0.2 % (w/v) autoclaved *M. lysodeikticus* ATCC 4698 (ML), 0.2 % (w/v) autoclaved *E. coli* ATCC 25922 (EC) and 0.1 % (w/v) autoclaved *L. monocytogenes* serotype 4b (LM) or gels containing no bacteria (CB, WB). Hydrolysis of the peptidoglycan substrates occurred in 25 mM Tris-HCl (pH7.5) containing 1 % Triton X-100. ML, EC, LM, peptidoglycan hydrolase activity staining; CB, Coomassie Blue staining; WB, Western blot probed with anti-His mAb. The hydrolyase activity bands corresponding to the IspC protein band are indicated by an arrow. **(B)** The peptidoglycan hydrolase activity of the full-length recombinant IspC as a function of pH. Renaturing SDS-PAGE was performed using *M. lysodeikticus* ATCC 4698 substrate (0.2 % w/v) as described above. Sodium citrate-citric acid (pH 3-6), Tris-HCl (pH 7.5-9) and glycine-NaOH (pH 10) buffers were used.

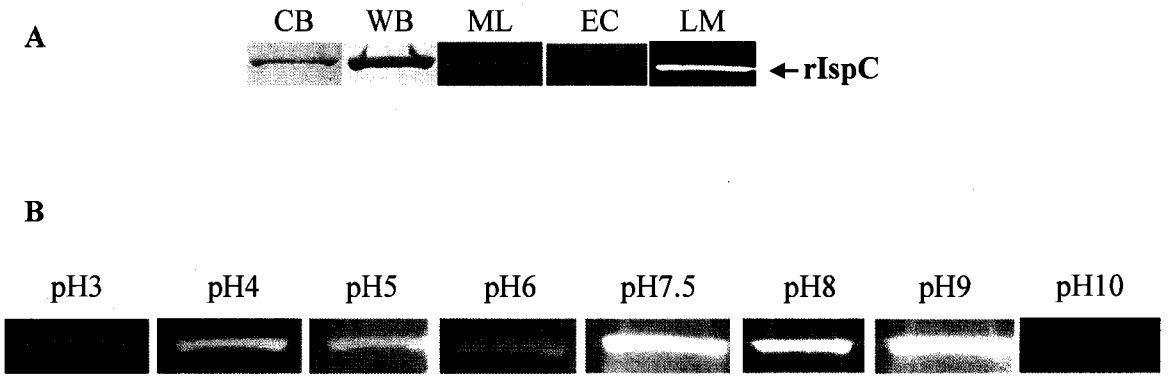
A
CB
WB
ML
EC
LM
←rIspC
B
pH3
pH4
pH5
pH6
pH7.5
pH8
pH9
pH10

FIG. 5-2. Expression of the *ispC* gene in *in vitro* cultured *L. monocytogenes*. The bacteria samples were taken at various time points (i.e., different OD_{620} values) over a 22 h growth period and analyzed for the *ispC* transcript by RT-PCR and for the protein by Western blot probed with RαIspC at a dilution of 1:1000. The RT-PCR products shown in each lane (i.e,. each time point) were derived from the same amount of total RNA (~100 ng). For Western blot analysis, the whole cell proteins from cells equivalent to 0.5 ml of culture at OD_{620} of 0.5 at each time point and purified rIspC (1 μg) were used. (a), PCR analysis of the *ispC* DNA without the reverse transcriptase step; (b), RT-PCR detection of the *ispC* mRNA; (c), PCR analysis of the 16S rRNA gene without the reverse transcriptase step; (d), RT-PCR detection of 16S rRNA as an internal control; (e), Western blot analysis of *L. monocytogenes* proteins and rIspC using the RαIspC antisera.

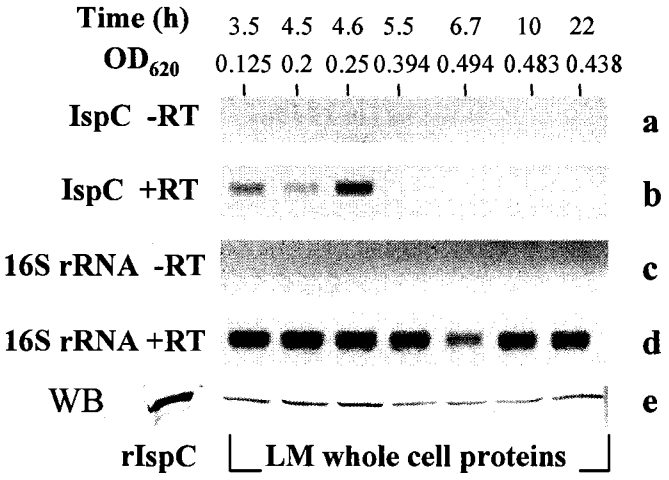
Time (h)
3.5 4.5 4.6 5.5 6.7 10 22
OD620
0.125 0.2 0.25 0.394 0.494 0.483 0.438
IspC -RT
a
IspC +RT
b
16S rRNA -RT
c
16S rRNA +RT
d
WB
e
rIspC
LM whole cell proteins

growth (Fig. 5-2b). Surprisingly, the authentic IspC protein, similar in molecular mass to rIspC, was detected on Western blots probed with RαIspC in all growth phases (Fig. 5-2e). Although the IspC protein exhibited a relatively stable level during the 22 h growth period, it appeared to reach a peak level at 4.6 h, in good agreement with that of the transcript (Fig. 5-2b). An independent experiment (Appendix 3, Fig. S1) showed these results were reproducible. The absence of the *ispC* transcript after the mid-exponential growth indicated that the protein was not actively expressed in later growth phases and that the protein detected in these growth phases most likely represented the undegraded protein synthesized earlier.

5.2.4 Localization of the IspC protein

The immunogenicity and sequence characteristics of IspC suggested that IspC was surface localized. To demonstrate this experimentally, live *L. monocytogenes* was probed with the RαIspC antiserum followed by immunofluorescence staining. IspC was detected by immunofluorescence microscopy, distributing unevenly in clusters on the cell surface (Fig. 5-3A (a)). Preimmune serum showed no fluorescence staining on the cell surface (Fig. 5-3A (c)), indicating the specific binding of RαIspC to the protein. These results were further confirmed by immunogold labeling of the bacterial cells with RαIspC (Fig. 5-3B (a)) but not with preimmune serum (Fig. 5-3B (b)). In addition, Western blot analysis of total TCA-precipitated proteins from the culture supernatant failed to detect any protein bands by RαIspC (data not shown). Collectively, these data indicate that IspC is localized exclusively on the bacterial surface.

5.2.5 Cell wall binding domain analysis

Four C-terminal fragments, CBD1 (aa 198-774), CBD2 (aa 234-774), CBD3 (aa 249-774) and CBD4 (aa 264-774), were produced in fusion with the green fluorescent

FIG. 5-3. Localization of IspC on the cell surface of *monocytogenes* serotype 4b by immunofluorescence staining and immunogold labeling. (A) Bacterial cells (3×10^8) were probed with the RαIspC antiserum (a) or preimmume serum (c) followed by the reaction with FITC-conjugated goat anti-rabbit antibody as described in Materials and Methods. Cells were visualized with a fluorescence microscope. Fluorescence images (left: a, c) and phase contrast images (right: b, d) of the bacterial cells in the same field were shown here. **(B)** Bacteria were incubated with primary antibodies described as above followed by reaction with gold (12 nm)-conjugated goat anti-rabbit IgG (H+L) as described in Materials and Methods. Cells were visualized with a transmission electron microscope at a magnification of 30 K, showing gold particles on the surface. Bar, 0.6 μm.

A

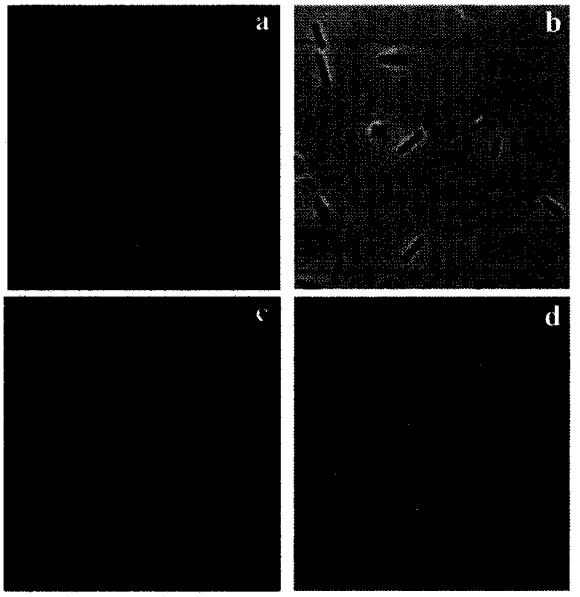

B

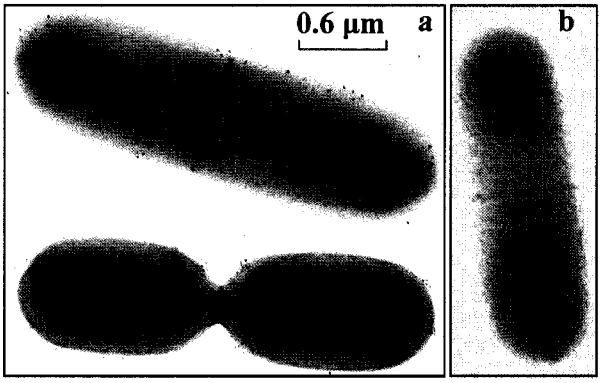

protein variant GFPuv (Fig. 5-4) to define the cell wall binding domain (CWBD) responsible for anchoring IspC to the surface. The C-terminal region (aa 198-774) was targeted for fusion protein constructions because it contains several GW modules which are similarly found in the CWBD of other *L. monocytogenes* proteins such as InlB and Ami. All the four GFPuv fusions bound evenly to the cell surface of *L. monocytogenes* serotype 4b as revealed by fluorescence microscopy (Fig. 5-5). However, the four hybrid proteins are different in binding affinity for the cell surface. Under the same assay conditions, only the fluorescence emitted from the GFPuv-CBD1 bound to the cell surface was detected with an exposure time of as short as 0.5 sec. Binding of CBD2 and CBD3 to the surface was detected at a longer exposure time (1.5 sec). Detection of CBD4 binding required an extended exposure time of 3.5 sec. A longer exposure time required for the detection indicated that a smaller number of fusion proteins are present on the cell surface. Binding of the CBDs to the bacterial surface are specific, as the interaction of the purified GFPuv with the cell surface was not detected at an exposure time of 3.5 sec.

5.2.6 Enzyme catalytic domain analysis

To define the catalytic domain of IspC, the 197-amino-acid N-terminal region encompassing a sequence (aa 58-197) highly homologous to the catalytic domain of the muramidase FlgJ from *S.* Typhimurium (Nambu et al., 1999) was targeted for deletion analysis. Three deletion constructs were generated to synthesize recombinant EAD1 (aa 58-197), EAD2 (aa 58-263) and EAD3 (aa 1-197) for renaturing SDS-PAGE analysis of their hydrolytic activities over a broad pH range from 3 to 10 (Fig. 5-6). At pH 7.5 where the full-length IspC showed its strong hydrolytic activity (Fig. 5-1B), EAD3 did not appear to hydrolyze the substrate efficiently (Fig. 5-6, Lane 3), although the IPTG-induced EAD3 expression in *E. coli* led to the cell lysis (i.e., a decrease in optical density and formation of

FIG. 5-4. IspC and its deletion variants. The polypeptides encoded by the expression constructs described in Materials and Methods are depicted by: IspC, aa 1-774; EAD1, aa 58-197; EAD2, aa 58-263; EAD3, aa 1-197; CBD1, aa 198-774; CBD2, aa 234-774; CBD3, aa 249-774; CBD4, aa 264-774.

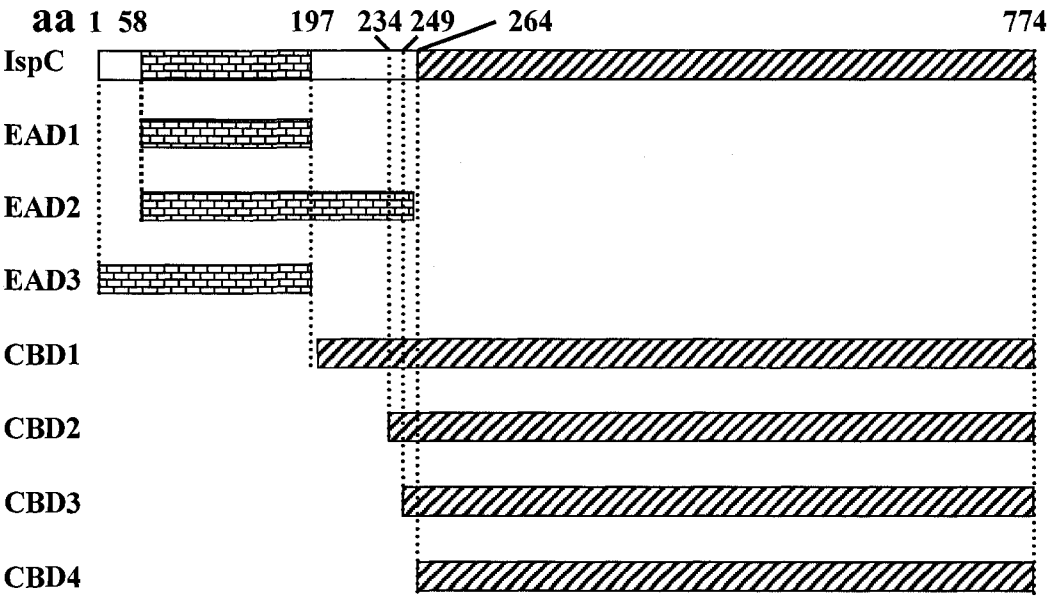
aa 1 58 197 234 249 264 774
IspC
EAD1
EAD2
EAD3
CBD1
CBD2
CBD3
CBD4

FIG. 5-5. Binding of the IspC C-terminal regions fused with GFPuv to the cell surface of *L. monocytogenes* serotype 4b. Live *L. monocytogenes* (6×10^8 cells), harvested from the late exponential growth, were incubated with GFPuv-CBD fusions or GFPuv each at 0.564 nM at room temperature for 5 min and imaged with a fluorescence microscope (left panels). The C-terminal regions of IspC are CBD1 (aa 198-774), CBD2 (aa 234-774), CBD3 (aa 249-774), and CBD4 (aa 264-774). The exposure time for capturing images is indicated by the numbers in parentheses. Right panels show corresponding phase contrast images of the bacterial cells in the same field.

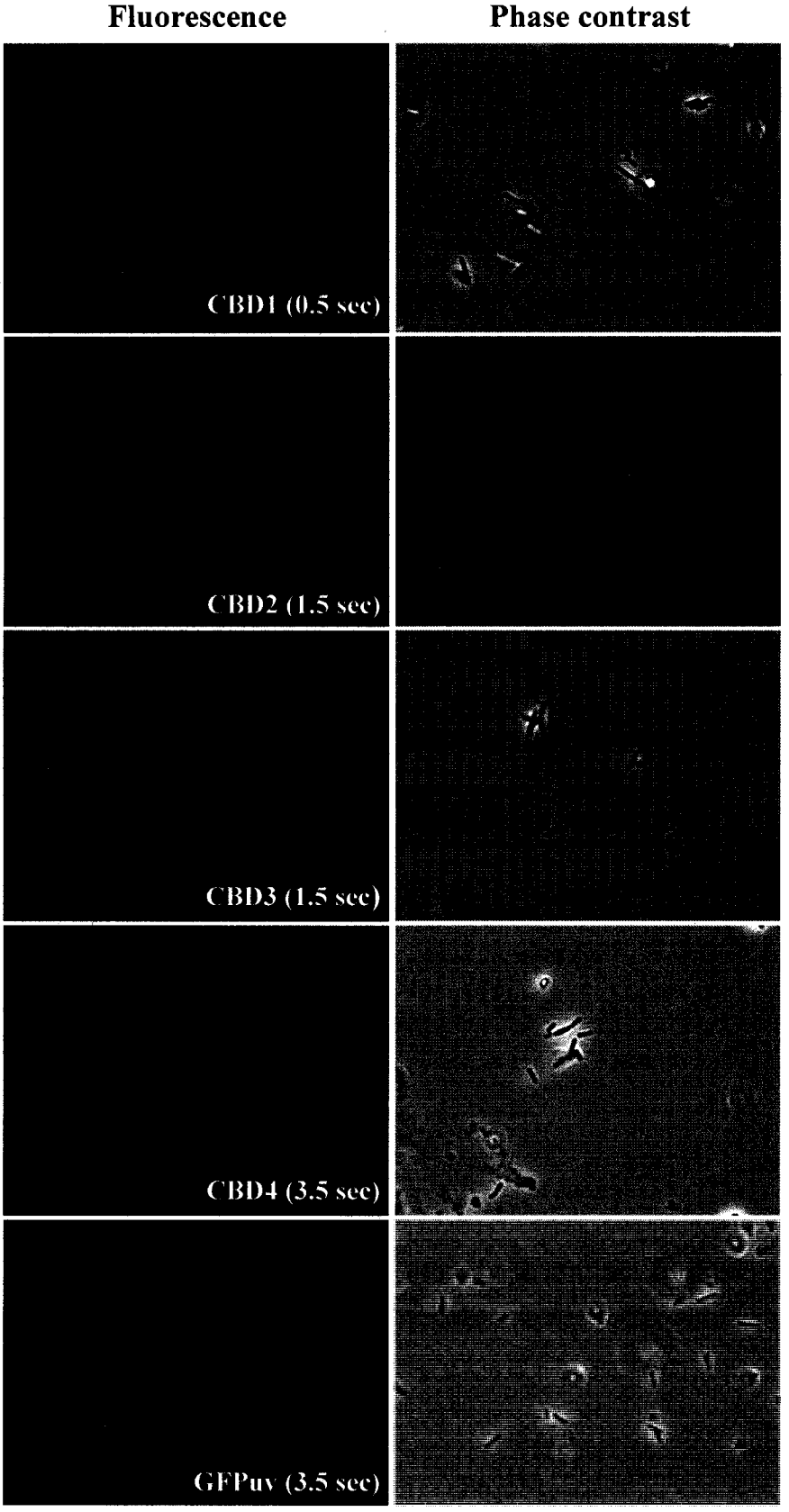
Fluorescence
Phase contrast
CBD1 (0.5 sec)
CBD2 (1.5 sec)
CBD3 (1.5 sec)
CBD4 (3.5 sec)
GFPuv (3.5 sec)

FIG. 5-6. Mapping of a peptidoglycan hydrolase domain in the N-terminal region of IspC. Renaturing SDS-PAGE analysis of the purified recombinant proteins derived from the N-terminal region (Lane 1: EAD1 aa 58-197; Lane 2: EAD2 aa 58-263; Lane 3: EAD3 aa 1-197) were performed using the *M. lysodeikticus* ATCC 4698 substrate (0.2 %, w/v) at various pHs. The same buffers as in Fig. 5-1B were used. The positions to which the purified EADs migrated were shown by Western blots (WB) probed with an anti-His mAb.

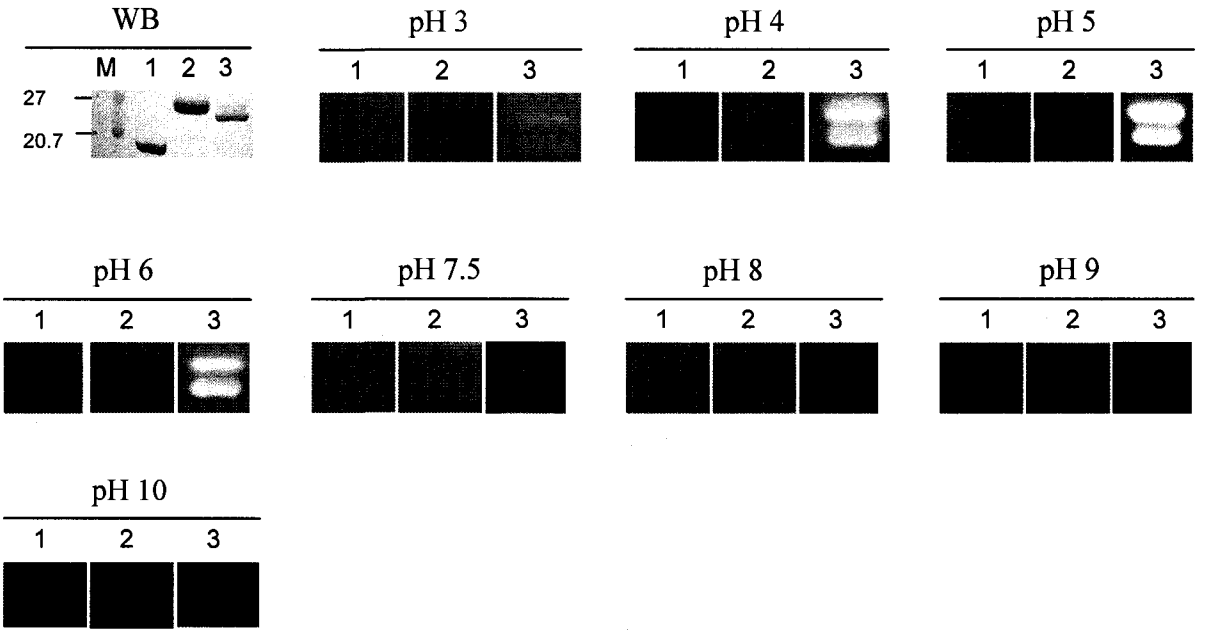
WB
M 1 2 3
27
20.7
pH 3
1 2 3
pH 4
1 2 3
pH 5
1 2 3
pH 6
1 2 3
pH 7.5
1 2 3
pH 8
1 2 3
pH 9
1 2 3
pH 10
1 2 3

fibrous materials) and thus suggested it possesses peptidoglycan hydrolase activity. Cell lysis was similarly observed during induced expression of the full length IspC. In contrast to the full-length IspC, EAD3 showed activity at acidic pH values but not at alkaline pH values with a pH optimum between 4 and 6. A double activity band was unexpectedly observed with EAD3 with a strong activity associated with the smaller fragment, which is most likely to be the degraded product of EAD3. In contrast, neither EAD1 nor EAD2 exhibited the hydrolytic activity over the broad range of pH values tested.

5.3 Discussion

This part of the study has demonstrated that a *L. monocytogenes* immunogenic protein of unknown function, IspC, identified previously by differential immunoscreening of an expression library of *L. monocytogenes* serotype 4b genomic DNA (Yu et al., 2007), is a novel surface localized autolysin comprising an N-terminal enzyme catalytic domain and a C-terminal cell wall binding domain. The data from RT-PCR analysis of the *ispC* transcript and Western blot analysis of the encoded protein under the *in vitro* culture condition revealed that the *ispC* gene was, in fact, expressed *in vitro* but only in the early exponential growth in a transient fashion. A relatively constant low level of the IspC protein observed in the stationary growth may indicate that the protein was quite stable and less susceptible to proteolytic degradation. This provides further evidence to support the hypothesis that IspC is significantly induced *in vivo* during infection and thus may play a role in virulence.

The combined results from both immunofluorescence microscopy and immunogold transmission electron microscopy showed that IspC is unevenly localized in clusters on the cell surface, in contrast to (i) the ring distribution of the *S. aureus* autolysin Atl on the cell surface at the septal region, which is proposed to be required for efficient partitioning of daughter cells after cell division (Yamada et al., 1996) and (ii) the polar position of a *S.*

pneumoniae peptidoglycan hydrolase LytB on the surface, which is believed to be involved in separation of the daughter cells or chain dispersing, the final event of the cell division cycle (De Las Rivas et al., 2002). Further characterization of binding of several GFP_{uv}-tagged CBDs of various lengths to *L. monocytogenes* has defined a C-terminal domain responsible for anchoring IspC to the surface. The GFP_{uv}-CBDs stained the bacterial surface evenly in contrast to the uneven surface display of the authentic IspC, suggesting that targeting IspC to certain areas of the surface may be crucial for its biological functions different from those proposed for the *S. aureus* Atl and the *S. pneumoniae* LytB. The C-terminal cell wall binding domain of IspC contains seven GW modules, the function of which has been ascribed to displaying the GW proteins on the surface via binding to the cell wall component lipoteichoic acid, as demonstrated in a number of other surface proteins from Gram-positive bacteria including *Listeria* (Baba and Schneewind, 1996; Braun et al., 1997; Jonquieres et al., 1999; Milohanic et al., 2004). Decoration of *L. monocytogenes* surface with GFPuv-tagged CBDs showed that a CBD with all 7 GW modules (i.e., CBD1) binds much stronger than the one with the first GW module being partially (i.e., CBD2 and CBD3) or nearly completely deleted (i.e., CBD4). This suggests that the sequence integrity within a GW module is crucial for cell wall binding function. Related findings were obtained with the *L. monocytogenes* InlB for which the strength of cell wall binding is influenced by the number of GW modules (Braun et al., 1997; Jonquieres et al., 1999; Jonquieres et al., 2001). InlB with 3 GW modules was found in both cell surface-associated and released forms (Jonquieres et al., 2001). Deletion or addition of GW modules resulted in a complete dissociation of an InlB variant bearing only one GW module and a complete retention of one containing 8 GW modules (Braun et al., 1997; Jonquieres et al., 1999). In *in vitro* or *in vivo* grown *L. monocytogenes*, IspC with seven GW modules would be expected to be bound

tightly on the surface. This notion is supported by two lines of experimental evidence reported here: (i) GFPuv-tagged CBD1 (7 GW modules) binds strongly to the surface as compared to the CDB4 (~ 6 GW modules); (ii) IspC was not detected by RαIspC antibody in the culture supernatant of *L. monocytogenes* serotype 4b (data not shown).

Bioinformatic analysis of the IspC sequence predicted a peptidoglycan hydrolase domain between aa 58 and aa 197 (Yu et al., 2007; H. Dan and M. Lin, unpublished data). Renaturing gel analysis showed that IspC was capable of hydrolyzing the cell wall substrates of not only *L. monocytogenes* but also other bacteria such as *M. lysodeikticus* ATCC 4698 and *E. coli* ATCC 25922. The immunogenic protein IspC is thus first identified from experimental evidence as an autolysin according to the definition of autolysins, i.e., bacteriolytic enzymes that degrade the cell wall peptidoglycan (murein) of the bacteria that produce them (Shockman and Holtje, 1994). The catalytic domain of IspC was further experimentally defined in the N-terminal region (aa 1-197) with IspC deletion variants. IspC possesses an N-terminal signal peptide of 23 residues that is cleavable by an *E. coli* signal peptidase. Thus, the catalytic domain of IspC is redefined to the N-terminal region (aa 24-197). The hydrolase activity analysis of these variants using renaturing gels revealed that the sequence N- but not C-terminal to the putative catalytic domain (aa 58-197) was required for a hydrolytic function. Autolysins are ubiquitous among bacteria that can cleave covalent bonds in peptidoglycan substrates of their own cell walls (Shockman and Holtje, 1994) and thus can be potentially lethal. Regulation of antolysin activity would be expected to be important for the survival of bacteria, even though regulatory mechanisms are not known. Because of the extracellular nature of the IspC and other known autolysins such as *L. monocytogenes* Ami (Milohanic et al., 2001), at least the microenvironment factors such as the pH surrounding and within the cell walls are expected to contribute a great deal to regulate the bacteriolytic

activity of autolysins. Although IspC exhibited its hydrolytic activity over a wide range of pH values, the enzyme functions much more efficiently at alkaline pHs than acidic pHs with an optimum pH of 7.5 to 9. In comparison, SKl, an *N*-acetylmuramoyl L-alanine amidase from *Streptococcus mitis* SK137, shows an optimum activity at pH 6.5 (Llull et al., 2006). These optimum pH values ranged from near neutral to alkaline suggest that the autolysins such as IspC should show limited enzymatic activity and thus avoid a potential lethal bacteriolytic effect on bacteria when exposed to a relatively low pH at several stages during infection, including the acidic environment of the stomach and phagosome, and low pH in acidified foods such as dairy products. The cell wall of *B. subtilis* was observed to be protonated during growth, suggesting a relatively low pH environment in the cell wall may provide one means of regulating autolysins during growth (Calamita et al., 2001). In contrast to the full length protein IspC, its N-terminal catalytic domain (i.e., EAD3) functions optimally at acidic pH values from 4 to 6. The covalent linkage to the EAD3 of the C-terminal cell wall binding domain (i.e., CBD1) with a predicted alkaline pI of 9.6 has resulted in a dramatic shift in the pH optimum from neutral to alkaline. This suggests that the IspC CWBD may be of importance in modulating the activity of the N-terminal enzyme domain. The importance of the C-terminal GW repeats for the autolytic function of an enzyme has been described for Atl in *S. aureus* (Baba and Schneewind, 1998) and Aas in *S. saprophyticus* (Hell et al., 2003). Similarly, targeting of IspC to the cell wall through its C-terminal region containing GW modules may be necessary for the autolytic function. The separate N-terminal catalytic domain of IspC, however, exhibited hydrolytic activity in renaturing gels in the absence of the cell wall binding domain. Likely, the IspC enzyme domain was retained in gels in close contact with the bacterial cell walls embedded, mimicking the cell wall targeting of the entire protein. IspC was anchored on the cell surface

through its C-terminal CWBD made up of seven GW modules (Wang and Lin, 2007). This, together with the N-terminal signal peptide, leads to proposal that the newly synthesized IspC in the cytoplasm is anchored on the cell surface with the aid of the N-terminal signal peptide, which directs the targeting of the IspC precursor to the cytoplasmic membrane and then the translocation across this membrane. Following the removal of the signal peptide by a signal peptidase and the release of the protein from the extracytoplasmic side of the membrane, the mature IspC protein is displayed on the surface via binding of its CWBD to the cell wall component lipoteichoic acid, as demonstrated in a number of other surface proteins from Gram-positive bacteria including *Listeria* (Baba and Schneewind, 1996; Braun et al., 1997; Jonquieres et al., 1999). GW modules in the *L. monocytogenes* Ami and InlB have been shown to be directly involved in pathogenesis through binding to host cell components (Marino et al., 2002; Milohanic et al., 2001). Further study would be needed to determine if the CWBD of IspC containing 7 GW modules is involved in mediating binding to host cells.

The present study has resulted in addition of a novel peptidoglycan hydrolase, IspC, to the list of *L. monocytogenes* autolysins identified earlier, namely P60, P45, Ami, MurA and Auto (Popowska, 2004). In *L. monocytogenes*, murein-hydrolyzing activity of a flagellin FlaA was demonstrated (Popowska and Markiewicz, 2004), but its autolytic activity remained in question. Bacterial autolysins are implicated in a number of cellular processes including cell wall turnover, cell division, cell separation, chemotaxis, biofilm formation, genetic competence, protein secretion, antibiotic-induced lysis, sporulation, formation of flagella (Shockman et al., 1996; Smith et al., 2000), and in pathogenesis (Berry and Paton, 2000; Canvin et al., 1995; Heilmann et al., 2005; Hell et al., 1998; Milohanic et al., 2001; Valisena et al., 1991). Although further studies are required to elucidate the biological

functions of the autolysin IspC and its role in virulence, it may be expected that IspC is involved in at least some of the cellular processes described for bacterial autolysins. Given that two *L. monocytogenes* autolysins Ami and Auto, similar in structural organization to IspC, play a role in pathogenesis (Cabanes et al., 2004; Milohanic et al., 2001), it is suggested that the immunogenic autolysin IspC may contribute to the virulence of *L. monocytogenes*.

CHAPTER VI

Study on the Role of IspC in *L. monocytogenes* Virulence Using Mouse and Mammalian Cell Culture Models

Some of the data from Chapter VI has been published in:
Wang, L., and Lin, M. (2008). A novel cell wall-anchored peptidoglycan hydrolase (autolysin) IspC essential for *Listeria monocytogenes* virulence: genetic and proteomic analysis. Microbiology *154 (Pt 7)*:1900-1913.

6.1 Introduction

L. monocytogenes IspC is a cell wall-anchored peptidoglycan hydrolase (autolysin), capable of degrading the cell wall peptidoglycan of the bacterium itself (Chapter V). Bacterial autolysins are involved or implicated in pathogenesis (Berry et al., 1989; Cabanes et al., 2004; Canvin et al., 1995; Lenz et al., 2003; Lock et al., 1992; Mani et al., 1994; Milohanic et al., 2001) in addition to their biological functions involving cell wall expansion, cell division, cell separation, chemotaxis, biofilm formation, genetic competence, protein secretion, antibiotic-induced lysis, sporulation, and formation of flagella (Smith et al., 2000). Autolysin-deficient mutants including a LytA mutant of *S. pneumoniae* (Berry and Paton, 2000), an AtlE mutant of *S. epidermidis* (Rupp et al., 1999), and Ami, Auto, p60 and MurA mutants of *L. monocytogenes* (Cabanes et al., 2004; Lenz et al., 2003; Milohanic et al., 2001; Pilgrim et al., 2003) are less virulent in animal models than their parental wild type strains. The mechanisms underlying how autolysins are involved in virulence are not fully understood and need to be investigated further. The autolytic activity and the cell wall binding domain of bacterial autolysins have been shown to be involved in virulence. LytA of *S. pneumoniae* and MurA and p60 of *L. monocytogenes* are thought to mediate the release of cytoplasmic toxins or proinflammatory degraded cell wall components resulting in subsequent tissue injuries (Jedrzejas, 2001; Lenz et al., 2003; Lock et al., 1992; Tuomanen, 2000). Restoration of virulence in a *L. monocytogenes* p60-defective mutant strain requires expression of the full-length autolysin p60 with an intact catalytic domain (Lenz et al., 2003). The cell wall binding domains of autolysins, made up of repeated GW modules, contribute to

bacterial virulence by promoting adherence to eukaryotic cells as shown for Ami of *L. monocytogenes* (Milohanic et al., 2001) and to extracellular matrix proteins as shown for Aas of *S. saprophyticus* (Hell et al., 1998) and AtlC of *S. caprae* (Allignet et al., 2002).

Several lines of experimental evidence accumulated from this and previous studies (Yu et al., 2007) have suggested that IspC is an important candidate potentially involved in pathogenesis. Such evidence includes (i) antibody to IspC is present in rabbits infected with live *L. monocytogenes* but not in animals receiving heat-killed bacteria, suggesting that this protein is specifically induced or upregulated *in vivo* during infection, (ii) IspC is localized on the cell surface, and (iii) IspC is an autolysin. Both Ami and Auto of *L. monocytogenes* are involved in pathogenesis but they act via different mechanisms (Cabanes et al., 2004; Milohanic et al., 2001). Ami contributes to bacterial adhesion to eukaryotic cells via its C-terminal GW modules, whereas Auto with four GW modules is not involved in adhesion but contributes to the entry of *L. monocytogenes* into eukaryotic cells. This suggests the necessity for examining the role of a newly identified *L. moncytogenes* autolysin IspC in pathogenesis.

This part of the study was conducted to analyze the *L. monocytogenes ispC* gene and its product using genetic and proteomic approaches in an attempt to define the biological function of this cell wall-anchored peptidoglycan hydrolase and its role in virulence. Data obtained here indicate that IspC is a novel factor contributing to the virulence of *L. monocytogenes* through the mechanisms involving its adhesive properties of the C-terminal CWBD and regulating the surface display of other virulence factors presumably by the

autolytic activity of its N-terminal catalytic domain.

6.2 Results

6.2.1 Construction and Phenotypic Characterization of an *ispC* in-frame Deletion Mutant

To elucidate the biological function of the 86-kDa autolysin IspC (Wang and Lin, 2007) and its potential role in virulence, an IspC-deficient *L. monocytogenes* strain was successfully created from the parental strain *L. monocytogenes* serotype 4b via homologous recombination using the pAUL-A-based integration-excision technique. This mutant, having a chromosomal in-frame deletion of 2292 bp within the 2325-bp *ispC* ORF (Fig. 6-1A), designated Δ*ispC*, was confirmed by PCR with two sets of primer pairs (Fig. 6-1B) followed by DNA sequencing. With the primers P304 and P285 targeting the deleted region, no PCR product was obtained from the Δ*ispC* mutant chromosome DNA, in contrast to a product derived from the WT corresponding to its calculated size of 452 bp. With the primers P481 and P518 annealing outside the deleted region, a PCR product close to the expected size of 993 bp was amplified from the mutant chromosome DNA and, as expected, was smaller than that (~ 3200 bp) derived from the WT. DNA sequencing of the PCR product derived with P481 and P518 from the Δ*ispC* mutant also confirmed a target deletion of 2292 bp within the *ispC* ORF.

The Δ*ispC* mutant exhibited the abrogation of IspC expression in *in vitro* culture, as evidenced by the data from three separate experiments: (i) Western blot analysis of total bacterial proteins revealed that a protein band of ~86 kDa from the WT recognized by rabbit

FIG. 6-1. Comparison of a Δ*ispC* mutant strain of *L. monocytogenes* with the WT at DNA, protein and microscopic levels. **(A)** Schematic representation of the *ispC* gene locus of the WT strain and the corresponding gene deletion in the mutant. The annealing positions of the primer pairs P304/P285 and P481/P518 used to confirm the Δ*ispC* mutant are indicated by arrows. The numbers in the parenthesis indicates the predicted sizes of PCR products amplified from the WT genomic DNA using the corresponding primers. The deleted sequence coding for aa 4-767 of IspC, the first three codons and the last eight codons of IspC are depicted by an open bar, a solid bar and a hachet bar, respectively. **(B)** Gel electrophoresis analysis of PCR products derived from the chromosomal DNAs of the mutant and the WT. Lane 1, the product from WT with the primer pair P304/P285; Lane 2, the product from the Δ*ispC* mutant with the primer pair P304/P285; Lane 3, the product from WT with the primer pair P481/P518; Lane 4, the product from the Δ*ispC* mutant with the primer pair P481/P518. **(C)** Western blot analysis of the total proteins extracted from the mutant and WT strains. Each lane containing the proteins from bacterial cells equivalent to 0.1 ml of culture with an OD_{620} of 1.0 was probed with rabbit anti-IspC antiserum (RαIspC). The molecular masses of protein standards (in kDa) are shown by the numbers on the left. **(D)** The bacteriolytic profiles of the surface proteins from the mutant and WT strains. The bacteriolytic activity was analysed in a renaturing SDS-PAGE (12%) gel containing 0.2% (w/v) *M. lysodeikticus*. Each lane contains the surface proteins extracted from bacterial cells equivalent to 1 ml of culture with an OD_{620} of 0.5. The bacteriolytic band of ~86 kDa corresponding to the IspC protein is indicated by an arrow. **(E)** Detection of the surface expression of IspC in the mutant and WT strains by immunofluorescence staining with RαIspC. **(F)** Phase contrast micrographs of the mutant and the WT harvested at the mid-log growth phase. **(G)** Sectional TEM micrographs of the mutant and WT strains at the mid-log growth phase. The bacterial cell walls are indicated by arrows. Magnification, 50 K. Bar, 0.16 μm.

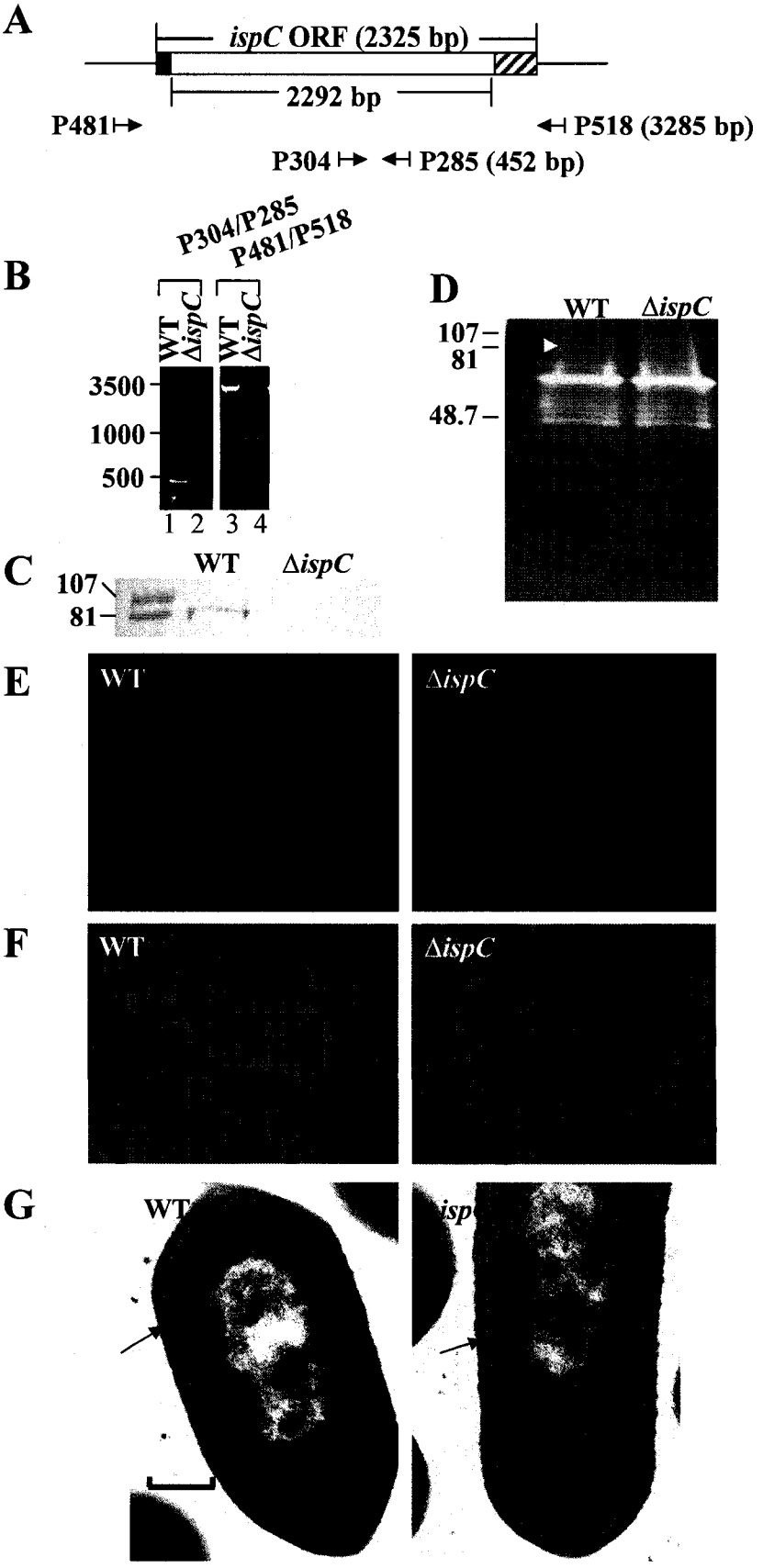
A
ispC ORF (2325 bp)
2292 bp
P481
P518 (3285 bp)
P304
P285 (452 bp)
B
P304/P285
P481/P518
WT
ΔispC
WT
ΔispC
3500
1000
500
1 2 3 4
C
WT
ΔispC
107
81
D
WT
ΔispC
107
81
48.7
E
WT
ΔispC
F
WT
ΔispC
G
WT
isp

anti-IspC polyclonal antibody (RαIspC) was not present in the mutant (Fig. 6-1C), (ii) immunofluorescence microscopy with RαIspC showed no fluorescence staining on live mutant bacteria but detected the IspC on the surface of WT bacteria (Fig. 6-1E), and (iii) renaturing SDS-PAGE analysis of the surface protein extract for peptidoglycan hydrolase activity with respect to *M. lysodeikticus* cell wall showed that a bacteriolytic band of ~86 kDa associated with the WT was not found in the mutant (Fig. 6-1D). Interestingly, surface peptidoglycan hydrolase activity profiles from the WT and the Δ*ispC* mutant showed that IspC is a minor autolysin in *in vitro* culture.

The Δ*ispC* mutant was indistinguishable from the WT with respect to: colony morphology on TSBA plates, bacterial morphology at various growth phases in BHI broth at 37 °C as revealed by phase contrast microscopy (Fig. 6-1F), transmission electron microscopy (data not shown), and sectional transmission electron microscopy (Fig. 6-1G), motility at 25 °C and 35 °C, hemolysis on sheep blood agar plates, carbohydrate utilization on API 50 CH strips, growth curve at 37 °C in BHI broth or growth in BHI under acidic (pH 4.5) or osmotic stress (0.3 M NaCl), and a number of biochemical tests (i.e. catalase test, CAMP test (*S. aureus* and *Rhodococcus equi*), H_2S test, oxidase test, nitrate reduction test).

6.2.2 IspC is Required for Virulence *in vivo*

To evaluate whether the *ispC* gene contributes to virulence, BALB/c mice were infected intravenously with the Δ*ispC* mutant and the WT. The deficiency of *ispC* in bacteria significantly ($P < 0.01$) reduced the bacterial load in the target organs by ~5-fold in brain and ~7-fold in liver at 48 h post infection with the exception of the spleen, where the bacterial

counts were similar between the mutant and the WT at 6 and 24 h (Fig. 6-2). The requirement of IspC for virulence was further demonstrated by the fact that the mutant did not cause any mortality at 72 h, in contrast to the death of 2 out of 6 mice infected with the WT. This result prompted further investigation into the role of IspC in virulence at the various stages of the infectious cycle using cultured eukaryotic cells.

6.2.3 Involvement of IspC in Bacterial Adhesion in a Cell Type-Dependent Manner

In earlier studies, GW modules of several autolysins including Ami of *L. monocytogenes* (Milohanic et al., 2001), Aas of *S. saprophyticus* (Hell et al., 1998), and AtlC of *S. caprae* (Allignet et al., 2002) were shown to be involved in bacterial adhesion. To determine if the surface autolysin IspC containing 7 GW modules in its C-terminal CWBD (Wang and Lin, 2007) promotes the adherence of bacteria to eukaryotic cells, the Δ*ispC* mutant and the WT were assayed for binding to several types of eukaryotic cells (Fig. 6-3A). The primary attachment of the Δ*ispC* mutant to Hep-G2, Vero and SCP was reduced by approximately two- to three-fold ($P < 0.01$) in comparison to that of the WT, while both strains adhered in a similar fashion to Caco-2, L132, Hela, HBMEC and the mouse macrophage J774. This indicates that IspC may play a role in mediating bacterial adhesion to normally nonphagocytic cells in a cell type-dependent manner.

6.2.4 IspC is Required for Invasion in a Cell-type Dependent Manner

To determine if IspC contributes to the invading capability of *L. monocytogenes*, internalization of the Δ*ispC* mutant and the WT into various normally nonphagocytic eukaryotic cells were investigated (Fig. 6-3B). The mutant exhibited a reduction in

FIG. 6-2. Bacterial counts in the target organs of mice infected with the *ΔispC* mutant and the WT. Groups of BALB/c mice (six mice per group) were intravenously inoculated with 5×10^4 bacteria of each strain. The number of viable bacteria in brains, livers, spleens obtained at 6, 24, and 48 h post infection was presented as the mean ± standard deviation (SD) (n=6). Bacterial organ counts were not available at 72 h because 2 out of 6 mice infected with the WT died.

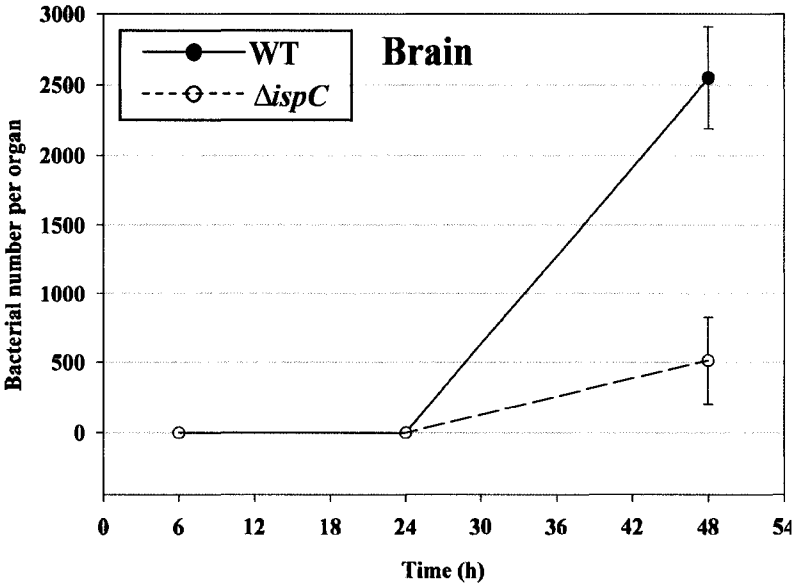
Brain
WT
ΔispC
Bacterial number per organ
3000
2500
2000
1500
1000
500
0
0
6
12
18
24
30
36
42
48
54
Time (h)

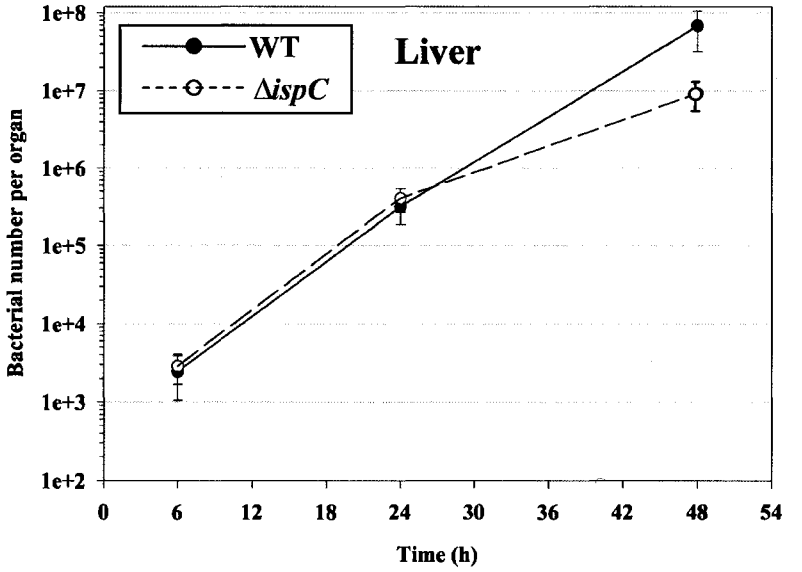
Liver
WT
ΔispC
Bacterial number per organ
1e+8
1e+7
1e+6
1e+5
1e+4
1e+3
1e+2
0
6
12
18
24
30
36
42
48
54
Time (h)

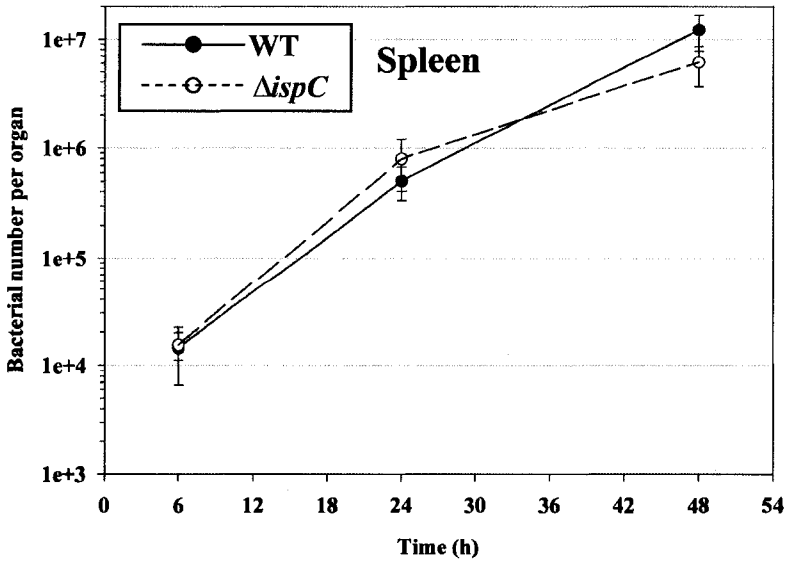
Spleen
WT
ΔispC
Bacterial number per organ
1e+7
1e+6
1e+5
1e+4
1e+3
0
6
12
18
24
30
36
42
48
54
Time (h)

FIG. 6-3. Contributions of IspC expression to bacterial adherence to and invasion of eukaryotic cells. (A) Quantitative analysis of adhesion of the Δ*ispC* mutant to various eukaryotic cell lines in comparison to the WT. The mutant and WT strains were used to infect one particular cell line in triplicate at a predetermined MOI (see Materials and Methods) for 1 h and the bacteria associated with the eukaryotic cells were quantified by plating the cell lysates after washing away free bacteria. The quantity of mutant bacteria was calculated relative to that of the WT set at 100% and presented as the mean ± SD (n=3). The asterisk indicates that difference is statistically significant ($P < 0.05$). **(B)** Quantitative analysis of entry of the Δ*ispC* mutant into various eukaryotic cell lines. The mutant and WT strains were used to infect one particular cell line in triplicate at a predetermined MOI (see Materials and Methods) for 1 h followed by further incubation with 100 μg/ml gentamicin for 1.5 h. The intracellular bacteria were determined as in A. The quantity of mutant bacteria was calculated relative to that of the WT set at 100% and presented as the mean ± SD (n=3). The asterisk indicates that difference is statistically significant ($P < 0.05$).

A

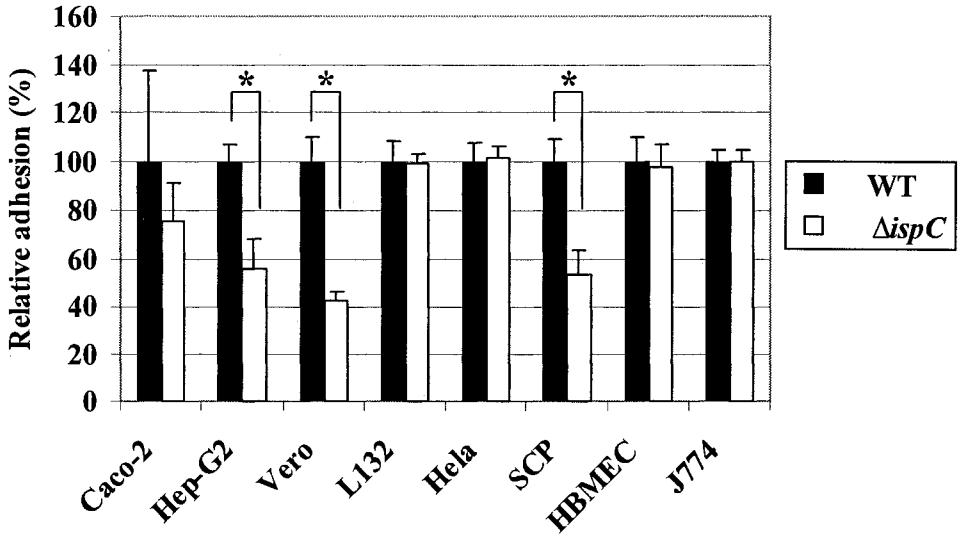
Relative adhesion (%)
160
140
120
100
80
60
40
20
0
*
*
*
Caco-2
Hep-G2
Vero
L132
Hela
SCP
HBMEC
J774
WT
ΔispC

B

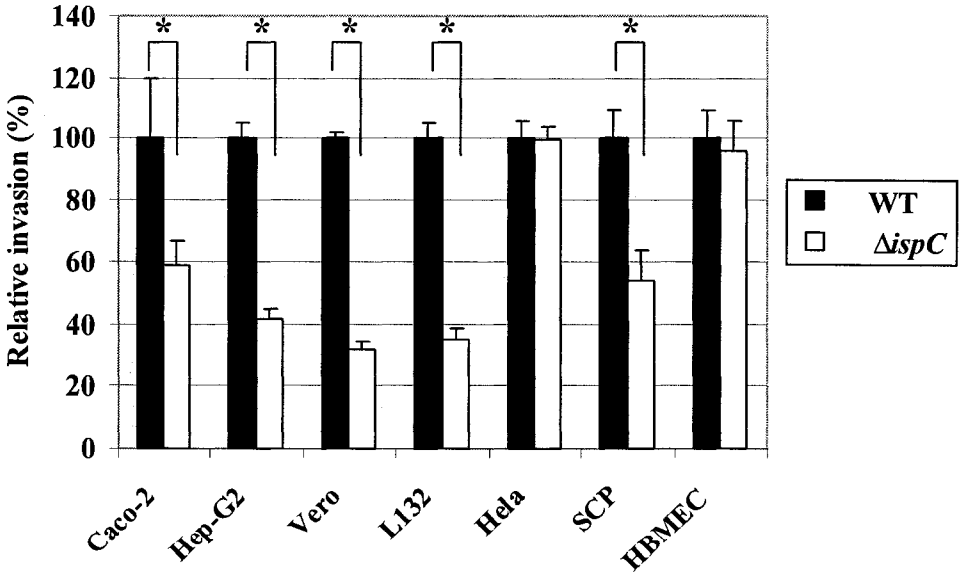
Relative invasion (%)
140
120
100
80
60
40
20
0
*
*
*
*
*
Caco-2
Hep-G2
Vero
L132
Hela
SCP
HBMEC
WT
ΔispC

internalization into Caco-2, Hep-G2, Vero, L132, and SCP by two- to three-fold ($P < 0.01$) relative to the WT, while it entered Hela and HBMEC as efficiently as the WT. Thus, IspC is involved in invading normally non-phagocytic cells by *L. monocytogenes* in a cell type-dependent manner.

6.2.5 Direct Binding of Recombinant IspC and its C-terminal CWBD to the Surface of SCP and Vero cells

The observation that the Δ*ispC* mutant possessed less adhesive and invasive characteristics for certain eukaryotic cell types prompted us to further study the adhesive properties of purified IspC and its C-terminal CWBD (aa 198-774) fused to GFPuv (GFPuv-CBD1) with respect to SCP and Vero cells in which the mutant exhibited an impaired adhesion and invasion ability. Fluorescence microscopy showed that both the purified recombinant IspC and GFPuv-CBD1 bound to SCP and Vero (Fig. 6-4). Stronger fluorescent signals were observed for binding of these proteins to SCP than binding to Vero. Fixation or fixation followed by permeabilization of these eukaryotic cells prior to fluorescence staining resulted in similar fluorescence images of cells (data not shown), indicating the binding event occurred on the cell surface. Binding of IspC or its C-terminal CWBD to the cell surfaces of SCP and Vero was specific, as no fluorescence staining on the cell surfaces was observed when probed with rabbit preimmune serum or purified GFPuv. Under the same assay condition, almost no fluorescence staining was observed on the surface of HBMEC probed with purified IspC or GFPuv-CBD1 (data not shown).

FIG. 6-4. Binding of purified recombinant IspC and an IspC cell wall binding domain (aa 198-774) fused with GFPuv (GFPuv-CBD1) to SCP and Vero cells. Paraformaldehyde-fixed SCP and Vero cells were incubated with purified recombinant IspC (3.5 μg/ml) or GFPuv-CBD1 (1.14 μM). The bound IspC was detected by interaction with RαIspC followed by staining with FITC-conjugated goat anti-rabbit IgG. The bound GFPuv-CBD1 was detected with the intrinsic fluorescence of the fusion protein. The rabbit preimmune serum (Pre) or GFPuv was used as a negative control. Fluorescence and phase contrast images of eukaryotic cells to which IspC or GFPuv-CBD1 bound were viewed using a fluorescence microscope.

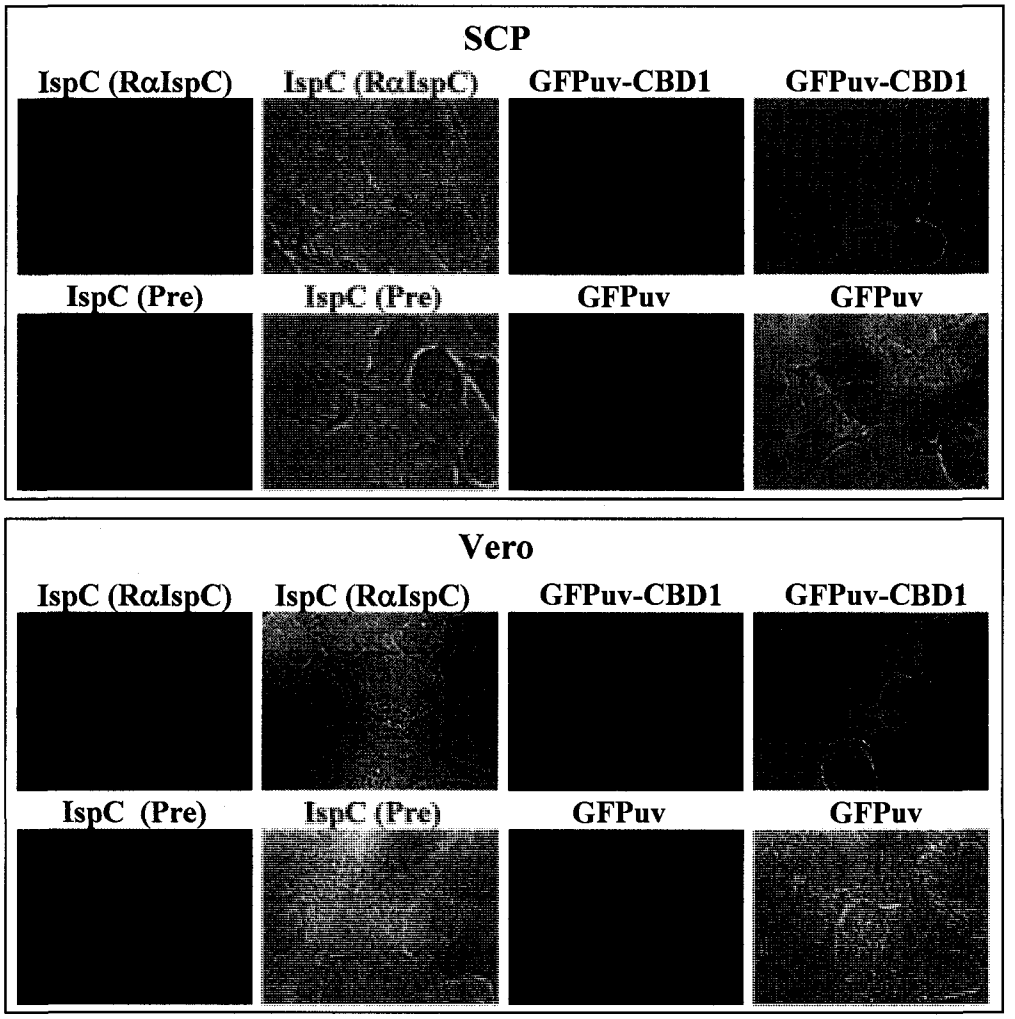
SCP
IspC (RαIspC)
IspC (RαIspC)
GFPuv-CBD1
GFPuv-CBD1
IspC (Pre)
IspC (Pre)
GFPuv
GFPuv
Vero
IspC (RαIspC)
IspC (RαIspC)
GFPuv-CBD1
GFPuv-CBD1
IspC (Pre)
IspC (Pre)
GFPuv
GFPuv

6.2.6 Deletion of *ispC* Impairs Displaying of Surface Proteins

To determine if the chromosomal deletion of *ispC* would alter the display of bacterial surface proteins including known virulence factors as an alternative mechanism leading to the reduced adhesive and invasive capacity of the mutant, surface proteins from the Δ*ispC* mutant and the WT at various growth phases were analyzed by SDS-PAGE followed by mass spectrometry (Fig. 6-5A) or by Western blots (Fig. 6-5B) using specific antibodies. Two protein bands of ~90 kDa and ~30 kDa present in the WT were undetectable in the mutant by SDS-PAGE and subsequently identified as ActA and a flagellin protein (a FlaA homologue) by mass spectrometry, respectively. Western blot analysis using rabbit antiserum to ActA showed that expression of ActA was not abolished in the mutant but dramatically reduced at all growth phases in contrast to the WT. The decrease in the amount of ActA was also observed with Western blot analysis of total cell lysates of the mutant (data not shown). Reduced surface display of ActA in the mutant was further demonstrated by immunofluorescence microscopy (Fig. 6-5C, top panel) and immunogold TEM (Fig. 6-5C, bottom panel) probed with rabbit anti-ActA antibody. Western blot analysis using rabbit anti-InlC2 antibody revealed a significant reduction in InlC2 expression in the mutant, although this protein was invisible from the SDS-PAGE gel. Three surface proteins having a similar expression level between the mutant and the WT were identified to be InlB precursor and p60 by mass spectrometry and InlA by Western blot analysis using rabbit anti-InlA antibody. No alteration in InlB expression was further confirmed by Western blot analysis using rabbit anti-InlB antibody.

FIG. 6-5. Analysis of the cell surface proteins of the Δ*ispC* mutant and the WT by SDS-PAGE and Western blots. (A) Surface proteins were extracted from the mutant and WT strains at the early-log (E), mid-log (M), late-log (L) and stationary (S) growth phases using 2 × SDS-PAGE sample buffer and loaded into each lane for SDS-PAGE analysis. The proteins identified by in-gel digestion of excised bands with trypsin followed by mass spectrometry analysis are shown on the left of the gel. Each lane was loaded with the surface proteins derived from bacterial cells equivalent to 7.5 ml of culture with an OD_{620} of 0.5. The molecular masses of protein standards (in kDa) are shown by the numbers on the right. **(B)** The surface protein extracts from the mutant and WT strains were resolved by SDS-PAGE followed by Western blot analysis using rabbit anti-ActA, -InlB, -InlA, and -InlC2 antibodies at a 1:1000 dilution. Surface proteins derived from bacterial cells equivalent to 1 ml of culture with an OD_{620} of 0.5 were loaded into each lane. **(C)** Detection of the surface expression of ActA protein of the mutant and WT bacteria at the mid-log growth phase by immunofluorescence staining (left top panel, immunofluorescence micrographs; right top panel, phase contrast micrographs) and immunogold labeling TEM (bottom panel), probed with rabbit anti-ActA antiserum. Bar, 0.2 μM.

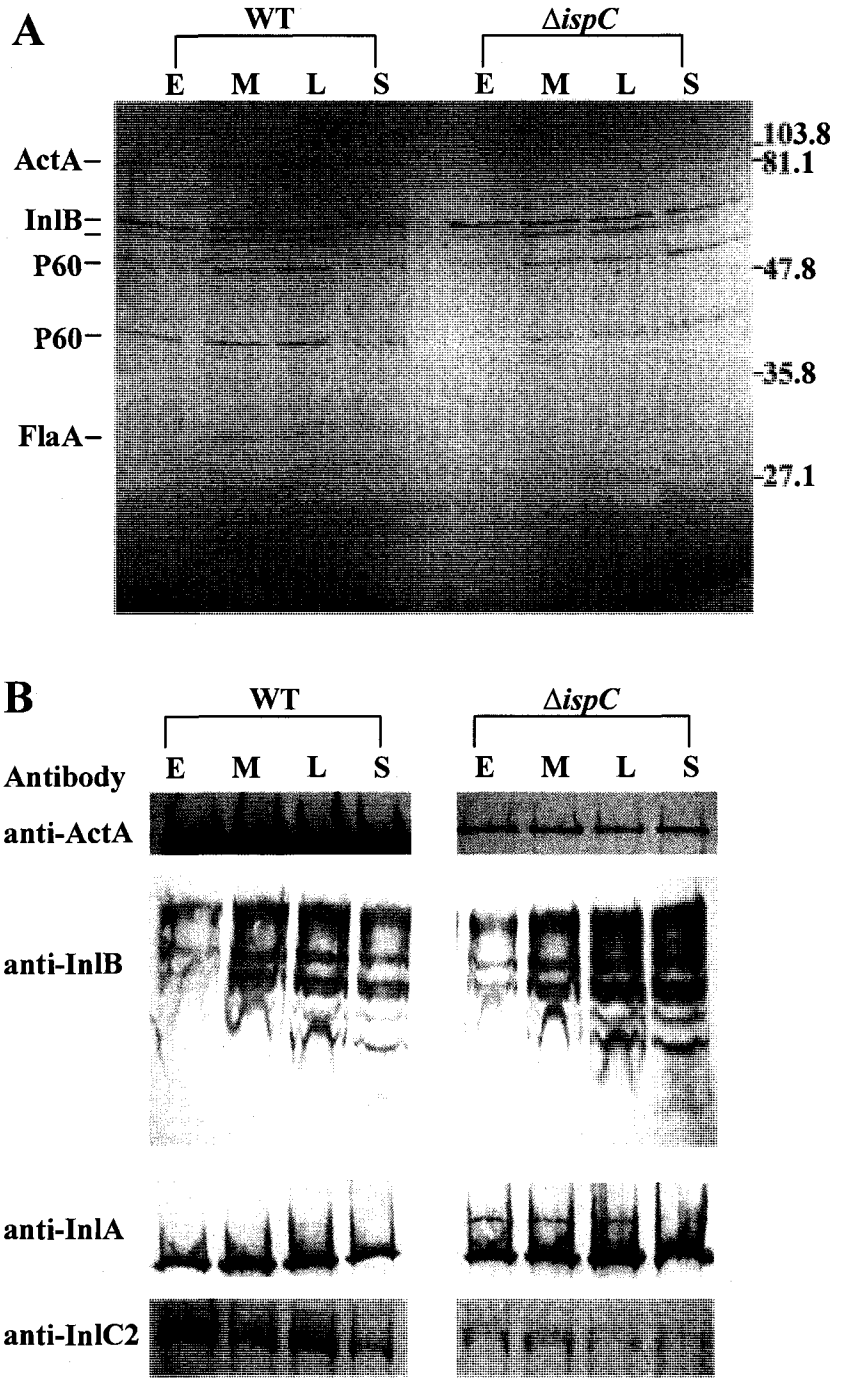
A
WT
ΔispC
E M L S E M L S
ActA
InlB
P60
P60
FlaA
103.8
81.1
47.8
35.8
27.1
B
WT
ΔispC
Antibody
E M L S E M L S
anti-ActA
anti-InlB
anti-InlA
anti-InlC2

C

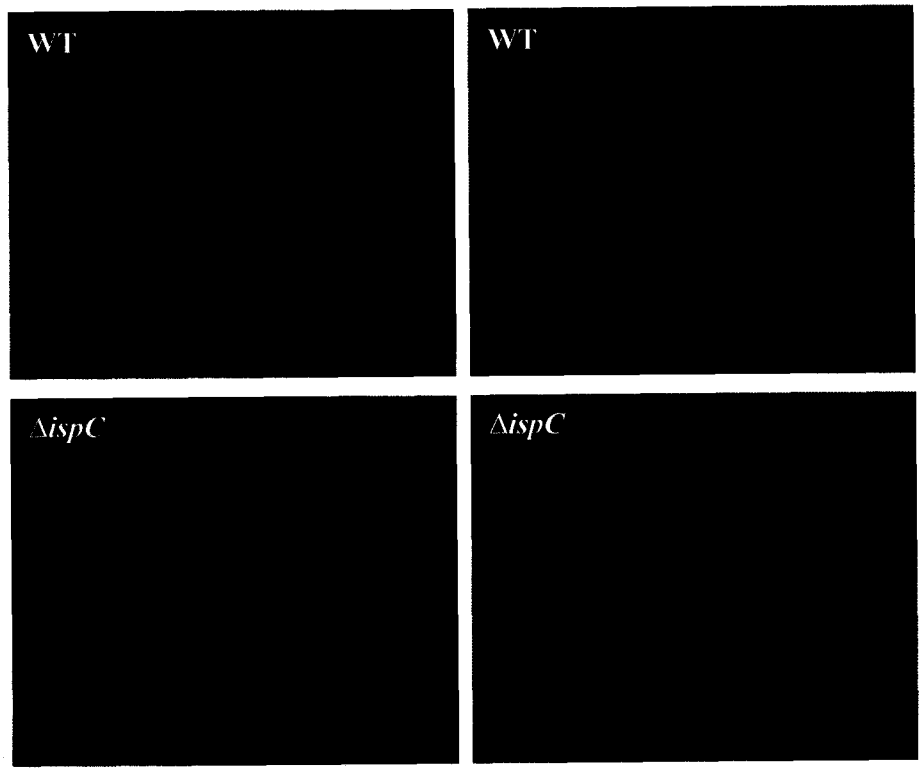

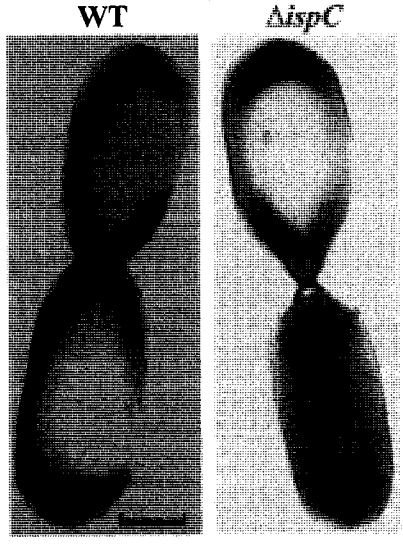

6.2.7 IspC is Involved in Actin Tail Formation at the Early Stage of Intracellular Infection

The observation that the surface display of a few proteins including ActA was strikingly reduced in the Δ*ispC* mutant prompted us to further investigate whether the abrogation of IspC expression affects the intracellular motility of bacteria by examining the formation of actin tails in the intracellular niche after infection of mouse macrophage J774 cells with the mutant in comparison to the WT. The mutant strain produced much shorter and weaker actin tails at the early infection stage (i.e., 3 h) than the WT, while at the late infection stage (i.e., 6 h), formation of the actin tails were similar between the mutant and the WT (Fig. 6-6).

6.2.8 IspC Contributes to Cell-to-cell Spread

Contribution of IspC to cell-to-cell spread of bacteria may be expected, as the formation of actin tails was impaired in early stage of infection with the Δ*ispC* mutant. This was macroscopically confirmed by the plaque assay of murine L2 fibroblast monolayer infected with the mutant as compared to the WT. The relative plaque size (expressed in arbitrary units (a. u.)) formed by the mutant strain (175.5±18.444 a. u., n=22) was significantly smaller ($P < 0.01$) than that of the WT (206.375± 25.595 a. u., n=24) (Fig. 6-7) indicating the reduced capacity of bacterial cell-to-cell spread for the Δ*ispC* strain.

6.2.9 IspC Contributes to Bacterial Intracellular Growth at the Later Infection Stage

Autolysins have dual effects on bacterial growth and survival (favoring growth and causing bacterial death). The impact of IspC on intracellular survival and growth was assessed in three cell lines (Vero, Hela and J774) following infection with the

FIG. 6-6. Detection of actin tail formation in mouse macrophage J774 following infection with the Δ*ispC* mutant and the WT. Actin tail formation promoted by ActA from the mutant and WT strains was examined at the early (3 h) and later stages (6 h) of J774 infection. The actin tails, bacteria and nuclei were stained with Alexa Fluor 488 Phalloidin (green), rabbit anti-ActA antibody followed by interaction with Alexa Fluor 647 goat anti-rabbit antibody (red), and DAPI (blue), respectively. The images were visualized with a fluorescence microscope equipped with a digital video camera.

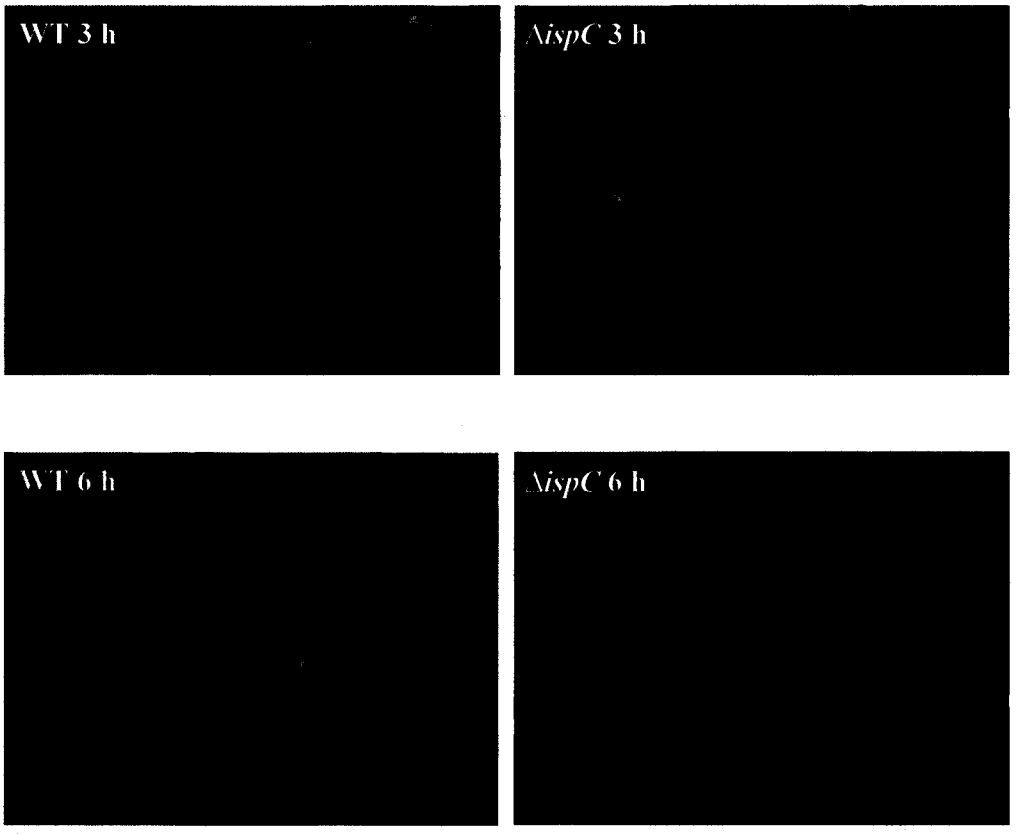
WT 3 h
ΔispC 3 h
WT 6 h
ΔispC 6 h

Fig. 6-7. Comparison of the sizes of plaques formed from murine L2 cells infected with the *ΔispC* mutant and the WT in a box plot. At least 20 plaques were randomly selected for each strain for determination of their relative sizes (diameter in arbitrary units (a. u.)) by analyzing the plaque images with the ImageJ software. The lower boundary of the box, a line within the box, and the upper boundary of the box correspond to the lower quartile (the 25th percentile), the median, and the upper quartile (the 75th percentile), respectively. Error bars above and below the box marks the 90th and 10th percentiles. Solid circles represent the unusual observations (outliers) greater than the 90th percentile or less than the 10th percentile.

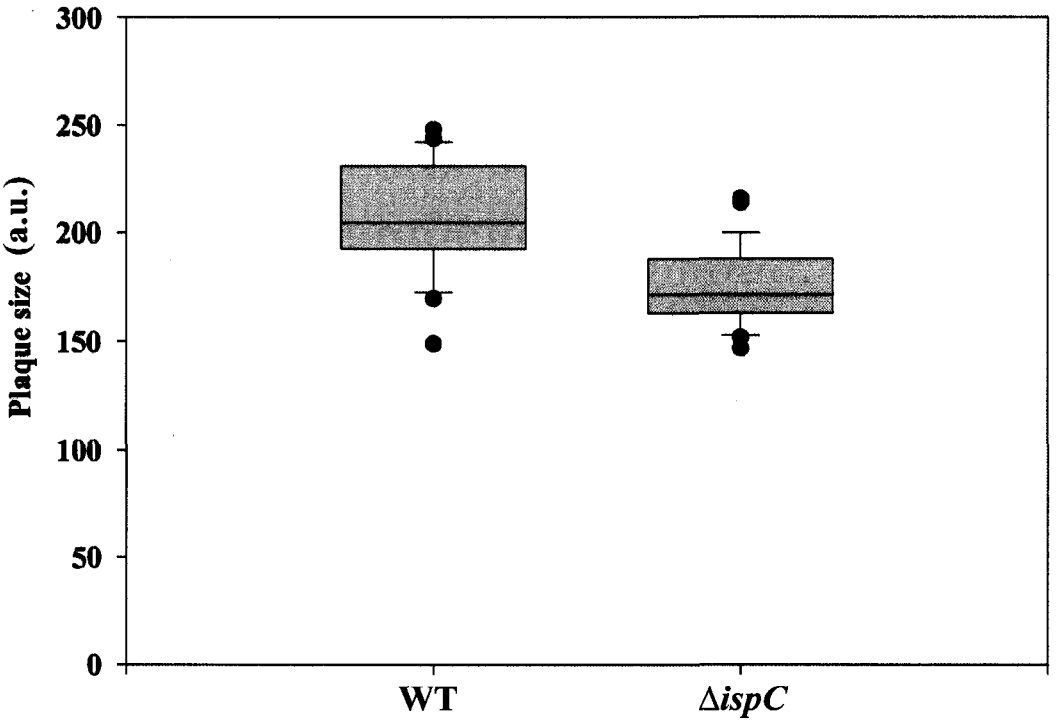
300
250
200
150
100
50
0
Plaque size (a.u.)
WT
ΔispC

Δ*ispC* mutant and the WT over an 8 h time course. The mutant showed an approximate two-fold reduction in growth within Vero and J774 and an approximate four-fold reduction within Hela, as compared to the WT (Fig. 6-8, Vero, $P < 0.01$; Hela, J774, $P < 0.05$) at 8 h post infection, although it had a similar growth rate to the WT before 8 h (Vero and J774) and 6 h (Hela). At 6 h, lack of IspC expression also produced about two-fold reduction in intracellular growth within Hela. These results indicate that IspC extends the existence of intracellular bacteria and promotes bacterial intracellular growth at the later infection stage.

6.3 Discussion

In this study, I showed evidence that a cell-wall anchored peptidoglycan hydrolase (autolysin) IspC (Wang and Lin, 2007), recognized also as the target of humoral immune response to listerial infection (Yu et al., 2007) and expressed as a minor autolysin *in vitro* (this study), is not important for cell division or separation during *in vitro* growth but required for full virulence of *L. monocytogenes*. By in-frame deleting the *ispC* gene, I have determined the effect of IspC deficiency on the phenotypic characteristics of *L. monocytogenes* (i.e., *in vitro* growth, colony/cell morphologies, and biochemical properties), virulence of the bacterium in mouse and eukaryotic cell models of infection, and display of other surface proteins. The findings from these analyses and from the analysis of binding of the purified IspC and its C-terminal CWBD (aa 198-774) fused to GFP (Wang and Lin, 2007) to eukaryotic cells, have shed new light on our understanding of the molecular mechanisms by which a surface peptidoglycan hydrolase contributes to bacterial pathogenesis.

The *in vivo* study demonstrated a significant attenuation of virulence of the Δ*ispC*

FIG. 6-8. Quantitative analysis of the intracellular growth of the Δ*ispC* mutant in Vero, Hela and J774. The intracellular growth assay (see Materials and Methods) was performed to assess the bacterial intracellular growth. The mutant and WT bacteria were used to infect three representative cell lines (Vero, Hela and J774) at a predetermined MOI for 1 h followed by further incubation with 100 μg/ml gentamicin. The intracellular viable bacteria were determined at the time points of 2, 4, 6 and 8 h after addition of gentamicin as in Fig. 6-3A and were presented as the mean ± SD (n=3). The asterisk indicates that difference is statistically significant ($P < 0.05$).

Vero

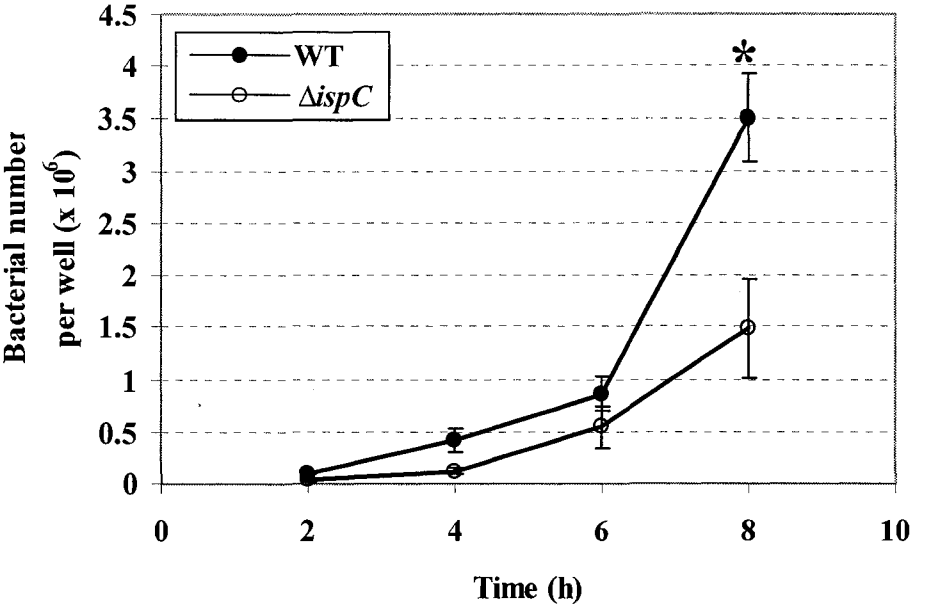

Hela

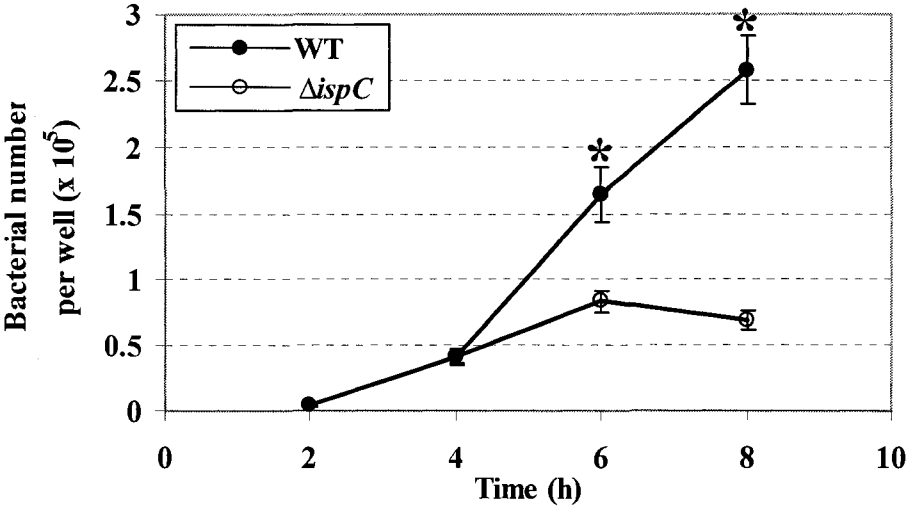

J774

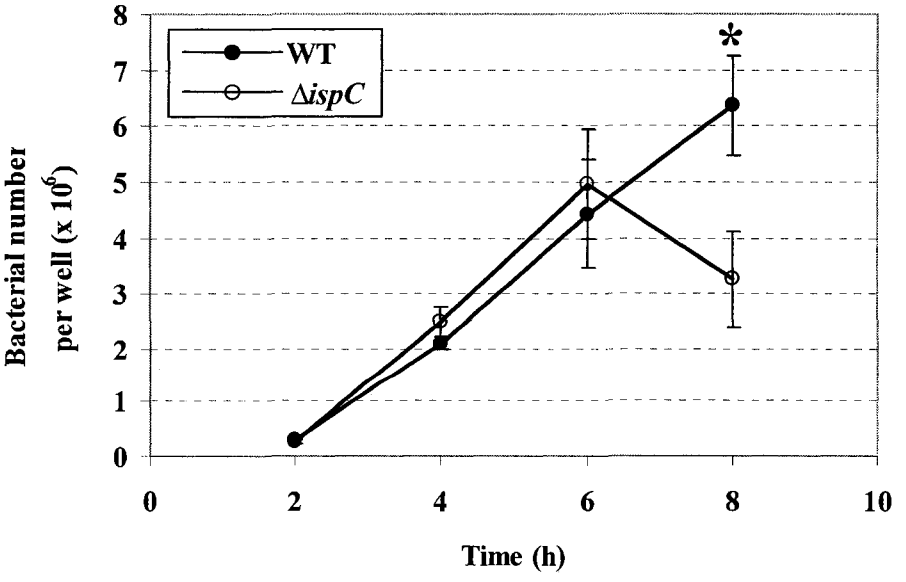

mutant for mice. Similarly, *in vivo* studies with animal models (mice, rats, and guinea pigs) of infection have shown that mutant strains defective in the synthesis of autolysins including AtlE of *S. epidermidis* (Rupp et al., 2001), p60, Ami and Auto of *L. monocytogenes* (Cabanes et al., 2004; Milohanic et al., 2001; Pilgrim et al., 2003), and LytA of *S. pneunoniae* (Berry and Paton, 2000) are less virulent than the wild type strains. Colonization in liver and brain by *L. monocytogenes* was much more IspC-dependent than was that in spleen. The observed effect on virulence, as reflected by the impaired ability to colonize the target organs (liver and brain) by the Δ*ispC* mutant, is unlikely attributable to the growth rate, colony or microscopic cell morphology or biochemical characteristics of the mutant strain, because the Δ*ispC* mutant was similar in these aspects to the WT strain *in vitro*. These findings suggest that IspC does not function in cell division or separation during *in vitro* growth for which other autolysins p60 and MurA (NamA) are shown to be necessary in *L. monocytogenes* (Carroll et al., 2003; Machata et al., 2005; Pilgrim et al., 2003). Therefore, IspC, deficiency of which is responsible for the observed attenuated virulence in mice, is involved in the establishment of *L. monocytogenes* infection *in vivo*.

This study has further characterized the Δ*ispC* mutant in detail using a cell culture infection model involving various eukaryotic cell types that the bacterium normally encounters during *in vivo* infection, leading to a better understanding of the principal role of IspC in pathogenesis. The results obtained from these experiments demonstrated that IspC significantly facilitated the infectious process of *L. monocytogenes* at multiple steps, which are known to require several key virulence factors (Vazquez-Boland et al., 2001) such as

internalins (InlA and InlB) responsible for bacterial entry into host cells, phospholipases (PlcA and PlcB) and LLO for escape from the phagosomes, and the actin polymerization (actin tail) promoting protein ActA for intracellular movement and cell-to-cell spread. The impaired capability of the Δ*ispC* mutant to adhere to Hep-G2, Vero and SCP cells but not to other eukaryotic cells (Caco-2, L132, Hela, HBMEC, and J774) suggests that IspC functions in pathogenesis as an adhesin mediating the attachment of the bacterium to some eukaryotic cells which presumably express the unidentified receptor(s) specific for IspC. Localization of IspC onto the cell surface (Wang and Lin, 2007) meets the requirement for this protein to act as an adhesin. The adhesin nature of IspC was further confirmed by the observation that purified IspC was capable of binding to SCP and Vero via its C-terminal CWBD made of 7 GW modules. The adhesive properties of autolysins have been shown in other autolysins, including Aas of *S. saprophyticus* (Hell et al., 1998), AtlC of *S. caprae* (Allignet et al., 2002), AtlE of *S. epidermidis* (Heilmann et al., 1997), and Ami of *L. monocytogenes* (Milohanic et al., 2001). Comparison of the adherence of the Δ*ispC* mutant to various eukaryotic cells with the invasion of these cells by the mutant points to some interesting facts that (i) the mutant with the impaired ability to adhere to the cell lines Hep-G2, Vero and SCP is less invasive to these cells, and (ii) the mutant strain with no reduced ability to adhere to Hela and HBMEC is fully capable of invading these cells. One exception to this is that the Δ*ispC* mutant capable of adhering to Caco-2 and L132 showed the impaired ability to invade these cells. These results indicate that IspC is necessary for entry of *L. monocytogenes* into specific types of eukaryotic cells, which may not always be dependent on IspC-mediated adhesion.

Surprisingly, the autolysin Auto of *L. monocytogenes*, similar in domain organization to two other *L. monocytogenes* autolysins Ami and IspC with an affinity for certain eukaryotic cells (Milohanic et al., 2001; Wang and Lin, 2007; this study), is not required for adhesion to but required for entry into eukaryotic cells (Cabanes et al., 2004). It appears that the importance of a particular autolysin in *L. monocytogenes* pathogenesis is dependent on the cell types (epithelial cells, fibroblasts, hepatocytes, endothelial cells, and macrophages) that the bacterium encounters during *in vivo* infection.

It was interesting to observe that adhesion to and invasion of SCP epithelial cells but not HBMEC by *L. monocytogenes* was dependent on the product of *ispC*. This is a novel finding for the role that IspC plays in *L. monocytogenes* infection of the brain. There are two brain barriers: the cerebral capillary endothelium as the barrier between the blood and the brain parenchyma and the choroid plexus epithelium as the barrier between blood and the cerebrospinal fluid (CSF) (Tuomanen, 1996). It has been shown that efficient invasion of HBMEC by *L. monocytogenes* depends on InlB (Greiffenberg et al., 1998). I have first used SCP cells to demonstrate that *L. monocytogenes* invades these cells in an IspC-dependent manner. This suggests that when cultured human epithelial cells from the choroid plexus are not available, SCP cells are a good cell culture model for *in vitro* study of adhesion to and entry into the epithelial cells of choroid plexus by *L. monocytogenes* that was shown to cause significant meningitis in sheep (Vandegraaff et al., 1981). Strong adhesion of *L. monocytogenes* to choroid plexus was also observed in a mouse infection model (Schluter et al., 1996). Based on the observations reported here and elsewhere (Prats et al., 1992; Schluter

et al., 1996), I propose a model for *L. monocytogenes* to breach the blood-brain barrier causing meningitis or encephalitis. The entry of the bacterium into the epithelial cells of choroid plexus is mediated at least by IspC via interaction with an unknown receptor. When within the epithelial cells, the bacterium undergoes cell-to-cell spread or enters into the CSF to undergo an extracellular phase prior to causing brain infection (meningitis). The demonstration of *L. monocytogenes* present in CSF (Brouwer et al., 2006, Schluter et al., 1996) supports the notion of *L monocytogenes* undergoing an extracellular phase. Alternatively, *L. monocytogenes* could invade the microvascular endothelial cells through InlB interacting with a specific as yet unidentified receptor, leading to encephalitis. The important but different functions of both IspC and InlB in brain pathogenesis caused by *L. monocytogenes* may be explained by the facts that both proteins similarly contain the C-terminal CWBD made up of repeated GW modules with variation in number and amino acid sequence for each protein (Braun et al., 1997; Wang and Lin, 2007). This domain was shown to be responsible for the interaction of IspC with SCP epithelial cells (this study) and presumably accounted for the binding of InlB to HBMEC.

Formation of shorter and weaker actin tails at the early stage of infection of J774 cells with the Δ*ispC* mutant and of smaller sizes of plaques following infection of L2 fibroblasts with the mutant, and significant reduction in growth of the mutant within Vero and J744 cells suggest that efficient intracellular movement, cell-to-cell spread, and intracellular survival of the bacterium necessarily depend on the expression of the *ispC* gene. I observed a marked reduction in the amount of the surface protein ActA due to the absence of IspC during *in*

vitro growth. This seems to suggest that IspC regulates the surface display of ActA presumably through its autolytic activity and thus promotes intracellular movement and cell-to-cell spread. However, the expression of ActA on the bacterial surface within the infected cells (J774) did not seem to be affected by lack of IspC expression in the Δ*ispC* mutant (L. Wang and M. Lin, unpublished data). Deletion of the *p60* gene from *L. monocytogenes* has been shown to affect the polarization of ActA on the bacterial surface, leading to loss of actin-based motility (Pilgrim et al., 2003). It may be speculated that the deletion of *ispC* alters the polarization of ActA on the surface of bacteria during the intracellular phase of growth, resulting in shorter and weaker actin tails in early stages of infection.

I have assessed the effect of IspC deficiency on the display of surface proteins by proteomic and immunological analysis. The reduced surface expression in the Δ*ispC* mutant of ActA, a putative LPXTG-containing internalin InlC2 and a flagellin-like protein homologous to the 30-kDa flagellin FlaA with peptidoglycan hydrolase activity of *L. monocytogenes* EGD-e (Popowska and Markiewicz, 2004) suggests that IspC may also be indirectly involved in pathogenesis, because these surface proteins were demonstrated or implicated as virulence factors. In addition to the role of ActA in promoting the actin-based intra- and intercellular movement of *L. monocytogenes*, this protein has been shown to mediate the attachment and entry of the bacterium into eukaryotic cells (Alvarez-Dominguez et al., 1997). Although the role of InlC2 in pathogenesis remains undefined, this protein may be required for bacterial survival under osmotic and/or stationary-phase stress (Dramsi et al.,

1997; Kazmierczak et al., 2003). The FlaA protein, a structural component of flagella, is capable of facilitating the initial association of the bacterium with and effective invasion of epithelial cells (Dons et al., 2004) and enhances the *L. monocytogenes* infectivity after ingestion (O'Neil and Marquis, 2006). Thus, the attenuated virulence of the Δ*ispC* mutant observed with mouse and cell culture infection models may be partly due to the reduced surface expression or display of other known or putative virulence factors. It is unlikely that the C-terminal region of IspC made up of 7 GW modules that functions to anchor the protein to the cell wall (Wang and Lin, 2007) is responsible for maintaining the proper display of other surface proteins. I propose that the autolytic activity conferred by the N-terminal catalytic domain of IspC (Wang and Lin, 2007) breaks the chemical bonds within cell wall peptidoglycan so as to alter the surface properties (e.g., structure, charge, and surface modification) as has been shown for p60 of *L. monocytogenes* (Pilgrim et al., 2003) and Atl of *S. aureus* (Takahashi et al., 2002), providing a cell wall architecture necessary for the proper polarization or display of the virulence factors such as ActA for their function. This is also supported by my unpublished observation that the mutant strain was harder to be disrupted by a physical (ultrasonication) or enzymatic (lysozyme digestion) method than was the WT. Inspection of both the proteins (ActA, InlC2 and a FlaA homologue) that exhibited a reduced surface expression and those unaffected (InlB, InlA and p60) appears to indicate that influence on the display of surface proteins by IspC is independent of a particular surface targeting mechanism, because various surface targeting mechanisms (Bierne and Cossart, 2007; Cabanes et al., 2002) such as LPXTG motif in InlA and InlC2, a C-terminal hydrophobic

domain in ActA, a C-terminal domain consisting of repeated GW modules in InlB, and LysM domain in p60 are employed in these proteins. The indirect role of IspC in virulence as promoting the surface display of other virulence factors is in contrast to the findings that the autolysins Auto and p60 of *L. monocytogenes* do not alter the expression of other major virulence factors such as InlA, InlB, ActA and LLO (Cabanes et al., 2004; Pilgrim et al., 2003). Thus, the present study is the first to demonstrate a dual role for a minor *L. monocytogenes* autolysin in virulence.

CHAPTER VII

Investigation into Interaction of IspC with Cellular Components of Eukaryotic Cells

7.1 Introduction

Virulence studies of the WT and Δ*ispC* mutant strains in mouse and cell culture models have established that IspC is essential for *L. monocytogenes* pathogenesis (Chapter VI). The present findings that (i) the mutant was impaired for adhesion to certain eukaryotic cells and (ii) both purified IspC and its C-terminal CWBD were capable of binding Vero and SCP cells supported the role of IspC as an adhesin in virulence. This has greatly stimulated interest in the identification of a host cellular receptor for IspC. The first two surface proteins of *L. monocytogenes* known to promote entry of the bacterium into host cells are InlA, which interacts with a species-specific receptor E-cadherin (Lecuit et al., 2001), and InlB, which binds multiple host receptors, the receptor tyrosine kinase Met/the hepatocyte growth factor (HGF) receptor (Shen et al., 2000), glycosaminoglycans (GAGs) (Jonquieres et al., 2001) -unbranched polysaccharides consisting of repeating disaccharide units, and the receptor for the globular part of the complement C1q molecule (gC1q-R) (Braun et al., 2000). The C-terminal GW modules of InlB responsible for anchoring the protein to the bacterial cell wall bind both GAGs and gC1q-R specifically, whereas the LRR domain binds Met (Marino et al., 2002). Given that IspC contains a C-terminal CWBD made of 7 GW modules (Chapter V) sharing some degree of modular and functional similarities with InlB, it may be worthy of determining if IspC interacts with a GAG heparin and gC1q-R.

InlB functionally mimics HGF by binding and activating the Met receptor, resulting in phosphorylation of Met and the adaptor proteins Cbl, Shc and Gabl (Ireton et al., 1999; Shen et al., 2000), which in turn recruit and stimulate the activity of the p85/p110 class I PI

3-kinase that is a key signalling protein necessary for and controlling the entry of *L. monocytogenes* into target cells (Cossart and Lecuit, 1998; Seveau et al., 2007). InlB-Met interaction induces signalling cascades that ultimately produce the actin cytoskeleton rearrangement (membrane ruffling) and bacterial internalization. Infection of Vero cells with the Δ*inlB* mutant results in ~ 30% of the cellular increase in the product PI3,4,5P3 of PI 3-kinase reaction that occurs upon infection with the WT (Ireton et al., 1999), indicating that InlB is not the only factor of *L. monocytogenes* that controls the activation of PI 3-kinase. It would be interesting to analyse whether IspC could have the capability to induce tyrosine phosphorylation of eukaryotic cell proteins including the adaptor proteins leading to membrane ruffling required for bacterial entry.

7. 2 Results

7.2.1 IspC and its CWBD bind to heparin glycosaminoglycans

Binding of IspC and its C-terminal CWBD to heparin glycosaminoglycans (GAGs) was assessed in an *in vitro* binding assay with heparin conjugated agarose beads. SDS-PAGE revealed that free rIspC was undetectable in the supernatant but found in the NaCl-eluted fractions from heparin-agarose beads that had pre-interacted with purified rIspC (Fig. 7-1A). Analysis of the interaction of rIspC with agarose beads in the same fashion showed that rIspC did not bind to the agarose matrix. These results indicated that IspC specifically bound to heparin. Further, the C-terminal CWBD (aa 198-774) fused to the C-terminus of GFPuv (GFPuv-CBD1) was able to bind heparin, revealed in the *in vitro* binding assay by the disappearance of a fluorescent band corresponding to GFPuv-CBD1 in the supernatant but its

FIG. 7-1. *In vitro* binding of IspC and its CWBD to heparin glycosaminoglycans. (A) The purified rIspC (0.073 mg/ml, 0.3 ml) was mixed with heparin-agarose (HA) or agarose (A), incubated at room temperature for 1 h, and centrifuged to collect the supernatant (S). The agarose beads were then washed with 5 × 0.3 ml of 10 mM phosphate buffer (pH 7.5) (here showing the first two washes W1, W2) and serially eluted with 5 × 0.3 ml of elution buffer (50 mM Tris-HCl, pH 7.5, 2 M NaCl) (E1, E2, E3, E4, E5). All the samples collected above and the purified rIspC (P) prior to mixing with agarose were analyzed by SDS-PAGE. Each lane contains an equal volume (10 µl) of samples. Protein standards with their molecular mass in kDa are indicated on the left. **(B)** GFPuv-CBD1 (11.3 nM, 0.3 ml) or GFPuv (11.3 nM, 0.3 ml) were incubated with heparin-agarose at room temperature and analyzed by SDS-PAGE. Samples were collected essentially as described in Panel A except for elution with 5 × 0.15 ml of elution buffer (here showing the first three washes W1, W2, W3 and four elutions E1, E2, E3, E4). The protein bands were visualized by a Molecular Imager ChemiDoc XRS System using UV light source.

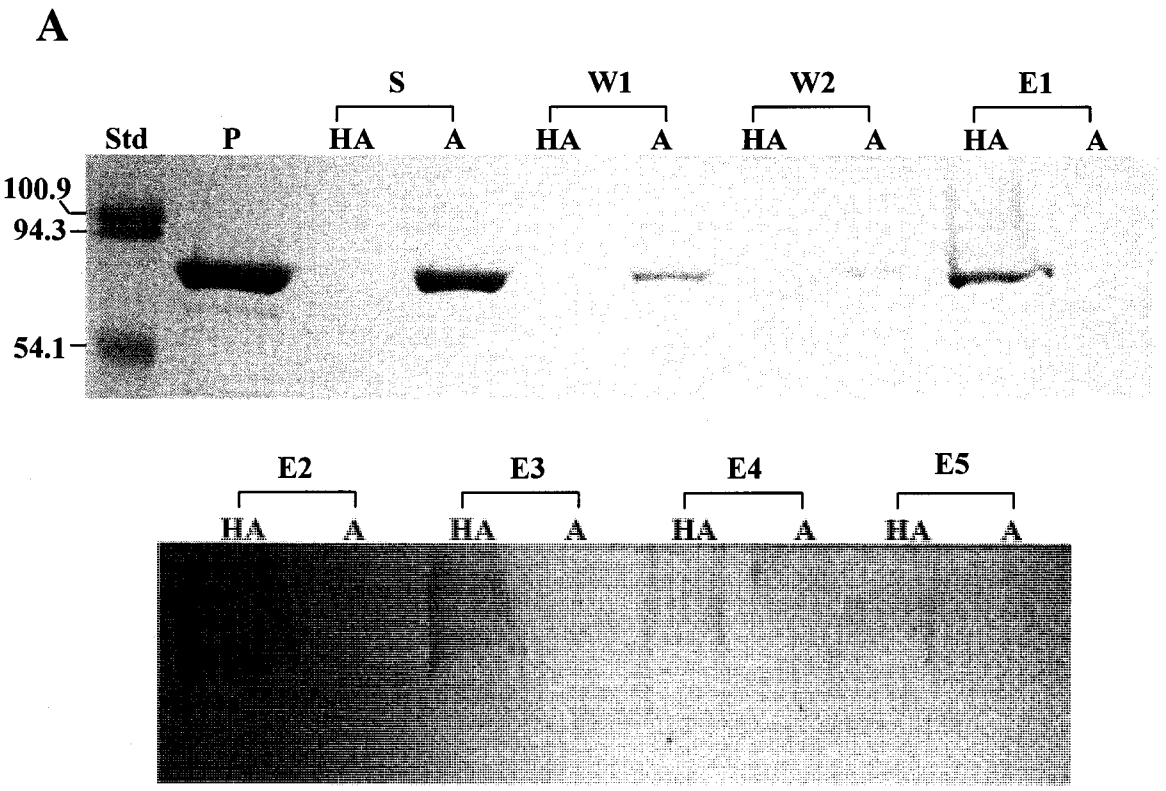
A
S
W1
W2
E1
Std
P
HA
A
HA
A
HA
A
HA
A
100.9
94.3
54.1
E2
E3
E4
E5
HA
A
HA
A
HA
A
HA
A

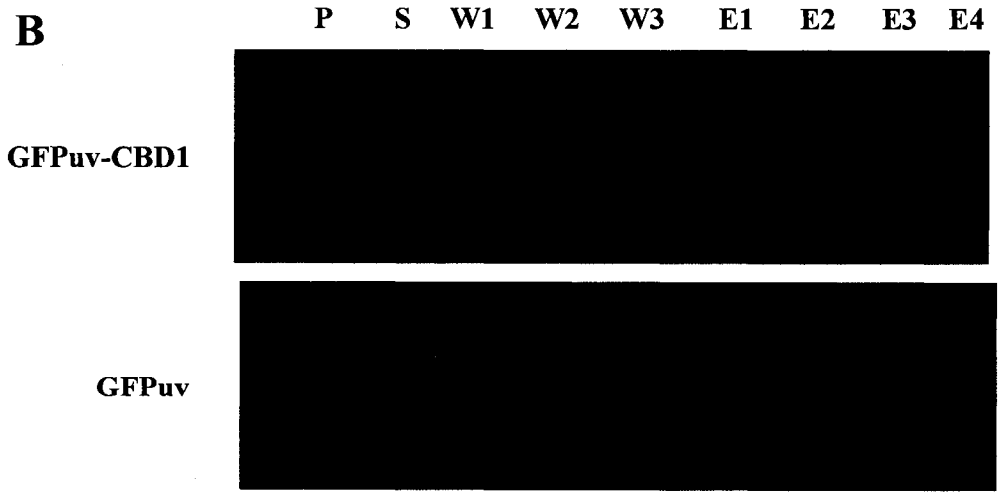
B
P
S
W1
W2
W3
E1
E2
E3
E4
GFPuv-CBD1
GFPuv

presence in the eluted fractions from heparin-agarose complexed with the fusion protein (Fig. 7-1B). The control protein GFPuv did not bind to heparin-agarose. Together, these results indicate that IspC binds heparin GAGs through its C-terminal CWBD.

7.2.2 IspC fails to interact with protein targets including gC1q-R

SDS-PAGE analysis of solubilized proteins from Vero or SCP cells co-immunoprecipitated with rIspC by RαIspC reveals no specific IspC-binding proteins on the gels (Fig. 7-2A), in comparison to the protein bands resolved from co-immunoprecitation controls with rIspC plus rabbit preimmune serum or with RαIspC antiserum alone and from electrophoresis analysis of RαIspC, rabbit preimmune serum and rIspC. Further analysis of anti-IspC co-immunoprecipitates from Vero or SCP cells and of their cell lysates by a ligand overlay assay probed with rIspC demonstrated no protein bands specifically interacting with rIspC (Fig. 7-2B). A protein band of ~ 86 kDa appeared in anti-IspC co-immunoprecipitates was clearly the rIspC protein (Fig. 7-2B, lanes 1, 5 and 9). The gC1q-R protein, which is a host cell receptor for InlB (Braun et al., 2000), was not detected in anti-IspC co-immunoprecipitates from Vero cells but was detectable as a protein band of ~ 33 kDa in the Vero cell lysates with Western blotting using anti-gC1q-R antibody (Fig. 7-2C), the ligand overlay assay probed with InlB (Appendix 3, Fig. S2), and Western blot analysis of the anti-InlB co-immunoprecipitates (Appendix 3, Fig. S3). Together, these results indicated that IspC did not interact with a receptor of protein nature in Vero or SCP cells.

FIG. 7-2. IspC fails to interact with protein targets including gC1q-R in Vero and SCP cells. (A) Proteins from Vero or SCP cell lysates were co-immunoprecipitated as described in Materials and Methods in the presence (+) or absence (-) of rIspC, RαIspC, rabbit preimmune sera (Pre). The immunoprecipitates were analyzed by SDS-PAGE (lanes 1-6). SDS-PAGE analysis of RαIspC, rabbit preimmune sera, and rIspC, identical to the amount used in Co-IP was presented in lanes 7-9 for comparison of protein pattern. Protein standards with their molecular mass in kDa are indicated on the left. **(B)** Co-immunoprecipitates (as in A), solubilized Vero or SCP cell lysate (40 μg), rIspC (1 μg) were analyzed in a ligand overlay assay as described in Materials and Methods using RαIspC as a probe. Protein standards with their molecular mass in kDa are indicated on the left. **(C)** Co-immunoprecipitates from Vero cell lysates (as in A) and Vero cell lysates (40 μg) were analyzed by Western blotting using anti-gC1q-R. The presence of gC1q-R in Vero cell lysates is indicated by an arrow.

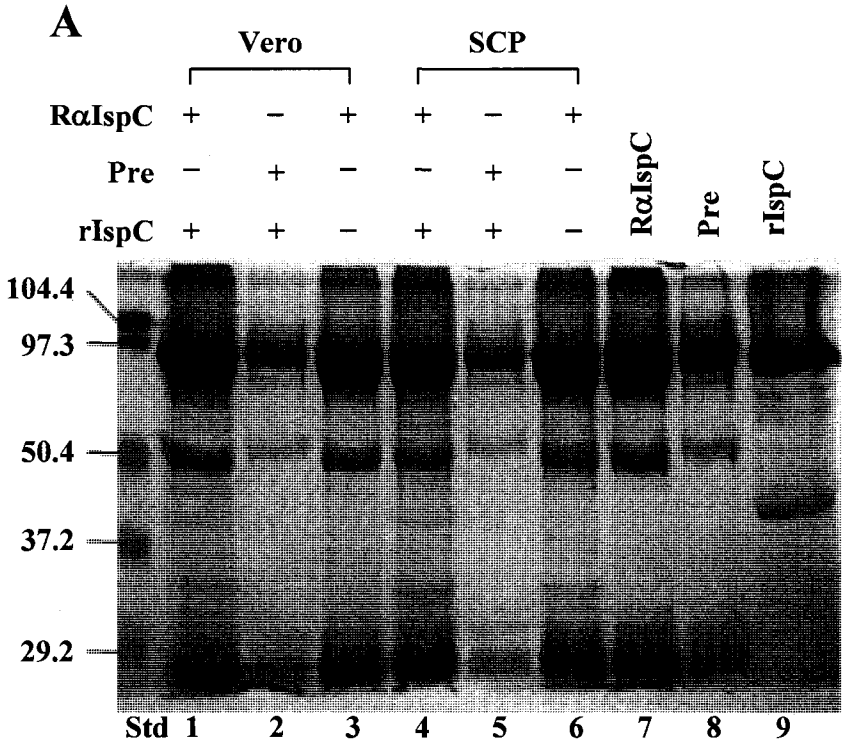
A
Vero
SCP
RαIspC + − + + − +
Pre − + − − + −
rIspC + + − + + −
RαIspC
Pre
rIspC
104.4
97.3
50.4
37.2
29.2
Std 1 2 3 4 5 6 7 8 9

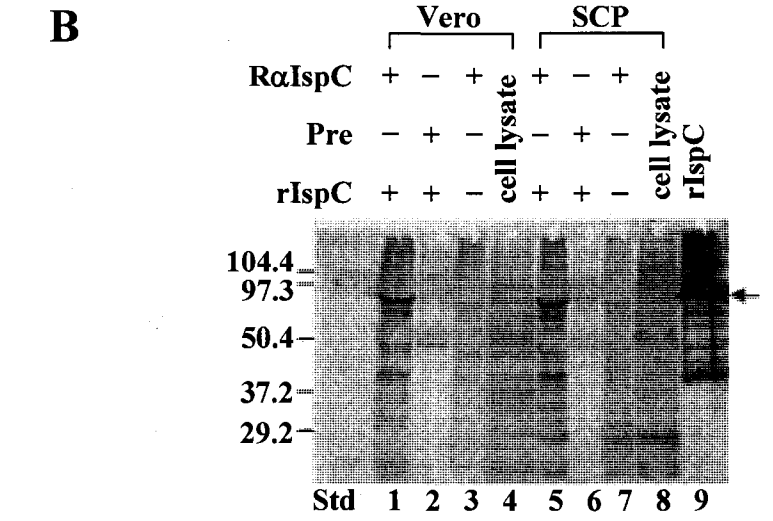
B
Vero
SCP
RαIspC + − + + − +
Pre − + − − + −
rIspC + + − + + −
cell lysate
cell lysate
rIspC
104.4
97.3
50.4
37.2
29.2
Std 1 2 3 4 5 6 7 8 9

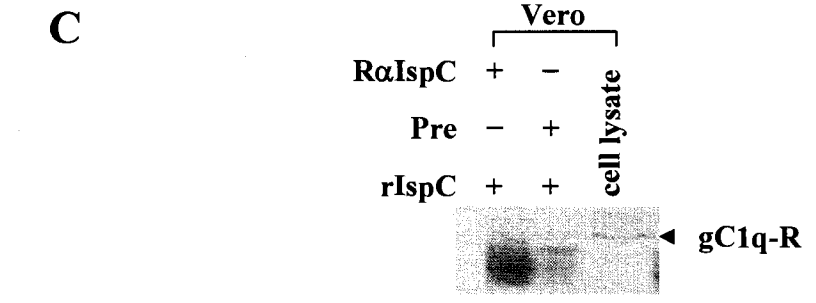
C
Vero
RαIspC + −
Pre − +
rIspC + +
cell lysate
gC1q-R

7.2.3 IspC does not influence tyrosine phosphorylation of Vero cell proteins

Western blotting using anti-phosphotyrosine antibody (anti-Tyr(P)) showed the presence of tyrosine phosphorylated proteins from IspC-treated or untreated Vero cells following the immunoprecipitation with anti-Tyr(P) but no difference was observed in the overall tyrosine phosphorylation state of both IspC-treated and untreated cells. However, the difference was observed between EGF-treated and untreated cells (Appendix 3, Fig. S4a). The p85 of PI 3-kinase was not detected in IspC-treated and untreated Vero cells by Western blotting with anti-P85 antibody in the anti-Tyr(P) immunoprecipitates; this protein was detected in EGF-treated Vero cells (Appendix 3, Fig. S4b). Tyrosine phosphorylation of the adaptor proteins Gab1 and Shc was undetectable in the anti-Tyr(P) immunoprecipitates from IspC-treated and untreated Vero cells by Western blotting with corresponding antibodies against the tyrosine phosphorylated form of Gab1 and Shc (anti-Gab1(P) and anti-Shc(P)) (data not shown). Thus, IspC does not stimulate tyrosine phosphorylation of Vero cell proteins including the Gab1 and Shc adaptor proteins. Further, tyrosine-phosphorylated Gab1 or Shc was not detected as expected in anti-PI 3-kinase p85 subunit immmunoprecipitates from Vero cells treated or untreated with IspC (data not shown).

7.2.4. IspC does not provoke significant actin cytoskeleton rearrangement

Vero cells, after treatment with purified IspC, were morphologically examined for actin cytoskeletal rearrangement (i.e., membrane ruffling). Of 200 cells examined, no cells were found apparently positive for membrane ruffling in both treated (3 nM IspC for 1 and 5 min) and untreated cells. Treatment for a longer time (10, 15 and 20 min) or at higher

concentrations of IspC (6 and 30 nM) did not result in any noticeable changes in actin rearrangement. In contrast, about 13% of the EGF-treated cells (200 cells) showed actin cytoskeletal rearrangement, exemplified by membrane ruffling of a Vero cell (Appendix 3, Fig. 5S). These results indicate that IspC is not important for triggering actin cytoskeletal rearrangement required for the entry of *L. monocytogenes* serotype 4b into Vero cells.

7. 3 Discussion

The binding assays performed here provided evidence that IspC had an affinity for heparin, a representative GAG from the glycosaminoglycan family consisting of five other most common structures: chondroitin sulfate (CS), dermatan sulfate (DS), heparan sulfate (HS), keratan sulfate (KS), and hyaluronic acid (HA) (Jackson et al., 1991). Heparin is closely related in structure to HS found in many tissues and cells of mammals (Powell et al., 2004) and often used to study the interaction between GAGs and GAG-binding proteins, exemplified by characterization of binding to heparin of bacterial proteins including *L. monocytogenes* InlB (Jonquieres et al., 2001) and *Bordetella pertussis* Fim2 subunit (Geuijen et al., 1998). The IspC protein was shown to bind to heparin through its C-terminal CWBD composed of 7 GW modules, as was similarly found for *L. monocytogenes* InlB that bound to GAG heparin by its C-terminus containing GW modules (Geuijen et al., 1998). Given that GAGs function as a receptor for InlB (Marino et al., 2002) and that there is a similarity between IspC and InlB in binding to the GAG heparin, it is suggested that GAGs act as a nonprotein receptor for IspC during *L. monocytogenes* invasion. Consistent with this is the observation that both purified IspC and its C-terminal CWBD were capable of binding Vero

and SCP cells (Chapter VI).

Electrostatic interactions are anticipated to be responsible for the binding of IspC to heparin by its C-terminal CWBD, since IspC and its CWBD consisting of 7 GW modules have theoretical pIs of 9.4 and 9.6, respectively (Wang and Lin, 2007) and heparin is a highly negatively charged macromolecule (Jackson et al., 1991). The domains of heparin-binding proteins actively involved in binding GAG are usually α-helical structures with the positively charged residues clustered on one face of the helix (Jackson et al., 1991). *L. monocytogenes* ActA, being suggested to be involved in HS receptor recognition in addition to promoting actin-based bacterial motility and cell-to-cell spread, was found to contain clusters of positively charged basic amino acids in predicted α-helices in the N-terminal region (Alvarez-Dominguez et al., 1997). Similarly, secondary structure prediction analysis revealed the presence of clusters of positively charged basic amino acids (**KK**AFD (aa 524-528), **KK**A (aa 605-607, aa 686-688), **KR**A (aa 767-769)) in four α-helices in the C-terminal CWBD (Fig. 4-7), a characteristic presumably favoring the interaction with a negatively charged GAG receptor such as HS or heparin. However, it has been shown that pretreatment of *L. monocytogenes* with heparin or HS, but not with other GAGs such as CS and KS in spite of being negatively charged, inhibited bacterial attachment to and invasion of IC-21 murine macrophages and CHO epithelial-like cells (Alvarez-Dominguez et al., 1997), suggesting that binding to heparin or HS is more than a simple electronic interaction and requires specific determinants of listerial adhesins such as InlB, ActA, and IspC for GAG receptor recognition.

Interestingly, IspC failed to interact with any protein components of Vero and SCP cells including gC1q-R, which was demonstrated as an additional specific receptor to the GW domains of InlB (Marino et al., 2002). It may be noted that the C-terminal GW domains of *L. monocytogenes* Ami also failed to bind gC1q-R (Marino et al., 2002). The binding specificity of InlB for gC1q-R may arise from the characteristics of the GW domains that display variation in amino acid sequence amongst the GW domains of *L. monocytogenes* InlB, IspC, and Ami.

The observation that treatment with purified rIspC did not result in a change in the overall tyrosine phosphorylation state of Vero and SCP cells and tyrosine phosphorylation of the adaptor proteins such as Gab1 and Shc suggested that the interaction of IspC with host cells was incapable of triggering signalling cascades necessary for bacterial internalization, as found with activation of the Met receptor by *L. monocytogenes* InlB (Cossart and Lecuit, 1998; Ireton et al., 1999; Seveau et al., 2007; Shen et al., 2000). Consistent with this is the unnoticeable actin rearrangement (membrane ruffling) observed with Vero and SCP cells after being treated with rIspC. In contrast, *L. monocytogenes* InlB binds to and activates the Met receptor through its LRR and IR domains (Braun et al., 1999; Freiberg et al., 2004) which in turn activates at least one signalling pathway involving the PI 3-kinase, leading ultimately to the production of membrane ruffling and bacterial engulfment. Lack of the LRR and IR domains in IspC well explains the inability of IspC to generate the same signalling effect in host cells as InlB. However, interaction of IspC with a GAG receptor could recruit other listerial factors to the sites where their specific signalling receptors are

located and thus enhance listerial factor-signalling receptor interactions which are necessary for triggering actin cytoskeletal rearrangement and bacterial entry.

CHAPTER VIII

General Discussion

8.1 General Discussion

Considerable effort was devoted in my thesis research to the characterization of an *L. monocytogenes* IspC protein of unknown function using biochemical, spectroscopic, molecular, genetic, proteomic approaches, *etc.* The significance of this research is highlighted by several major findings. First, IspC was experimentally demonstrated as a novel surface peptidoglycan hydrolase (autolysin) with an N-terminal catalytic domain (aa 24 to 197) for the peptidoglycan hydrolytic activity and a C-terminal CWBD (aa 198 to 774) composed of 7 GW modules for cell wall anchoring. Subsequent studies with the Δ*ispC* mutant, derived from the parental strain *L. monocytogenes* serotype 4b by in-frame deleting the gene from the chromosome, provided evidence that IspC was not involved in cell division or separation but essential for full virulence of *L. monocytogenes*. Further experiments with the Δ*ispC* mutant, purified rIspC and its C-terminal CWBD established a dual role for a minor autolysin IspC in *L. monocytogenes* virulence, i.e., a direct role as an adhesin promoting the bacterium-host cell interaction and an indirect role regulating the surface display of other known or putative virulence factors. These novel findings have advanced our understanding of the molecular mechanisms by which a surface peptidoglycan hydrolase contributes to bacterial pathogenesis. Because *L. monocytogenes* IspC is a recently identified antigen for humoral immune response to listerial infection (Yu et al., 2007), knowledge gained from this thesis research about *L. monocytogenes* IspC should have set the stage for future studies on this protein.

It should be noted that several attempts were made to clone the full length *ispC* gene into a plasmid vector (provided by another researcher) that could be used to complement the Δ*ispC* mutant. The cloning, however, has proved to be difficult with that particular vector.

Therefore, experiments were not performed with the complemented Δ*ispC* mutant. Complementation experiments were not always included in the study of bacterial gene deletion mutants including the a*ut* gene (coding for the autolysin Auto) deletion mutant of *L. monocytogenes* (Cabanes et al., 2004). It is unlikely that in-frame deletion of the *ispC* from the chromosome has any polar effects on the mutant strain, because the mutant is indistinguishable from the WT in a number of phenotypic characteristics including biochemical characteristics. Further analysis of the genome organization surrounding the *ispC* gene homolog (i.e., LMOf2365_1093) in *L. monocytogenes* 4b strain F2365 (Nelson et al., 2004) revealed that a polar effect on the expression of the upstream or downstream genes due to deletion of the *ispC* seems unlikely, because the upstream gene LMOf2365_1092 lies on the same strand and in the same orientation as the *ispC* homolog and the downstream gene LMOf2365_1094 is located on the complementary strand and in the opposite direction.

IspC is a surface-localized autolysin with a domain organization similar to that of two other *L. monocytogenes* surface autolysins Ami and Auto (Cabanes et al., 2004; Milohanic et al., 2001). This similarity may have formed a structural basis for IspC to be functionally and pathogenically similar to Ami and Auto. All these three autolysins are not important for bacterial growth *in vitro*, cell division, cell separation, or cell wall morphology but required for the full virulence of *L. monocytogenes* (Cabanes et al., 2004; Milohanic et al., 2001; this study). In spite of this, each of these *L. monocytogenes* autolysins appears to play a distinct role in virulence. IspC promotes not only bacterial adherence and invasion in a cell type-dependent manner but also bacterial intracellular growth and actin tail formation in cultured eukaryotic cells. In contrast, Ami mediates bacterial adhesion to but not bacterial entry into eukaryotic cells (Milohanic et al., 2001); Auto is required for entry into but not for

adhesion to nonprofessional phagocytic cells (Cabanes et al., 2004).

IspC contributes to the adherence of *L. monocytogenes* to eukaryotic cells via its C-terminal CWBD composed of GW modules that are capable of binding to the cell surface, as similarly found with Ami of *L. monocytogenes* (Milohanic et al., 2001). The observed similarity between IspC and InlB in binding to the GAG heparin suggests that GAGs are nonprotein receptors for IspC. Whether the C-terminal CWBD of Ami also interacts with a GAG receptor and why Auto is not involved in the adhesion of bacteria to eukaryotic cells are not known and require further investigation. Since the C-terminal CWBD of IspC is responsible for anchoring the protein to the bacterial cell wall, how this domain becomes available for interaction with a host GAG receptor needs some explanations. Perhaps some portions of the GW modules in the CWBD are surface-exposed and are responsible for GAG receptor recognition.

L. monocytogenes is capable of crossing the intestinal epithelial barrier, the maternofetal barrier and the blood-brain barrier. The interaction of InlA and E-cadherin plays an essential role in crossing the former two barriers by *L. monocytogenes.* It has been shown that efficient invasion of HBMEC by *L. monocytogenes* depends on InlB (Greiffenberg et al., 1998). This study is the first to demonstrate that adhesion to and invasion of SCP cells but not HBMEC cells by *L. monocytogenes* is dependent on the expression of IspC. Binding study indicates that bacterial adhesion to SCP cells was mediated by the C-terminal CWBD of IspC. This novel finding suggests that IspC plays a role in *L. monocytogenes* infection of the brain by facilitating bacterial translocation of the blood-CSF barrier. The observation that the Δ*ispC* mutant exhibited the impaired ability to colonize the mouse brain further supports that IspC contributes to the brain infection by *L. monocytogenes*. IspC- and InlB-dependent invasion of

SCP cells and HBMEC cells, respectively, by *L. monocytogenes* suggests that the brain infection may be a consequence of the combined actions of multiple virulence factors, or that of a critical as yet unidentified virulence factor. Much effort is still needed to elucidate how *L. monocytogenes* crosses the blood-CSF barrier to cause infection of the human brain, a primary cause of death. Identification of the virulence factors such as IspC and InlB may help elucidate the molecular pathogenic mechanism(s) of brain infection and thus help develop new antibacterial drugs.

The indirect role of IspC in *L. monocytogenes* virulence is suggested by proteomic and immunological analysis showing that reduced surface expression of some known or putative virulence factors (e.g., ActA, InlC2, and a flagellin homologue FlaA) is due to the IspC deficiency. In contrast, lack of the autolysins Auto and p60 of *L. monocytogenes* does not reduce the expression of other major virulence factors such as InlA, InlB, ActA or LLO (Cabanes et al., 2004; Pilgrim et al., 2003). Deletion of the *p60* gene from *L. monocytogenes*, however, has been shown to affect the polarization of ActA on the bacterial surface, leading to loss of actin-based motility (Pilgrim et al., 2003). It is not known how IspC regulates the surface display of these proteins (e.g., ActA, InlC2 and FlaA). It may be speculated that the peptidoglycan hydrolase activity conferred by the N-terminal catalytic domain of IspC is necessary to break the cell wall peptidoglycan bonds to alter the surface properties, which allows the proper polarization and display of the other virulence factors such as ActA for their function.

This study has identified a novel autolysin IspC of *L. monocytogenes*, which was previously shown to be targeted by the humoral immune response to listerial infection (Yu et al., 2007) and shown here to be an important virulence factor. Thus, the surface autolysin IspC, together with other putative autolysins encoded by the *L. monocytogenes* genome,

represents an interesting area worthy of further investigations.

8.2 Conclusions

Several conclusions can be drawn from the findings of the present study. (i) *L. monocytogenes* IspC contains a 23-residue N-terminal signal peptide being cleaved by a signal peptidase between Thr 23 and Thr 24 during heterologous expression in *E. coli*, resulting in an 84-kDa mature protein; (ii) *L. monocytogenes* IspC posseses a dominant β-sheet secondary structure; (iii) *L. monocytogenes* IspC is a surface autolysin with two separate functional domains: the N-terminal catalytic domain (aa 24 to 197) responsible for the peptidoglycan hydrolytic activity and the C-terminal domain (aa 198 to 774) made up of seven GW modules responsible for anchoring the protein to the cell wall; (iv) The C-terminal CWBD is important in modulating the peptidoglycan hydrolytic activity of the N-terminal catalytic domain; (v) IspC, expressed as a minor autolysin *in vitro*, is not important for cell division and separation in broth medium but essential for full virulence of *L. monocytogenes in vivo*; (vi) IspC facilitates the infectious process of *L. monocytogenes* at multiple steps for which the importance of this protein is dependent on the type of eukaryotic cells; (vii) IspC plays a dual role in *L. monocytogenes* pathogenesis as an adhesin and as being involved in the regulation of the surface display of some known or putative virulence factors; and (viii) IspC binds to GAG heparin but not to gC1q-R and is incapable of triggering signalling cascades necessary for bacterial internalization (actin cytoskeletal rearrangement) as observed with activation of the Met receptor by *L. monocytogenes* InlB.

8. 3 Future Work

Although this research has led to a better understanding of the biochemical, molecular, and structural (secondary) properties of *L. monocytogenes* IspC and its role in pathogenesis, many research questions relating to the present study need to be explored to gain a deeper

and more comprehensive knowledge of the cell surface autolysin IspC in the future. What is the peptidoglycan cleavage site of IspC? This is quite an interesting question, because none of the *L. monocytogenes* autolysins identified to date have been analyzed with regard to the peptidoglycan hydrolytic bond specificities. With the availability of a sufficient amount of highly purified rIspC and an effective protocol for protein preparation from this study, a high-resolution crystal structure of IspC may be solved to give further functional insights into the protein. *L. monocytogenes* IspC is not important for cell division or separation, but whether this protein is involved in other biological functions such as biofilm formation, genetic competence, protein secretion, antibiotic-induced lysis, *etc.*, remains unknown and requires further investigation. Do various strains of *Listeria* express the IspC homologues recognized by rabbit polyclonal antibody RαIspC? What is the molecular mechanism(s) underlying the reduced surface display of some known or putative virulence factors in *L. monocytogenes* due to a deficiency in IspC? How important is the peptidoglycan hydrolytic activity of IspC in regulating the display of surface proteins in *L. monocytogenes*? Whether *L. monocytogenes* IspC interacts with a GAG receptor on eukaryotic cells remain to be confirmed. Are any protein receptors of host cells involved in recognition of *L. monocytogenes* IspC? Given that IspC is a virulence factor targeted by the humoral immune response to listerial infection, it would be interesting to determine if antibodies to IspC play a role in protective immunity against infection with intracellular *L. monocytogenes*. This might provide new insights into the role of humoral immunity in host defense against an intracellular bacterial pathogen. All these represent interesting questions to ponder in the future study of *L. monocytogenes* IspC.

References

Alberti-Segui, C., Goeden, K.R., and Higgins, D.E. (2007). Differential function of *Listeria monocytogenes* listeriolysin O and phospholipases C in vacuolar dissolution following cell-to-cell spread. Cell Microbiol. *9*, 179-195.

Allignet, J., England, P., Old, I., and El Solh, N. (2002). Several regions of the repeat domain of the *Staphylococcus caprae* autolysin, AtlC, are involved in fibronectin binding. FEMS Microbiol. Lett. *213*, 193-197.

Alvarez-Dominguez, C., Vazquez-Boland, J.A., Carrasco-Marin, E., Lopez-Mato, P., and Leyva-Cobian, F. (1997). Host cell heparan sulfate proteoglycans mediate attachment and entry of *Listeria monocytogenes*, and the listerial surface protein ActA is involved in heparan sulfate receptor recognition. Infect. Immun. *65*, 78-88.

Anantharaman, V., and Aravind, L. (2003). Evolutionary history, structural features and biochemical diversity of the NlpC/P60 superfamily of enzymes. Genome Biol. *4*, R11.

Armstrong, B.A., and Sword, C.P. (1966). Electron microscopy of *Listeria monocytogenes*-infected mouse spleen. J. Bacteriol. *91*, 1346-1355.

Baba, T., and Schneewind, O. (1996). Target cell specificity of a bacteriocin molecule: a C-terminal signal directs lysostaphin to the cell wall of *Staphylococcus aureus*. EMBO J. *15*, 4789-4797.

Baba, T., and Schneewind, O. (1998). Targeting of muralytic enzymes to the cell division site of Gram-positive bacteria: repeat domains direct autolysin to the equatorial surface ring of *Staphylococcus aureus*. EMBO J. *17*, 4639-4646.

Bakardjiev, A.I., Stacy, B.A., Fisher, S.J., and Portnoy, D.A. (2004). Listeriosis in the pregnant guinea pig: a model of vertical transmission. Infect. Immun. *72*, 489-497.

Barry, R.A., Bouwer, H.G., Portnoy, D.A., and Hinrichs, D.J. (1992). Pathogenicity and immunogenicity of *Listeria monocytogenes* small-plaque mutants defective for intracellular growth and cell-to-cell spread. Infect. Immun. *60*, 1625-1632.

Baumgartner, M., Karst, U., Gerstel, B., Loessner, M., Wehland, J., and Jansch, L. (2007). Inactivation of Lgt allows systematic characterization of lipoproteins from *Listeria monocytogenes*. J. Bacteriol. *189*, 313-324.

Berche, P., Gaillard, J.L., and Richard, S. (1988). Invasiveness and intracellular growth of *Listeria monocytogenes*. Infection *16 Suppl 2*, S145-148.

Berche, P., Gaillard, J.L., and Sansonetti, P.J. (1987). Intracellular growth of *Listeria monocytogenes* as a prerequisite for induction of T cell-mediated immunity. J. Immunol. *138*, 2266-2271.

Bergmann, B., Raffelsbauer, D., Kuhn, M., Goetz, M., Hom, S., and Goebel, W. (2002). InlA- but not InlB-mediated internalization of *Listeria monocytogenes* by non-phagocytic mammalian cells needs the support of other internalins. Mol. Microbiol. *43*, 557-570.

Bernadsky, G., Beveridge, T.J., and Clarke, A.J. (1994). Analysis of the sodium dodecyl sulfate-stable peptidoglycan autolysins of select gram-negative pathogens by using renaturing polyacrylamide gel electrophoresis. J. Bacteriol. *176*, 5225-5232.

Berry, A.M., Lock, R.A., Hansman, D., and Paton, J.C. (1989). Contribution of autolysin to virulence of *Streptococcus pneumoniae*. Infect. Immun. *57*, 2324-2330.

Berry, A.M., and Paton, J.C. (2000). Additive attenuation of virulence of *Streptococcus pneumoniae* by mutation of the genes encoding pneumolysin and other putative pneumococcal virulence proteins. Infect. Immun. *68*, 133-140.

Bielecki, J., Youngman, P., Connelly, P., and Portnoy, D.A. (1990). *Bacillus subtilis* expressing a haemolysin gene from *Listeria monocytogenes* can grow in mammalian cells. Nature *345*, 175-176.

Bierne, H., and Cossart, P. (2002). InlB, a surface protein of *Listeria monocytogenes* that behaves as an invasin and a growth factor. J. Cell Sci. *115*, 3357-3367.

Bierne, H., and Cossart, P. (2007). *Listeria monocytogenes* surface proteins: from genome predictions to function. Microbiol. Mol. Biol. Rev. *71*, 377-397.

Bierne, H., Mazmanian, S.K., Trost, M., Pucciarelli, M.G., Liu, G., Dehoux, P., Jansch, L., Garcia-del Portillo, F., Schneewind, O., and Cossart, P. (2002). Inactivation of the *srtA* gene in *Listeria monocytogenes* inhibits anchoring of surface proteins and affects virulence. Mol. Microbiol. *43*, 869-881.
Notes: CORPORATE NAME: the European *Listeria* Genome Consortium.

Birkeland, N.K. (1994). Cloning, molecular characterization, and expression of the genes encoding the lytic functions of lactococcal bacteriophage phi LC3: a dual lysis system of modular design. Can. J. Microbiol. *40*, 658-665.

Bockmann, R., Dickneite, C., Goebel, W., and Bohne, J. (2000). PrfA mediates specific binding of RNA polymerase of *Listeria monocytogenes* to PrfA-dependent virulence gene promoters resulting in a transcriptionally active complex. Mol. Microbiol. *36*, 487-497.

Bonnemain, C., Raynaud, C., Reglier-Poupet, H., Dubail, I., Frehel, C., Lety, M.A., Berche,

P., and Charbit, A. (2004). Differential roles of multiple signal peptidases in the virulence of *Listeria monocytogenes*. Mol. Microbiol. *51*, 1251-1266.

Bouwer, H.G., Barry, R.A., and Hinrichs, D.J. (1997). Acquired immunity to an intracellular pathogen: immunologic recognition of *L. monocytogenes*-infected cells. Immunol. Rev. *158*, 137-146.

Bradford, M.M. (1976). A rapid and sensitive method for the quantitation of microgram quantities of protein utilizing the principle of protein-dye binding. Anal. Biochem. *72*, 248-254.

Braun, L., Dramsi, S., Dehoux, P., Bierne, H., Lindahl, G., and Cossart, P. (1997). InlB: an invasion protein of *Listeria monocytogenes* with a novel type of surface association. Mol. Microbiol. *25*, 285-294.

Braun, L., Ghebrehiwet, B., and Cossart, P. (2000). gC1q-R/p32, a C1q-binding protein, is a receptor for the InlB invasion protein of *Listeria monocytogenes*. EMBO J. *19*, 1458-1466.

Braun, L., Nato, F., Payrastre, B., Mazie, J.C., and Cossart, P. (1999). The 213-amino-acid leucine-rich repeat region of the *Listeria monocytogenes* InlB protein is sufficient for entry into mammalian cells, stimulation of PI 3-kinase and membrane ruffling. Mol. Microbiol. *34*, 10-23.

Braun, L., Ohayon, H., and Cossart, P. (1998). The InlB protein of *Listeria monocytogenes* is sufficient to promote entry into mammalian cells. Mol. Microbiol. *27*, 1077-1087.

Brouwer, M.C., van de Beek, D., Heckenberg, S.G., Spanjaard, L., and de Gans, J. (2006). Community-acquired *Listeria monocytogenes* meningitis in adults. Clin. Infect. Dis. *43*, 1233-1238.

Bubert, A., Kestler, H., Gotz, M., Bockmann, R., and Goebel, W. (1997). The *Listeria monocytogenes iap* gene as an indicator gene for the study of PrfA-dependent regulation. Mol. Gen. Genet. *256*, 54-62.

Bubert, A., Kohler, S., and Goebel, W. (1992a). The homologous and heterologous regions within the *iap* gene allow genus- and species-specific identification of *Listeria* spp. by polymerase chain reaction. Appl. Environ. Microbiol. *58*, 2625-2632.

Bubert, A., Kuhn, M., Goebel, W., and Kohler, S. (1992b). Structural and functional properties of the p60 proteins from different *Listeria* species. J. Bacteriol. *174*, 8166-8171.

Bubert, A., Sokolovic, Z., Chun, S.K., Papatheodorou, L., Simm, A., and Goebel, W. (1999). Differential expression of *Listeria monocytogenes* virulence genes in mammalian host cells. Mol. Gen. Genet. *261*, 323-336.

Buchrieser, C. (2007). Biodiversity of the species *Listeria monocytogenes* and the genus *Listeria*. Microbes Infect. *9*, 1147-1155.

Cabanes, D., Dehoux, P., Dussurget, O., Frangeul, L., and Cossart, P. (2002). Surface proteins and the pathogenic potential of *Listeria monocytogenes*. Trends Microbiol. *10*, 238-245.

Cabanes, D., Dussurget, O., Dehoux, P., and Cossart, P. (2004). Auto, a surface associated autolysin of *Listeria monocytogenes* required for entry into eukaryotic cells and virulence. Mol. Microbiol. *51*, 1601-1614.

Calamita, H.G., Ehringer, W.D., Koch, A.L., and Doyle, R.J. (2001). Evidence that the cell wall of *Bacillus subtilis* is protonated during respiration. Proc. Natl. Acad. Sci. U S A *98*, 15260-15263.

Calvo, E., Pucciarelli, M.G., Bierne, H., Cossart, P., Pablo Albar, J., and Garcia-Del Portillo, F. (2005). Analysis of the *Listeria* cell wall proteome by two-dimensional nanoliquid chromatography coupled to mass spectrometry. Proteomics *5*, 433-443.

Camilli, A., Goldfine, H., and Portnoy, D.A. (1991). *Listeria monocytogenes* mutants lacking phosphatidylinositol-specific phospholipase C are avirulent. J. Exp. Med. *173*, 751-754.

Camilli, A., Tilney, L.G., and Portnoy, D.A. (1993). Dual roles of *plcA* in *Listeria monocytogenes* pathogenesis. Mol. Microbiol. *8*, 143-157.

Canvin, J.R., Marvin, A.P., Sivakumaran, M., Paton, J.C., Boulnois, G.J., Andrew, P.W., and Mitchell, T.J. (1995). The role of pneumolysin and autolysin in the pathology of pneumonia and septicemia in mice infected with a type 2 *pneumococcus*. J. Infect. Dis. *172*, 119-123.

Carroll, S.A., Hain, T., Technow, U., Darji, A., Pashalidis, P., Joseph, S.W., and Chakraborty, T. (2003). Identification and characterization of a peptidoglycan hydrolase, MurA, of *Listeria monocytogenes*, a muramidase needed for cell separation. J. Bacteriol. *185*, 6801-6808.

Chakraborty, T., Ebel, F., Domann, E., Niebuhr, K., Gerstel, B., Pistor, S., Temm-Grove, C.J., Jockusch, B.M., Reinhard, M., Walter, U., and et, a.l. (1995). A focal adhesion factor directly linking intracellularly motile *Listeria monocytogenes* and *Listeria ivanovii* to the actin-based cytoskeleton of mammalian cells. EMBO J. *14*, 1314-1321.

Chakraborty, T., Leimeister-Wachter, M., Domann, E., Hartl, M., Goebel, W., Nichterlein, T., and Notermans, S. (1992). Coordinate regulation of virulence genes in *Listeria monocytogenes* requires the product of the *prfA* gene. J. Bacteriol. *174*, 568-574.

Chico-Calero, I., Suarez, M., Gonzalez-Zorn, B., Scortti, M., Slaghuis, J., Goebel, W., and Vazquez-Boland, J.A. (2002). Hpt, a bacterial homolog of the microsomal glucose-

6-phosphate translocase, mediates rapid intracellular proliferation in *Listeria*. Proc. Natl. Acad. Sci. U S A *99*, 431-436.

Choi, J.H., and Lee, S.Y. (2004). Secretory and extracellular production of recombinant proteins using *Escherichia coli*. Appl. Microbiol. Biotechnol. *64*, 625-635.

Coffey, A., Rombouts, F.M., and Abee, T. (1996). Influence of environmental parameters on phosphatidylcholine phospholipase C production in *Listeria monocytogenes*: a convenient method to differentiate *L. monocytogenes* from other *Listeria* species. Appl. Environ. Microbiol. *62*, 1252-1256.

Conlan, J.W., and North, R.J. (1991). Neutrophil-mediated dissolution of infected host cells as a defense strategy against a facultative intracellular bacterium. J. Exp. Med. *174*, 741-744.

Conlan, J.W., and North, R.J. (1992). Early pathogenesis of infection in the liver with the facultative intracellular bacteria *Listeria monocytogenes*, *Francisella tularensis*, and *Salmonella typhimurium* involves lysis of infected hepatocytes by leukocytes. Infect. Immun. *60*, 5164-5171.

Cossart, P. (2000). Actin-based motility of pathogens: the Arp2/3 complex is a central player. Cell Microbiol. *2*, 195-205.

Cossart, P., and Lecuit, M. (1998). Interactions of *Listeria monocytogenes* with mammalian cells during entry and actin-based movement: bacterial factors, cellular ligands and signaling. EMBO J. *17*, 3797-3806.

Cossart, P., and Mengaud, J. (1989). *Listeria monocytogenes*. A model system for the molecular study of intracellular parasitism. Mol. Biol. Med. *6*, 463-474.

Cossart, P., Pizarro-Cerda, J., and Lecuit, M. (2003). Invasion of mammalian cells by *Listeria monocytogenes*: functional mimicry to subvert cellular functions. Trends Cell Biol. *13*, 23-31.

Cossart, P., Vicente, M.F., Mengaud, J., Baquero, F., Perez-Diaz, J.C., and Berche, P. (1989). Listeriolysin O is essential for virulence of *Listeria monocytogenes*: direct evidence obtained by gene complementation. Infect. Immun. *57*, 3629-3636.

Cousens, L.P., and Wing, E.J. (2000). Innate defenses in the liver during *Listeria* infection. Immunol. Rev. *174*, 150-159.

Czajkowsky, D.M., Hotze, E.M., Shao, Z., and Tweten, R.K. (2004). Vertical collapse of a cytolysin prepore moves its transmembrane beta-hairpins to the membrane. EMBO J. *23*, 3206-3215.

Czuprynski, C.J., and Brown, J.F. (1990). Effects of purified anti-Lyt-2 mAb treatment on murine listeriosis: comparative roles of Lyt-2+ and L3T4+ cells in resistance to primary and secondary infection, delayed-type hypersensitivity and adoptive transfer of resistance. Immunology *71*, 107-112.

Dabiri, G.A., Sanger, J.M., Portnoy, D.A., and Southwick, F.S. (1990). *Listeria monocytogenes* moves rapidly through the host-cell cytoplasm by inducing directional actin assembly. Proc. Natl. Acad. Sci. U S A *87*, 6068-6072.

Davies, J.W., Ewan, E.P., Varughese, P., and Acres, S.E. (1984). *Listeria monocytogenes* infections in Canada. Clin. Invest. Med. *7*, 315-320.

de Chastellier, C., and Berche, P. (1994). Fate of *Listeria monocytogenes* in murine macrophages: evidence for simultaneous killing and survival of intracellular bacteria. Infect. Immun. *62*, 543-553.

De Las Rivas, B., Garcia, J.L., Lopez, R., and Garcia, P. (2002). Purification and polar localization of pneumococcal LytB, a putative endo-beta-N-acetylglucosaminidase: the chain-dispersing murein hydrolase. J. Bacteriol. *184*, 4988-5000.

Dhar, G., Faull, K.F., and Schneewind, O. (2000). Anchor structure of cell wall surface proteins in *Listeria monocytogenes*. Biochemistry *39*, 3725-3733.

Domann, E., Wehland, J., Rohde, M., Pistor, S., Hartl, M., Goebel, W., Leimeister-Wachter, M., Wuenscher, M., and Chakraborty, T. (1992). A novel bacterial virulence gene in *Listeria monocytogenes* required for host cell microfilament interaction with homology to the proline-rich region of vinculin. EMBO J. *11*, 1981-1990.

Domann, E., Zechel, S., Lingnau, A., Hain, T., Darji, A., Nichterlein, T., Wehland, J., and Chakraborty, T. (1997). Identification and characterization of a novel PrfA-regulated gene in *Listeria monocytogenes* whose product, IrpA, is highly homologous to internalin proteins, which contain leucine-rich repeats. Infect. Immun. *65*, 101-109.

Donnelly, C.W. (2001). *Listeria monocytogenes*: a continuing challenge. Nutr. Rev. *59*, 183-194.

Dons, L., Eriksson, E., Jin, Y., Rottenberg, M.E., Kristensson, K., Larsen, C.N., Bresciani, J., and Olsen, J.E. (2004). Role of flagellin and the two-component CheA/CheY system of *Listeria monocytogenes* in host cell invasion and virulence. Infect. Immun. *72*, 3237-3244.

Dons, L., Rasmussen, O.F., and Olsen, J.E. (1992). Cloning and characterization of a gene encoding flagellin of *Listeria monocytogenes*. Mol. Microbiol. *6*, 2919-2929.

Dramsi, S., Biswas, I., Maguin, E., Braun, L., Mastroeni, P., and Cossart, P. (1995). Entry of

Listeria monocytogenes into hepatocytes requires expression of InlB, a surface protein of the internalin multigene family. Mol. Microbiol. *16*, 251-261.

Dramsi, S., Dehoux, P., Lebrun, M., Goossens, P.L., and Cossart, P. (1997). Identification of four new members of the internalin multigene family of *Listeria monocytogenes* EGD. Infect. Immun. *65*, 1615-1625.

Drevets, D.A., Sawyer, R.T., Potter, T.A., and Campbell, P.A. (1995). *Listeria monocytogenes* infects human endothelial cells by two distinct mechanisms. Infect. Immun. *63*, 4268-4276.

Dussurget, O., Pizarro-Cerda, J., and Cossart, P. (2004). Molecular determinants of *Listeria monocytogenes* virulence. Annu. Rev. Microbiol. *58*, 587-610.

Dustoor, M., Croft, W., Fulton, A., and Blazkovec, A. (1977). Bacteriological and histopathological evaluation of guinea pigs after infection with *Listeria monocytogenes*. Infect. Immun. *15*, 916-924.

Ebe, Y., Hasegawa, G., Takatsuka, H., Umezu, H., Mitsuyama, M., Arakawa, M., Mukaida, N., and Naito, M. (1999). The role of Kupffer cells and regulation of neutrophil migration into the liver by macrophage inflammatory protein-2 in primary listeriosis in mice. Pathol. Int. *49*, 519-532.

Eckert, C., Lecerf, M., Dubost, L., Arthur, M., and Mesnage, S. (2006). Functional analysis of AtlA, the major N-acetylglucosaminidase of *Enterococcus faecalis*. J. Bacteriol. *188*, 8513-8519.

Edelson, B.T., and Unanue, E.R. (2001). Intracellular antibody neutralizes *Listeria* growth. Immunity *14*, 503-512.

Farber, J.M., and Peterkin, P.I. (1991). *Listeria monocytogenes*, a food-borne pathogen. Microbiol. Rev. *55*, 476-511.

Finelli, A., Kerksiek, K.M., Allen, S.E., Marshall, N., Mercado, R., Pilip, I., Busch, D.H., and Pamer, E.G. (1999). MHC class I restricted T cell responses to *Listeria monocytogenes*, an intracellular bacterial pathogen. Immunol. Res. *19*, 211-223.

Fleming, A.D., Ehrlich, D.W., Miller, N.A., and Monif, G.R. (1985). Successful treatment of maternal septicemia due to *Listeria monocytogenes* at 26 weeks' gestation. Obstet. Gynecol. *66*, 52S-53S.

Foster, S.J. (1992). Analysis of the autolysins of *Bacillus subtilis* 168 during vegetative growth and differentiation by using renaturing polyacrylamide gel electrophoresis. J. Bacteriol. *174*, 464-470.

Foster, S.J. (1995). Molecular characterization and functional analysis of the major autolysin of *Staphylococcus aureus* 8325/4. J. Bacteriol. *177*, 5723-5725.

Francis, M.S., and Thomas, C.J. (1996). Effect of multiplicity of infection on *Listeria monocytogenes* pathogenicity for HeLa and Caco-2 cell lines. J. Med. Microbiol. *45*, 323-330.

Freiberg, A., Machner, M.P., Pfeil, W., Schubert, W.D., Heinz, D.W., and Seckler, R. (2004). Folding and stability of the leucine-rich repeat domain of internalin B from *Listeria monocytogenes*. J. Mol. Biol. *337*, 453-461.

Gaillard, J.L., Berche, P., Frehel, C., Gouin, E., and Cossart, P. (1991). Entry of *L. monocytogenes* into cells is mediated by internalin, a repeat protein reminiscent of surface antigens from gram-positive *cocci*. Cell *65*, 1127-1141.

Gaillard, J.L., Berche, P., Mounier, J., Richard, S., and Sansonetti, P. (1987). *In vitro* model of penetration and intracellular growth of *Listeria monocytogenes* in the human enterocyte-like cell line Caco-2. Infect. Immun. *55*, 2822-2829.

Gaillard, J.L., Berche, P., and Sansonetti, P. (1986). Transposon mutagenesis as a tool to study the role of hemolysin in the virulence of *Listeria monocytogenes*. Infect. Immun. *52*, 50-55.

Gaillard, J.L., and Finlay, B.B. (1996). Effect of cell polarization and differentiation on entry of *Listeria monocytogenes* into the enterocyte-like Caco-2 cell line. Infect. Immun. *64*, 1299-1308.

Gaillard, J.L., Jaubert, F., and Berche, P. (1996). The *inlAB* locus mediates the entry of *Listeria monocytogenes* into hepatocytes *in vivo*. J. Exp. Med. *183*, 359-369.

Garandeau, C., Reglier-Poupet, H., Dubail, I., Beretti, J.L., Berche, P., and Charbit, A. (2002). The sortase SrtA of *Listeria monocytogenes* is involved in processing of internalin and in virulence. Infect. Immun. *70*, 1382-1390.

Garifulin, O., and Boyartchuk, V. (2005). *Listeria monocytogenes* as a probe of immune function. Brief Funct. Genomic. Proteomic. *4*, 258-269.

Geiger, B., and Ayalon, O. (1992). Cadherins. Annu. Rev. Cell Biol. *8*, 307-332.

Geoffroy, C., Gaillard, J.L., Alouf, J.E., and Berche, P. (1987). Purification, characterization, and toxicity of the sulfhydryl-activated hemolysin listeriolysin O from *Listeria monocytogenes*. Infect. Immun. *55*, 1641-1646.

Geoffroy, C., Raveneau, J., Beretti, J.L., Lecroisey, A., Vazquez-Boland, J.A., Alouf, J.E.,

and Berche, P. (1991). Purification and characterization of an extracellular 29-kilodalton phospholipase C from *Listeria monocytogenes*. Infect. Immun. *59*, 2382-2388.

Geuijen, C.A., Willems, R.J., Hoogerhout, P., Puijk, W.C., Meloen, R.H., and Mooi, F.R. (1998). Identification and characterization of heparin binding regions of the Fim2 subunit of *Bordetella pertussis*. Infect. Immun. *66*, 2256-2263.

Gill, S.C., and von Hippel, P.H. (1989). Calculation of protein extinction coefficients from amino acid sequence data. Anal. Biochem. *182*, 319-326.

Glaser, P., Frangeul, L., Buchrieser, C., Rusniok, C., Amend, A., Baquero, F., Berche, P., Bloecker, H., Brandt, P., Chakraborty, T., Charbit, A., Chetouani, F., Couve, E., de Daruvar, A., Dehoux, P., Domann, E., Dominguez-Bernal, G., Duchaud, E., Durant, L., Dussurget, O., Entian, K.D., Fsihi, H., Portillo, F.G., Garrido, P., Gautier, L., Goebel, W., Gomez-Lopez, N., Hain, T., Hauf, J., Jackson, D., Jones, L.M., Kaerst, U., Kreft, J., Kuhn, M., Kunst, F., Kurapkat, G., Madueno, E., Maitournam, A., Vicente, J.M., Ng, E., Nedjari, H., Nordsiek, G., Novella, S., de Pablos, B., Perez-Diaz, J.C., Purcell, R., Remmel, B., Rose, M., Schlueter, T., Simoes, N., Tierrez, A., Vazquez-Boland, J.A., Voss, H., Wehland, J., and Cossart, P. (2001). Comparative genomics of *Listeria* species. Science *294*, 849-852.

Glomski, I.J., Decatur, A.L., and Portnoy, D.A. (2003). *Listeria monocytogenes* mutants that fail to compartmentalize listerolysin O activity are cytotoxic, avirulent, and unable to evade host extracellular defenses. Infect. Immun. *71*, 6754-6765.

Goebel, W., Kathariou, S., Kuhn, M., Sokolovic, Z., Kreft, J., Kohler, S., Funke, D., Chakraborty, T., and Leimeister-Wachter, M. (1988). Hemolysin from *Listeria*--biochemistry, genetics and function in pathogenesis. Infection *16 Suppl 2*, S149-156.

Goetz, M., Bubert, A., Wang, G., Chico-Calero, I., Vazquez-Boland, J.A., Beck, M., Slaghuis, J., Szalay, A.A., and Goebel, W. (2001). Microinjection and growth of bacteria in the cytosol of mammalian host cells. Proc. Natl. Acad. Sci. U S A *98*, 12221-12226.

Goldfine, H., and Knob, C. (1992). Purification and characterization of *Listeria monocytogenes* phosphatidylinositol-specific phospholipase C. Infect. Immun. *60*, 4059-4067.

Goldfine, H., Knob, C., Alford, D., and Bentz, J. (1995). Membrane permeabilization by *Listeria monocytogenes* phosphatidylinositol-specific phospholipase C is independent of phospholipid hydrolysis and cooperative with listeriolysin O. Proc. Natl. Acad. Sci. U S A *92*, 2979-2983.

Gottlieb, S.L., Newbern, E.C., Griffin, P.M., Graves, L.M., Hoekstra, R.M., Baker, N.L., Hunter, S.B., Holt, K.G., Ramsey, F., Head, M., Levine, P., Johnson, G., Schoonmaker-Bopp,

D., Reddy, V., Kornstein, L., Gerwel, M., Nsubuga, J., Edwards, L., Stonecipher, S., Hurd, S., Austin, D., Jefferson, M.A., Young, S.D., Hise, K., Chernak, E.D., and Sobel, J. (2006). Multistate outbreak of Listeriosis Linked to turkey deli meat and subsequent changes in US regulatory policy. Clin. Infect. Dis. *42*, 29-36.
Notes: CORPORATE NAME: Listeriosis Outbreak Working Group.

Gouin, E., Mengaud, J., and Cossart, P. (1994). The virulence gene cluster of *Listeria monocytogenes* is also present in *Listeria ivanovii*, an animal pathogen, and *Listeria seeligeri*, a nonpathogenic species. Infect. Immun. *62*, 3550-3553.

Gregory, S.H., Sagnimeni, A.J., and Wing, E.J. (1996). Expression of the *inlAB* operon by *Listeria monocytogenes* is not required for entry into hepatic cells *in vivo*. Infect. Immun. *64*, 3983-3986.

Greiffenberg, L., Goebel, W., Kim, K.S., Daniels, J., and Kuhn, M. (2000). Interaction of *Listeria monocytogenes* with human brain microvascular endothelial cells: an electron microscopic study. Infect. Immun. *68*, 3275-3279.

Greiffenberg, L., Goebel, W., Kim, K.S., Weiglein, I., Bubert, A., Engelbrecht, F., Stins, M., and Kuhn, M. (1998). Interaction of *Listeria monocytogenes* with human brain microvascular endothelial cells: InlB-dependent invasion, long-term intracellular growth, and spread from macrophages to endothelial cells. Infect. Immun. *66*, 5260-5267.

Groves, R.D., and Welshimer, H.J. (1977). Separation of pathogenic from apathogenic *Listeria monocytogenes* by three *in vitro* reactions. J. Clin. Microbiol. *5*, 559-563.

Grundling, A., Gonzalez, M.D., and Higgins, D.E. (2003). Requirement of the *Listeria monocytogenes* broad-range phospholipase PC-PLC during infection of human epithelial cells. J. Bacteriol. *185*, 6295-6307.

Gutekunst, K.A., Pine, L., White, E., Kathariou, S., and Carlone, G.M. (1992). A filamentous-like mutant of *Listeria monocytogenes* with reduced expression of a 60-kilodalton extracellular protein invades and grows in 3T6 and Caco-2 cells. Can. J. Microbiol. *38*, 843-851.

Hain, T., Steinweg, C., Kuenne, C.T., Billion, A., Ghai, R., Chatterjee, S.S., Domann, E., Karst, U., Goesmann, A., Bekel, T., Bartels, D., Kaiser, O., Meyer, F., Puhler, A., Weisshaar, B., Wehland, J., Liang, C., Dandekar, T., Lampidis, R., Kreft, J., Goebel, W., and Chakraborty, T. (2006). Whole-genome sequence of *Listeria welshimeri* reveals common steps in genome reduction with *Listeria innocua* as compared to *Listeria monocytogenes*. J. Bacteriol. *188*, 7405-7415.

Hamon, M., Bierne, H., and Cossart, P. (2006). *Listeria monocytogenes*: a multifaceted

model. Nat. Rev. Microbiol. *4*, 423-434.

Hearty, S., Leonard, P., Quinn, J., and O'kennedy, R. (2006). Production, characterisation and potential application of a novel monoclonal antibody for rapid identification of virulent *Listeria monocytogenes*. J. Microbiol. Methods, *66*, 294-312.

Heidrich, C., Ursinus, A., Berger, J., Schwarz, H., and Holtje, J.V. (2002). Effects of multiple deletions of murein hydrolases on viability, septum cleavage, and sensitivity to large toxic molecules in *Escherichia coli*. J. Bacteriol. *184*, 6093-6099.

Heilmann, C., Hartleib, J., Hussain, M.S., and Peters, G. (2005). The multifunctional *Staphylococcus aureus* autolysin *aaa* mediates adherence to immobilized fibrinogen and fibronectin. Infect. Immun. *73*, 4793-4802.

Heilmann, C., Hussain, M., Peters, G., and Gotz, F. (1997). Evidence for autolysin-mediated primary attachment of *Staphylococcus epidermidis* to a polystyrene surface. Mol. Microbiol. *24*, 1013-1024.

Hell, W., Meyer, H.G., and Gatermann, S.G. (1998). Cloning of *aas*, a gene encoding a *Staphylococcus saprophyticus* surface protein with adhesive and autolytic properties. Mol. Microbiol. *29*, 871-881.

Hell, W., Reichl, S., Anders, A., and Gatermann, S. (2003). The autolytic activity of the recombinant amidase of *Staphylococcus saprophyticus* is inhibited by its own recombinant GW repeats. FEMS Microbiol. Lett. *227*, 47-51.

Hess, J., Gentschev, I., Szalay, G., Ladel, C., Bubert, A., Goebel, W., and Kaufmann, S.H. (1995). *Listeria monocytogenes* p60 supports host cell invasion by and *in vivo* survival of attenuated *Salmonella typhimurium*. Infect. Immun. *63*, 2047-2053.

Heuck, A.P., Savva, C.G., Holzenburg, A., and Johnson, A.E. (2007). Conformational changes that effect oligomerization and initiate pore formation are triggered throughout perfringolysin O upon binding to cholesterol. J. Biol. Chem. *282*, 22629-22637.

Hochuli, E., Dobeli, H., and Schacher, A. (1987). New metal chelate adsorbent selective for proteins and peptides containing neighbouring histidine residues. J. Chromatogr. *411*, 177-184.

Hof, H. (1984). Virulence of different strains of *Listeria monocytogenes* serovar 1/2a. Med. Microbiol. Immunol. (Berl) *173*, 207-218.

Hof, H., Nichterlein, T., and Kretschmar, M. (1997). Management of listeriosis. Clin Microbiol. Rev. *10*, 345-357.

Humann, J., Bjordahl, R., Andreasen, K., and Lenz, L.L. (2007). Expression of the p60 autolysin enhances NK cell activation and is required for *Listeria monocytogenes* expansion in IFN-gamma-responsive mice. J. Immunol. *178*, 2407-2414.

Inoue, S., Itagaki, S., and Amano, F. (1995). Intracellular killing of *Listeria monocytogenes* in the J774.1 macrophage-like cell line and the lipopolysaccharide (LPS)-resistant mutant LPS1916 cell line defective in the generation of reactive oxygen intermediates after LPS treatment. Infect. Immun. *63*, 1876-1886.

Ireton, K., Payrastre, B., Chap, H., Ogawa, W., Sakaue, H., Kasuga, M., and Cossart, P. (1996). A role for phosphoinositide 3-kinase in bacterial invasion. Science *274*, 780-782.

Ireton, K., Payrastre, B., and Cossart, P. (1999). The *Listeria monocytogenes* protein InlB is an agonist of mammalian phosphoinositide 3-kinase. J. Biol. Chem. *274*, 17025-17032.

Jackson, R.L., Busch, S.J., and Cardin, A.D. (1991). Glycosaminoglycans: molecular properties, protein interactions, and role in physiological processes. Physiol. Rev. *71*, 481-539.

Jacobs, T., Darji, A., Frahm, N., Rohde, M., Wehland, J., Chakraborty, T., and Weiss, S. (1998). Listeriolysin O: cholesterol inhibits cytolysis but not binding to cellular membranes. Mol. Microbiol. *28*, 1081-1089.

Jacquet, C., Doumith, M., Gordon, J.I., Martin, P.M., Cossart, P., and Lecuit, M. (2004). A molecular marker for evaluating the pathogenic potential of foodborne *Listeria monocytogenes*. J. Infect. Dis. *189*, 2094-2100.

Jaradat, Z.W., Wampler, J.W., and Bhunia, A.W. (2003). A *Listeria* adhesion protein-deficient *Listeria monocytogenes* strain shows reduced adhesion primarily to intestinal cell lines. Med. Microbiol. Immunol. (Berl) *192*, 85-91.

Jedrzejas, M.J. (2001). Pneumococcal virulence factors: structure and function. Microbiol. Mol. Biol. Rev. *65*, 187-207.

Johansson, J., Mandin, P., Renzoni, A., Chiaruttini, C., Springer, M., and Cossart, P. (2002). An RNA Thermosensor Controls Expression of Virulence Genes in *Listeria monocytogenes*. Cell *110*, 551.

Jonquieres, R., Bierne, H., Fiedler, F., Gounon, P., and Cossart, P. (1999). Interaction between the protein InlB of *Listeria monocytogenes* and lipoteichoic acid: a novel mechanism of protein association at the surface of gram-positive bacteria. Mol. Microbiol. *34*, 902-914.

Jonquieres, R., Pizarro-Cerda, J., and Cossart, P. (2001). Synergy between the N- and

C-terminal domains of InlB for efficient invasion of non-phagocytic cells by *Listeria monocytogenes*. Mol. Microbiol. *42*, 955-965.

Kamisango, K., Saiki, I., Tanio, Y., Okumura, H., Araki, Y., Sekikawa, I., Azuma, I., and Yamamura, Y. (1982). Structures and biological activities of peptidoglycans of *Listeria monocytogenes* and *Propionibacterium acnes*. J. Biochem. (Tokyo) *92*, 23-33.

Kathariou, S., Metz, P., Hof, H., and Goebel, W. (1987). Tn916-induced mutations in the hemolysin determinant affecting virulence of *Listeria monocytogenes*. J. Bacteriol. *169*, 1291-1297.

Kaufmann, S.H., Emoto, M., Szalay, G., Barsig, J., and Flesch, I.E. (1997). Interleukin-4 and listeriosis. Immunol. Rev. *158*, 95-105.

Kazmierczak, M.J., Mithoe, S.C., Boor, K.J., and Wiedmann, M. (2003). *Listeria monocytogenes* sigma B regulates stress response and virulence functions. J. Bacteriol. *185*, 5722-5734.

Keeney, K.M., Stuckey, J.A., and O'Riordan, M.X. (2007). LplA1-dependent utilization of host lipoyl peptides enables *Listeria* cytosolic growth and virulence. Mol. Microbiol. *66*, 758-770.

Khelef, N., Lecuit, M., Bierne, H., and Cossart, P. (2006). Species specificity of the *Listeria monocytogenes* InlB protein. Cell Microbiol. *8*, 457-470.

Kim, K.P., Jagadeesan, B., Burkholder, K.M., Jaradat, Z.W., Wampler, J.L., Lathrop, A.A., Morgan, M.T., and Bhunia, A.K. (2006). Adhesion characteristics of *Listeria* adhesion protein (LAP)-expressing *Escherichia coli* to Caco-2 cells and of recombinant LAP to eukaryotic receptor Hsp60 as examined in a surface plasmon resonance sensor. FEMS Microbiol. Lett. *256*, 324-332.

Kingdon, G.C., and Sword, C.P. (1970). Cardiotoxic and lethal effects of *Listeria monocytogenes* hemolysin. Infect. Immun. *1*, 373-379.

Kocks, C., Gouin, E., Tabouret, M., Berche, P., Ohayon, H., and Cossart, P. (1992). *L. monocytogenes*-induced actin assembly requires the *actA* gene product, a surface protein. Cell *68*, 521-531.

Kocks, C., Hellio, R., Gounon, P., Ohayon, H., and Cossart, P. (1993). Polarized distribution of *Listeria monocytogenes* surface protein ActA at the site of directional actin assembly. J. Cell Sci. *105 (Pt 3)*, 699-710.

Kohler, S., Bubert, A., Vogel, M., and Goebel, W. (1991). Expression of the *iap* gene coding for protein p60 of *Listeria monocytogenes* is controlled on the posttranscriptional level. J.

Bacteriol. *173*, 4668-4674.

Kohler, S., Leimeister-Wachter, M., Chakraborty, T., Lottspeich, F., and Goebel, W. (1990). The gene coding for protein p60 of *Listeria monocytogenes* and its use as a specific probe for *Listeria monocytogenes*. Infect. Immun. *58*, 1943-1950.

Kuhn, M. (1998). The microtubule depolymerizing drugs nocodazole and colchicine inhibit the uptake of *Listeria monocytogenes* by P388D1 macrophages. FEMS Microbiol. Lett. *160*, 87-90.

Kuhn, M., and Goebel, W. (1989). Identification of an extracellular protein of *Listeria monocytogenes* possibly involved in intracellular uptake by mammalian cells. Infect. Immun. *57*, 55-61.

Kuhn, M., and Goebel, W. (1994). Induction of cytokines in phagocytic mammalian cells infected with virulent and avirulent *Listeria* strains. Infect. Immun. *62*, 348-356.

Kuhn, M., and Goebel, W. (1997). Responses by murine macrophages infected with *Listeria monocytogenes* crucial for the development of immunity to this pathogen. Immunol. Rev. *158*, 57-67.

Kuhn, M., and Goebel, W. (1998). Host cell signalling during *Listeria monocytogenes* infection. Trends Microbiol. *6*, 11-15.

Kuhn, M., Kathariou, S., and Goebel, W. (1988). Hemolysin supports survival but not entry of the intracellular bacterium *Listeria monocytogenes*. Infect. Immun. *56*, 79-82.

Kvenberg, J.E. (1988). Outbreaks of listeriosis/*Listeria*-contaminated foods. Microbiol. Sci. *5*, 355-358.

Laemmli, U.K. (1970). Cleavage of structural proteins during the assembly of the head of bacteriophage T4. Nature *227*, 680-685.

Lasa, I., David, V., Gouin, E., Marchand, J.B., and Cossart, P. (1995). The amino-terminal part of ActA is critical for the actin-based motility of *Listeria monocytogenes*; the central proline-rich region acts as a stimulator. Mol. Microbiol. *18*, 425-436.

Lasa, I., Gouin, E., Goethals, M., Vancompernolle, K., David, V., Vandekerckhove, J., and Cossart, P. (1997). Identification of two regions in the N-terminal domain of ActA involved in the actin comet tail formation by *Listeria monocytogenes*. EMBO J. *16*, 1531-1540.

Laurent, V., Loisel, T.P., Harbeck, B., Wehman, A., Grobe, L., Jockusch, B.M., Wehland, J., Gertler, F.B., and Carlier, M.F. (1999). Role of proteins of the Ena/VASP family in actin-based motility of *Listeria monocytogenes*. J. Cell Biol. *144*, 1245-1258.

Lecuit, M. (2005). Understanding how *Listeria monocytogenes* targets and crosses host barriers. Clin. Microbiol. Infect. *11*, 430-436.

Lecuit, M., and Cossart, P. (2002). Genetically-modified-animal models for human infections: the *Listeria* paradigm. Trends Mol. Med. *8*, 537-542.

Lecuit, M., Dramsi, S., Gottardi, C., Fedor-Chaiken, M., Gumbiner, B., and Cossart, P. (1999). A single amino acid in E-cadherin responsible for host specificity towards the human pathogen *Listeria monocytogenes*. EMBO J. *18*, 3956-3963.

Lecuit, M., Hurme, R., Pizarro-Cerda, J., Ohayon, H., Geiger, B., and Cossart, P. (2000). A role for alpha-and beta-catenins in bacterial uptake. Proc. Natl. Acad. Sci. U S A *97*, 10008-10013.

Lecuit, M., Nelson, D.M., Smith, S.D., Khun, H., Huerre, M., Vacher-Lavenu, M.C., Gordon, J.I., and Cossart, P. (2004). Targeting and crossing of the human maternofetal barrier by *Listeria monocytogenes*: role of internalin interaction with trophoblast E-cadherin. Proc. Natl. Acad. Sci. U S A *101*, 6152-6157.

Lecuit, M., Ohayon, H., Braun, L., Mengaud, J., and Cossart, P. (1997). Internalin of *Listeria monocytogenes* with an intact leucine-rich repeat region is sufficient to promote internalization. Infect. Immun. *65*, 5309-5319.

Lecuit, M., Vandormael-Pournin, S., Lefort, J., Huerre, M., Gounon, P., Dupuy, C., Babinet, C., and Cossart, P. (2001). A transgenic model for listeriosis: role of internalin in crossing the intestinal barrier. Science *292*, 1722-1725.

Leimeister-Wachter, M., Domann, E., and Chakraborty, T. (1992). The expression of virulence genes in *Listeria monocytogenes* is thermoregulated. J. Bacteriol. *174*, 947-952.

Leimeister-Wachter, M., Haffner, C., Domann, E., Goebel, W., and Chakraborty, T. (1990). Identification of a gene that positively regulates expression of listeriolysin, the major virulence factor of *Listeria monocytogenes*. Proc. Natl. Acad. Sci. U S A *87*, 8336-8340.

Lemon, K.P., Higgins, D.E., and Kolter, R. (2007). Flagellar motility is critical for *Listeria monocytogenes* biofilm formation. J. Bacteriol. *189*, 4418-4424.

Lenz, L.L., Mohammadi, S., Geissler, A., and Portnoy, D.A. (2003). SecA2-dependent secretion of autolytic enzymes promotes *Listeria monocytogenes* pathogenesis. Proc. Natl. Acad. Sci. U S A *100*, 12432-12437.

Lepay, D.A., Steinman, R.M., Nathan, C.F., Murray, H.W., and Cohn, Z.A. (1985). Liver macrophages in murine listeriosis. Cell-mediated immunity is correlated with an influx of macrophages capable of generating reactive oxygen intermediates. J. Exp. Med. *161*,

1503-1512.

Lin, M., Dan, H., and Li, Y. (2004). Identification of a second flagellin gene and functional characterization of a sigma70-like promoter upstream of a *Leptospira borgpetersenii flaB* gene. Curr. Microbiol. *48*, 145-152.

Lin, M., Surujballi, O., Nielsen, K., Nadin-Davis, S., and Randall, G. (1997). Identification of a 35-kilodalton serovar-cross-reactive flagellar protein, FlaB, from *Leptospira interrogans* by N-terminal sequencing, gene cloning, and sequence analysis. Infect. Immun. *65*, 4355-4359.

Lin, M., Todoric, D., Mallory, M., Luo, B.S., Trottier, E., and Dan, H. (2006). Monoclonal antibodies binding to the cell surface of *Listeria monocytogenes* serotype 4b. J. Med. Microbiol. *55*, 291-299.

Lingnau, A., Domann, E., Hudel, M., Bock, M., Nichterlein, T., Wehland, J., and Chakraborty, T. (1995). Expression of the *Listeria monocytogenes* EGD *inlA* and *inlB* genes, whose products mediate bacterial entry into tissue culture cell lines, by PrfA-dependent and -independent mechanisms. Infect. Immun. *63*, 3896-3903.

Llull, D., Lopez, R., and Garcia, E. (2006). Skl, a novel choline-binding N-acetylmuramoyl-L-alanine amidase of *Streptococcus mitis* SK137 containing a CHAP domain. FEBS Lett. *580*, 1959-1964.

Lock, R.A., Hansman, D., and Paton, J.C. (1992). Comparative efficacy of autolysin and pneumolysin as immunogens protecting mice against infection by *Streptococcus pneumoniae*. Microb. Pathog. *12*, 137-143.

Loessner, M.J., Kramer, K., Ebel, F., and Scherer, S. (2002). C-terminal domains of *Listeria monocytogenes* bacteriophage murein hydrolases determine specific recognition and high-affinity binding to bacterial cell wall carbohydrates. Mol. Microbiol. *44*, 335-349.

Lorber, B. (1997). Listeriosis. Clin. Infect. Dis. *24*, 1-9; quiz 10-1.

Luo, Q., Herler, M., Muller-Altrock, S., and Goebel, W. (2005). Supportive and inhibitory elements of a putative PrfA-dependent promoter in *Listeria monocytogenes*. Mol. Microbiol. *55*, 986-997.

Luo, Q., Rauch, M., Marr, A.K., Muller-Altrock, S., and Goebel, W. (2004). *In vitro* transcription of the *Listeria monocytogenes* virulence genes *inlC* and *mpl* reveals overlapping PrfA-dependent and -independent promoters that are differentially activated by GTP. Mol. Microbiol. *52*, 39-52.

Lyytikainen, O., Autio, T., Maijala, R., Ruutu, P., Honkanen-Buzalski, T., Miettinen, M.,

Hatakka, M., Mikkola, J., Anttila, V.J., Johansson, T., Rantala, L., Aalto, T., Korkeala, H., and Siitonen, A. (2000). An outbreak of *Listeria monocytogenes* serotype 3a infections from butter in Finland. J. Infect. Dis. *181*, 1838-1841.

MacDonald, P.D., Whitwam, R.E., Boggs, J.D., MacCormack, J.N., Anderson, K.L., Reardon, J.W., Saah, J.R., Graves, L.M., Hunter, S.B., and Sobel, J. (2005). Outbreak of listeriosis among Mexican immigrants as a result of consumption of illicitly produced Mexican-style cheese. Clin. Infect. Dis. *40*, 677-682.

MacDonald, T.T., and Carter, P.B. (1980). Cell-mediated immunity to intestinal infection. Infect. Immun. *28*, 516-523.

MacFaddin, J. F. (2000). Biochemical tests for identification of medical bacteria (New York: Lippincott Williams & Wilkin).

Machata, S., Hain, T., Rohde, M., and Chakraborty, T. (2005). Simultaneous deficiency of both MurA and p60 proteins generates a rough phenotype in *Listeria monocytogenes*. J. Bacteriol. *187*, 8385-8394.

Machner, M.P., Urbanke, C., Barzik, M., Otten, S., Sechi, A.S., Wehland, J., and Heinz, D.W. (2001). ActA from *Listeria monocytogenes* can interact with up to four Ena/VASP homology 1 domains simultaneously. J. Biol. Chem. *276*, 40096-40103.

Mackaness, G.B. (1962). Cellular resistance to infection. J. Exp. Med. *116*, 381-406.

Madigan, M. M., Parker, J., Madigan, M. T., and Martinko, J. M. (2002). Brock Biology of Microorganisms (Upper Saddle River, New Jersey: Prentice Hall).

Makino, S.I., Kawamoto, K., Takeshi, K., Okada, Y., Yamasaki, M., Yamamoto, S., and Igimi, S. (2005). An outbreak of food-borne listeriosis due to cheese in Japan, during 2001. Int. J. Food Microbiol. *104*, 189-196.

Mandel, T.E., and Cheers, C. (1980). Resistance and susceptibility of mice to bacterial infection: histopathology of listeriosis in resistant and susceptible strains. Infect. Immun. *30*, 851-861.

Mani, N., Baddour, L.M., Offutt, D.Q., Vijaranakul, U., Nadakavukaren, M.J., and Jayaswal, R.K. (1994). Autolysis-defective mutant of *Staphylococcus aureus*: pathological considerations, genetic mapping, and electron microscopic studies. Infect. Immun. *62*, 1406-1409.

March, P.E., and Inouye, M. (1985). Characterization of the *lep* operon of *Escherichia coli*. Identification of the promoter and the gene upstream of the signal peptidase I gene. J. Biol. Chem. *260*, 7206-7213.

Marchand, J.B., Moreau, P., Paoletti, A., Cossart, P., Carlier, M.F., and Pantaloni, D. (1995). Actin-based movement of *Listeria monocytogenes*: actin assembly results from the local maintenance of uncapped filament barbed ends at the bacterium surface. J. Cell Biol. *130*, 331-343.

Marco, A.J., Domingo, M., Ruberte, J., Carretero, A., Briones, V., and Dominguez, L. (1992a). Lymphatic drainage of *Listeria monocytogenes* and Indian ink inoculated in the peritoneal cavity of the mouse. Lab Anim. *26*, 200-205.

Marco, A.J., Prats, N., Ramos, J.A., Briones, V., Blanco, M., Dominguez, L., and Domingo, M. (1992b). A microbiological, histopathological and immunohistological study of the intragastric inoculation of *Listeria monocytogenes* in mice. J. Comp. Pathol. *107*, 1-9.

Margot, P., Wahlen, M., Gholamhoseinian, A., Piggot, P., and Karamata, D. (1998). The *lytE* gene of *Bacillus subtilis* 168 encodes a cell wall hydrolase. J. Bacteriol. *180*, 749-752.

Marino, M., Banerjee, M., Jonquieres, R., Cossart, P., and Ghosh, P. (2002). GW domains of the *Listeria monocytogenes* invasion protein InlB are SH3-like and mediate binding to host ligands. EMBO J. *21*, 5623-5634.

Marino, M., Braun, L., Cossart, P., and Ghosh, P. (1999). Structure of the InlB leucine-rich repeats, a domain that triggers host cell invasion by the bacterial pathogen *L. monocytogenes*. Mol. Cell *4*, 1063-1072.

Marquis, H., Doshi, V., and Portnoy, D.A. (1995). The broad-range phospholipase C and a metalloprotease mediate listeriolysin O-independent escape of *Listeria monocytogenes* from a primary vacuole in human epithelial cells. Infect. Immun. *63*, 4531-4534.

Marquis, H., Goldfine, H., and Portnoy, D.A. (1997). Proteolytic pathways of activation and degradation of a bacterial phospholipase C during intracellular infection by *Listeria monocytogenes*. J. Cell Biol. *137*, 1381-1392.

Mauder, N., Ecke, R., Mertins, S., Loeffler, D.I., Seidel, G., Sprehe, M., Hillen, W., Goebel, W., and Muller-Altrock, S. (2006). Species-specific differences in the activity of PrfA, the key regulator of listerial virulence genes. J. Bacteriol. *188*, 7941-7956.

Mazmanian, S.K., Liu, G., Ton-That, H., and Schneewind, O. (1999). *Staphylococcus aureus* sortase, an enzyme that anchors surface proteins to the cell wall. Science *285*, 760-763.

McLaughlan, A.M., and Foster, S.J. (1998). Molecular characterization of an autolytic amidase of *Listeria monocytogenes* EGD. Microbiology *144 (Pt 5)*, 1359-1367.

Mead, P.S., Dunne, E.F., Graves, L., Wiedmann, M., Patrick, M., Hunter, S., Salehi, E., Mostashari, F., Craig, A., Mshar, P., Bannerman, T., Sauders, B.D., Hayes, P., Dewitt, W.,

Sparling, P., Griffin, P., Morse, D., Slutsker, L., and Swaminathan, B. (2006). Nationwide outbreak of listeriosis due to contaminated meat. Epidemiol. Infect. *134*, 744-751.
Notes: CORPORATE NAME: *Listeria* Outbreak Working Group

Mengaud, J., Braun-Breton, C., and Cossart, P. (1991a). Identification of phosphatidylinositol-specific phospholipase C activity in *Listeria monocytogenes*: a novel type of virulence factor? Mol. Microbiol. *5*, 367-372.

Mengaud, J., Dramsi, S., Gouin, E., Vazquez-Boland, J.A., Milon, G., and Cossart, P. (1991b). Pleiotropic control of *Listeria monocytogenes* virulence factors by a gene that is autoregulated. Mol. Microbiol. *5*, 2273-2283.

Mengaud, J., Ohayon, H., Gounon, P., Mege, R.M., and Cossart, P. (1996). E-cadherin is the receptor for internalin, a surface protein required for entry of *L. monocytogenes* into epithelial cells. Cell *84*, 923-932.

Mengaud, J., Vicente, M.F., Chenevert, J., Geoffroy, C., Baquero, F., Perez-Diaz, J.C., and Cossart, P. (1989). A genetic approach to demonstrate the role of listeriolysin O in the virulence of *Listeria monocytogenes*. Acta Microbiol. Hung. *36*, 177-182.

Mergulhao, F.J., Summers, D.K., and Monteiro, G.A. (2005). Recombinant protein secretion in *Escherichia coli*. Biotechnol. Adv. *23*, 177-202.

Michel, E., Reich, K.A., Favier, R., Berche, P., and Cossart, P. (1990). Attenuated mutants of the intracellular bacterium *Listeria monocytogenes* obtained by single amino acid substitutions in listeriolysin O. Mol. Microbiol. *4*, 2167-2178.

Milohanic, E., Glaser, P., Coppee, J.Y., Frangeul, L., Vega, Y., Vazquez-Boland, J.A., Kunst, F., Cossart, P., and Buchrieser, C. (2003). Transcriptome analysis of *Listeria monocytogenes* identifies three groups of genes differently regulated by PrfA. Mol. Microbiol. *47*, 1613-1625.

Milohanic, E., Jonquieres, R., Cossart, P., Berche, P., and Gaillard, J.L. (2001). The autolysin Ami contributes to the adhesion of *Listeria monocytogenes* to eukaryotic cells via its cell wall anchor. Mol. Microbiol. *39*, 1212-1224.

Milohanic, E., Jonquieres, R., Glaser, P., Dehoux, P., Jacquet, C., Berche, P., Cossart, P., and Gaillard, J.L. (2004). Sequence and binding activity of the autolysin-adhesin Ami from epidemic *Listeria monocytogenes* 4b. Infect. Immun. *72*, 4401-4409.

Milohanic, E., Pron, B., Berche, P., and Gaillard, J.L. (2000). Identification of new loci involved in adhesion of *Listeria monocytogenes* to eukaryotic cells. European *Listeria* Genome Consortium. Microbiology *146 (Pt 3)*, 731-739.

Milon, G. (1997). *Listeria monocytogenes* in laboratory mice: a model of short-term infectious and pathogenic processes controllable by regulated protective immune responses. Immunol. Rev. *158*, 37-46.

Moat, A. G., and Foster, J. W. (2002). Microbial Physiology (New York: John Wiley).

Monack, D.M., and Theriot, J.A. (2001). Actin-based motility is sufficient for bacterial membrane protrusion formation and host cell uptake. Cell Microbiol. *3*, 633-647.

Mondal, M.S., Ruiz, A., Bok, D., and Rando, R.R. (2000). Lecithin retinol acyltransferase contains cysteine residues essential for catalysis. Biochemistry *39*, 5215-5220.

Mounier, J., Ryter, A., Coquis-Rondon, M., and Sansonetti, P.J. (1990). Intracellular and cell-to-cell spread of *Listeria monocytogenes* involves interaction with F-actin in the enterocytelike cell line Caco-2. Infect. Immun. *58*, 1048-1058.

Nambu, T., Minamino, T., Macnab, R.M., and Kutsukake, K. (1999). Peptidoglycan-hydrolyzing activity of the FlgJ protein, essential for flagellar rod formation in *Salmonella typhimurium*. J. Bacteriol. *181*, 1555-1561.

Nanninga, N. (1991). Cell division and peptidoglycan assembly in *Escherichia coli*. Mol. Microbiol. *5*, 791-795.

Navarre, W.W., and Schneewind, O. (1999). Surface proteins of gram-positive bacteria and mechanisms of their targeting to the cell wall envelope. Microbiol. Mol. Biol. Rev. *63*, 174-229.

Nelson, K.E., Fouts, D.E., Mongodin, E.F., Ravel, J., DeBoy, R.T., Kolonay, J.F., Rasko, D.A., Angiuoli, S.V., Gill, S.R., Paulsen, I.T., Peterson, J., White, O., Nelson, W.C., Nierman, W., Beanan, M.J., Brinkac, L.M., Daugherty, S.C., Dodson, R.J., Durkin, A.S., Madupu, R., Haft, D.H., Selengut, J., Van Aken, S., Khouri, H., Fedorova, N., Forberger, H., Tran, B., Kathariou, S., Wonderling, L.D., Uhlich, G.A., Bayles, D.O., Luchansky, J.B., and Fraser, C.M. (2004). Whole genome comparisons of serotype 4b and 1/2a strains of the food-borne pathogen *Listeria monocytogenes* reveal new insights into the core genome components of this species. Nucleic Acids Res. *32*, 2386-2395.

Niebuhr, K., Ebel, F., Frank, R., Reinhard, M., Domann, E., Carl, U.D., Walter, U., Gertler, F.B., Wehland, J., and Chakraborty, T. (1997). A novel proline-rich motif present in ActA of *Listeria monocytogenes* and cytoskeletal proteins is the ligand for the EVH1 domain, a protein module present in the Ena/VASP family. EMBO J. *16*, 5433-5444.

Niemann, H.H., Jager, V., Butler, P.J., van den Heuvel, J., Schmidt, S., Ferraris, D., Gherardi, E., and Heinz, D.W. (2007). Structure of the human receptor tyrosine kinase met in complex with the *Listeria* invasion protein InlB. Cell *130*, 235-246.

Nomura, T., Kawamura, I., Kohda, C., Baba, H., Ito, Y., Kimoto, T., Watanabe, I., and Mitsuyama, M. (2007). Irreversible loss of membrane-binding activity of *Listeria*-derived cytolysins in non-acidic conditions: a distinct difference from allied cytolysins produced by other Gram-positive bacteria. Microbiology *153*, 2250-2258.

O'Neil, H.S., and Marquis, H. (2006). *Listeria monocytogenes* flagella are used for motility, not as adhesins, to increase host cell invasion. Infect. Immun. *74*, 6675-6681.

O'Riordan, M., Moors, M.A., and Portnoy, D.A. (2003). *Listeria* intracellular growth and virulence require host-derived lipoic acid. Science *302*, 462-464.

Ohnishi, R., Ishikawa, S., and Sekiguchi, J. (1999). Peptidoglycan hydrolase LytF plays a role in cell separation with CwlF during vegetative growth of *Bacillus subtilis*. J. Bacteriol. *181*, 3178-3184.

Oshida, T., Sugai, M., Komatsuzawa, H., Hong, Y.M., Suginaka, H., and Tomasz, A. (1995). A *Staphylococcus aureus* autolysin that has an N-acetylmuramoyl-L-alanine amidase domain and an endo-beta-N-acetylglucosaminidase domain: cloning, sequence analysis, and characterization. Proc. Natl. Acad. Sci. U S A *92*, 285-289.

Pamer, E.G. (2004). Immune responses to *Listeria monocytogenes*. Nat. Rev. Immunol. *4*, 812-823.

Pandiripally, V.K., Westbrook, D.G., Sunki, G.R., and Bhunia, A.K. (1999). Surface protein p104 is involved in adhesion of *Listeria monocytogenes* to human intestinal cell line, Caco-2. J. Med. Microbiol. *48*, 117-124.

Park, J.H., Lee, Y.S., Lim, Y.K., Kwon, S.H., Lee, C.U., and Yoon, B.S. (2000). Specific binding of recombinant *Listeria monocytogenes* p60 protein to Caco-2 cells. FEMS Microbiol. Lett. *186*, 35-40.

Park, S.F., and Stewart, G.S. (1990). High-efficiency transformation of *Listeria monocytogenes* by electroporation of penicillin-treated cells. Gene *94*, 129-132.

Pilgrim, S., Kolb-Maurer, A., Gentschev, I., Goebel, W., and Kuhn, M. (2003). Deletion of the gene encoding p60 in *Listeria monocytogenes* leads to abnormal cell division and loss of actin-based motility. Infect. Immun. *71*, 3473-3484.

Pine, L., Malcolm, G.B., and Plikaytis, B.D. (1990). *Listeria monocytogenes* intragastric and intraperitoneal approximate 50% lethal doses for mice are comparable, but death occurs earlier by intragastric feeding. Infect. Immun. *58*, 2940-2945.

Pistor, S., Chakraborty, T., Walter, U., and Wehland, J. (1995). The bacterial actin nucleator protein ActA of *Listeria monocytogenes* contains multiple binding sites for host

microfilament proteins. Curr. Biol. *5*, 517-525.

Popowska, M. (2004). Analysis of the peptidoglycan hydrolases of *Listeria monocytogenes*: multiple enzymes with multiple functions. Pol. J. Microbiol. *53 Suppl*, 29-34.

Popowska, M., and Markiewicz, Z. (2004). Murein-hydrolyzing activity of flagellin FlaA of *Listeria monocytogenes*. Pol. J. Microbiol. *53*, 237-241.

Popowska, M., and Markiewicz, Z. (2006). Characterization of *Listeria monocytogenes* protein Lmo0327 with murein hydrolase activity. Arch. Microbiol. *186*, 69-86.

Porath, J., Carlsson, J., Olsson, I., and Belfrage, G. (1975). Metal chelate affinity chromatography, a new approach to protein fractionation. Nature *258*, 598-599.

Portnoy, D.A., Auerbuch, V., and Glomski, I.J. (2002). The cell biology of *Listeria monocytogenes* infection: the intersection of bacterial pathogenesis and cell-mediated immunity. J. Cell Biol. *158*, 409-414.

Portnoy, D.A., Chakraborty, T., Goebel, W., and Cossart, P. (1992). Molecular determinants of *Listeria monocytogenes* pathogenesis. Infect. Immun. *60*, 1263-1267.

Portnoy, D.A., Jacks, P.S., and Hinrichs, D.J. (1988). Role of hemolysin for the intracellular growth of *Listeria monocytogenes*. J. Exp. Med. *167*, 1459-1471.

Potvin, C., Leclerc, D., Tremblay, G., Asselin, A., and Bellemare, G. (1988). Cloning, sequencing and expression of a *Bacillus* bacteriolytic enzyme in *Escherichia coli*. Mol. Gen. Genet. *214*, 241-248.

Powell, A.K., Yates, E.A., Fernig, D.G., and Turnbull, J.E. (2004). Interactions of heparin/heparan sulfate with proteins: appraisal of structural factors and experimental approaches. Glycobiology *14*, 17R-30R.

Prats, N., Briones, V., Blanco, M.M., Altimira, J., Ramos, J.A., Dominguez, L., and Marco, A. (1992). Choroiditis and meningitis in experimental murine infection with *Listeria monocytogenes*. Eur. J. Clin. Microbiol. Infect. Dis. *11*, 744-747.

Pron, B., Boumaila, C., Jaubert, F., Sarnacki, S., Monnet, J.P., Berche, P., and Gaillard, J.L. (1998). Comprehensive study of the intestinal stage of listeriosis in a rat ligated ileal loop system. Infect. Immun. *66*, 747-755.

Pucciarelli, M.G., Calvo, E., Sabet, C., Bierne, H., Cossart, P., and Garcia-del Portillo, F. (2005). Identification of substrates of the *Listeria monocytogenes* sortases A and B by a non-gel proteomic analysis. Proteomics *5*, 4808-4817.

Pugsley, A.P. (1993). The complete general secretory pathway in gram-negative bacteria. Microbiol. Rev. *57*, 50-108.

Racz, P., Kaiserling, E., Tenner, K., and Wuthe, H.H. (1973). Experimental *Listeria* cystitis. II. Further evidence of the epithelial phase in experimental *Listeria* infection. An electron microscopic study. Virchows Arch. B Cell Pathol. *13*, 24-37.

Racz, P., Tenner, K., and Szivessy, K. (1970). Electron microscopic studies in experimental keratoconjunctivitis listeriosa. I. Penetration of *Listeria monocytogenes* into corneal epithelial cells. Acta Microbiol. Acad. Sci. Hung. *17*, 221-236.

Rafelski, S.M., and Theriot, J.A. (2005). Bacterial shape and ActA distribution affect initiation of *Listeria monocytogenes* actin-based motility. Biophys. J. *89*, 2146-2158.

Rafelski, S.M., and Theriot, J.A. (2006). Mechanism of polarization of *Listeria monocytogenes* surface protein ActA. Mol. Microbiol. *59*, 1262-1279.

Ramachandran, R., Tweten, R.K., and Johnson, A.E. (2005). The domains of a cholesterol-dependent cytolysin undergo a major FRET-detected rearrangement during pore formation. Proc. Natl. Acad. Sci. U S A *102*, 7139-7144.

Raveneau, J., Geoffroy, C., Beretti, J.L., Gaillard, J.L., Alouf, J.E., and Berche, P. (1992). Reduced virulence of a *Listeria monocytogenes* phospholipase-deficient mutant obtained by transposon insertion into the zinc metalloprotease gene. Infect. Immun. *60*, 916-921.

Reinscheid, D.J., Gottschalk, B., Schubert, A., Eikmanns, B.J., and Chhatwal, G.S. (2001). Identification and molecular analysis of PcsB, a protein required for cell wall separation of group B *streptococcus*. J. Bacteriol. *183*, 1175-1183.

Rocourt, J., Alonso, J.M., and Seeliger, H.P. (1983). [Comparative virulence of the 5 genomic groups of *Listeria monocytogenes* (sensu lato)]. Ann. Microbiol. (Paris) *134A*, 359-364.

Rocourt, J., and Bille, J. (1997). Foodborne listeriosis. World Health Stat. Q. *50*, 67-73.

Rocourt, J., Jacquet, C., and Reilly, A. (2000). Epidemiology of human listeriosis and seafoods. Int. J. Food Microbiol. *62*, 197-209.

Rocourt, J., Schrettenbrunner, A., and Seeliger, H.P. (1983). [Biochemical differentiation of the "*Listeria monocytogenes*" (sensu lato) genomic groups]. Ann. Microbiol. (Paris) *134A*, 65-71.

Rossjohn, J., Feil, S.C., McKinstry, W.J., Tweten, R.K., and Parker, M.W. (1997). Structure of a cholesterol-binding, thiol-activated cytolysin and a model of its membrane form. Cell *89*,

685-692.

Rowan, N.J., Candlish, A.A., Bubert, A., Anderson, J.G., Kramer, K., and McLauchlin, J. (2000). Virulent rough filaments of *Listeria monocytogenes* from clinical and food samples secreting wild-type levels of cell-free p60 protein. J. Clin. Microbiol. *38*, 2643-2648.

Rupp, M.E., Fey, P.D., Heilmann, C., and Gotz, F. (2001). Characterization of the importance of *Staphylococcus epidermidis* autolysin and polysaccharide intercellular adhesin in the pathogenesis of intravascular catheter-associated infection in a rat model. J. Infect. Dis. *183*, 1038-1042.

Rupp, M.E., Ulphani, J.S., Fey, P.D., Bartscht, K., and Mack, D. (1999). Characterization of the importance of polysaccharide intercellular adhesin/hemagglutinin of *Staphylococcus epidermidis* in the pathogenesis of biomaterial-based infection in a mouse foreign body infection model. Infect. Immun. *67*, 2627-2632.

Rusch, S.L., and Kendall, D.A. (2007). Interactions that drive Sec-dependent bacterial protein transport. Biochemistry *46*, 9665-9673.

Sambrook, J., and Russel, D. W. (2000). Molecular cloning: a laboratory manual (Cold Spring Harbor, New York: Cold Spring Harbor Laboratory Press).

Schaferkordt, S., and Chakraborty, T. (1995). Vector plasmid for insertional mutagenesis and directional cloning in *Listeria* spp. Biotechniques *19*, 720-722, 724-725.

Schaferkordt, S., Domann, E., and Chakraborty, T. (1998). Molecular approaches for the study of *Listeria*. In Methods in Microbiology: Bacterial Pathogenesis, P. Williams, J. Ketley, and G. Salmond, eds. (San Diego, California: Acadamic Press), pp. 424-428.

Schlech, W.F. 3rd (1993). An animal model of foodborne *Listeria monocytogenes* virulence: effect of alterations in local and systemic immunity on invasive infection. Clin. Invest. Med. *16*, 219-225.

Schleifer, K.H., and Kandler, O. (1972). Peptidoglycan types of bacterial cell walls and their taxonomic implications. Bacteriol. Rev. *36*, 407-477.

Schluter, D., Chahoud, S., Lassmann, H., Schumann, A., Hof, H., and Deckert-Schluter, M. (1996). Intracerebral targets and immunomodulation of murine *Listeria monocytogenes* meningoencephalitis. J. Neuropathol. Exp. Neurol. *55*, 14-24.

Schmid, M.W., Ng, E.Y., Lampidis, R., Emmerth, M., Walcher, M., Kreft, J., Goebel, W., Wagner, M., and Schleifer, K.H. (2005). Evolutionary history of the genus *Listeria* and its virulence genes. Syst. Appl. Microbiol. *28*, 1-18.

Schubert, K., Bichlmaier, A.M., Mager, E., Wolff, K., Ruhland, G., and Fiedler, F. (2000). P45, an extracellular 45 kDa protein of *Listeria monocytogenes* with similarity to protein p60 and exhibiting peptidoglycan lytic activity. Arch. Microbiol. *173*, 21-28.

Schubert, W.D., Gobel, G., Diepholz, M., Darji, A., Kloer, D., Hain, T., Chakraborty, T., Wehland, J., Domann, E., and Heinz, D.W. (2001). Internalins from the human pathogen *Listeria monocytogenes* combine three distinct folds into a contiguous internalin domain. J. Mol. Biol. *312*, 783-794.

Schubert, W.D., Urbanke, C., Ziehm, T., Beier, V., Machner, M.P., Domann, E., Wehland, J., Chakraborty, T., and Heinz, D.W. (2002). Structure of internalin, a major invasion protein of *Listeria monocytogenes*, in complex with its human receptor E-cadherin. Cell *111*, 825-836.

Scortti, M., Monzo, H.J., Lacharme-Lora, L., Lewis, D.A., and Vazquez-Boland, J.A. (2007). The PrfA virulence regulon. Microbes Infect. *9*, 1196-1207.

Scott, J.R., and Barnett, T.C. (2006). Surface proteins of gram-positive bacteria and how they get there. Annu. Rev. Microbiol. *60*, 397-423.

Seveau, S., Pizarro-Cerda, J., and Cossart, P. (2007). Molecular mechanisms exploited by *Listeria monocytogenes* during host cell invasion. Microbes Infect. *9*, 1167-1175.

Sheehan, B., Klarsfeld, A., Msadek, T., and Cossart, P. (1995). Differential activation of virulence gene expression by PrfA, the *Listeria monocytogenes* virulence regulator. J. Bacteriol. *177*, 6469-6476.

Sheehan, B., Kocks, C., Dramsi, S., Gouin, E., Klarsfeld, A.D., Mengaud, J., and Cossart, P. (1994). Molecular and genetic determinants of the *Listeria monocytogenes* infectious process. Curr. Top Microbiol. Immunol. *192*, 187-216.

Shen, A., and Higgins, D.E. (2006). The MogR transcriptional repressor regulates nonhierarchal expression of flagellar motility genes and virulence in *Listeria monocytogenes*. PLoS Pathog. *2*, e30.

Shen, Y., Naujokas, M., Park, M., and Ireton, K. (2000). InIB-dependent internalization of *Listeria* is mediated by the Met receptor tyrosine kinase. Cell *103*, 501-510.

Shockman, G.D., and Barrett, J.F. (1983). Structure, function, and assembly of cell walls of gram-positive bacteria. Annu. Rev. Microbiol. *37*, 501-527.

Shockman, G.D., Daneo-Moore, L., Kariyama, R., and Massidda, O. (1996). Bacterial walls, peptidoglycan hydrolases, autolysins, and autolysis. Microb. Drug Resist. *2*, 95-98.

Shockman, G.D., and Holtje, J.-V. (1994). Microbial peptidoglycan (murein) hydrolases. In

Bacterial cell wall, J.-M. Ghuysen, and R. Hakenbeck, eds. (Amsterdam: Elsevier), pp. 160-166.

Siddique, I.H. (1969). Cytotoxic activity of hemolysin from *Listeria monocytogenes* onL-M strain of mouse cells. Can. J. Microbiol. *15*, 955-957.

Simonen, M., and Palva, I. (1993). Protein secretion in *Bacillus* species. Microbiol. Rev. *57*, 109-137.

Skalka, B., Smola, J., and Elischerova, K. (1982). Routine test for *in vitro* differentiation of pathogenic and apathogenic *Listeria monocytogenes* strains. J. Clin. Microbiol. *15*, 503-507.

Slaghuis, J., Goetz, M., Engelbrecht, F., and Goebel, W. (2004). Inefficient replication of *Listeria innocua* in the cytosol of mammalian cells. J. Infect. Dis. *189*, 393-401.

Smith, G.A., Marquis, H., Jones, S., Johnston, N.C., Portnoy, D.A., and Goldfine, H. (1995). The two distinct phospholipases C of *Listeria monocytogenes* have overlapping roles in escape from a vacuole and cell-to-cell spread. Infect. Immun. *63*, 4231-4237.

Smith, G.A., Theriot, J.A., and Portnoy, D.A. (1996). The tandem repeat domain in the *Listeria monocytogenes* ActA protein controls the rate of actin-based motility, the percentage of moving bacteria, and the localization of vasodilator-stimulated phosphoprotein and profilin. J. Cell Biol. *135*, 647-660.

Smith, T.J., Blackman, S.A., and Foster, S.J. (2000). Autolysins of *Bacillus subtilis*: multiple enzymes with multiple functions. Microbiology *146 (Pt 2)*, 249-262.

Snapir, Y.M., Vaisbein, E., and Nassar, F. (2006). Low virulence but potentially fatal outcome-*Listeria ivanovii*. Eur. J. Intern. Med. *17*, 286-287.

Stathopoulos, C., Hendrixson, D.R., Thanassi, D.G., Hultgren, S.J., St Geme, J.W. 3rd, and Curtiss, R. 3rd (2000). Secretion of virulence determinants by the general secretory pathway in gram-negative pathogens: an evolving story. Microbes Infect. *2*, 1061-1072.

Steen, A., Buist, G., Leenhouts, K.J., El Khattabi, M., Grijpstra, F., Zomer, A.L., Venema, G., Kuipers, O.P., and Kok, J. (2003). Cell wall attachment of a widely distributed peptidoglycan binding domain is hindered by cell wall constituents. J. Biol. Chem. *278*, 23874-23881.

Suarez, M., Gonzalez-Zorn, B., Vega, Y., Chico-Calero, I., and Vazquez-Boland, J.A. (2001). A role for ActA in epithelial cell invasion by *Listeria monocytogenes*. Cell Microbiol. *3*, 853-864.

Sun, A.N., Camilli, A., and Portnoy, D.A. (1990). Isolation of *Listeria monocytogenes* small-plaque mutants defective for intracellular growth and cell-to-cell spread. Infect.

Immun. *58*, 3770-3778.

Sutcliffe, I.C., and Harrington, D.J. (2002). Pattern searches for the identification of putative lipoprotein genes in Gram-positive bacterial genomes. Microbiology *148*, 2065-2077.

Takahashi, J., Komatsuzawa, H., Yamada, S., Nishida, T., Labischinski, H., Fujiwara, T., Ohara, M., Yamagishi, J., and Sugai, M. (2002). Molecular characterization of an *atl* null mutant of *Staphylococcus aureus*. Microbiol. Immunol. *46*, 601-612.

Tang, P., Rosenshine, I., and Finlay, B.B. (1994). *Listeria monocytogenes*, an invasive bacterium, stimulates MAP kinase upon attachment to epithelial cells. Mol. Biol. Cell *5*, 455-464.

Temm-Grove, C.J., Jockusch, B.M., Rohde, M., Niebuhr, K., Chakraborty, T., and Wehland, J. (1994). Exploitation of microfilament proteins by *Listeria monocytogenes*: microvillus-like composition of the comet tails and vectorial spreading in polarized epithelial sheets. J. Cell Sci. *107 (Pt 10)*, 2951-2960.

Tilley, S.J., Orlova, E.V., Gilbert, R.J., Andrew, P.W., and Saibil, H.R. (2005). Structural basis of pore formation by the bacterial toxin pneumolysin. Cell *121*, 247-256.

Tilney, L.G., and Portnoy, D.A. (1989). Actin filaments and the growth, movement, and spread of the intracellular bacterial parasite, *Listeria monocytogenes*. J. Cell Biol. *109*, 1597-1608.

Tilney, L.G., and Tilney, M.S. (1993). The wily ways of a parasite: induction of actin assembly by *Listeria*. Trends Microbiol. *1*, 25-31.

Tokuda, H., and Matsuyama, S. (2004). Sorting of lipoproteins to the outer membrane in *E. coli*. Biochim. Biophys. Acta *1694*, IN1-9.

Tomasz, A. (1984). Building and breaking of bonds in the cell wall of bacteria - the role for autolysins. In Microbial cell wall synthesis and autolysis, C. Nombela, ed. (Amsterdam, The Netherlands: Elsevier Science), pp. 3-12.

Tuomanen, E. (1996). Entry of pathogens into the central nervous system. FEMS Microbiol. Rev. *18*, 289-299.

Tuomanen, E.I. (2000). Pathogenesis of pneumococcal inflammation: otitis media. Vaccine *19 Suppl 1*, S38-40.

Tuteja, R. (2005). Type I signal peptidase: an overview. Arch. Biochem. Biophys. *441*, 107-111.

Valisena, S., Varaldo, P.E., and Satta, G. (1991). Staphylococcal endo-beta-N-acetylglucosaminidase inhibits response of human lymphocytes to mitogens and interferes with production of antibodies in mice. J. Clin. Invest. *87*, 1969-1976.

van Roosmalen, M.L., Geukens, N., Jongbloed, J.D., Tjalsma, H., Dubois, J.Y., Bron, S., van Dijl, J.M., and Anne, J. (2004). Type I signal peptidases of Gram-positive bacteria. Biochim. Biophys. Acta *1694*, 279-297.

Vandegraaff, R., Borland, N.A., and Browning, J.W. (1981). An outbreak of listerial meningo-encephalitis in sheep. Aust. Vet. J. *57*, 94-96.

Vasilescu, J., Smith, J.C., Ethier, M., and Figeys, D. (2005). Proteomic analysis of ubiquitinated proteins from human MCF-7 breast cancer cells by immunoaffinity purification and mass spectrometry. J. Proteome Res. *4*, 2192-2200.

Vatanyoopaisarn, S., Nazli, A., Dodd, C.E., Rees, C.E., and Waites, W.M. (2000). Effect of flagella on initial attachment of *Listeria monocytogenes* to stainless steel. Appl. Environ. Microbiol. *66*, 860-863.

Vazquez-Boland, J.A., Kocks, C., Dramsi, S., Ohayon, H., Geoffroy, C., Mengaud, J., and Cossart, P. (1992). Nucleotide sequence of the lecithinase operon of *Listeria monocytogenes* and possible role of lecithinase in cell-to-cell spread. Infect. Immun. *60*, 219-230.

Vazquez-Boland, J.A., Kuhn, M., Berche, P., Chakraborty, T., Dominguez-Bernal, G., Goebel, W., Gonzalez-Zorn, B., Wehland, J., and Kreft, J. (2001). *Listeria* pathogenesis and molecular virulence determinants. Clin. Microbiol. Rev. *14*, 584-640.

Vega, Y., Dickneite, C., Ripio, M.T., Bockmann, R., Gonzalez-Zorn, B., Novella, S., Dominguez-Bernal, G., Goebel, W., and Vazquez-Boland, J.A. (1998). Functional similarities between the *Listeria monocytogenes* virulence regulator PrfA and cyclic AMP receptor protein: the PrfA* (Gly145Ser) mutation increases binding affinity for target DNA. J. Bacteriol. *180*, 6655-6660.

Vega, Y., Rauch, M., Banfield, M.J., Ermolaeva, S., Scortti, M., Goebel, W., and Vazquez-Boland, J.A. (2004). New *Listeria monocytogenes* prfA* mutants, transcriptional properties of PrfA* proteins and structure-function of the virulence regulator PrfA. Mol. Microbiol. *52*, 1553-1565.

Velge, P., Bottreau, E., Kaeffer, B., Yurdusev, N., Pardon, P., and Van Langendonck, N. (1994). Protein tyrosine kinase inhibitors block the entries of *Listeria monocytogenes* and *Listeria ivanovii* into epithelial cells. Microb. Pathog. *17*, 37-50.

Vines, A., and Swaminathan, B. (1998). Identification and characterization of nucleotide sequence differences in three virulence-associated genes of *Listeria monocytogenes* strains

representing clinically important serotypes. Curr. Microbiol. *36*, 309-318.

Wampler, J.L., Kim, K.P., Jaradat, Z., and Bhunia, A.K. (2004). Heat shock protein 60 acts as a receptor for the *Listeria* adhesion protein in Caco-2 cells. Infect. Immun. *72*, 931-936.

Wang, L., and Lin, M. (2007). Identification of IspC, an 86-kilodalton protein target of humoral immune response to infection with *Listeria monocytogenes* serotype 4b, as a novel surface autolysin. J. Bacteriol. *189*, 2046-2054.

Wang, L., Walrond, L., Cyr, T.D., and Lin, M. (2007). A novel surface autolysin of *Listeria monocytogenes* serotype 4b, IspC, contains a 23-residue N-terminal signal peptide being processed in *E. coli*. Biochem. Biophys. Res. Commun. *354*, 403-408.

Watson, B.B., and Lavizzo, J.C. (1973). Extracellular antigens from *Listeria monocytogenes*. II. Cytotoxicity of hemolytic and lipolytic antigens of *Listeria* for cultured mouse macrophages. Infect. Immun. *7*, 753-758.

Welch, M.D., Rosenblatt, J., Skoble, J., Portnoy, D.A., and Mitchison, T.J. (1998). Interaction of human Arp2/3 complex and the *Listeria monocytogenes* ActA protein in actin filament nucleation. Science *281*, 105-108.

Williams, D., Irvin, E.A., Chmielewski, R.A., Frank, J.F., and Smith, M.A. (2007). Dose-response of *Listeria monocytogenes* after oral exposure in pregnant guinea pigs. J. Food. Prot. *70*, 1122-1128.

Wolfe, P.B., Silver, P., and Wickner, W. (1982). The isolation of homogeneous leader peptidase from a strain of *Escherichia coli* which overproduces the enzyme. J. Biol. Chem. *257*, 7898-7902.

Wuenscher, M.D., Kohler, S., Bubert, A., Gerike, U., and Goebel, W. (1993). The *iap* gene of *Listeria monocytogenes* is essential for cell viability, and its gene product, p60, has bacteriolytic activity. J. Bacteriol. *175*, 3491-3501.

Yamabhai, M., Emrat, S., Sukasem, S., Pesatcha, P., Jaruseranee, N., and Buranabanyat, B. (2008). Secretion of recombinant *Bacillus* hydrolytic enzymes using *Escherichia coli* expression systems. J. Biotechnol. *133*, 50-57.

Yamada, S., Sugai, M., Komatsuzawa, H., Nakashima, S., Oshida, T., Matsumoto, A., and Suginaka, H. (1996). An autolysin ring associated with cell separation of *Staphylococcus aureus*. J. Bacteriol. *178*, 1565-1571.

Yu, W.L., Dan, H., and Lin, M. (2007). Novel protein targets of humoral immune response to *Listeria monocytogenes* infection in rabbits. J. Med. Microbiol. *56*, 888-895.

Zachar, Z., and Savage, D.C. (1979). Microbial interference and colonization of the murine gastrointestinal tract by *Listeria monocytogenes*. Infect. Immun. *23*, 168-174.

APPENDIX 1

Nucleotide and Deduced Amino Acid Sequences of the *ispC* Gene from *L. monocytogenes* serotype 4b

```
   1                ATATGATGAGTTTGTAAAATGGTTTAACAAACAACCAAATGATT
  45 ATAAGAAAAAATATCAAAAAGAGCATAAGGAAAATCAAAAAGCTCCTCAGAAAAAAATCT
 105 ATCCTAATCCTAATGCCAATAAATACAGGCTAACTCTTTTTGATAAAATATTTTTAACTG
 165 TGCTAATTGCATTAACGATACTATTTGGAACACTAGTGGCGACAGGGAAATCTTTTAAAG
 225 GCTTAATTAGTGAAGAATCCACAACACAAATTGAAAAAGTAGTACATGTTGATAATTACG
 285 ATTTAAAATTGAATTAACTGTAAAAAACTTCCAAAAGTTATCTATCTTTTGGAAGTTTTT
 345 ATTTAAAATTGAAGAAGTAAAGCATTTTATCATAAAATGAAATAAAAATTTTGTCTAAAT
 405 GTTTAACAAATTTGTTGTTATAATACCATTTATTTTTTTTGTAATAAATTTGTAACTTAC
 465 GGAGGCATAAAGTTTGGTAAAATTAGGACAATAAACAAATTAAGGAGTGGTTGGAGAATA
 525 atgataaataaaaagtggatgaaaattgtaatgattccgatgctagttgttccaatgtac
   1  M  I  N  K  K  W  M  K  I  V  M  I  P  M  L  V  V  P  M  Y
 585 ggtttgacaactgttggcggacaattacaagattcattaactggagaaaattccttttgtt
  21  G  L  T  T  V  G  G  Q  L  Q  D  S  L  T  G  E  N  S  F  V
 645 aaagaggttgaagctgcaacgacagcatcgcaacaagcatttatcgacaaaatagcacct
  41  K  E  V  E  A  A  T  T  A  S  Q  Q  A  F  I  D  K  I  A  P
 705 gctgcccaggcatctcaagaaaaatatcatctgttatctagtataactttagctcaagca
  61  A  A  Q  A  S  Q  E  K  Y  H  L  L  S  S  I  T  L  A  Q  A
 765 attctagaatctggttggggaaaaagtggacttgctacacaaggatataatttatttggt
  81  I  L  E  S  G  W  G  K  S  G  L  A  T  Q  G  Y  N  L  F  G
 825 ataaaagggaaatataatggacaatcagttatcatgacaacttctgaatatgtgaacggt
 101  I  K  G  K  Y  N  G  Q  S  V  I  M  T  T  S  E  Y  V  N  G
 885 gagtggattaaaattgatgctgaattccgcaaataccctagctggaatgaatctgtcact
 121  E  W  I  K  I  D  A  E  F  R  K  Y  P  S  W  N  E  S  V  T
 945 gaccatactcttttattagtgaacggaacttcttggaataaagacttatataagaaagtt
 141  D  H  T  L  L  L  V  N  G  T  S  W  N  K  D  L  Y  K  K  V
1005 gtcgacgcaacggattataaagtaactgcaatggagcctcaaaaagctggatatgcaacc
 161  V  D  A  T  D  Y  K  V  T  A  M  E  P  Q  K  A  G  Y  A  T
1065 tctcctacatatggtgctagcttaattcaagtaattgagaattatgatttagccaaatat
 181  S  P  T  Y  G  A  S  L  I  Q  V  I  E  N  Y  D  L  A  K  Y
1125 gatgttttatacgacaaaattcttactcaaaaatccacttccggaaaagcaactgttaca
 201  D  V  L  Y  D  K  I  L  T  Q  K  S  T  S  G  K  A  T  V  T
1185 agtccgactggaaatggtgtatggactttaccgtataaagtaaaaggagtgcaatctgtt
 221  S  P  T  G  N  G  V  W  T  L  P  Y  K  V  K  G  V  Q  S  V
1245 agtccagctagcacatacgctaacaaggatatcgatttagtatctgttgctacaacaaag
 241  S  P  A  S  T  Y  A  N  K  D  I  D  L  V  S  V  A  T  T  K
1305 agaggtacgtactatcaatttaaatataatggtaaagtagttggttgggtagatggcaaa
 261  R  G  T  Y  Y  Q  F  K  Y  N  G  K  V  V  G  W  V  D  G  K
1365 gcattaactatttatgatagtgtcaattatgataaagtaaatgtcggacgtgctaaaatt
 281  A  L  T  I  Y  D  S  V  N  Y  D  K  V  N  V  G  R  A  K  I
```

```
1425 actagcccagtaagtaacggtatctggtctaaaccatacaatgtttatggaagagaattt
 301  T  S  P  V  S  N  G  I  W  S  K  P  Y  N  V  Y  G  R  E  F
1485 gttacgaatgcaacaacttacgcacaacaagaaattaaacttttacgcgaagcacaaact
 321  V  T  N  A  T  T  Y  A  Q  Q  E  I  K  L  L  R  E  A  Q  T
1545 gctaaaggtacttattaccaatttagcataaataataaaactattggttggattgataaa
 341  A  K  G  T  Y  Y  Q  F  S  I  N  N  K  T  I  G  W  I  D  K
1605 cgagctctcactatctatccgtatgattccattatttcaagtaaaaatgtgaaccttgac
 361  R  A  L  T  I  Y  P  Y  D  S  I  I  S  S  K  N  V  N  L  D
1665 ggacaaattactaatccaaccggaaatggtatttggactaaagcgtacaaacttgaagga
 381  G  Q  I  T  N  P  T  G  N  G  I  W  T  K  A  Y  K  L  E  G
1725 acaacttctgtggcgcaggctacgaaatatgcaaataaagatgtgaaaatcagccaacaa
 401  T  T  S  V  A  Q  A  T  K  Y  A  N  K  D  V  K  I  S  Q  Q
1785 atcgaaactcaacatggtacttattacaatatcagtatcgatgggaaagcaattggttgg
 421  I  E  T  Q  H  G  T  Y  Y  N  I  S  I  D  G  K  A  I  G  W
1845 ttagatagaaacgctattacactgtatgatcaagaggaatacaataaaacagttgctatt
 441  L  D  R  N  A  I  T  L  Y  D  Q  E  E  Y  N  K  T  V  A  I
1905 gacgcagtagtaaaaaatgtgaagggtaatgctgtatggacagaaccttaccgtacagtt
 461  D  A  V  V  K  N  V  K  G  N  A  V  W  T  E  P  Y  R  T  V
1965 ggtacaaaattaatcggaccagcggaaacttacttgaataaagaagtggaagtcgtccgt
 481  G  T  K  L  I  G  P  A  E  T  Y  L  N  K  E  V  E  V  V  R
2025 gaagcaaaaacgccaaaaggaacttactaccaatttaaatctggtggcaaagtaatcggc
 501  E  A  K  T  P  K  G  T  Y  Y  Q  F  K  S  G  G  K  V  I  G
2085 tggttagataaaaaagctttcgatgtatatgacaatattaattacaacaaagcggttaat
 521  W  L  D  K  K  A  F  D  V  Y  D  N  I  N  Y  N  K  A  V  N
2145 ttagatactgtagtggaaaatgtgacaggtaatgcagtttggacggctccttataagagt
 541  L  D  T  V  V  E  N  V  T  G  N  A  V  W  T  A  P  Y  K  S
2205 aaaggtgttaaacttgttacttcagcagcaacctataaaggcaaggcaacaaaaataact
 561  K  G  V  K  L  V  T  S  A  A  T  Y  K  G  K  A  T  K  I  T
2265 cgtgaagcgcaaacaagtagaggaacatattacgagtttagtgttgatggtaaagtcatt
      R  E  A  Q  T  S  R  G  T  Y  Y  E  F  S  V  D  G  K  V  I
2325 ggctggttagataaaaaagctttcgatgtatatgacaatattaattacaacaaagcggtt
      G  W  L  D  K  K  A  F  D  V  Y  D  N  I  N  Y  N  K  A  V
2385 aacttagatgctgtagtggaaaatgtgacaggcaacgcagtttggactgctccatataag
       N  L  D  A  V  V  E  N  V  T  G  N  A  V  W  T  A  P  Y  K
2445 agtaagggtgttaaattagttacttcagcagccacatataaagataaagcaactaaaata
      S  K  G  V  K  L  V  T  S  A  A  T  Y  K  D  K  A  T  K  I
2505 actcgagaagcgcaaacaagtagaggaacttactacgaatttagcgtaaacggcaaagta
      T  R  E  A  Q  T  S  R  G  T  Y  Y  E  F  S  V  N  G  K  V
2565 atcggttggttagataaaaaagcttttgatgtatatgattctattgagtacaataaagcg
      I  G  W  L  D  K  K  A  F  D  V  Y  D  S  I  E  Y  N  K  A
2625 attaatatgactggattacttagcaacgcgccaggtaatggcatttggacagagccgtat
```

```
     I  N  M  T  G  L  L  S  N  A  P  G  N  G  I  W  T  E  P  Y
2685 agagttattggcacaaaaaatgtaggacaagcaactgcttatgctaacaagacagtacag
     R  V  I  G  T  K  N  V  G  Q  A  T  A  Y  A  N  K  T  V  Q
2745 ttgatacgcgaggctaagactacacgtgcaacttactatcaaatgagtgtaaatggtaaa
     L  I  R  E  A  K  T  T  R  A  T  Y  Y  Q  M  S  V  N  G  K
2805 atagttggttgggtagataaacgagctttacaaacgttaaatagACTAAAAATAATCAT
     I  V  G  W  V  D  K  R  A  F  T  N  V  K  *
2865 ATAAAAACAGAGTGAGATTTCTCACTCTGTTTTTATATGATTATAGATTAAGATTTAGTG
2925 ATGTAAATAAGTTCCTTCAAGAAGTCTTTATAATAAGGGGATTCGAAGTGAGAAAAGGAA
2985 TGCCCAAATGGATAGTTGAAATCACCTATATAGCCTTTTTTCGAAAAGTCGATTACTTTT
3045 GCTTCAGGCAATTTAGATAAGAAATAATTATTTAAACGTTCCCAGAAGTAATTATTCTTT
3105 TCGATGGCCATTTTGTTTTTGTAAGTTGCGACTTCTCCATCTTCATCATAATAAGACGTT
3165 GTAAATCCACCTAGGTTTAAAATAACCCGATCAGTAGGAATTATTTCTGTAAGTTTTTCG
3225 ATAAATTGATCAGCATAGCCTTTCCACTCATTGAAGTAGGTTTCATTATCAATATGATCT
3285 AAAATTCTCTCGTAAGAAATGTCATTAAGTAATTGGCTTTGTTCTATAACATAAGATAAT
3345 GTAATAGCTGAATTATTATTTAACCAAAT
```

APPENDIX 2

Buffers, Solutions, Culture Media, and Experimental Protocols

50 × TAE Buffer (Tris-Acetate Buffer)

2 M TRIZMA® Base
5.7% (v/v) Acetic acid, glacial
50 mM EDTA (pH 8.0)
Store at room temperature.

10 × DNA Sample or Loading Buffer

0.4% (w/v) Bromophenol blue
0.4% (w/v) Xylene cyanol
25% (w/v) Ficoll (type 400)
10 mM EDTA (pH 8.0)
Sterilize with 0.22-μm filter and store at room temperature.

6 × DNA Sample or Loading Buffer

30% (v/v) Glycerol
50 mM EDTA (pH 8.0)
0.25% (w/v) Bromophenol blue
Store at 4 °C.

SOB medium (Sambrook and Russel, 2000)

Per 1 L:
Tryptone: 20 g
Yeast extract: 5 g
NaCl: 0.5 g
Add dH_2O to 950 ml

Shake until the solutes have dissolved. Add 10 ml of 250 mM KCl (This solution is made by dissolving 1.86 g KCl in 100 ml of dH_2O). Adjust the pH of the medium to 7.0 with 5 M NaOH (~0.2 ml). Adjust the volume of the solution to 1 L with dH_2O. Sterilize by autoclaving for 20 min at 15 psi on liquid cycle. Just before use, add 5 ml of a sterile solution of 2 M $MgCl_2$ (This solution is made by dissolving 0.4066 g $MgCl_2 \cdot 6H_2O$ in 100 ml of dH_2O and sterilized by autoclaving for 20 min at 15 psi on liquid cycle.).

SOC medium

SOC medium is identical to SOB medium, except that it contains 20 mM glucose. After the SOB medium has been autoclaved, allow it to cool to 60 °C or less. Add 20 ml of a sterile 1 M solution of glucose (This solution is made by dissolving 18 g glucose in 100 ml of dH_2O. and sterilized by passing it through a 0.22-μm filter).

25 × PBS

Per 1 L:
Sodium phosphate dibasic (Na_2HPO_4): 27.5 g
Sodium phosphate monobasic monohydrate ($NaH_2PO_4 \cdot H_2O$): 7.88 g
NaCl: 212.5 g
Add dH_2O to 1 L
Autoclave for 20 min at 15 psi on liquid cycle.

Acrylamide/Bis Solution (30%T, 2.67%C)

Acrylamide: 146 g
Bis N, N'-Methylene-bis-acrylamide: 4 g

Dissolve first with ~200 ml of dH_2O and then adjust volume to 500 ml, sterilize using a 0.22-μm filter and store at 4 °C.

Note: Make solution in fume hood and wear a chemical mask!

10% (w/v) APS

1 g Ammonium Persulfate is dissolved in 10 ml of dH_2O, aliquot and store at -20 °C.

4% Stacking Gel

Per 5 ml:
Acrylamide/bis (30% T, 2.67% C): 0.65 ml
0.5 M Tris-HCl, pH 6.8 (4 °C): 1.25 ml
dH_2O: 3.05 ml
10% (w/v) SDS: 50 µl
10% (w/v) APS (add last): 25 µl
TEMED (add last): 5 µl

10% Separating Gel

Per 10 ml:
Acrylamide/bis (30% T, 2.67% C): 3.3 ml
1.5 M Tris-HCl, pH 8.8 (4 °C): 2.5 ml
dH_2O: 4.05 ml
10% (w/v) SDS: 100 µl
10% (w/v) APS (add last): 50 µl
TEMED (add last): 5 µl

12% Separating Gel:

Per 10 ml:
Acrylamide/bis (30% T, 2.67% C): 4.0 ml
1.5 M Tris-HCl, pH 8.8: 2.5 ml
dH_2O: 3.35 ml
10% (w/v) SDS: 100 µl
10% (w/v) APS (add last): 50 µl
TEMED (add last): 5 µl

Leave 2.2 cm to the top of short glass for stacking gel; Add slowly 100 µl of n-Butanol or 0.2 ml of dH_2O after loading the separating gel solution.

2 × Protein Sample Buffer

0.1 M Tris-HCl, pH 6.8
40% (v/v) Glycerol
20% (v/v) β-Mercaptoethanol
4% (w/v) SDS
0.02% (w/v) Bromophenol Blue

10 × SDS-PAGE Running Buffer

Per 1 L
TRIZMA® Base: 30 g
Glycine: 144 g
SDS: 6 g
Add dH_2O to 1 L and store at room temperature.

Coomassie Blue Stain

0.5% (w/v) Coomassie Brilliant Blue
40% (v/v) methanol
10% (v/v) acetic acid
Store at room temperature.

Coomassie Blue Destain Solution

40% (v/v) methanol
10% (v/v) acetic acid

50% (v/v) dH_2O
Store at room temperature.

Protein Transfer Buffer

Per 1 L:
TRIZMA® Base: 5.82 g
Glycine: 2.93 g
Add dH_2O to 1 L and store at 4 °C.

1 × PBST·T

Per 10 L:
25 × PBS: 400 ml
Tween 20: 5 ml
Triton X-100: 20 ml
Add dH_2O to 10 L and store at room temperature.

3% (w/v) BSA+1 × PBST·T

3 g BSA (Bovine Serum Albumin Fraction V, heat shock) is dissolved in 100 ml of 1 × PBST·T, aliquot and store at -20 °C.

0.1% (w/v) Ponceau S

0.1 g Ponceau S is dissolved in 100 ml of 5% (v/v) Acetic Acid and store at room temperature in brown bottle.

LBMOPS Broth

Per 500ml:
Tryptone: 5 g
Yeast Extract: 2.5 g
NaCl: 5 g
MOPS: 5.25 g

Make up to 500 ml with dH_2O, adjust pH to 7.0, and autoclave at 121 ° C for 30 min.

0.5 M Sucrose LBMOPS

Per 500ml:
Tryptone: 5 g
Yeast Extract: 2.5 g
NaCl: 5 g
MOPS: 5.25 g
Sucrose: 85.575 g

Make up to 500 ml with dH_2O, adjust pH to 7.0, and autoclave at 110 °C for 30 min.

Sucrose Electroporation Buffer

1 mM Hepes
0.5 M sucrose

Adjust pH to 7.0 and autoclave at 110 °C for 30 min.

Preparation of $CaCl_2$-Competent *E. coli* DH5α Cells

1. Streak out *E. coli* DH5α from -80 °C stock on LB agar plate and grow at 37 °C overnight. (DO NOT ADD antibiotic, since these cells do not have a plasmid in them.).
2. Pick one isolated colony and grow a 5-ml culture in LB broth without antibiotics at 37 °C for 13.5 h with shaking (200 rpm).
3. Dilute overnight culture 1:100 in LB broth.
4. Grow culture at 37 °C, 200 rpm for 2.7 h to reach an OD_{600} of 0.39.

5. Chill culture on ice for 10 min.
6. Spin down cells from 225 ml of culture at 2700 × g at 4 °C for 10 min.
7. Resuspend the pellet in 135 ml of ice cold 80 mM $MgCl_2$-20 mM $CaCl_2$ solution and rotate on ice for 20 min.
8. Pellet at 2700 × g at 4 °C for 10 min.
9. Resuspend cells in 10 ml of 0.1 M $CaCl_2$ containing 10% (v/v) glycerol and rotate on ice.
10. Dispense in 200-µl aliquots of competent cells into chilled 1.5-ml microcentrifuge tube.
11. Place on dry ice.
12. Transfer cells to -80 °C freezer.
13. Test for transformation efficiency: Use a stock of pUC19 solution (0.01 ng/µl) to determine transformation efficiency.

Purification of PCR Products or Digested DNAs

The PCR amplified products or digested DNAs are purified using Wizard™ PCR Preps DNA Purification System (Promega) as follows:

1. PCR amplified products or digested DNAs containing 1 × DNA loading buffer were incubated at 65 °C for 5 min.
2. Samples were loaded at negative (black) cathode. Appropriate DNA Ladder is used as a reference for estimation of the DNA size.
3. Electrophoresis at 70 vol. on ice in 1% (w/v) low-melting agarose gel (0.25 g in 25 ml of 1 × TAE buffer) containing 0.05% (w/v) ethidium bromide (5 µl of 10 mg/ml stock per 100 ml gel) on a Mini-Sub Cell GT System (BioRad) in 1 × TAE buffer. (Optional) Add 10 µl of ethidium bromide (10 mg/ml) into the buffer at the positive (red) anode.
4. Excise the desired DNA band using a clean razor blade or scalpel on a clean glass plate and put into a 1.5-ml microcentrifuge tube.

Note: The band should be visualized with a medium or long wavelength (e. g., ≥300 nm) UV light (Model UVM-57 302 NM Lamp, Mid range UV; UVP, Inc., upland, California) and should be excised quickly to minimize the exposure of the DNA to UV light. Faceshield should be used for protection from ultraviolet radiation.

5. Melt the gel at 70 °C in water bath for 2 min.
6. Prepare one Wizard® Minicolumn: remove and set aside the plunger from a 3-ml syringe. Attach the barrel to each Minicolumn.
7. Add 1 ml of resin into the melted agarose slice and mix thoroughly for 20 sec but do not vortex.
8. Pipet the resin/DNA mix into the barrel. Insert the plunger slowly and gently push the slurry into the Minicolumn with the plunger.
9. Detach the syringe from the Minicolumn, and remove the plunger. Reattach the barrel to the minicolumn.
10. Wash with 2 ml of 80% (v/v) isopropanol (either 1-Propanol or 2-propanol, reagent grade).
11. Remove the syringe and transfer the Minicolumn to a new 1.5-ml microcentrifuge tube.
12. Centrifuge at 14,100 × g for 2 min to dry the membrane.
13. Transfer the Minicolumn to a new tube.
14. Elute with 50 µl of dH_2O or elution buffer provided at 14,100 × g for 1 min (DNA

will remain intact on the Minicolumn for up to 30 min).

15. Store at -20 °C.

DNA Dephosphorylation

DNA: ~8 pmol

Alkaline phosphatase Calf Intestinal (CIP) (10 U/μl): 1 μl

37 °C overnight and then 75 °C for 10 min for enzyme inactivation, and purify using Wizard™ PCR Preps DNA Purification System.

DNA Phosphorylation

10 × T4 Polynucleotide Kinase Buffer: 2.5 μl

DNA: 20 μl

T4 Polynucleotide Kinase (10 U/μl): 1 μl

10 mM ATP: 2.5 μl

37 °C for 30 min, 65 °C for 20 min for enzyme inactivation, and purify using Wizard™ PCR Preps DNA Purification System.

Transformation of Plasmid into $CaCl_2$-Competent *E. coli* Cells

1. Thaw and keep $CaCl_2$-competent *E. coli* cells (30-50 μl) on ice.
2. Add plasmid (0.5 μl of 20-fold dilution) or ligation mixture (8 μl). Move the pipette through the cells while dispensing. Gently tap the tube to mix.
3. Incubate cells on ice 30 min.
4. Heat shock cells for 45 sec in a 42 °C water bath.
5. Place on ice for 2 min.
6. Add 0.2 ml of warm SOC medium.
7. Incubate at 37 °C for 1 h with shaking (225 rpm).
8. Plate on appropriate antibiotic plate.
9. Incubate the plate at 37 °C overnight.

Ligation of Insert DNA into Plasmid

Insert DNA: x μl

Linear vector DNA: y μl (100 ng)

5 × Ligation buffer: 2 μl

T4 DNA ligase (400 U/μl): 1 μl

Total volume: 10 μl

Insert DNA and plasmid were mixed at a 3:1 molar ratio to reach a volume of 7 μl. Incubate ligation mixture at room temperature for ~4 h or 16 °C overnight. Use the mixture (8 μl) for transformation.

TA Cloning

Purified PCR product: 6 μl

10 × Ligation buffer: 1 μl

pCR2.1 vector (25 ng/μl): 2 μl

T4 DNA ligase (4 U/μl): 1 μl

Reaction mix: 10 μl

Incubate at 16 °C overnight.

NdeI-XhoI Double Digestion of pET30a

Autoclaved dH_2O: 2 μl

10 × NEBuffer 4: 6 μl

Plasmid DNA: 40 μl (4~5 μg)

1 mg/ml BSA (10 ×): 6 μl

NdeI (20 U/μl): 3 μl

XhoI (20 U/µl): 3 µl
Reaction mixture: 60 µl

37 °C overnight.

Fill-In NdeI/XhoI Double Digested-pET30a

Add the components to a final concentration of

50 ng/µl NdeI/XhoI digested-pET30a
1 × EcoPol Buffer
33 µM dNTPs
Klenow: U/1 µg DNA

Fill-in was carried out at 25 °C for 15 min followed by 75 °C for 30 min for enzyme inactivation. The filled-in plasmids were stored at -20 °C for blunt end cloning. Use this reaction buffer to dilute klenow.

PCR

1. **Platinum® *Pfx* DNA Polymerase (Invitrogen):**

Components	Vol. (µl)
dH_2O	68
10 × buffer	20
10 mM dNTPs	3
50 mM $MgSO_4$	2
Primer 1 (25 µM)	2
Primer 2 (25 µM)	2
Genomic DNA (40 ng/µl)	2
Platinum® *Pfx* DNA Polymerase (2.5 U/µl)	1
Total vol.	100

Program:

(1) 94 °C 2 min
(2) 94 °C 30 sec
(3) 55 °C 45 sec
(4) 72 °C 1 kb/min
(5) Go to step (2), repeat 34 cycles
(6) 72 °C 10 min
(7) 4 °C Hold

Store at -20 °C.

2. **TA colony PCR (pCR2.1 derivatives)**

Components	Vol. (µl)
dH_2O	79
10 × PCR-mg buffer	10
10 mM dNTPs	2
50 mM MgCl2	6
M13 Reverse Primer (25 µM)	1
T7 Promoter Primer (25 µM)	1
Colony template	0

Taq DNA polymerase (5 U/μl)	1
Total vol.	100

Program as above.

3. **pET30a colony PCR (pET30a derivatives)**

Components	Vol. (μl)
dH_2O	79
10 × PCR-mg buffer	10
10 mM dNTPs	2
50 mM $MgCl_2$	6
T7 Promoter Primer (25 μM)	1
T7 Terminator Primer (25 μM)	1
Taq DNA polymerase (5 U/μl)	1
Colony template	0
Total vol.	100

Program as above.

4. **QuickChange site-directed mutagenesis mutant strand synthesis reaction**

Components	Vol. (μl)
10 × reaction buffer	5
40 ng/ul pET30a-398/399 (minipreped from *E. coli* DH5α strain)	1
Primer 1 (25 μM)	1
Primer 2 (25 μM)	1
10 mM dNTPs	1.5
dH_2O	39.5
Pfu Turbo DNA polymerase (2.5 U/μl)	1
Total vol.	50

Program:
(1) 95 °C 2 min
(2) 95 °C 30 sec
(3) 55 °C 1 min
(4) 68 °C 8 min
(5) Goto Step 2 Rep 17
(6) 4 °C Hold

The PCR products were subsequently digested with 1 μl of DpnI (20 U/μl) at 37 °C for 1 h to remove the wild type DNA strand. The digested PCR products (5 μl) were used to transform $CaCl_2$-competent DH5α cells (50 μl).

Protein Concentration Measurement

1. Prepare Bovine Albumin Serum Standard (Pierce) at various concentrations

Vol. of Stock Standard (0.1 or 1.0 mg/ml)	**Standard concentration** (μg/ml)

0 µl	0
10 µl of 0.1 mg/ml stock	1
25 µl of 0.1 mg/ml stock	2.5
50 µl of 0.1 mg/ml stock	5.0
75 µl of 0.1 mg/ml stock	7.5
10 µl of 1.0 mg/ml stock	10
12 µl of 1.0 mg/ml stock	12

2. Color development: Add 0.2 ml of stock dye (BioRad, 4 °C) to 0.8 ml of dH_2O to a total volume of 1.0 ml. Standards (above) or sample (5 µl (i.e., 200 × dilution) and 10 µl (i.e., 100 × dilution)) were added to dye solution and mixed by inverting followed by incubation at room temperature for 10 min.
3. Protein concentration was determined using a Bradford Micro-protein assay by determination absorbance at 595 nm (A_{595}nm) with minus BSA solution (0 µg/ml BSA) as blank.

Blue-White Screening

Blue white screening is based on the Lac operon in the vectors (e.g., pCR2.1, pUC118, pAUL-A) containing the Lac Z gene encoding β-galactosidase within an internal Multiple Cloning Site (MCS).

After transformation, bacteria were grown on plates containing appropriate antibiotics, 100 µl of 8 mg/ml IPTG, and 16 µl of 50 mg/ml X-Gal at 37 °C overnight. X-Gal, functions as indicator. IPTG, functions as inducer of the Lac operon. If the DNA of interest was successfully ligated into the vector, the bacterial colony will be white; if not, the colony will be blue. The white colonies were picked for subsequent identification by colony PCR.

Section Transmission Electron Microscopy

1. Fixation: Mid-log phase cultures (1 ml) of bacteria (Δ*ispC* [OD_{620}=0.848] and WT [OD_{620}= 0.822]) were washed 3 × with PBS (1st wash with 1ml of PBS and the 2nd and 3rd washes with 0.5 ml of buffer) and fixed in 0.8 ml of 2.5% (w/v) Glutaraldehyde (GA) in 0.1 M PO4 buffer (pH 7.4) and stored at 4 °C.
2. Embed bacteria in agarose:
   a) 4% (w/v) low melting agarose were hydrated for 15 min before heating;
   b) Melt agarose and cool down to ~40 °C with stirring;
   c) Bacteria were spun down into pellet and resuspended in 4% (w/v) low melting agarose;
   d) Spun down again, cooled the pellet on ice and cut into small blocks (~1 m^3);
3. Wash in 0.1 M PO4 buffer (pH 7.4) (EMCO34) as follows:
   a) 4 × at room temperature for 3 h;
   b) 1 × at 4 °C overnight;
   c) 1 × at room temperature for 15 min;
4. Postfix in 1% (w/v) OsO_4 in 0.1 M PO4 buffer (pH 7.4) at room temperature for 1 h.
5. Rinse in distilled/deionized water (d.d H_2O) 4 × at room temperature for 2 h.
6. Stain with 3% (w/v) uranyl acetate at room temperature for 2 h.
7. Rinse in d.d. H_2O at room temperature for 10 min.
8. Dehydrate in 30% (v/v) ethanol (ETOH) at room temperature for 10 min, in 50% (v/v) for 10 min, in 70% (v/v) at 4 °C overnight, in 85% (v/v) for 10 min, in 95% (v/v) ETOH for 10 min, and 3 × in 100% (v/v) for 1.5 h.
9. Embed 2 × in Propylene Oxide at room temperature for 10 min each, in 3:1 Propylene

Oxide/Epon for 2 h, in 1:1 Propylene Oxide/Epon for 2 h, and in 1:3 Propylene Oxide/Epon overnight.

10. Polymerization at 54 °C oven for the weekend.
11. Stain with 3% (w/v) uranyl acetate for 20 min.
12. Stain in 0.4% (w/v) lead acetate for 10 min.

Preparation of Peptidoglycan of *L. monocytogenes*

1. Overnight cultures of *L. monocytogenes* serotype 4b (WT) and Δ*ispC* mutant were diluted 1:100 in 1 L of BHI broth and incubated at 37 °C to mid-log growth of phase.
2. Collect bacteria by centrifugation at 3500 × g at 4 °C for 10 min.
3. Resuspend cell pellet in 50 ml of 4% (w/v) SDS and boiled for 30 min.
4. Centrifuge at 10,000 × g at room temperature for 20 min.
5. Wash 6 × with water.
6. Pellet was stored at -80 °C overnight.
7. Cells were broken by 3 × passages through a French press at 1500 lb/in^2.
8. Centrifuge to remove unbroken cells at 3000 × g for 5 min.
9. Centrifuge supernatant at 10,000 × g for 20 min.
10. Resuspend the pellet in 13 ml of 100 mM Tris·HCl (pH 7.5), add 0.7 mg α-amylase at 37 °C for 2 h.
11. Add $MgSO_4$ (20 mM), 100 μg DNase I and 500 μg RNaseA, at 37 °C for 2 h.
12. Add $CaCl_2$ (10 mM) and 1mg trypsin, at 37 °C overnight.
13. Add 1% (w/v) SDS and boil for 15 min.
14. Centrifuge at 10,000 × g for 20 min at 20 °C.
15. Wash 2 × in maximal volume of water.
16. Wash 1 × in 20 ml of 8 M LiCl.
17. Wash 3 × in water.
18. Pellet.
19. Resuspend the pellet in 10 ml of 49% hydrofluoric acid.
20. Rock for 48 h at 4 °C to remove teichoic acids.
21. Centrifuge at 10,000 × g for 20 min at 4 °C.
22. Wash 3 × with water.
23. Pellet.
24. Neutralize with 100 mM Tris·HCl (pH 7.5) and washed 2 × with water.
25. Suspend in 10 ml of 1 × NEBuffer 3 and 50 units of alkaline phosphatase, at 37 °C overnight.
26. Boil 5 min to inactivate enzymes.
27. Centrifuge at 10,000 × g for 20 min.
28. Wash 3 × with water.
29. Weigh empty bottle, add 2.5 ml of water, and frozen at -80 °C for at least 2 h.
30. Lyophilize for ~2 d.
31. Weigh and store at -20 °C.

Miniprep Plasmids from *E. coli* Host Strains

The plasmids were prepared from 5 ml of overnight culture of *E. coli* DH5α using QIAprep Spin Miniprep kit (QIAGEN) as per manufacturer's instruction. The plasmids are eluted in dH_2O (30 μl) and stored at -20 °C and the concentration was determined at 100-fold dilution (i.e., 5 μl in 0.5 ml dH_2O) on a GENEQUANT / 80210398 RNA/DNA CALCULATOR (Phoenix Equipment Inc., Rochester, NY).

Extraction of the *L. monocytogenes* Genomic DNA

The total genomic DNA of *L. monocytogenes* was extracted from 40 ml of *L. monocytogenes* culture using a GenomicPrep™Cells and Tissue DNA Isolation Kit (Amersham) with some modifications (Yu et al., 2007). According to the manufacturer's instructions, the cells (40 ml) were centrifuged in microcentrifuge tubes at 14,100 × g for 1 min, washed 3 × with 1 ml of PBS and pelleted at the same speed. The cell pellets were resuspended in 1 ml of PBS and mixed with lysozyme (Sigma), added to a final concentration of 2.5 mg/ml (50 µl of 50 mg/ml lysozyme in 50% (v/v) glycerol (freshly made)). After incubation at 37 °C for 1 h, proteinase K (Sigma) was added to the cell suspension to a final concentration of 2 mg/ml and incubated for another 1 hour. A cell lysis solution (600 µl) was added to 600 µl of the cell suspension, mixed well, and incubated at 80 °C for 15 min. The cell lysate was cooled to the room temperature, mixed with 3 µl of RNase A (100 mg/ml) solution and incubated at 37 °C for 15 min. The RNase A-treated cell lysate was cooled to room temperature and mixed with 200 µl of protein precipitation solution. The cell lysate was centrifuged at 14,100 × g for 5 min to remove the precipitated materials. The supernatant containing the genomic DNA was collected in a new 1.5-ml centrifuge tube and mixed with 600 µl of 100% (v/v) isopropanol by inverting gently 50 times. The DNA was collected by centrifugation at 14,100 × g for 1 min, washed with 600 µl of 70% (v/v) ethanol, and air dried for 15 min. The DNA pellet was dissolved in 100 µl of DNA hydration solution at room temperature overnight and stored at -20°C.

Preparation of Electroporation Competent *L. monocytogenes*

The competent *L. monocytogenes* cells were prepared by Penicillin (PnG) treatment essentially as described (Park and Stewart, 1990). Briefly, one colony of *L. monocytogenes* LI0521 (serotype 4b) was inoculated from TSBA agar plate into 5 ml of LBMOPS broth and aerobically grown at 37 °C overnight. The overnight cultures were diluted 1:10 into LBMOPS containing 0.5 M sucrose and grown until reaching an OD_{600} = 0.2 (~3 h). PnG was added in the culture to a final concentration of 10 µg/ml and the incubation continued for a further 2.5 h (A_{600} = 0.36). Bacteria (44 ml) were harvested by centrifugation (8000 × g, 10 min, 4 °C) and washed a total of three times (i.e. the 1st wash with an equal volume and the last two washes with half vol. of ice-cold PBS) with Sucrose Electroporation Buffer (1 mM Hepes, 0.5 M sucrose, pH 7.0). The final cell pellet was resuspended in the same buffer (250 µl) to reach a final concentration of 1.03 × 10^{11}/ml. The competent cells for electroporation were used within 30 min of their preparation or stored in 15% (v/v) glycerol at -80 °C.

Transformation of Recombinant pAUL-A Plasmid into Competent *L. monocytogenes* by Electroporation

The recombinant plasmid was transformed into competent *L. monocytogenes* serotype 4b prepared as above by electroporation on a BioRad *E coli* Pulser. Plasmid in dH_2O (1 µl) was added into 50 µl of competent *L. monocytogenes*, gently mixed with an eppendorf tip and chilled on ice for 1 min. Electroporation was performed at 2.5 kv for 5 ms in a precooled Gene Pulser Cuvette (0.2 cm electrode gap) on a BioRad *E. coli* Pulser. SOC (1 ml) was added immediately and mixed by pipeting. Cell suspension was incubated at 30 °C for 3 h at 225 rpm and cell suspension (250 µl) was plated onto the 5 µg/ml erythromycin-containing LB agar plate and incubated at 30 °C for 4 days.

Examination of Transformants

Erythromycin resistant colonies from the above 5 µg/ml erythromycin-containing LB agar plate were examined for presence of pAUL-A-517/518 by extraction of plasmid followed by confirmation by PCR using the vector specific primers. One colony was

inoculated into 5 ml of LBMOPS containing 5 μg/ml erythromycin and incubated at 30 °C overnight at 100 rpm for plasmid extraction. The cell pellet was digested with 30 μl of 10 mg/ml lysozyme (in water) in 100 μl of TE buffer (10 mM Tris-HCl, pH 8.0, 1 mM EDTA) at 37 °C for 10 min. The lysozyme-digested cells were subjected to miniprep as described above for *E. coli*. PCR was used to confirm the presence of correct plasmid by PCR using vector specific primers (M13 Forward Primer and M13 Reverse Primer).

Allelic Exchange

The generation of the *ispC* in-frame deletion mutant strain (designated Δ*ispC*) was performed basically as described (Schaferkordt and Chakraborty, 1995). Briefly, the verified colony containing correct pAUL-A-517/518 plasmid was streaked on a LB agar plate containing 5 μg/ml erythromycin and incubated at the non-permissive temperature of 42 °C overnight and this procedure was repeated twice to achieve the integration of the recombinant plasmid on the chromosome. To obtain spontaneous excision of the integrated plasmid through intramolecular homologous recombination, an integrated colony was inoculated into 20 ml of LBMOPS minus erythromycin and incubated at 30 °C overnight with gentle shaking (100 rpm) followed by a subculture at a 1:2000 dilution in fresh LBMOPS medium minus erythromycin (20 μl overnight culture in 40 ml of medium) at 30°C overnight with gentle shaking. To eliminate the excised plasmid, the overnight culture was diluted 1:100 in fresh LBMOPS minus erythromycin (400 μl of overnight culture in 40 ml of medium) and incubated at the non-permissive temperature of 42 °C with gentle shaking. The overnight bacterial suspension was serially diluted with LBMOPS minus erythromycin to a final concentration of 10^3 bacteria/ml and cell suspension (100 μl per plate) was plated on LB agar plate minus erythromycin and incubated at 37 °C overnight. The colonies were screened for erythromycin-sensitive colonies by duplicating colonies on erythromycin (5 μg/ml)-containing and -minus LB agar plates. The genomic DNAs of the erythromycin-sensitive colonies were extracted using DNAzol (invitrogen) according to the manufacturer's instruction. The mutants were confirmed by PCR analysis of the genomic DNA using the primer pair internal to the deletion region P304 and P285 and the primer pair external to the deletion region P481 and P518 and by sequencing the PCR products.

APPENDIX 3

Supplementary Data

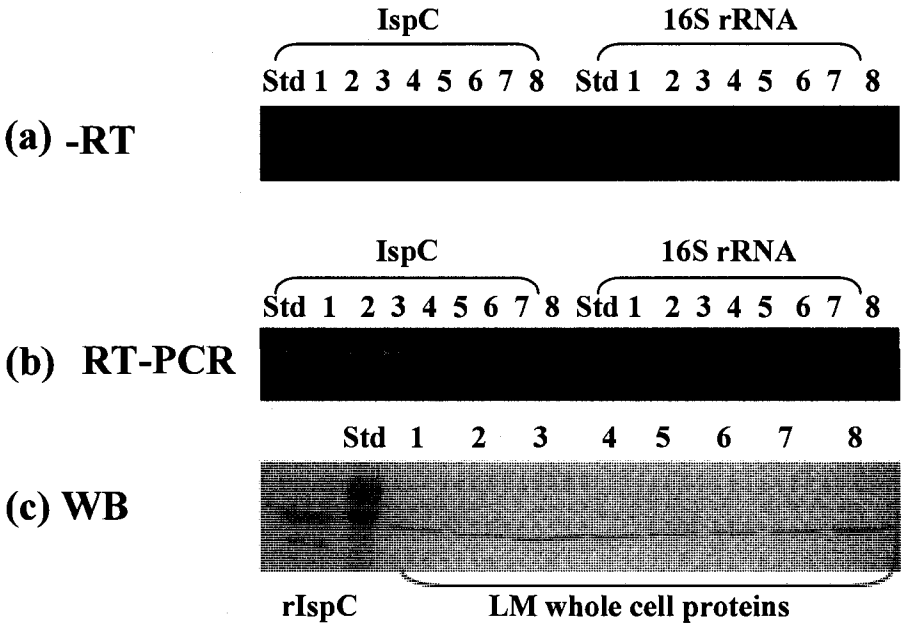

(d)

Time point	1	2	3	4	5	6	7	8
OD_{620}	0.125	0.2	0.25	0.3	0.4	0.5	0.483	0.437

FIG. S1. Expression of the *ispC* gene in *in vitro* cultured *L. monocytogenes*. The bacteria samples were taken at various time points (i.e., different OD620 values) over a 24 h growth period and analyzed for the *ispC* transcript by RT-PCR and for the protein by Western blot probed with RαIspC at a dilution of 1:1000. The RT-PCR products shown in each lane (i.e., each time point) were derived from the same amount of total RNA (~100 ng). For Western blot analysis, the whole cell proteins from cells equivalent to 0.5 ml of culture at OD620 of 0.5 at each time point and purified rIspC (1 μg) were used. **(a)**, PCR analysis of the DNAs of *ispC* and 16S rRNA without the reverse transcriptase step; **(b)**, RT-PCR detection of the mRNAs of *ispC* and 16S rRNA; **(c)**, Western blot (WB) analysis of *L. monocytogenes* (LM) proteins and rIspC using the RαIspC antiserum; **(d)**, the OD_{620} values of *L. monocytogenes* culture collected at various time points.

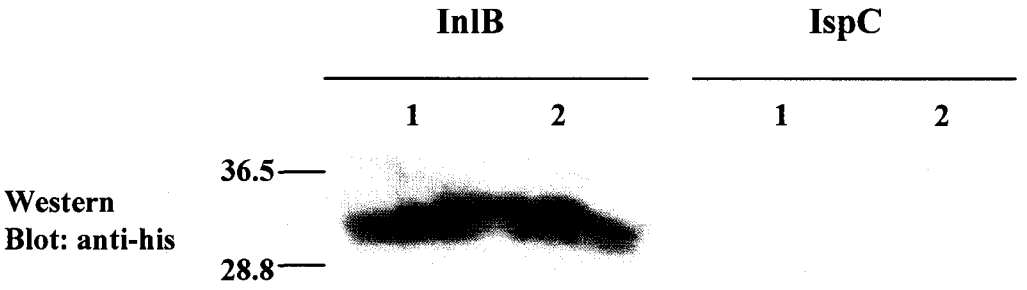

FIG. S2 Ligand overlay assay. Vero cell lysates (40 μg) were separated by SDS-PAGE and electrotransferred onto nitrocellulose membranes. The bound proteins were probed using IspC or InlB (25 μg/ml) followed by detection using anti-his monoclonal antibody. Samples were analyzed in duplicate (Lanes 1 and 2). Protein standards with their molecular masses in kDa are shown on the left of the blots.

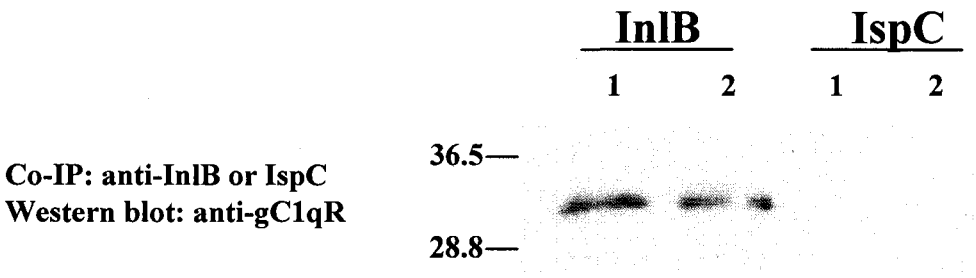

FIG. S3. Co-immunoprecipitation. Precleared Vero cell lysates were incubated with recombinant IspC or InlB (25 μg) that had been attached through specific antibodies to Protein A agarose beads. The co-immunoprecipitates were detected by Western blotting probed with anti-gC1qR antibody. Samples were analyzed in duplicate (Lanes 1 and 2). Protein standards with their molecular masses in kDa are shown on the left of the blots.

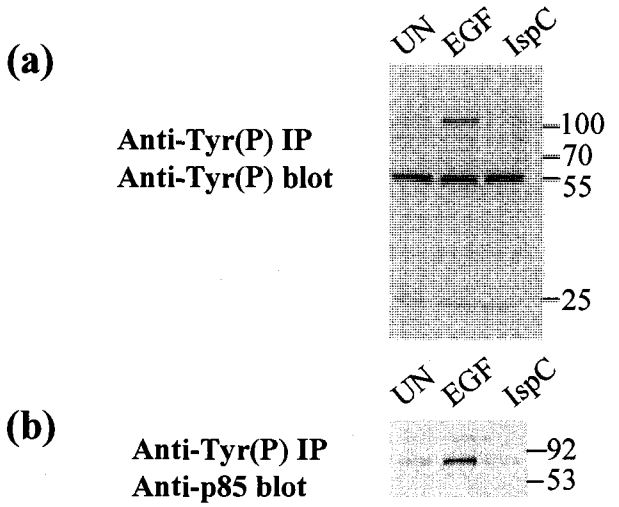

FIG. S4. Effects of IspC on tyrosine phosphorylation. (**a**) Vero cells were treated in triplicate with either IspC (3 nM), or EGF (100 ng/ml), or left untreated (UN) for 1 min. The anti-Tyr(P) immunoprecipitates were analyzed for overall tyrosine phosphorylation by Western blotting probed with anti-Tyr(P) antibody. (**b**) The association of phosphorylated proteins with the p85 subunit of PI 3-kinase was further detected by Western blotting using anti-Tyr(P) immunoprecipitates with anti-p85 antibody. Protein standards with their molecular masses in kDa are shown on the right of the blots.

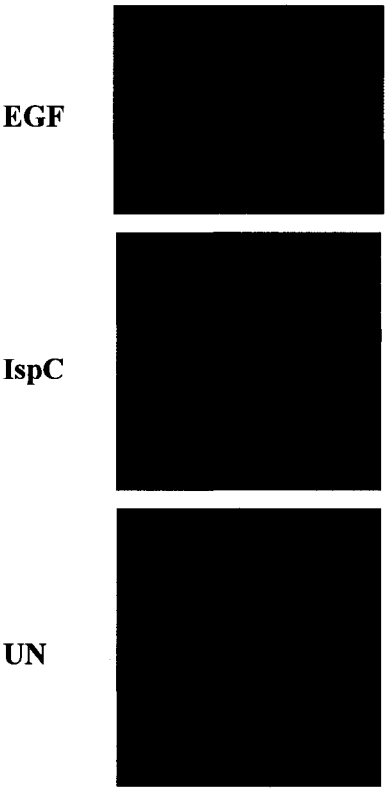

FIG. S5. Actin rearrangement. Vero cells were treated in duplicate with either EGF (100 ng/ml) or IspC (3 nM) for 5 min. Cells were then stained with phalloidin and examined morphologically on a fluorescence microscope at a magnification of 40 ×. Untreated cells (UN) were used as negative control.

CURRICULUM VITAE

PERSONAL DATA:

Name: **Lin Ru Wang**
Phone:
e-mail:
Address:

EDUCATION:

01/2004-present, Ph. D. candidate, Department of Biochemistry, Microbiology and Immunology, University of Ottawa, Canada

Project: Biochemical and Genetic Characterization of IspC, an Immunogenic Surface Protein with Peptidoglycan Hydrolase Activity Essential for Virulence of *Listeria monocytogenes*

09/1992-07/1997, Bachelor in Medicine, Department of Medical Laboratory Science, Dalian Medical University, China

WORKING EXPERIENCE:

09/2003-01/2004, Research assistant, Canadian Food Inspection Agency, Canada

12/2002-05/2003, Team leader, the 2nd branch of the Clinical Laboratory of the 2nd affiliated hospital of China Medical University, China

09/1997-12/2002, Technologist, the Clinical Laboratory of the affiliated hospital of China Medical University, China

AWARDS/ HONOURS/SCHOLARSHIPS:

02/2007, First prize in Research Seminar Symposium, University of Ottawa, Canada

09/2005 to present, Admission Scholarship, University of Ottawa, Canada

07/1997, My undergraduate graduation thesis entitled "The extraction and purification of collagen I" was conferred as Excellent Graduation Thesis.

09/1992-07/1997, Seven awards as per Excellence Comprehensive Performances, Department of Medical Laboratory Science, Dalian Medical University, China

Fall of 1995 and Winter of 1996, Conferred as Excellent Investigator in Social Investigation Activity, Dalian Medical University, China

EXPERTISES:

Studying host-pathogen interaction using animal and mammalian cell culture model systems,

target genetic mutagenesis, molecular mechanisms of pathogenesis, protein expression, protein purification, and molecular/biochemical/structural characterization of virulence factor.

Culture, isolation, and identification of human pathogens (primarily bacteria including *Mycobacterium tuberculosis*, enteropathogenic bacteria such as *Vibrio cholera*, and *Staphylococci etc.*) from various clinical samples, antimicrobial testing, efficiency of chemical/physical disinfection and sterilization monitoring, and hospital-acquired infection monitoring.

Lab management, supervise, and train students and technicians.

RECENT PUBLICATIONS:

Wang, L., and Lin, M. (2007). Identification of IspC, an 86-kilodalton protein target of humoral immune response to infection with *Listeria monocytogenes* serotype 4b, as a novel surface autolysin. J. Bacteriol. *189*, 2046-2054.

Wang, L., Walrond, L., Cyr, T.D., and Lin, M. (2007). A novel surface autolysin of *Listeria monocytogenes* serotype 4b, IspC, contains a 23-residue N-terminal signal peptide being processed in *E. coli*. Biochem. Biophys. Res. Commun. *354*, 403-408.

Wang, L., and Lin, M. (2008). A novel cell wall-anchored peptidoglycan hydrolase (autolysin) IspC essential for *Listeria monocytogenes* virulence: genetic and proteomic analysis. Microbiology *154 (Pt 7)*:1900-1913.

PRESENTATIONS:

Lin Ru Wang and Min Lin. Characterization of a novel immunogenic protein IspC from *Listeria monocytogenes* serotype 4b, a potential target for bacterial detection. Poster presented at Federal Food Safety and Nutrition Research Meeting, Ottawa, Canada, Oct 19-21, 2005